THERMODYNAMICS OF GAS HYDRATE EQUILIBRIA

by

Dimitrios Anaştassios Avlonitis

Submitted for the Degree of Doctor of Philosophy

Department of Petroleum Engineering
Heriot-Watt University
Edinburgh

February 1992

This copy of the thesis has been supplied on condition that anyone who consults it is understood to recognize that the copyright rests with its author and that no quotation from the thesis and no information derived from it may be published without the prior written consent of the author or the University(as may be appropriate).

TABLE OF CONTENTS

LIST OF TABLES

LIST OF FIGURES

ACKNOWLEDGEMENTS

This work was supported by the (Greek) State Scholarships Foundation and the Department of Petroleum Engineering/Heriot-Watt University.

Thermodynamics of Gas Hydrate Equilibria

Dimitrios Anastassios Avlonitis

ABSTRACT

Reservoir fluids are usually saturated with water at reservoir conditions and may form gas hydrates in transfer lines, which potentially may plug the system. For long subsea pipelines, methanol injection is the practical means for preventing hydrate formation and for decomposing blockages. For efficient and economical pipeline design and operation, phase boundaries, phase fractions and distribution of water and methanol among the equilibrium phases of the system must be accurately known. The system comprising reservoir fluids, water and methanol demonstrates a complex multiphase behaviour and currently no quantitatively adequate description for it has been detailed in the open literature. The problem is addressed in this thesis by a consistent application of classical equilibrium thermodynamics.

At ordinary operating conditions any combination of as many as six phases can be potentially present. For the description of the vapour and all liquid phases, we use one cubic equation of state with nonconventional mixing rules developed as part of this work. Classical thermodynamics together with the cell theory of van der Waals and Platteeuw were employed for the development of a general model for the calculation of heat capacities of gas hydrates. A consistent methodology has also been developed for obtaining the potential parameters of the cell model. Thereafter, application of the model demonstrates that for nearly spherical guest molecules the classical cell theory is a strictly valid description of gas hydrates. However, complex guest molecules distort the hydrate lattice, resulting in variation of the numerical values of certain parameters of the model.

This work presents an efficient algorithm for the solution of the problem of the identity of the equilibrium phases in multiphase systems where gas hydrates are potentially present. The algorithm is based on the alternative use of two equivalent forms of the Gibbs tangent plane criterion and it is believed to be more appropriate for systems involving gas hydrate equilibria than previous methods. Application of the proposed algorithm in several regions of the phase diagram of both binary and multicomponent systems shows that it can be used

reliably to solve any phase equilibria problem, including the location of phase boundaries.

In summary this work presents a consistent, efficient and reliable scheme for multiphase equilibrium calculations of systems containing reservoir fluids, water and methanol. Favourable results have been obtained by comparison with diverse experimental data reported in the open literature and it is believed that the proposed correlation can be used reliably for pipeline design and operation.

INTRODUCTION

Gas hydrates are solid crystalline compounds formed by inclusion of small gas molecules (guest molecules) into a lattice constructed by water. The whole structure is stabilised by hydrogen bonds and van der Waals forces. The crystal structure of gas hydrates was elucidated by X-ray diffraction experiments (von Stackelberg and Müller, 1954) and the most common gas hydrates form in either of two distinct structures, designated I and II correspondingly, each of which contains two types of cavities. The unit cell of structure I and II are illustrated in figures 1a and 1b correspondingly, according to von Stackelberg and Müller. The former consists of 46 water molecules which constitute two small pentagonal dodecahedra cavities and six tetradecahedral large cavities, having two opposite hexagonal faces and twelve pentagonal faces. The unit cell of structure II consists of 136 water molecules comprising sixteen pentagonal dodecahedra small cavities and eight hexadecahedra large cavities, having twelve pentagonal faces symmetrically arranged around four hexagonal faces. The average cavity radii of these three types of cavities are about 3.9 Å for the pentagonal dodecahedra, 4.3 Å for the tetradecahedra and 4.7 Å for the hexadecahedra (Sloan, 1990). The large cavity of structure I and the small cavities of both structures are nearly spherical, but the tetradecahedral cavity of structure I is rather oblate.

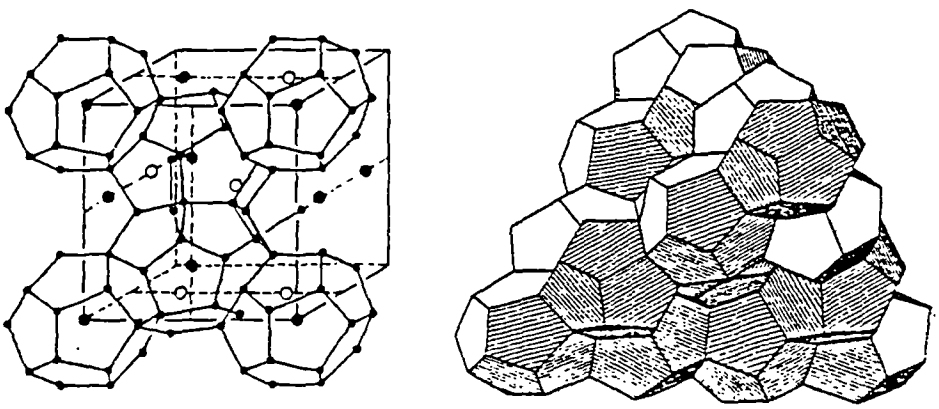

a. b.

Figure I.1. The unit cell of hydrate structure I (a) and II (b).

Hydrates resemble snow or ice in appearance but unlike ice they may form at temperatures well above the triple point when the pressure is sufficiently high. Since reservoir fluids are typically saturated with water, in downstream transfer lines from the well-head, hydrates are likely to form with subsequent reduction of the transportation capacity or even total blockage of the system. Clearly, offshore and arctic pipelines are particularly prone to hydrate formation. A number of options are available for the prevention of hydrate formation which include insulation and/or heating of the pipeline, dehydration at the well head and inhibitor injection. For long subsea pipelines, however, only inhibitor injection is of practical significance. Any water-soluble substance, which lowers the chemical potential of water, is in effect a hydrate inhibitor but methanol is the universally accepted chemical, both for continuous injection and for decomposing blockages.

For efficient and economical pipeline design and operation, the boundary of hydrate formation with and without methanol must be precisely known. In addition, the mass and properties of each of the equilibrium phases and in particular the distribution of water and methanol among them must be predicted as accurately as possible. While this was the main task undertaken with the present work, as an aside, a number of associated problems(as discussed below) had to be addressed.

It has been long established that the ideal solid solution theory of van der Waals and Platteeuw(1959) can cope well with all hydrate equilibrium problems (Parrish and Prausnitz, 1972; Ng and Robinson, 1976; Sloan et al, 1976; Holder et al, 1980; Englezos and Bishnoi, 1988; Avlonitis et al, 1989). However, the reliability of the classical model of van der Waals and Platteeuw(1959) depends on adequate description of coexisting phases and it is dependent on reliable values of the incorporated thermodynamic and potential parameters. The theory itself cannot provide values of these parameters, which have to be based on experimental data. It appears that the values of the thermodynamic properties of the empty hydrate lattice relative to ice at the ice point and zero pressure (*reference properties*), reported by Dharmawardhana et al(1980) are correct within the reported experimental error, since Davidson et al(1987) have found a nearly identical value for the chemical potential difference from an altogether different experimental approach. Unfortunately, the same is not true for the values of the potential parameters of the model, where every author reports his own values (see for instance Parrish and Prausnitz, 1972; Anderson and Prausnitz, 1986 and Sloan, 1990), although the same data were available and used by all of them and presumably the same methodology has also been

employed in regressing the parameters. The important differences in predictive quality reported by these authors may be attributed to incorrect values of the potential parameters. This paradoxical phenomenon did not lack the attention of Holder and his coworkers. Their proposed rectification of the problem (John et al, 1985), which is based on the introduction of new assumptions and further complexities has been found to be inefficient for real and multicomponent gases. The present investigation reveals the nature of the problem, proposes a consistent methodology for determining the potential parameters and eventually evaluates the model by an extensive comparison of predictions with experimental data for natural and synthetic multicomponent systems.

Most of the previous theoretical studies use the classical cell model for PVT predictions. It is well known, however, that the model can also be used to calculate enthalpy changes, as accurately as dissociation pressures. This is expected due to the applicability of the Clausius-Clapeyron equation along a phase transition line (Barrer and Edge, 1967). However, no rigorous scheme has been proposed so far for the prediction of heat capacities of gas hydrates for real and multicomponent systems. In view of the significant practical interest in the knowledge of the thermal properties of gas hydrates, the present study extends the ideal solid solution theory to the prediction of heat capacities of gas hydrates. The proposed methodology is theoretically rigorous and it does not introduce additional assumptions, but the values of the parameters it depends upon have to be provided by experimental data. The model is tested against the only set of experimental heat capacity measurements available in the open literature of a multicomponent gas hydrate system.

An equation of state has always been the preferred method for representing a vapour phase in equilibrium with hydrates. For the water-rich liquid phase, Saito et al (1964) use the ideal liquid solution approach(*Raoult's Law*). Presumably, in doing so, they assume that the solubility of reservoir gases in water is negligible at usual conditions. Although, there are instances where the validity of this assumption can be questioned, it has been the preferred method in the past (Parrish and Prausnitz, 1972; Holder and Hand,1982). When inhibition calculations were needed, Raoult's Law was corrected by the activity coefficient, calculated separately from the appropriate model(Menten et al, 1981). Although, the reliability of this procedure has been proven to be superior to the Hammerschmidt (1939) equation, nonetheless, it is not a thermodynamically consistent scheme and it is unable to evaluate the distribution of an inhibitor such as methanol among the coexisting phases. An attempt to rectify this problem was carried out by Anderson and Prausnitz(1986), who used the

UNIQUAC equation to calculate the fugacities of all condensible components in a liquid phase. Henry's Law was used for supercritical components. Thus, four models had been necessary to perform simple inhibition calculations. Due to this inherent extreme complexity, it is not surprising that their program has been proven to be not useful in practice for representing systems other than those employed for fitting its own parameters. Also, it cannot serve as a platform for further development to carry out more elaborate calculations, such as stability analyses of complex systems, because of convergence problems which are acknowledged by these authors even for relatively simple problems. In the present study we use one single equation of state to represent the vapour as well as all liquid phases. In doing so we have developed new mixing rules for polar-nonpolar interactions. This approach vastly simplifies the calculation scheme and offers a series of advantages. In addition, our model is proven to be capable of predicting adequately the phase behaviour of adverse multicomponent systems. When the work on hydrate inhibition was completed and submitted for review (see Avlonitis et al, 1991), to our knowledge, it was the first time that reliable hydrate inhibition prediction had been demonstrated by the application of one cubic equation of state for all fluid phases.

The identity of the equilibrium phases had been a serious problem in multiphase equilibria calculations, until Michelsen(1982) presented numerical implementations of the Gibbs tangent plane criterion. The method of Michelsen has been applied to water-hydrocarbon multiphase systems at high temperatures by Nutakki et al(1988) and it was successfully adopted for some simple hydrate forming mixtures by Cole and Goodwin(1990). Evidently, the method of Gupta, as reported by Bishnoi et al(1989), is also based on the tangent plane criterion. This work presents an alternative algorithm for multiphase-multicomponent equilibria, which is particularly efficient when more than two phases may occur, i.e. when water is one of the components. The method could be used to solve any phase equilibrium problem, including the location of phase boundaries, with minimum information supplied by the user. The efficiency of the proposed algorithm is demonstrated by an extensive comparison with diverse experimental data of systems showing multiphase regions.

In summary this work presents a theoretically consistent scheme for the prediction of the PVT and thermodynamic properties of gas hydrates in the presence or absence of inhibitors with the minimum user-supplied information (ie the specifications of the problem only). As an aside, the model is capable of predicting the effect of water-methanol mixtures on the behaviour of reservoir fluids. The layout of this thesis is described below.

In Chapter I, a model for asymmetric systems containing water and methanol is developed. A brief description of the PVT behaviour of such systems, is followed by a presentation of the most successful or promising ideas reported in the open literature for modelling such systems. Next, the evolution of our suggestion is presented and tested against diverse experimental data in the range of our interest. A complete description is also given of the numerical methods for multiphase equilibria calculations.

In Chapter II the fundamental equations of the classical cell theory are presented. While the parameters reported by Dharmawardhana et al(1980) are accepted, all other parameters are regressed again on the basis of the latest experimental data. In particular a consistent methodology for the determination of the potential parameters is detailed.

The proposed hydrate model is extensively tested against experimental dissociation pressure data for natural and other multicomponent systems in Chapter III.

A new method for the prediction of the heat capacities of gas hydrates is detailed in Chapter IV. Though our treatment is purely phenomenological and macroscopic, as an aside, some interesting insights are gained regarding the molecular interactions of guest and host molecules.

In Chapter V the problem of the identity of the equilibrium phases is related the thermodynamic stability of the system. All the relevant thermodynamic equations are derived in an attempt to elucidate the nature of the problem. A methodology based on the idea of free flash calculations, which we consider appropriate for the solution of the specified multiphase equilibrium problem, is detailed. It is noted that although free flash calculations were carried out for some time as a means to enhance the performance of the flash algorithm (see for instance Sarkar, 1988) they have never been used successfully as an independent means of performing stability analyses of multiphase systems.

Finally, in Chapter VI, we summarize our conclusions from the current work. Despite the progress reported in this work, we declare, as expected, that the subject can not be considered closed and we indicate the areas where further experimental and theoretical work needs to be carried out.

References

Anderson, F.E. and Prausnitz, J.M., "Inhibition of gas hydrates by methanol", AIChE J., **32**(8),1321(1986).

Avlonitis, D.A., Danesh, A., Todd, A.C., Baxter,T., "The formation of hydrates in oil-water Systems", Multiphase Flow-Proc. 4th Internl Conf., p. 15, BHRA(1989).

Avlonitis, D.A., Todd, A.C., Danesh, A., "A rigorous method for the prediction of gas hydrate inhibition by methanol in multicomponent systems", The First Internl. Offshore and Polar Engin. Conf.,(ISOPE-91), Edinburgh, Scotland(1991).

Barrer, R.M., and Edge, A.V.J., "Gas Hydrates containing Argon, Krypton and Xenon: Kinetics and Energetics of Formation and Equilibria", Proc. Roy. Soc., **A300**, 1(1967).

Bishnoi, P.R., Gupta, A.K., Englezos, P., Kalogerakis, N., "Multiphase Equilibrium Flash Calculations for Systems Containing Gas Hydrates", Fluid Phase Equilibria, **53**, 97(1989).

Cole, W.A., Goodwin, S.P., "Flash Calculations for Gas Hydrates: A Rigorous Approach", Chem. Eng. Sci., **45**(3), 569(1990).

Dharmawardhana, P.B., Parrish, W.R., Sloan, E.D., "Experimental Thermodynamic Parameters for the Prediction of Natural gas Hydrate Dissociation Pressures", IEC Fund., **19**, 410(1980).

Englezos, P. and Bishnoi, P.R., "Prediction of Gas Hydrate Formation Conditions in Aqueous Electrolyte Solutions", AIChE J., **34**(10), 1717(1988).

Holder, G.D., Gorbin, G., Papadopoulos, K.D., "Thermodynamic and Molecular Properties of Gas Hydrates Containing Methane, Argon and Krypton", IEC Fund., **19**(3), 282(1980).

John, V.T., Papadopoulos, K.D.,Holder, G.D., "A Generalised Model for Predicting Equilibrium Conditions for Gas Hydrates", AIChE J., **31**(2), 252(1985).

Michelsen, M.L., "The Isothermal Flash Problem, Part I. Stability", Fluid Phase Equilibria, **9**, 1(1982).

Ng, H.J. and Robinson,D.B., "The Measurement and Prediction of Hydrate Formation in Liquid Hydrocarbon-Water Systems", IEC Fund., **15**(4), 293(1976).

Nutakki, R., Firoozabadi, A, Wong, T.W., Aziz, K., "Calculation of Multiphase Equilibrium for Water-Hydrocarbon Systems at High Temperature", SPE/DOE 17390, 733(1988).

Parrish, W.R. and Prausnitz, J.M., "Dissociation Pressures of Gas Hydrates Formed by Gas Mixtures", IEC Proc. Des. Dev., **11**(1), 26(1972).

Saito, S., Marshall, D.R., Kobayashi, R., "Hydrates at High Pressures", AIChE J., **10**(5) 734(1964).

Sarkar, R., PhD Thesis, Heriot-Watt University, Edinburgh (1988).

Sloan, E.D., Khoury, F.M., Kobayashi, R., "Water Content of Methane Gas in Equilibrium with Hydrates", IEC Fund., **15**(4) 318(1976).

Sloan, E.D., "Clathrate Hydrates of Natural Gases", Marcel Dekker Inc, New York(1990).

van der Waals, J.H. and Platteeuw, J.C., "Clathrate Solutions", Adv. Chem. Phys., **2**, 1(1959).

von Stackelberg, M. and Müller, H.R., "Feste Gashydrate", Z. für Elektrochemie, **58**, 25(1954).

CHAPTER I

MODELLING OF VAPOUR-LIQUID EQUILIBRIA OF ASYMMETRIC SYSTEMS

1.1. Objective

Water is often one of the components of hydrocarbon streams in transfer lines in various processes from gas and oil production through refining and distribution. For such systems, predictions of equilibrium phase boundaries as well as compositions and densities of equilibrium phases are required for proper design and operation of the various processing units. In this chapter vapour-liquid equilibria of multicomponent hydrocarbon systems containing water and methanol are modelled by the application of a cubic equation of state with non-conventional mixing rules. This study is confined to nitrogen, carbon dioxide, hydrogen sulfide and hydrocarbons up to n-octane. No adequate experimental data are available for heavier compounds. For our purposes, the present study is restricted to conditions below the critical and above the hydrate point of the mixture. No particular effort is directed towards modelling of the near critical region. The model is restricted to electrically neutral and non-reacting components and interfacial phases are ignored.

It will be demonstrated that the equation of state with the developed mixing rules can represent effectively diverse experimental P, V, T and compositional data for all fluid phases in the range of our interest. The equation of state, as an empirical correlation of macroscopic properties, does not need to refer to intermolecular forces and no reference is made to microscopic properties. To further improve the quality of predictions in a few cases the empirical principle of corresponding states is relaxed.

Overall the model is thermodynamically consistent and it applies equally well to all fluid phases. More components of interest might be included if binary experimental data were available. Simplicity and computational efficiency are also enhanced by application of a single equation of state.

1.2. Phase behaviour of mixtures of water, methanol and hydrocarbons above hydrating conditions

In the following the liquid and vapour phases are designated by the symbols L and V respectively. Subscripts to L indicate the important component in that liquid phase. Occasionally, a supercritical phase may be designated by the symbol G(for gas), when it emerges in the phase diagram from liquid regions.

Phase Diagrams

The phase behaviour of binary systems can be represented as a function of the independent variables T, P and the mole fraction of the first component x_1. Three variables would require construction of a spatial diagram but more advantageous are planar cross-sections of that at a fixed value of one of the variables. P(T) diagrams show comprehensively the general behaviour of the system but they do not show the composition. For binary systems, T(x) diagrams at constant pressure and P(x) diagrams at constant temperature are used to convey more detailed phase behaviour information. The following diagrams are only aimed to convey the most general features of a particular system and for the sake of clarity they may be severely distorted. For the same reason the scales of the axes are not indicated. Although the range of temperatures of our actual interest is limited from 20 K below the ice point to 20 K above that, to facilitate understanding, the regions depicted in the diagrams of this section cover a more extensive range of temperature.

The Methanol/Water Binary System

Methanol and water are miscible in all proportions. Azeotropy and three phase equilibria are not possible. The P(T) diagram of this system is the simplest possible and it is shown in figure 1a. Light solid lines are the vapour pressure curves of the pure methanol(1) and water(2) and end at the critical points of the pure components Cm and Cw respectively. The heavy solid line connecting these points represents the locus of the critical points of all methanol/water mixtures. A T(x) isobar at nearly atmospheric pressure($P_1 \ll P(Cm)$) is presented in figure 1b, which has a characteristic lenticular shape. Homogeneous vapour phases occur above the upper curve(dew-point line) and homogeneous liquid phases occur below the lower curve(bubble-point line). Points between the two lines describe states in which liquid and vapour phases

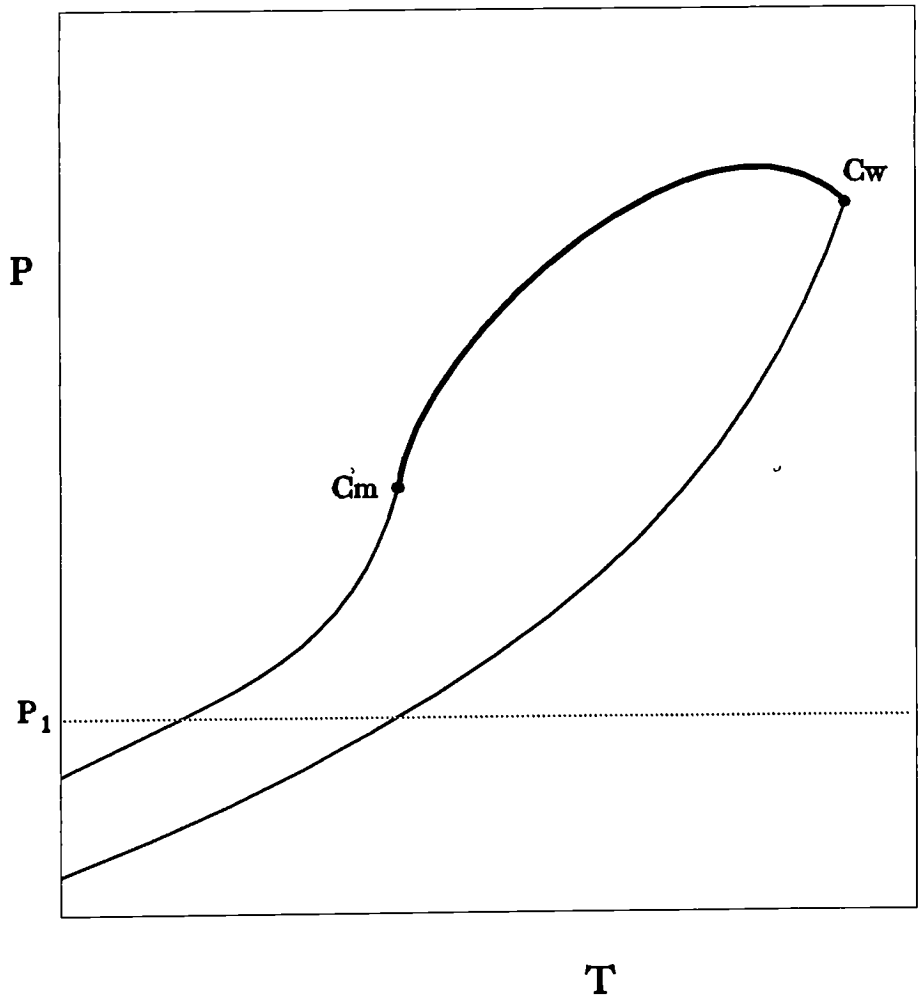

a. P(T) diagram

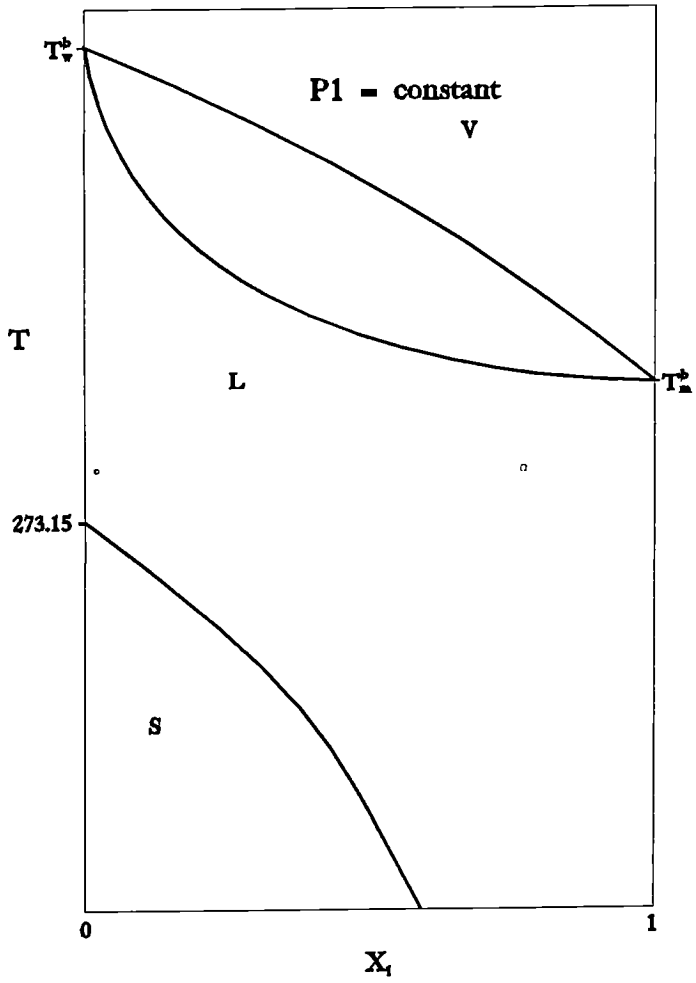

b. P(x) diagram.

Figure 1.1. Phase diagrams of methanol(1)/water(2).

coexist in equilibrium. For completeness, the freezing point curve of the methanol(1)/water(2) system is also included in the T(x) diagram. However, the region below 173 K, where a solid methanol monohydrate compound is formed, is not included in the figure.

Hydrocarbon/Water Binaries

The general characteristics of the phase behaviour of a hydrocarbon/water binary system are represented in figure 2a. The critical point of water(647.30K, 22.12MPa) is substantially higher than the critical point of common hydrocarbons and related gases. In the figure the pure component vapour pressure curves are shown as light solid lines. They end at the respective critical points, indicated as Ch and Cw. The gas-liquid critical curve, shown in the figure as a heavy solid line, which normally connects the critical points of the two pure components as a continuous line, in this case is broken into two parts because it is intersected by the liquid-liquid curve. The lower branch of the critical curve begins at the critical point of the hydrocarbon and ends at the three-phase critical end point (CEP), which is also the end point of the three-phase equilibrium line. Above the critical end point the hydrocarbon-rich liquid phase merges with the vapour phase. A point above the three phase equilibrium line but below the critical end point represents equilibria between a hydrocarbon-rich liquid and a water-rich liquid phase. Points below the three-phase equilibrium line represent equilibrium between a vapour phase and one of the two liquid phases. The lower critical curve corresponds to mixtures with very high hydrocarbon concentration. Other mixtures are represented by the branch of the critical curve which starts from the critical point of water and continues upward at very high pressures.

Figure 2b, 2c and 2d show T(x) phase diagrams at different pressures of a typical hydrocarbon/water binary system in the T, P region of figure 2a. T(x) phase diagrams for hydrocarbon/water binaries can show single-phase and two-phase areas as well as three-phase lines. As temperature increases, the hydrocarbon-rich liquid phase reaches first the three phase critical point and vanishes leaving a vapour phase or vapour in equilibrium with a water-rich liquid. In figure 2b the pressure is above the critical pressure of the hydrocarbon-rich liquid phase and this liquid does not appear. In figure 2c the pressure is lower than the three-phase critical end point pressure but higher than the critical pressure of pure hydrocarbon. There is one three phase equilibrium tie-line(Lw-V-Lh) but

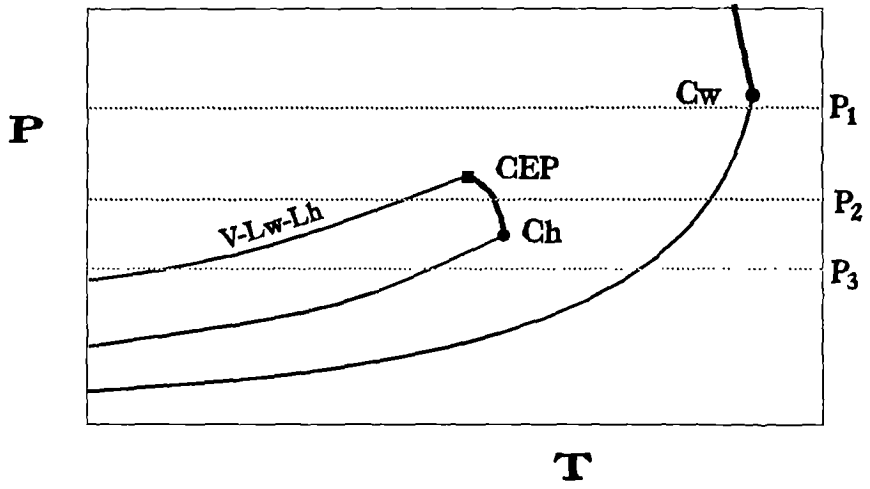

a. P(T) diagram.

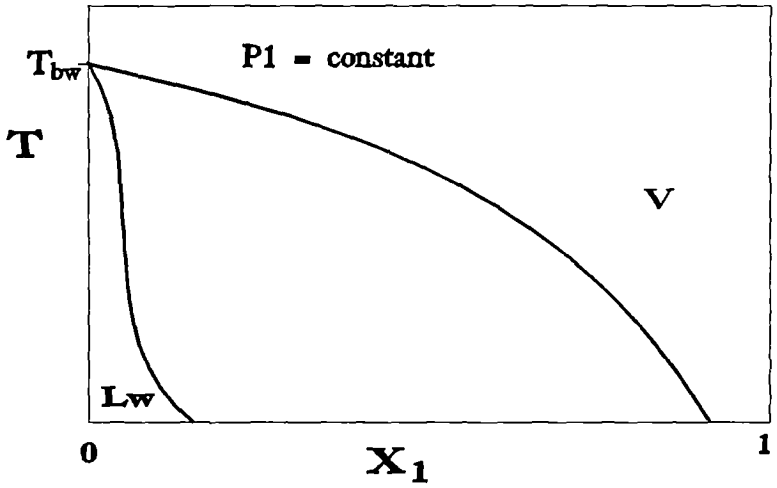

b. T(x) diagram at P > P(CEP).

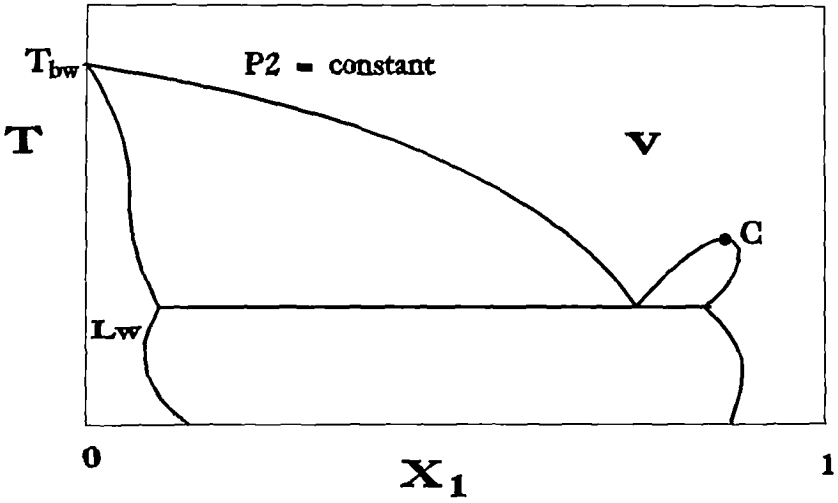

c. T(x) diagram at P(CEP) > P >P(Ch).

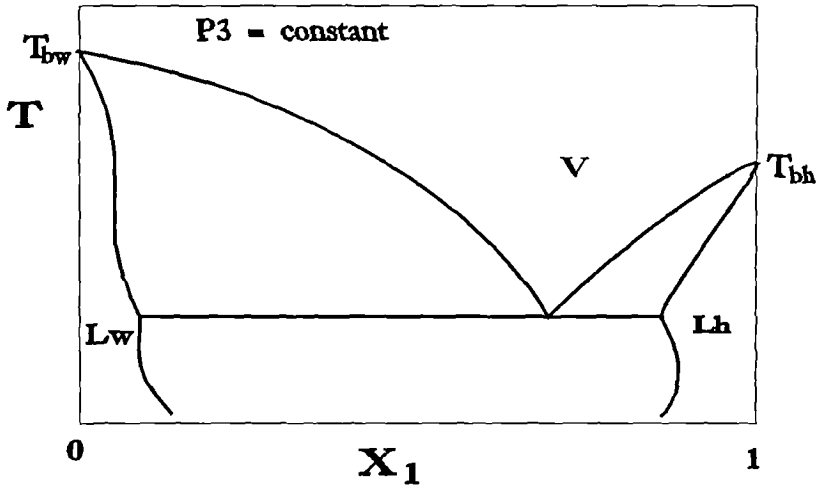

d. T(x) diagram at P(Ch) > P.

Figure 1.2. Phase diagrams of a typical hydrocarbon/water system.

the pure hydrocarbon can not show a boiling point and the hydrocarbon-rich vapour-liquid area can not attach the right ordinate. The intersections of the constant pressure line P_2 with the three-phase line, the lower critical line and the water vapour pressure line of the P(T) diagram, are represented in the T(x) diagram by the three-phase tie-line, the critical point C and the boiling temperature of water T_{bw}, respectively. In figure 2d the pressure has been further reduced below the critical pressure of the pure hydrocarbon and the phase diagram is fully developed. There are three single phase regions(Lw, V, Lh) and three two phase regions(Lw-Lh, Lw-V, V-Lh). Since the constant pressure line P_3 does not intersect critical lines in the P(T) diagram, critical points do not appear in the T(x) diagram. The boiling temperature points of pure water T_{bw} and hydrocarbon T_{bh} appearing in the T(x) diagram, are located at the intersections of the constant pressure P_3 line with the vapour pressure lines of water and hydrocarbon of the P(T) diagram.

The behaviour of all hydrocarbon and related gases included in this study is similar. It is noted that for a fixed temperature in any two-phase region the compositions of the equilibrium phases are fixed and do not depend on the overall composition of the binary mixture.

Methanol/Hydrocarbon Binaries

The phase behaviour of methanol binaries can not be generalized as that of water binaries even in the restricted area of our interest. Hence, a number of specific examples will be presented. Figure 3a corresponds to the pressure-temperature diagram of methane/methanol. The three-phase equilibrium line is below the vapour pressure line of methane. The region where Lh-Lm equilibrium exists, lies at very low temperatures and it is confined between the three-phase, the vapour pressure and the critical line. At ordinary temperatures only Lm-V equilibrium is possible, as shown in figure 3b.

Figure 4a corresponds to the P(T) diagram of the ethane/methanol binary system. The critical point of pure ethane is located at 305K/4.88Mpa and it is much higher in temperature than that of methane. Otherwise the significant features of this system are similar to those of methane/methanol. Qualitative P(x) phase diagrams for ethane/methanol are presented in figures 4b, c and d. Intersections of constant temperature lines with critical lines of the P(T) diagram

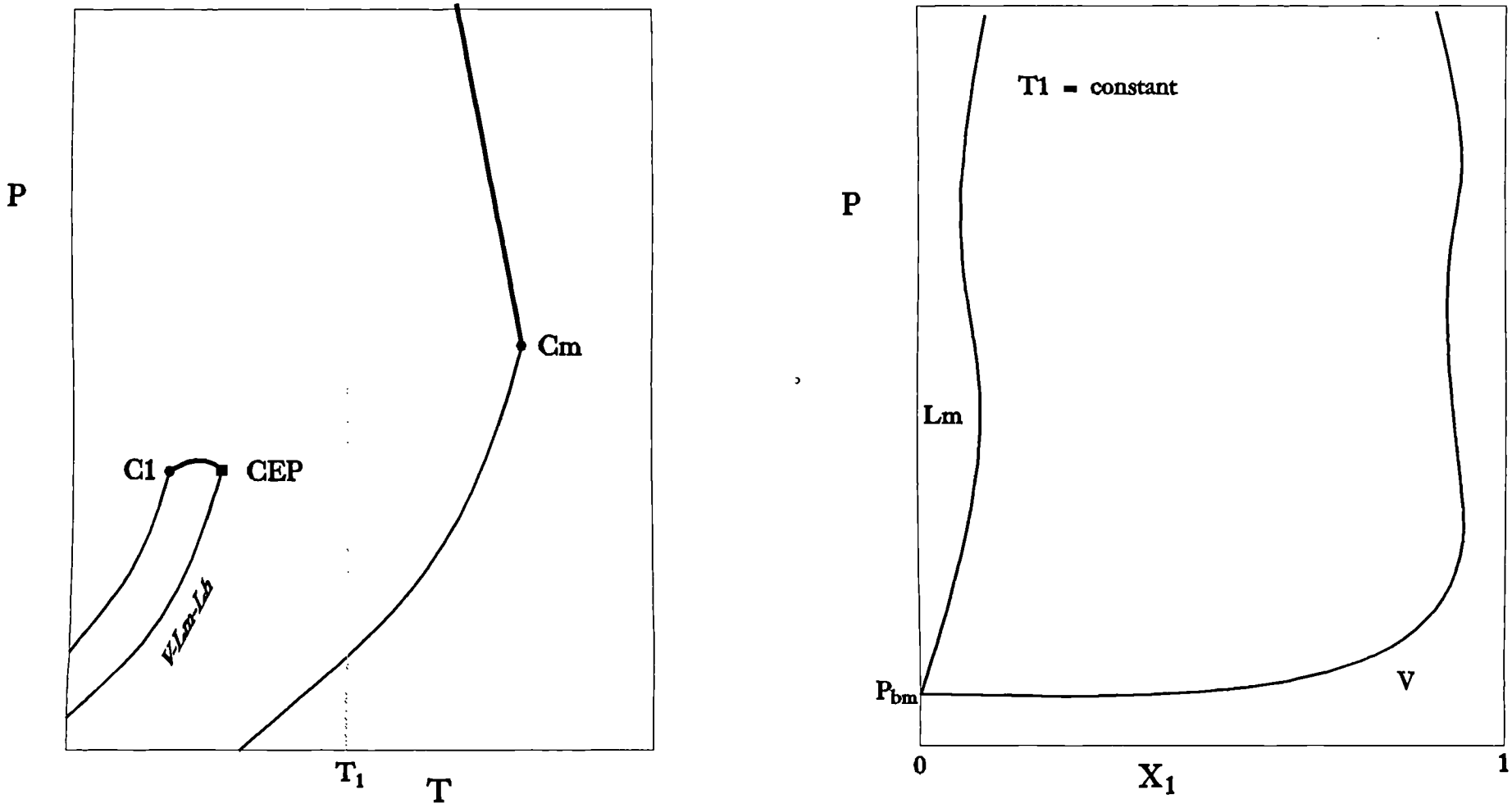

a. P(T) diagram

b. P(x) diagram

Figure 1.3. Phase diagrams of the system methane(1)/methanol(2).

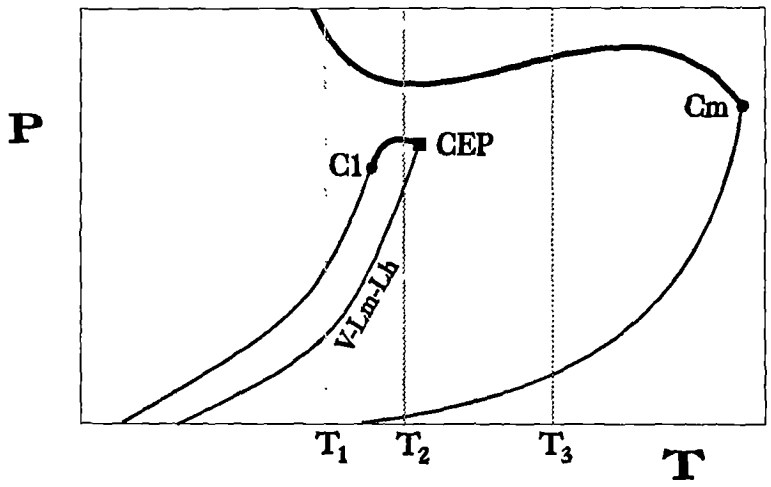

a. P(T) diagram.

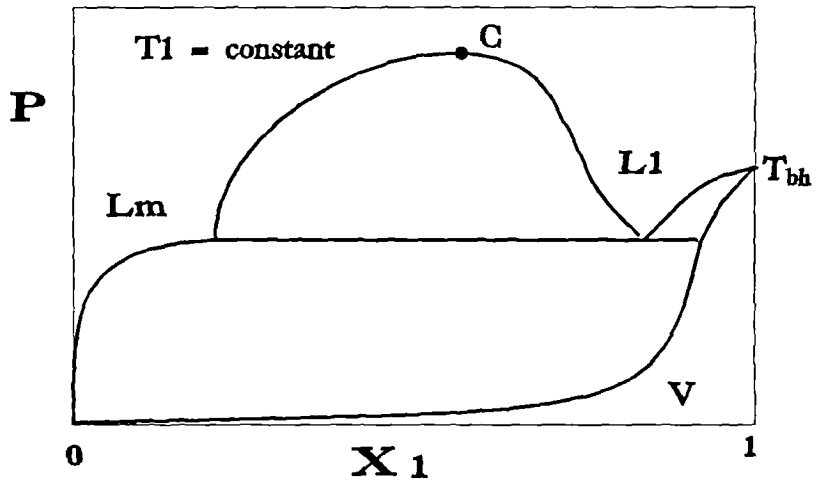

b. P(x) diagram at T < T(C1).

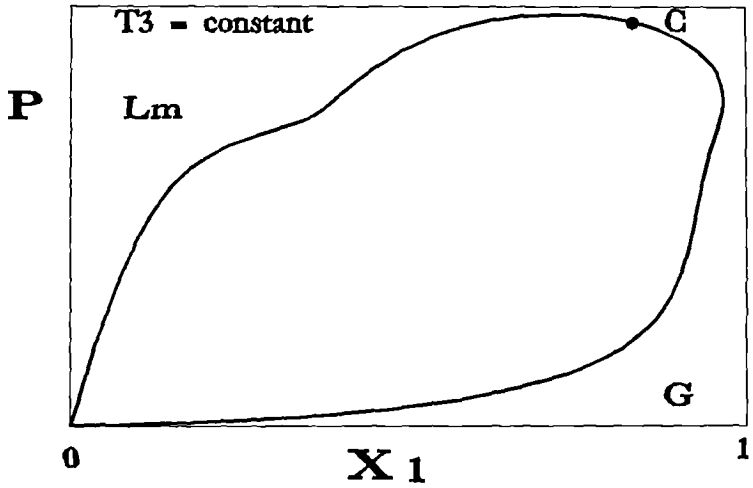

d. P(x) diagram at T > T(CEP).

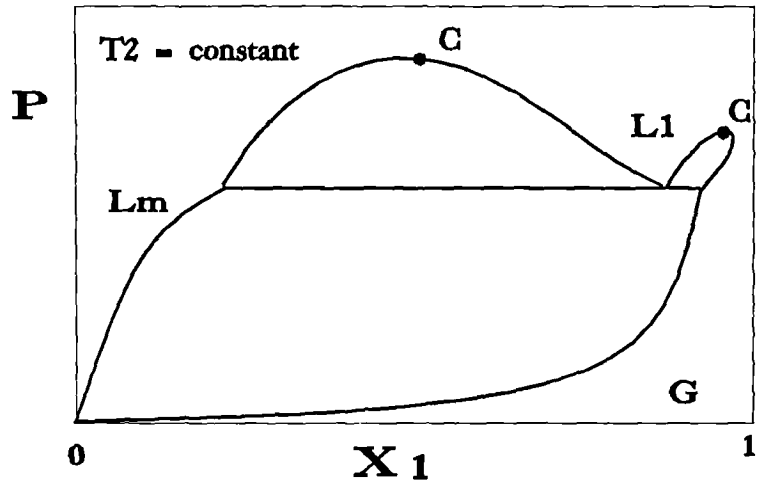

c. P(x) diagram at T(CEP) > T > T(C1).

Figure 1.4. Phase diagrams of the system ethane(1)/methanol(2).

locate corresponding critical points denoted in the P(x) diagrams by the symbol C.

Figure 5a corresponds to the P(T) diagram of heptane/methanol. Here, the critical temperature of heptane is higher than that of methanol but it has a significantly lower critical pressure. The three-phase equilibrium line is above the vapour pressure line of methanol and the critical end point is below the critical point of methanol. The hydrocarbon-rich liquid branch of the critical curve connects the critical point of methanol and heptane. The branch of the critical curve which represents the methanol-rich liquid starts at the critical end point and extends almost vertically to higher pressures. Figure 5b, c, d and e show corresponding T(x) diagrams for the heptane/methanol binary system.

Multicomponent systems

The phase behaviour of multicomponent systems may be represented effectively by P(T) diagrams at fixed mixture composition. The hydrocarbon-rich liquid phase ends at the critical point, where the dew point and bubble point curves are merging. If water is among the components, an additional three phase dew point curve appears which ends at the critical point of the water-rich liquid phase. Figure 6 represents the phase diagram of a typical multicomponent water/hydrocarbon mixture.

Summary

Phase equilibria diagrams of binary systems above hydrating conditions, can be classified on the basis of the shape of their critical curves. As it appears from the presentation above, a model capable of describing the PVT behaviour of mixtures of water-methanol-hydrocarbons, should represent effectively the properties of three distinct phases: a vapour or gas phase, a hydrocarbon-rich liquid and a water-rich liquid. Then, around the model there should be developed efficient algorithms to perform three-phase VLL as well as VL and LL calculations.

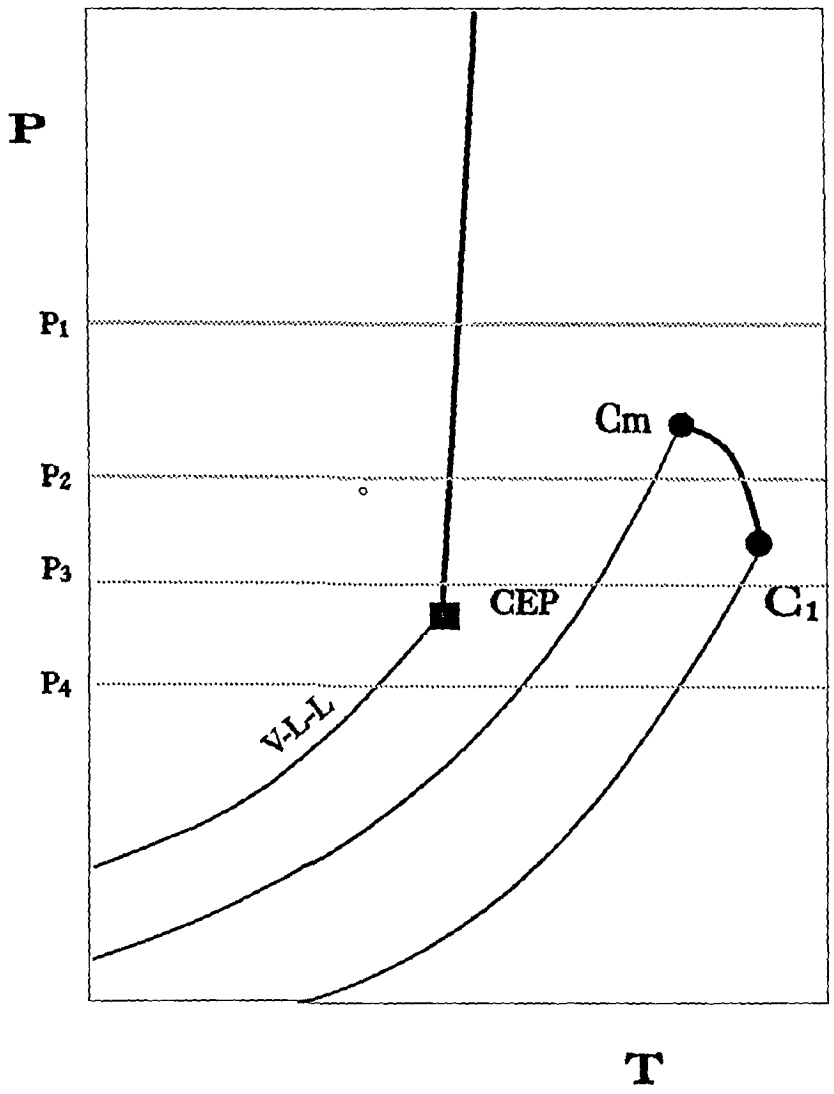

a. P(T) diagram.

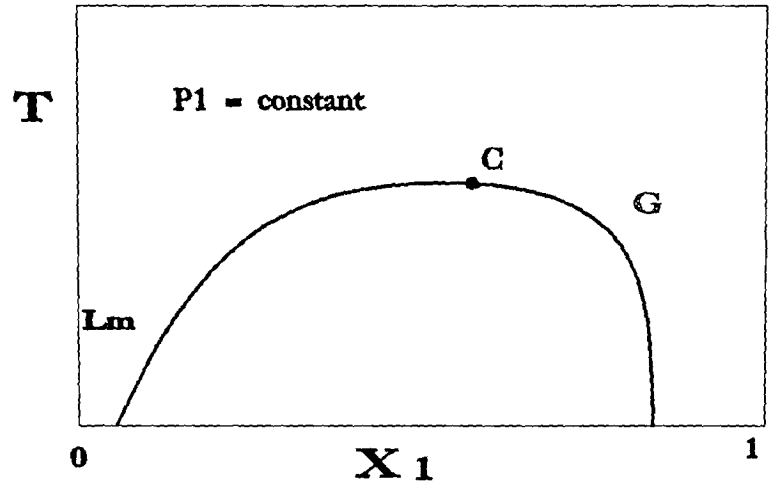

b. T(x) diagram at P > P(Cm).

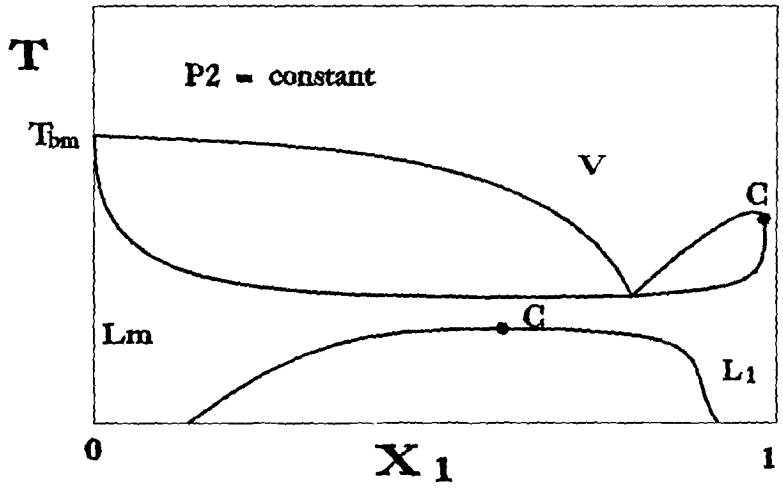

c. T(x) diagram at P(Cm)>P>P(C1).

Figure 1.5. Phase diagrams of the system heptane(1)/methanol(2).

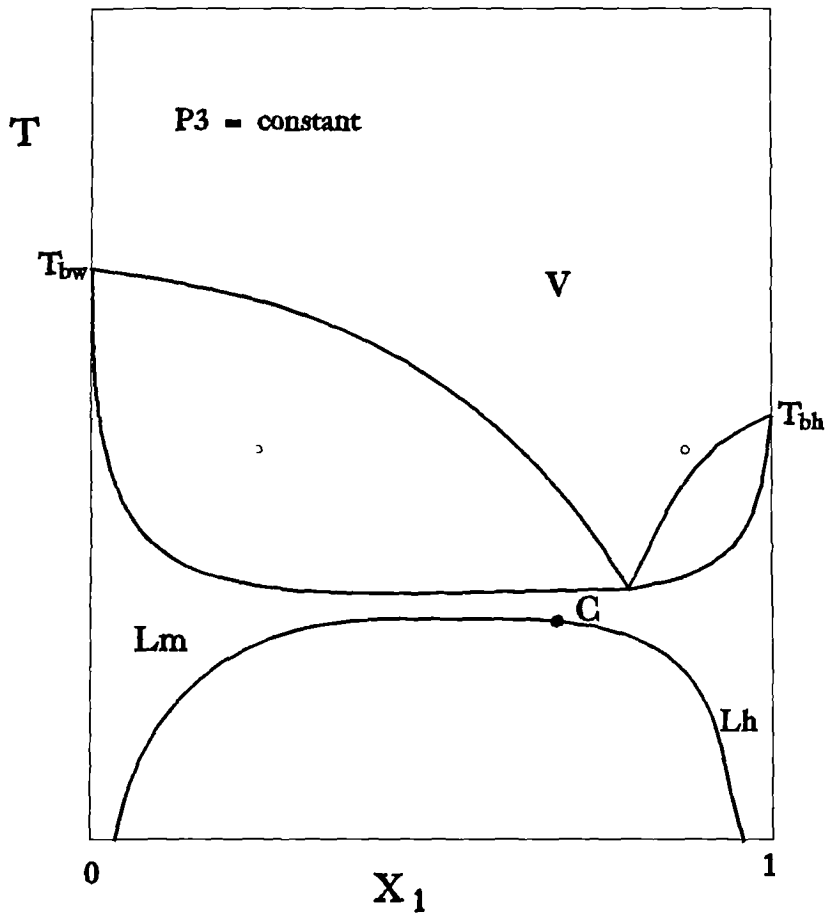

d. T(x) diagram at P(C1)>P>P(CEP)

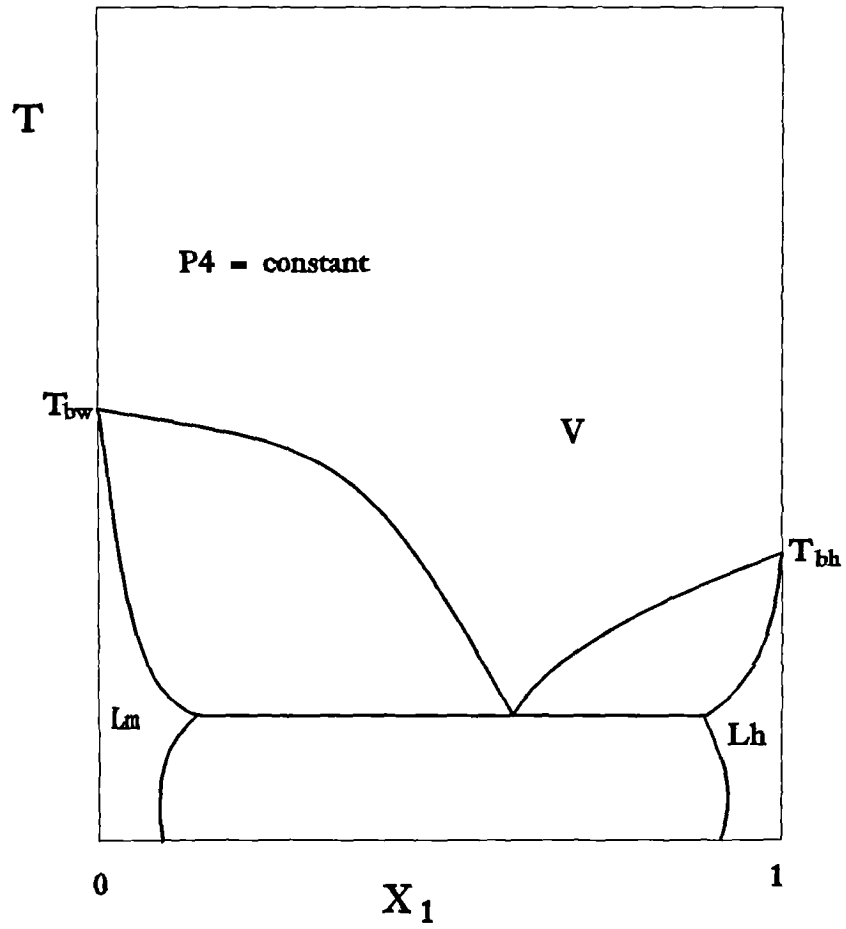

e. T(x) diagram at P < P(CEP)

Figure 1.5. Phase diagrams of the system heptane(1)/methanol(2).

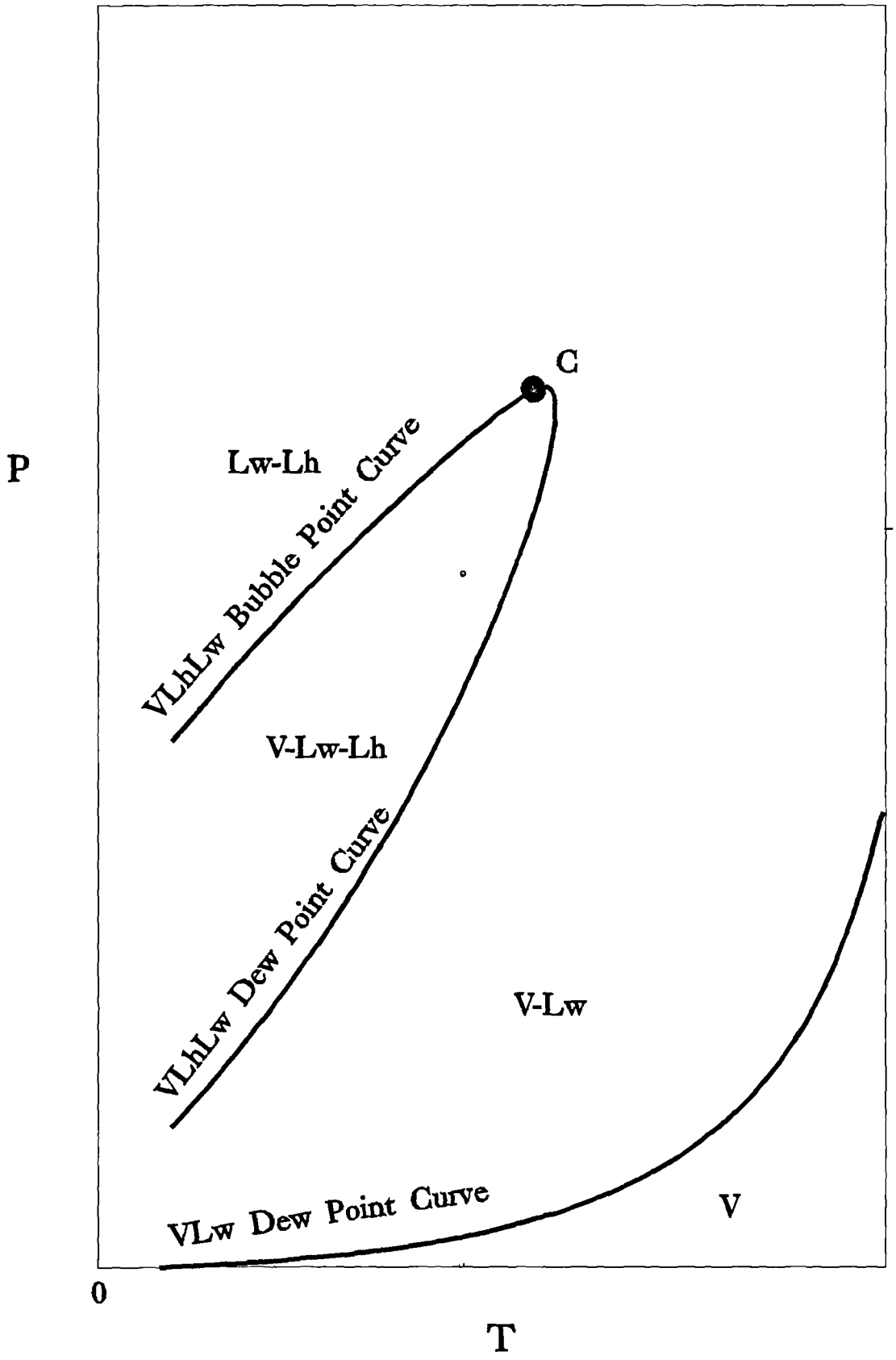

Figure 1.6. Phase diagram of a multicomponent system containing water.

1.3. Equations of state

Introduction

Equations of state (EoS), in contrast to fundamental equations, are mathematical relations between the pressure, temperature, volume and composition of a system. When such relations are combined with experimental knowledge of heat capacities they constitute fundamental equations and thermodynamic properties such as enthalpy, entropy, latent heat etc may be predicted. Classical thermodynamics provide certain rules and restrictions to the choice of an equation of state, but it can not supply the equation itself. This may be obtained by either of two approaches: An empirical approach, or from microscopic theories of intermolecular forces, such as statistical mechanics.

Formally equations of state may be distinguished in two categories: closed type analytical expressions of the type $f(P,v,T,\mathbf{x})=0$ and open ended series or virial equations where the compressibility factor is given as a power series of density at constant temperature. The latter, despite their fundamentally sound derivation from statistical mechanics are limited in application to the gas phase only and they are awkward in mathematical treatment. Most successful closed type equations of state are explicit in pressure, third degree polynomials of volume. The third degree is the least required to satisfy meaningfully the conditions of criticality and at the same time allow representation of liquid and vapour phases. An obvious advantage of cubic equations of state is that they are analytically solvable for volume when the pressure and temperature are known. The most celebrated of the these is the one developed by van der Waals more than one century ago. Despite their empirical nature, they have been applied equally well to gas and liquid phases at low or high pressures even in the near critical region.

Noncubic EoS with many parameters such as the Benedict-Webb-Rubin equation may be more successful in representing pure component data but they have been shown to be inferior when applied to real mixtures. In the following paragraphs a cubic equation of state is chosen to model all fluid phases. For mixtures, special empirical combining rules are developed and finally the model is validated by comparison with diverse experimental data and the advantages of the proposed approach are discussed.

Cubic Equations of State

Cubic EoS may be classified according to the number of constants appearing in the polynomial. The van der Waals(vdW) EoS contains two constants only: 'a' in the attractive term and 'b' for the repulsive term. These two constants may be calculated from the critical properties of the pure substance by application of the criticality conditions. The modified by Soave(1972) EoS of Redlich and Kwong(SRK) and the Peng-Robinson(PR) EoS, the latter probably being the most popular one in the petroleum industry, also contain two constants, which are correlated to the critical properties of the pure components and the accentric factor. The latter in turn relates to the vapour pressure of the pure substance. The significantly improved predictions of SRK over vdW is mainly attributed to the introduced allowance for temperature dependence of the attractive term. The popularity of PR EoS over SRK lies in the fact that the former is superior in predicting liquid densities. This has been achieved by an appropriate modification of the attractive term so that the produced constant value of the critical compressibility factor ζ_c is merely reduced to a more realistic value. For all substances vdW equation calculates ζ_c equal to 0.375, SRK 0.333 and PR 0.307, while for most fluids experimental critical compressibility factor Zc is close to 0.28.

Introduction of a third parameter in the equation of state relaxes the assumption of a fixed value for the critical compressibility factor and improves the prediction of volumetric properties. Peneloux et al(1982) introduced a third constant 'c' which translates the volume along its axis and it was so chosen that the EoS reproduces exactly the pure component saturated liquid volume at a reduced temperature equal to 0.7. This translation leaves the vapour-liquid equilibria calculations unaffected. For mixtures c is simply the mole fraction weighted sum of individual constants. Patel and Teja(1982) introduced a third parameter in the EoS in a such a way that the critical compressibility factor ζ_c may be chosen freely so that the EoS matches both the vapour pressure and the saturated liquid density data. For nonpolar fluids the third parameter may be evaluated from the critical properties and the accentric factor of the component through generalized correlations. It is shown that the optimum value of ζ_c is always larger than the experimental critical compressibility factor of the substance. The Patel and Teja EoS is a significant improvement on those of SRK and PR to which it reduces, if the constant ζ_c is made equal to 0.333 or

0.307 respectively. On the other hand, the third parameter has to be calculated by solution of a cubic equation and this is an added complexity not present in other EoS.

Valderrama(1990) presented a three parameter equation similar in form to PT EoS. Unlike PT however he uses the experimental critical compressibility factor Z_c as a generalizing parameter for the constants a_c, b and c and the product [accentric factor]x[critical compressibility factor] for the factor F in the Soave expression for $\alpha(T_r)$. In doing so he argues(Valderrama and Cisternas,1987) that the use of four substance dependent generalizing parameters(T_c, P_c, Z_c and ω) is needed for improved predictions of volumetric properties and vapour pressures of polar and nonpolar fluids. The Valderrama(1990) EoS has been extensively tested recently(Danesh et al, 1991) in complex reservoir fluids and it was found to be superior to other EoS in the prediction of volumetric properties without the use of adjustable parameters.

In this study we adopt the Valderrama(1990) EoS for the reasons outlined above. The definition of the equation is:

$$P = \frac{RT}{v-b} - \frac{a(T)}{v(v+b)+c(v-b)} \tag{1.1}$$

where

$$a = a_c a(T_r) \tag{1.2}$$

$$a_c = \Omega_a \frac{R^2 T_c^2}{P_c} \tag{1.3}$$

$$a(T_r) = [\, 1 + F(1 - \sqrt{T_r}) \,]^2 \tag{1.4}$$

$$b = \Omega_b \frac{RT_c}{P_c} \tag{1.5}$$

$$c = \Omega_c \frac{RT_c}{P_c} \tag{1.6}$$

$$\Omega_a = 0.66121 - 0.76105 \cdot Z_c \tag{1.7}$$

$$\Omega_b = 0.02207 - 0.20868 \cdot Z_c \tag{1.8}$$

$$\Omega_c = 0.57765 - 1.87080 \cdot Z_c \quad (1.9)$$

$$F = 0.46283 + 3.5823(\omega Z_c) + 8.19417(\omega Z_c)^2 \quad (1.10)$$

To further improve the accuracy of predictions of both the vapour pressure and the saturated volumes, for the polar components water and methanol the correlation for $a(T_r)$ of Valderrama is relaxed and a specific correlation is developed.

$$a(T_r) = \{ 1 + F[1 - (T_r)^{\Psi}] \}^2 \quad (1.11)$$

where for methanol F=0.76757, Ψ=0.67933 and for water F=0.72318, Ψ=0.52084. A temperature dependence of these parameters has not been considered necessary.

Mixing Rules

When an EoS is applied to mixtures, the parameters a, b, and c need to be calculated from the corresponding pure component parameters and the composition of the mixture. The rules governing the combination of pure component parameters and composition to derive mixture properties are termed mixing rules. Thermodynamics is again unable to supply such mixing rules and as a result mixing rules are developed empirically as suitable expressions for representing successfully a limited family of experimental data. A purely theoretical answer, however, stands for the virial coefficients: statistical mechanics show that the second, third etc virial coefficients are polynomials of second, third etc order in mole fraction correspondingly. For example, the second virial coefficient B(T,x) is given by:

$$B(T,\mathbf{x}) = \sum_i \sum_j x_i x_j B_{ij}(T) \quad (1.11)$$

where $B_{ij} = B_{ji}$. Cross virial coefficients B_{ij} may be calculated theoretically from statistical mechanics or they may be determined experimentally.

The second virial coefficient can be related to the vdW constants a and b. As v goes to infinity comparison of the virial and the vdW EoS shows that:

$$B = b - a/RT \quad (1.12)$$

For mixtures, direct comparison of (12) with (11) shows that:

$$a = \sum_i \sum_j x_i x_j a_{ij}(T) \tag{1.13}$$

$$b = \sum_i \sum_j x_i x_j b_{ij} \tag{1.14}$$

The cross parameters a_{ij} and b_{ij} are approximated by the following empirical relations, which are commonly referred to as the geometric mean and the hard sphere approximation:

$$a_{ij} = \sqrt{a_i a_j} \tag{1.15}$$

$$b_{ij} = \frac{bi+bj}{2} \tag{1.16}$$

Substitution of (16) into (14) leads to a much simpler expression:

$$b = \sum_i x_i b_i \tag{1.14a}$$

Equations (13) and (14a) constitute the classical mixing rules, originally proposed by van der Waals himself. A similar expression is chosen for the third parameter c:

$$c = \sum_i x_i c_i \tag{1.17}$$

A vast improvement in the predictions of the equation of state - particularly in cases of dissimilar components in complex reservoir fluids - can be achieved by empirically modifying (15):

$$a_{ij} = (1 - k_{ij})\sqrt{a_i a_j} \tag{1.15a}$$

where k_{ij} is the so called binary interaction parameter. By adjusting the value of k_{ij} any binary data of similarly behaving substances may be fitted. The real value of k_{ij} lies in the fact that ternary and higher order interactions are often comparatively small and it is beyond the accuracy of an EoS to account for them. Thus multicomponent systems can be represented from pure component and binary data only. Due to the lack of any theoretical significance, however, the numerical values of k_{ij} can not be generalized without significant loss of accuracy. Hydrocarbon-hydrocarbon binary interaction parameters are assumed to be equal to zero in this study. The nonzero numerical values for k_{ij}, that we

have obtained by an optimization process of binary data, are listed in Table 1. These are independent of temperature.

Summary

The most successful equations of state were briefly reviewed and a promising one was presented and has been chosen for further development. The presentation was restricted to nonpolar fluids. For polar-nonpolar interactions the mixing rules are strongly modified, as discussed in the next paragraph.

Table 1.1. Binary interaction parameters for the Valderrama(1990) EoS

Gas	CO2	N2	H2S
Methane	0.092	0.035	0.080
Ethane	0.134	0.038	0.095
Propane	0.128	0.070	0.088
i-Butane	0.126	0.134	0.050
n-Butane	0.138	0.114	0.050
n-Pentane	0.141	0.088	0.047
n-Hexane	0.118	0.150	0.047
n-Heptane	0.110	0.142	0.047
CO2	-	-0.036	0.088
Nitrogen	-	-	0.176

1.4. Mixing Rules for Asymmetric Systems

Introduction

Chemical potentials of individual components in asymmetric systems depend strongly on the identity of particular substances. This means that an interchange of indices in the mole fractions of an asymmetric system results in irrelevant changes in corresponding chemical potentials. Asymmetry in mixtures of molecules arises when unlike molecular interactions are substantially different from interactions between molecules of the same kind and it is the result of significant differences in size or shape or polarity of molecules. The last factor is by far the most important. It is clear that mixtures of polar substances are not necessarily asymmetric, if they are not substantially different in any of the above qualities. Also, the asymmetric character of a mixture becomes more pronounced as differences in these qualities increase. For example, the mixture methanol-methane is much more asymmetric in character than the system carbon dioxide-propanol while methanol-water is not considered asymmetric.

Cubic equations of state with mixing rules quadratic in mole fraction, as presented above, provide an efficient description of the behaviour of reservoir hydrocarbon fluids and have been successfully applied at all conditions of engineering interest including the critical and the retrograde region. However the same scheme is not applicable to asymmetric polar-nonpolar liquid mixtures. Traditionally, such liquids have been modelled by application of the so called activity coefficient models. In these models the excess chemical potential of any component(that is the difference between the chemical potential in the actual solution and that it would have in an ideal solution having the same composition) is given by a semiempirical function of temperature and composition. Popular activity models such as the Wilson equation, the UNIQUAC equation, the NRTL equation and others have demonstrated extreme flexibility in fitting binary data of highly asymmetric liquid mixtures. The fitting quality, however, is a necessary - but not an efficient - criterion for the validation of the theoretical background and more likely than not activity models are simply mathematical equations flexible enough to fit certain data. As such, activity models do have major shortcomings: they are not applicable for a vapour phase and thus another model is usually required for equilibria calculations, they are not reliable at higher pressures, they have difficulties in incorporating supercritical components and finally they may not be reliable for multicomponent systems.

In the past decade, the approach of most researchers to modelling of asymmetric mixtures, as it is evidenced by the number of publications on the subject, has been the appropriate modification of the mixing rules of cubic EoS in an apparent effort to increase mathematical flexibility. Most proposals originate from either of two sources: activity coefficient models and density dependence of the attractive term. Clearly, such modifications are empirical - or, at best, semiempirical - in nature. A third approach to the problem comes from the association models, where polymerization reactions of components are taken into account. Though there are few recent publications(Wenzel and Krop,1990; Elliot et al,1990; Peschel and Wenzel,1984) indicating success in fitting binary data(that is, with one polar fluid), association models are not discussed any further here, simply because they are impractical for real systems. In the following the most important recent developments on the choice of mixing rules for asymmetric systems, are briefly reviewed, followed by a presentation of our proposal.

Coupled EoS/Activity models

The first attempt was reported by Huron and Vidal(1979). For the relationship between mixing rules in the RK EoS and excess free energy models they derived

$$a/b = \sum_i x_i a_i/b_i - G^E_\infty/\lambda \qquad (1.18)$$

by taking the infinite pressure limit of the excess Gibbs free energy in the RK EoS where v=b. The expression for the excess free energy at infinite dilution G^E_∞ was taken from the NRTL equation. The factor λ is characteristic of the EoS used. For the RK EoS it is equal to ln2. Other EoS would lead to different factors. The values of the parameters of the excess Gibbs energy at infinite dilution in the above model have to be determined by fitting the EoS to experimental data. This is because already tabulated values of parameters were obtained at low pressures, while this model requires parameters at an infinite pressure. The model includes three temperature dependent parameters per binary but despite excellent results at high densities it was shown (Whiting and Prausnitz,1982) to be inconsistent and invalid at low densities.

Attempts to correct the deficiencies of the Huron-Vidal model were reported by Mollerup(1981) and Whiting and Prausnitz(1982). Both utilise the concept of density-dependent local composition mixing rules(DDLC) where the constants of the EoS depend not only on composition and temperature but on density as well - except for pure components. The final equations are extremely complicated and are not reproduced here. Since the correlation of Mollerup(1981) was shown to fail even with relatively simple systems such as methane-decane, different and significantly improved density-dependent mixing rules were presented by the same author(Mollerup,1983) under the name random-nonrandom-mixture equation. In the new equation a nonquadratic correction term is added to the classical mixing rules for the attractive term to account for asymmetric interactions. The mixing rule utilises two symmetric temperature dependent binary interaction parameters. The scheme originally was based on the SRK EoS and the NRTL model. All necessary equations are listed in the original publication. A three parameter version of the same model has been utilised by Mollerup(1985) to correlate ternary water-methanol-hydrocarbon gas solubilities. Again all parameters were symmetric and temperature dependent. Similarly, Mathias and Copeman(1983), utilize the UNIQUAC equation to arrive at their DDLC PR EoS. In this model three parameters were employed, where the two appearing in the LC part were temperature dependent. Good results were reported for the Liquid-Liquid equilibria of a few methanol-hydrocarbon and water-hydrocarbon binary systems. A truncated version with three temperature independent parameters was also presented. However according to Mollerup(1985) his model consumes only 20% of the computational time required by the Mathias and Copeman(1983) model and either of them consumes a lot more than the EoS with conventional mixing rules. This is attributed to excessive calculations(summations of mole fraction products) required to solve a non-cubic EoS for the molar volume of the mixture.

A new effort on coupling cubic EoS-activity models has been attempted by Michelsen(1990a, b) on the basis of an earlier idea of Mollerup(1986), that is instead of matching EoS and activity models at infinite pressure(Huron and Vidal, 1979), the matching is effected using a zero reference pressure. The obvious benefit of the new procedure lies in the fact that the parameters of the excess Gibbs energy model need not be recalculated but instead the already regressed and tabulated ones are directly incorporated into the mixing rules. The

resultant mixing rules are quite similar to those originally proposed by Huron and Vidal and are not density-dependent. The full details of equations and procedures are given by Dahl and Michelsen(1990), who also report results for the coupling of RK EoS with UNIFAC and these results might have been considered satisfactory if the binary systems chosen for application were really asymmetric and not just polar mixtures.

Density dependent mixing rules

A breakthrough in the modelling of asymmetric systems with a cubic EoS came from Luedecke and Prausnitz(1985), who abandoned the effort to couple EoS-activity models and instead they introduced density-dependent mixing rules in an empirical, phenomenological manner. Their model is simple and yet has as many as three binary interaction parameters any of which can be made temperature dependent for additional flexibility. At low density the mixing rule for 'a' reduces to the classical quadratic one, thus satisfying the second virial coefficient restriction. The original equation is:

$$a=\sum_i\sum_j x_i x_j (a_i a_j)^{1/2}(1 - k_{ij})+(\rho/RT)\sum_i\sum_j x_i x_j (x_i c_{ij}+x_j c_{ji}) \qquad (1.19)$$

where ρ is the density, k_{ij} is the conventional binary interaction parameter and c_{ij} is the new added binary parameters. The authors assumed that c_{ij} is not equal to c_{ji} . Their results for water-hydrocarbon binaries away from the critical region are considered very good. Serious discrepancies were recognized, however, in the LL equilibria predictions of ternary asymmetric systems and the authors relate this problem to the inability of their model to predict correctly the critical points of binary systems.

Dimitrelis and Prausnitz(1990) presented a new mixing rule, which can be seen as a modification of that of Luedecke and Prausnitz(1985). First, the classical mixing rules and the non-conventional mixing rules were connected by an interpolation function ranging from 0(at low densities) to 1(at high densities). Second, one of the three binary interaction parameters was made temperature dependent. Their results, despite the added sophistication, do not seem to be significantly better than those of Luedecke and Prausnitz(1985) and more importantly the same shortcomings as before have been observed.

It should be noted that when density dependent mixing rules are incorporated into a cubic EoS, the EoS is not strictly cubic and can no longer be solved by analytical methods. Instead a numerical procedure has to be adopted, thus rendering the model computationally more expensive. The subject is discussed in some detail by Topliss et al(1988).

Simple asymmetric mixing rules

A new purely empirical approach to the problem of modelling asymmetric mixtures was presented by Panagiotopoulos and Reid(1986a). These authors relax the assumption $k_{ij}=k_{ji}$ and this way they introduce a second parameter per binary. Their proposal is:

$$a_{ij} = (a_i a_j)^{1/2}[1 - k_{ij} + (k_{ij} - k_{ji})x_i] \qquad (1.20)$$

Equation (20) has the following characteristics: if $k_{ij}=k_{ji}$, the classical mixing rules are recovered. If x_i approaches unity the effective interaction parameter reduces to k_{ji}. If x_i approaches zero the effective interaction parameter reduces to k_{ij}. Application of this mixing rule for the calculation of the mixture parameter a results in cubic dependence on the mole fraction. Equivalent empirical mixing rules have been proposed independently by Kabadi and Danner(1985) and Stryjek and Vera(1986). Neither of these mixing rules reduces to the theoretically correct quadratic dependence on mole fractions at low density, since they all are density independent. Panagiotopoulos and Reid(1986b) have also compared their mixing rule eqn (20) with density-dependent mixing rules similar to those of Luedecke and Prausnitz(1985) for the ternary system water-butanol-carbon dioxide. As they report, these mixing rules are approximately equivalent in correlating phase equilibria at high and low pressures. The important difference, of course, is the computational superiority of the non-density dependent mixing rule, eqn(20). It is noted, however, that the chosen system does not have a pronounced asymmetric character.

Proposed mixing rules for mixtures of hydrocarbons with water and methanol

In the choice of an appropriate model for multicomponent-multiphase equilibria of highly asymmetric real systems at high pressures, one has first to exclude activity models for their many limitations as mentioned above. On the other hand, EoS/activity coefficient coupled models have been recognised to be computationally expensive. In addition they do not seem to be of any real

advantage(from the published fitting of binary data) over the much simpler semiempirical alternative of Luedecke and Prausnitz(1985) and those similar to it. Still further, the latter have not been recognized to be generally superior in representing complex mixtures over the purely empirical nondensity-dependent form presented by Panagiotopoulos and Reid(1986a) and the similar. In summary, for all these methods, which modify only the attractive term a of the classical mixing rules, it appears that increased complexity of the model does not result in improved predictions.

For our purposes, we develop two mixing rules, one density dependent and one nondensity-dependent, on the basis of our conclusion from the above review. The new mixing rules are incorporated in the Valderrama EoS and the EoS is extensively tested by application in difficult, highly asymmetric systems.

DEVELOPMENT OF NONDENSITY-DEPENDENT MIXING RULES

The attractive term a of the equation of state is separated into two parts:

$$a=a^C + a^A \tag{1.21}$$

where a^C is given by the classic quadratic mixing rules

$$a^C = \sum_i \sum_j x_i x_j (a_i a_j)^{1/2}(1-k_{ij}) \tag{1.22}$$

The term a^A accounts for asymmetric interactions and should vanish when the system approaches ideal behaviour, i.e. at high temperatures. It should also vanish when symmetric interactions become dominant, i.e. when the concentration of the polar component tends to zero or when the concentration of non-polars in a polar-rich phase tend to zero. For thermodynamic consistency the term a^A should be independent of pressure. The simplest possible mixing rule which satisfies our requirements is

$$a^A = \sum_p x_p^2 \sum_1 x_i a_{pi} l_{pi} \tag{1.23}$$

where p is the index of polar components, $a_{pi}=(a_p a_i)^{1/2}$ and l_{pi} is a binary interaction parameter. In accordance with our requirements, this binary parameter should be expected to be a *decreasing* function of temperature:

$$l_{pi} = l_{pi}^{\circ} - l_{pi}^{1} (T-T_o) \tag{1.24}$$

where l_{pi}° and l_{pi}^{1} are positive dimensionless constants and T_o is the ice point in K. Should our arguments be correct, it is further expected that these constants will increase with asymmetry in binary systems and will be close to zero for nearly symmetric systems. These parameters have been obtained by forcing agreement of the model to binary data reported in the open literature. A listing of the obtained binary interaction parameters is given in Table 2.

Equation (1) can be rewritten in cubic form as:

$$Z^3 + (C-1)Z^2 + [A-C-B(B+2C+1)]Z + B(BC+C-A) = 0 \qquad (1.25)$$

where Z is the compressibility factor of the mixture. Other symbols are defined below:

$$A = \frac{aP}{(RT)^2} \qquad (1.25a)$$

$$B = \frac{bP}{RT} \qquad (1.25b)$$

$$C = \frac{cP}{RT} \qquad (1.25c)$$

Fugacity coefficients may be calculated from the following expression, the derivation of which is detailed, as an example, in Appendix A.

$$\ln\phi_i = -\ln(Z-B) + \frac{B_i}{Z-B} - \frac{\ln\frac{Q+D}{Q-D}}{D}\sum_j y_j A_{ij}(1-k_{ij}) + \frac{A(B_i+C_i)}{2(Q^2-D^2)}$$
$$+ \frac{A}{8D^3}\left[\ln\frac{Q+D}{Q-D} - \frac{2QD}{Q^2-D^2}\right][C_i(3B+C) + B_i(3C+B)]$$
$$- \frac{\ln\frac{Q+D}{Q-D}}{D}\left[y_i\sum_j y_j A_{ij}l_{ij} + \frac{1}{2}\sum_i\sum_j y_i^2 A_{ij}l_{ij} - \frac{1}{2}\sum_i\sum_j y_i^2 y_j A_{ij}l_{ij}\right] \qquad (1.26)$$

It is noted that the last term is nonzero only if component i is a polar. The rest of the capital symbols have the following meaning:

$$A_{ij} = \frac{\sqrt{a_i a_j}P}{(RT)^2} \qquad (1.26a)$$

Table 1.2. Interaction parameters of methanol and water binaries for nondensity-dependent mixing rules

	Methanol(2)			Water(2)		
Component(1)	k	l_{21}^{o}	$l_{21}^{1}x10^{4}$	k	l_{21}^{o}	$l_{21}^{1}x10^{4}$
Methane	0.2538	0.7319	6.88	0.5028	1.8180	49.00
Ethane	0.0137	0.0519	21.70	0.4974	1.4870	45.40
Propane	0.0278	0.0779	0.00	0.5465	1.6070	39.30
i-Butane	0.1233	0.3209	17.60	0.5863	1.7863	37.40
n-Butane	0.1465	0.2917	0.00	0.5800	1.6885	33.57
n-Pentane	0.2528	0.7908	58.28	0.5525	1.6188	23.72
n-Hexane	0.2245	0.5607	17.54	0.4577	1.5730	31.41
n-Heptane	0.1461	0.4592	27.17	0.4165	1.5201	35.21
n-Octane	0.1403	0.5331	36.91	0.3901	1.5200	35.31
Xenon	-	-	-	0.2374	0.8870	47.50
Carbon dioxide	0.0510	0.0700	11.56	0.1965	0.7232	23.74
Nitrogen	0.2484	1.0440	7.22	0.4792	2.6575	64.46
Hydrogen sulfide	0.0694	0.1133	0.00	0.1382	0.3809	13.24
Methanol	0.0000	0.0000	0.00	-0.0789	0.0835	0.00
Water	-0.0789	-0.0149	0.00	0.0000	0.0000	0.00

$$Q = Z + \frac{(B+C)^2}{4} \tag{1.26b}$$

$$D = \sqrt{BC + \frac{(B+C)^2}{4}} \tag{1.26c}$$

Expressions for B_i and C_i are similar to eqn (25c).

DEVELOPMENT OF DENSITY-DEPENDENT MIXING RULES

A density-dependent term a^A of mixing rules for asymmetric systems should satisfy the boundary conditions put forward above and in addition it should tend to zero as the molar volume of the mixture tends to infinity. Accordingly, the simplest possible formulation may be directly derived from eqn(23):

$$a^A = \frac{1}{RTv}\sum_p x_p^2 a_p \sum_i x_i a_{pi} l_{pi} \qquad (1.27)$$

where v is the molar volume of the mixture. Other symbols have the same meaning as before. The introduction of a_p in the product was necessary to dimensionally rationalize the expression. Binary interaction parameters for the density dependent mixing rules are listed in Table 3. The following expression is obtained for fugacity coefficients:

$$\ln\phi_i = -\ln(Z-B) + \frac{B_i}{Z-B} + \frac{\ln\frac{Q-D}{Q+D}}{D}\sum_j y_j A_{ij}(1-k_{ij}) + \frac{A^C(B_i+C_i)}{2(Q^2-D^2)}$$

$$- \frac{A^C}{8D^3}\left[\ln\frac{Q-D}{Q+D} + \frac{2QD}{Q^2-D^2}\right][C_i(3B+C) + B_i(3C+B)]$$

$$+ \frac{A^A(B_i+C_i)}{4D^3}\left[\ln\frac{Q-D}{Q+D} + \frac{2QD}{Q^2-D^2}\right]$$

$$+ \frac{\ln\frac{Q^2-D^2}{Z^2} + \frac{B+C}{2D}\ln\frac{Q-D}{Q+D}}{2BC}\left[2y_i A_i \sum_j y_j A_{ij} l_{ij} + \sum_p y_p^2 A_{pi} A_p l_{pi}\right]$$

$$- \frac{A^A(BC_i+CB_i)}{2BC}\left[\frac{\ln\frac{Q^2-D^2}{Z^2}}{BC} + \frac{2D^2 + (B+C)Q}{2(Q^2-D^2)D^2} + (B+C)\ln\frac{Q-D}{Q+D}\left(\frac{1}{2BCD} + \frac{1}{4D^3}\right)\right]$$

(1.28)

Table 1.3. Binary interaction parameters of methanol and water for density-dependent mixing rules °

	Methanol(2)			Water(2)		
Component(1)	k	l_{21} °	$l_{21}{}^{1}$x10^4	k	l_{21} °	$l_{21}{}^{1}$x10^4
Methane	0.2460	0.0806	-6.50	0.5028	0.1756	-3.420
Ethane	0.0127	0.0064	2.914	0.4786	0.1373	-2.900
Propane	0.0166[1]	0.0068	-1.202	0.5465	0.1522	-4.440
i-Butane	0.1189	0.0386	0.000	0.5863	0.1690	-5.750
n-Butane	0.1028	0.0259	-1.661	0.5641	0.1580	-5.100
n-Pentane	0.1982	0.1294	12.34	0.5384	0.1429	-7.160
n-Hexane	0.1745	0.0674	1.000	0.4595	0.1498	-5.010
n-Heptane	0.1069	0.0713	3.769	0.4452	0.1492	-4.850
n-Octane	0.1144	0.2024	18.59	0.4437	0.1543	-5.200
Xenon	-	-	-	0.7868	0.1880	-5.640
Carbon dioxide	0.0551	0.0092	1.070	0.1948	0.0722	-0.750
Nitrogen	0.2374	0.1217	-6.833	0.4792	0.2531	-6.780
Hydrogen sulfide	0.0699	0.0130	-0.4727	0.1354	0.0386	0.000
Methanol	0.0000	0.0000	0.0000	-0.0647	0.0069	0.000
Water	-0.0647	0.0037	0.0000	0.0000	0.0000	0.000

[1]For propane k_{ij} is also temperature dependent: k_{pw}=0.0166+0.001013(T-T_O).

For density-dependent mixing rules, the binary interaction parameter l_{ij} does not depend on temperature in a consistent way, because of interference from the multiplication factor 1/RTv, which is also a function of temperature.

REGRESSION OF BINARY PARAMETERS

All binary interaction parameters have been obtained simultaneously, by forcing appropriate models to fit experimental binary data. Original sources of experimental data for binary mixtures of water and methanol with other components are given in Tables 4 and 5 respectively. References are listed at the end of the Chapter. In the regression, experimental data in the near critical region were excluded because the mixing rules and/or the equation of state are not considered adequate in this region-which anyway is not to our immediate interest-and large deviations are observed. Data at very low temperatures(below about 240 K) were also excluded, because it is understood that the linear dependence of the binary parameter 'l' on temperature is only an approximation; if coverage of the full temperature range were desired, a more complicated function would be more appropriate. Finally, experimental data showing significant deviation from mainstream trends were also not considered. Such deviations were very common reflecting severe experimental difficulties in determining the very small quantity which represents the solubility of a polar substance in a nonpolar-rich phase or the opposite. Another difficulty, particular to methanol-hydrocarbon systems, arises from the fact that very small quantities of water in methanol may change drastically the solubility of hydrocarbons in methanol. Unless extreme care was taken by the experimentalist to dry methanol and avoid subsequent condensation of water, the solubility data would be wrong and misleading. For the above reasons the number of data points utilised is limited and is given for every binary system in Table 6.

In fitting the data all experimental values reported by the experimentalist were considered and the square root of the sum of the squares of relative deviations of predictions were minimised by application of the simplex method of Nelder and Mead(1965). Predictions for three-phase data were generated from three-phase bubble point calculations. For two-phase data flash calculations were the preferred method for predicting of equilibrium phase compositions, because it is faster and more stable than the corresponding bubble point calculation, which is important at least initially when the values of the parameters are completely unknown. Respective phase equilibrium algorithms are detailed in the next paragraph. Specific weights were not attributed to data points.

An indication of the performance of either mixing rule may be directly estimated from the quality of fitting the binary data used in the regression of the

parameters. For both models the same data and the same numerical algorithms have been used. The results are summarized in Table 6. It is noted that density-dependent mixing rules consistently perform slightly better with water binaries but the results for methanol are mixed. As a visualization example, figure 7 compares predictions with the experimental data of Kobayashi and Katz(1953) for the three phase VLL equilibria of the system propane-water. It is noted that predictions from both mixing rules are identical for the hydrocarbon-rich vapour and liquid phases, while density-dependent mixing rules are slightly better in the water rich phase.

Table 1.4. Sources of vapour-liquid equilibrium data of water-hydrocarbon mixtures

Component	Reference
Methane	1,5,9,14,15,16,17,21,22,29,34,35,36,40,49,53,54
Ethane	1,6,7,15,16,25,40,47,53
Propane	1,2,8,10,15,16,23,30,42
i-Butane	15,16
n-Butane	7,12,15,16,17,26,27
n-Pentane	15,16,18,19,24,49
n-Hexane	4,11,13,15,16,19,24,28,39,51
n-Heptane	15,16,19,24,31,48,56
n-Octane	15,16,19,24
CO2	20,33,37,38,44,45,46,47,49,50
N2	3,14,21,29,43
H2S	32,49

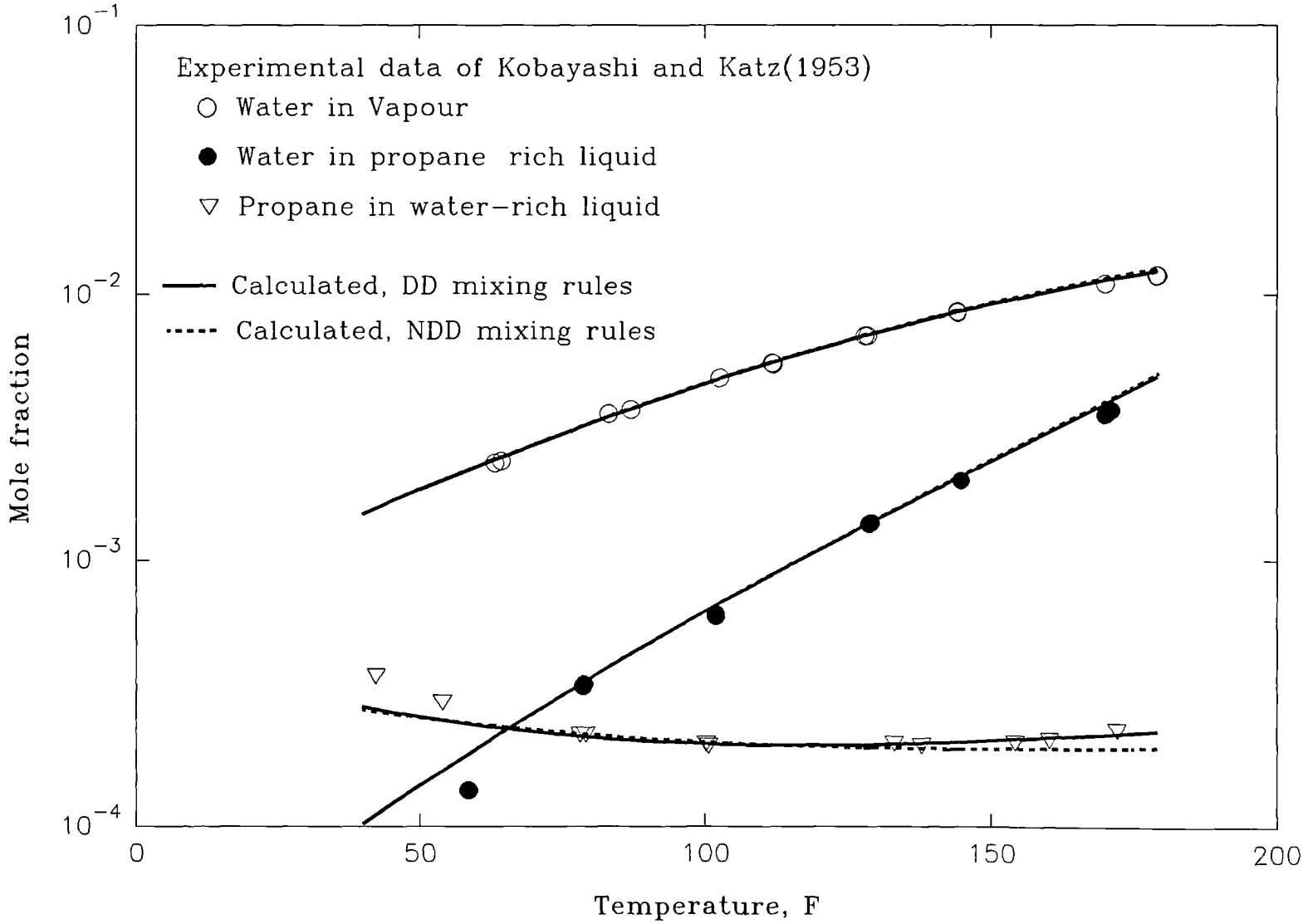

Figure 1.7. Phase compositions of the propane–water system at the three–phase VLL equilibria.

Table 1.5. Sources of vapour-liquid equilibrium data of methanol-hydrocarbon mixtures

Component	Reference
Methane	4,5,13,16,19,40,42,47
Ethane	16,27,32,45,46,47
Propane	14,23,29,47
i-Butane	23
n-Butane	10,23,28,30
n-Pentane	6,22,41
n-Hexane	2,7,11,12,17,20,22,34
n-Heptane	1,8,22,33
n-Octane	8,22,33
CO2	3,4,5,9,16,18,26,31,35,36,37,39,43,44,47
N2	4,5,15,16,21,24,25,26,40,44,46
H2S	38,43

PHYSICAL SIGNIFICANCE OF PARAMETER l

The second binary interaction parameter l_{ij} ,which was introduced empirically on the basis of the required behaviour of the model, does have some physical significance: If i is a polar substance, then l_{ij} reflects the effect on the attraction energy when an infinitesimal quantity of substance j is added to pure i to form an infinitely dilute solution. Since addition of a nonpolar in a polar substance always results in an increase of the potential energy of the solution the parameter l_{ij} is always positive. However, when a polar is added to another polar, the potential energy may be reduced due to chemical association of dissimilar molecules. In this case l_{ij} should be negative. Nondensity-dependent mixing

rules predict such a decrease in potential energy when water is added to methanol while for the inverse an increase is predicted.

Table 1.6. Comparison of quality of fitting(AAD%) of binary data by density and nondensity-dependent mixing rules with the Valderrama EoS.

Component	Methanol			Water		
	DD	NDD	#Points	DD	NDD	#Points
Methane	11.19	11.46	80	2.54	3.80	98
Ethane	12.73	11.35	66	4.26	5.41	59
Propane	6.76	6.75	40	2.35	3.34	32
i-Butane	2.36	0.76	5	1.52	2.25	9
n-Butane	11.77	9.40	16	6.38	10.31	58
n-Pentane	15.22	12.32	16	14.26	15.62	23
n-Hexane	15.40	9.48	93	15.71	17.19	26
n-Heptane	6.84	4.73	26	10.00	11.64	6
n-Octane	6.56	4.14	17	17.00	27.11	5
Carbon dioxide	5.76	5.51	184	4.54	4.88	73
Nitrogen	5.00	5.42	96	1.07	1.22	28
Hydrogen sulfide	4.73	4.30	24	5.77	4.39	50

Assuming $l_{ij}>0$ for a binary system, first and second order differentiation of eqn (22) with respect to the mole fraction of the polar component, reveals that the term a^A shows a maximum at $x_p=2/3$ and a minimum(zero) at $x_p=0$. As a consequence, for the addition of an infinitesimal quantity of a polar in a hydrocarbon-rich gas or liquid phase, the term a^A contributes positively to the

potential energy. Such a prediction corresponds to a reasonable physical situation. Mixing rules with more parameters show, in general, a minimum for the term a^A at $x_p>0$, thus predicting an initial negative contribution of the term a^A to the potential energy of the mixture with addition of the polar, which at higher concentrations(above the minimum) turns to a drastic increase.

Summary

The various approaches for modelling phase equilibria of asymmetric systems were reviewed and the governing ideas have been clearly stated. Next, these ideas were applied to derive simple models, which preserve any power of the more complex models reported in the literature and yet allow for efficient and fast computations.

1.5. Vapour-Liquid Equilibria Calculations

In the following it is assumed that the number and the identity of the equilibrium phases is known. For VLE calculations this is usually the case. The methods detailed in this paragraph will be extended to include the problem of the identity of the present phases in Chapter V.

Thermodynamic description of the phase equilibrium problem

The phase equilibrium problem is divided in two cases: the flash problem and the phase boundary problem. For a specified reservoir fluid at a fixed temperature the typical flash problem requires knowledge of the composition of all co-existing phases given the equilibrium pressure. For the same fluid , the typical phase boundary problem requires knowledge of the pressure where a phase just appears or disappears. In either case, the thermodynamic equivalent requires uniformity of the chemical potential of each component throughout the system. Analytical expressions for the dependence of the chemical potential on temperature, pressure and composition are available from the equation of state and we may write:

$$\mu_{i1} =... = \mu_{ij} =...= \mu_{i\pi}\ ,\ i=1,...,c \qquad (1.29)$$

where μ_{ij} is the chemical potential of component i in phase j, c the number of components and π the number of phases. In the most general case (i.e. when all components are present in all phases) these $c(\pi-1)$ such equations constitute the

thermodynamic diffusional stability requirement. In addition, material balance imposes another set of (c+π) equations:

$$z_i = \sum_{j}^{\pi} F_j x_{ij} \tag{1.30}$$

for every component i, and

$$\sum_{i}^{c} x_{ij} = 1 \tag{1.31}$$

for every phase j, where z_i is the specified(known and given) mole fraction of component i in the feed, F_j is the fraction in number of moles of phase j and x_{ij} is the mole fraction of component i in phase j. Totally there are π(c+1) equations with an equal number of unknowns, which may be chosen to be either (x_{ij}, F_j) at specified temperature T and pressure P or (x_{ij}, $F_{j\neq r}$, P) at specified T with $F_r = 0$. The first is the typical isothermal flash problem and the second the general phase boundary problem. In practice, instead of chemical potentials, fugacities are used in an equivalent manner and the set of nonlinear equations is solved by application of numerical methods as described below.

The same algorithms, with only slight modifications, will be used for flash and phase boundary problems. It is emphasized, however, that there is one fundamental difference between the two cases of phase equilibria calculations, and that is there is always a mathematical solution of the flash problem, sometimes even if the wrong phases were assumed present. It is not so for the general phase boundary problem, where there may be one solution or multiple solutions or even no solution at all. The Newton-Raphson and the Successive substitutions algorithms will be used to solve either of these phase equilibrium problems.

The Newton-Raphson multiphase equilibrium algorithm

It is necessary to assign one of the coexisting phases as the reference phase, which then is designated the indice 1. Though any present phase can serve as such, the vapour phase will be chosen whenever it is present. The system of nonlinear equations to be solved is formally defined by:

$$\mathbf{G}(\Psi) = 0 \tag{1.32}$$

where **G** is the vector of the $\pi(c+1)$ equations. These are defined below:

$$G_i = z_i - \sum_j^{\pi} F_j x_{ij} \tag{1.32a}$$

$$G_{c+1} = 1 - \sum_i^{c} x_{ij} \tag{1.32b}$$

$$G_{(m-1)(c+1)+i} = \ln\frac{f_{i1}}{f_{im}},\ m = 2,..,\pi \tag{1.32c}$$

$$G_{m(c+1)} = P - \sum_i^{c} \frac{f_{i1}}{\phi_{im}},\ m = 2,..,\pi \tag{1.32d}$$

where f_{im} and ϕ_{im} are respectively the fugacity and fugacity coefficient of component i in phase m. The vector of the unknowns Ψ is defined by:

$$\Psi = \Psi(x_1, F_1, x_2, F_2, ..., x_\pi, F_\pi)^T \tag{1.32e}$$

where $\mathbf{x}_j$ is the vector of the mole fractions composing phase j. This choice of the vector of functions and the vector of unknowns has an immediate advantage: it allows these vectors to expand or contract to accommodate more or less phases simply by assigning to π the exact number of present phases. This property of the matrices will be further exploited in Chapter V.

The Newton-Raphson method is based on a linear approximation of $\mathbf{G}^{t+1}$, where t is the iteration level, from the t-th iterate Ψ^t:

$$\mathbf{G}(\Psi^{t+1}) = \mathbf{G}(\Psi^t + \Delta^t) = \mathbf{G}(\Psi^t) + \lambda \mathbf{J}^t \Delta^t = 0 \tag{1.33}$$

where λ is a step limiting scalar and $\mathbf{J}^t$ is the Jacobian matrix of **G** at Ψ^t, defined by:

$$\mathbf{J}^t = \left[\frac{\vartheta \mathbf{G}}{\vartheta \Psi}\right]^t \tag{1.34}$$

Matrix eqn (33) can be solved for the unknown vector Δ^t by a number of methods. In our implementation we use the LU decomposition, which does not

require calculation of the inverse matrix. The Newton-Raphson algorithm is quadratically convergent if Ψ^t is close to the solution. Otherwise, convergence is not guaranteed. Convergence is considered achieved when the Euclidian norm of **G** , denoted as ||G||, becomes less than a tolerance $e=10^{-8}$.

If at any level of iteration, higher than the second, the algorithm starts diverging, as evidenced by an increase of the euclidian norm of **G**

$$||G(\Psi^{t+1})|| > ||G(\Psi^t)|| \tag{1.35}$$

then $G(\Psi^{t+1})$ is recalculated with λ halved until the euclidian norm of $G(\Psi^{t+1})$ improves. The technique is based on the concept that often the Newton-Raphson calculates better values for the slopes than for the values of the differences. Anyway, this procedure is not meaningful when λ becomes less than 0.01 and it is stopped.

The derivatives comprising the Jacobian matrix, eqn (34), can be calculated analytically. The respective formulas are given below.

$$\frac{\vartheta G_l}{\vartheta \Psi_{(j-1)(c+1)+i}} = \frac{\vartheta G_l}{\vartheta x_{ij}} = -\Psi_{j(c+1)}\delta_{li} = -F_j\delta_{li}\ ,\ l,i = 1,...,c \text{ and } j=1,...,\pi \tag{1.36}$$

where δ_{li} is the Kronecker delta.

$$\frac{\vartheta G_l}{\vartheta \Psi_{j(c+1)}} = \frac{\vartheta G_l}{\vartheta F_j} = -\Psi_{(j-1)(c+1)+l} = -x_{lj} \tag{1.37}$$

$$\frac{\vartheta G_{c+1}}{\vartheta \Psi_{(j-1)(c+1)+i}} = \frac{\vartheta G_l}{\vartheta x_{ij}} = -\delta_{j1} \tag{1.38}$$

$$\frac{\vartheta G_{c+1}}{\vartheta \Psi_{j(c+1)}} = \frac{\vartheta G_{c+1}}{\vartheta F_j} = 0 \tag{1.39}$$

$$\frac{\vartheta G_{(m-1)(c+1)+l}}{\vartheta \Psi_i} = \frac{\vartheta G_{(m-1)(c+1)+l}}{\vartheta x_{i1}} = \frac{1}{f_{l1}}\frac{\vartheta f_{l1}}{\vartheta x_{i1}}\ ,\ m=2,...,\pi \tag{1.40}$$

$$\frac{\vartheta G_{(m-1)(c+1)+l}}{\vartheta \Psi_{(m-1)(c+1)+i}} = \frac{\vartheta G_{(m-1)(c+1)+l}}{\vartheta x_{im}} = -\frac{1}{f_{lm}}\frac{\vartheta f_{lm}}{\vartheta x_{im}}\ ,\ m=2,...,\pi \tag{1.41}$$

$$\frac{\vartheta G_{(m-1)(c+1)+l}}{\vartheta \Psi_{(j-1)(c+1)+i}} = \frac{\vartheta G_{(m-1)(c+1)+l}}{\vartheta x_{ij}} = 0, j \neq m \tag{1.42}$$

$$\frac{\vartheta G_{(m-1)(c+1)+l}}{\vartheta \Psi_{j(c+1)}} = \frac{\vartheta G_{(m-1)(c+1)+l}}{\vartheta F_j} = 0 \tag{1.43}$$

$$\frac{\vartheta G_{m(c+1)}}{\vartheta \Psi_i} = \frac{\vartheta G_{m(c+1)}}{\vartheta x_{i1}} = -P\sum_k^c \frac{x_{km}\vartheta f_{k1}}{f_{km}\vartheta x_{i1}}, \quad m=2,...,\pi \tag{1.44}$$

$$\frac{\vartheta G_{m(c+1)}}{\vartheta \Psi_{(m-1)(c+1)+i}} = \frac{\vartheta G_{m(c+1)}}{\vartheta x_{im}} = -P\frac{f_{i1}}{f_{im}} + P\sum_k^c \frac{x_{k1}f_{k1}}{(f_{km})^2}\frac{\vartheta f_{km}}{\vartheta x_{im}}, \quad m=2,...,\pi \tag{1.45}$$

$$\frac{\vartheta G_{m(c+1)}}{\vartheta \Psi_{(j-1)(c+1)+i}} = \frac{\vartheta G_{m(c+1)}}{\vartheta x_{ij}} = 0\ , \ j \neq m \tag{1.46}$$

$$\frac{\vartheta G_{m(c+1)}}{\vartheta \Psi_{j(c+1)}} = \frac{\vartheta G_{c+1}}{\vartheta F_j} = 0 \tag{1.47}$$

Bubble point pressure calculations can be conducted using the same basic model by setting $F_1=0$ and substituting F_1 in the unknowns with pressure P. The vector of the unknowns becomes:

$$\Psi = \Psi(x_1, P, x_2, F_2,..., x_\pi, F_\pi)^T \tag{1.48}$$

Some elements of the Jacobian matrix need also to be replaced as indicated below:

$$\frac{\vartheta G_1}{\vartheta \Psi_{c+1}} = \frac{\vartheta G_1}{\vartheta P} = 0 \tag{1.49}$$

$$\frac{\vartheta G_{c+1}}{\vartheta \Psi_{c+1}} = \frac{\vartheta G_{c+1}}{\vartheta P} = 0 \tag{1.50}$$

$$\frac{\vartheta G_{(m-1)(c+1)+l}}{\vartheta \Psi_{c+1}} = \frac{\vartheta G_{(m-1)(c+1)+l}}{\vartheta P} = \frac{1}{f_{l1}}\frac{\vartheta f_{l1}}{\vartheta P} - \frac{1}{f_{lm}}\frac{\vartheta f_{lm}}{\vartheta P}, \quad m=2,...,\pi \tag{1.51}$$

$$\frac{\vartheta G_{m(c+1)}}{\vartheta \Psi_{c+1}} = \frac{\vartheta G_{m(c+1)}}{\vartheta P} = 1-P\sum_k^c \left[\frac{x_{km}}{f_{km}}\left(\frac{\vartheta f_{k1}}{\vartheta P} - \frac{f_{k1}}{f_{km}}\frac{\vartheta f_{km}}{\vartheta P} + \frac{f_{k1}}{P}\right)\right], \quad m=2,...,\pi \tag{1.52}$$

The derivatives of fugacities with respect to pressure and composition can be calculated analytically. Different expressions are obtained for different mixing rules. For more versatility, in this implementation numerical approximations are used. This does not affect convergence in any respect, but it may cause an increase in computational time.

Multiphase equilibrium calculations by the successive substitution algorithm

The condition for equality of fugacities is expressed by the equation:

$$x_{i1}\phi_{i1}P = ... = x_{ij}\phi_{ij}P = ... \tag{1.53}$$

from which the equilibrium ratios K_{ij} are introduced:

$$\frac{\phi_{ij}}{\phi_{i1}} = \frac{x_{i1}}{x_{ij}} = K_{ij}\ ,\ j = 2,...,\pi \tag{1.54}$$

The method of successive substitutions employs equilibrium ratios K_{ij} and phase fractions F_j as independent variables. Equations (30) and (31) give:

$$\sum_{j}^{\pi} F_j = 1 \tag{1.55}$$

and by combining equations (30), (54) and (55), we get:

$$x_{i1} = \frac{z_i}{1+\sum_{j=2}^{\pi} F_j\left(\frac{1}{K_{ij}} - 1\right)} \tag{1.56}$$

$$x_{im} = \frac{\frac{z_i}{K_{im}}}{1+\sum_{j=2}^{\pi} F_j\left(\frac{1}{K_{ij}} - 1\right)}\ ,\ m = 2,...,\pi \tag{1.57}$$

Finally, equations (56) and (57) are combined to eliminate mole fractions:

$$\sum_{i}^{c}(x_{im} - x_{i1}) = 0 \Rightarrow \sum_{i}^{c} \frac{(\frac{1}{K_{im}} - 1)z_i}{1+\sum_{j=2}^{\pi} F_j(\frac{1}{K_{ij}} - 1)} = 0 \qquad (1.58)$$

There are π-1 such equations, which may be solved for the unknown phase mole fractions F_j, if equilibrium ratios are known. A suitable method is the Newton-Raphson, defined by eqn (33). The elements of the Jacobian matrix, eqn (34), are calculated from the following equation:

$$\frac{\vartheta G_{m-1}}{\vartheta F_{k-1}} = \sum_{i}^{c} \frac{(\frac{1}{K_{im}} - 1)z_i}{\left[1+\sum_{j=2}^{\pi} F_j(\frac{1}{K_{ij}} - 1)\right]^2}\left[\frac{1}{K_{ik}} - 1\right], \; m, k = 2,...,\pi \qquad (1.59)$$

The successive substitutions algorithm is initiated by assuming values for the equilibrium ratios K_{ij}. Next, the phase fractions of all phases are calculated from equations (58) and (55). The composition of each phase is calculated from equations (56) and (57). From the calculated compositions and the specified temperature T and pressure P, the fugacities of each component in each phase are calculated from the equation of state. The decisive step in the successive substitutions algorithm is the re-evaluation of the equilibrium ratios from the following equation:

$$K_{ij}^{t+1} = K_{ij}^{t}\left[\frac{f_{ij}}{f_{i1}}\right]^t \qquad (1.60)$$

where the superscript t denotes the iteration level. It is emphasized that fugacities are calculated from mole fractions corresponding to equilibrium ratios of the same iteration level. All fugacity ratios will converge to unity at equilibrium. The algorithm is considered converged when the following condition is satisfied:

$$\sum_{j}^{\pi}\sum_{i}^{c}\left[\ln\frac{f_{ij}}{f_{i1}}\right]^2 < 10^{-8} \qquad (1.61)$$

For bubble point calculations, F_1 is set equal to zero in equation (55). In addition to the calculations detailed above, a value for the pressure must be

assumed to initiate the algorithm. The value of pressure is adjusted after each iteration according to the following equation:

$$P^{t+1} = P^t \sum_i^c (x_{im}K_{im})^t \qquad (1.62)$$

where m the indice of the vaporizing liquid phase.

Initial Estimates

All phase equilibria algorithms require initial estimates for the values of the unknown quantities. Good initial guesses help quick and smooth convergence of the algorithm. In fact, if the initial guesses are not close enough to the true values, the Newton-Raphson algorithm will not converge to a solution and the successive substitution method most likely will converge to the trivial solution, particularly in the near critical region. In our implementation, an initial estimate for the composition of a hydrocarbon-rich liquid phase is obtained from the equation:

$$x_{ih} = \frac{z_i}{1+V(K_i-1)} \qquad (1.63)$$

where x_{ih} and z_i are respectively the mole fraction of component i in hydrocarbon-rich liquid phase and in the feed on a dry basis, V is the estimated vapour phase fraction in moles, taken as 90% of the dry feed and K_i is the equilibrium ratio as taken from the Wilson equation(Wilson,1969). The dry-base composition of the vapour phase is estimated from the equation:

$$y_i = K_i x_{ih} \qquad (1.64)$$

where y_i is the mole fraction of component i in the vapour phase. The mole fraction of water in the vapour phase y_w is taken from Raoult's Law:

$$y_w = \frac{P_w^s}{P} \qquad (1.65)$$

where P_w^s is the saturated vapour pressure of water. The concentration of water in the hydrocarbon-rich liquid phase is assumed to be equal to 0.01 in mole fraction, since the algorithms are not sensitive to this value.

The concentrations of hydrocarbons and related gases in the water-rich phase are taken from the correlations appearing in the IUPAC Solubility Data Series(1987), assuming that individual solubilities are independent of the presence of other gases.

Summary

Two different algorithms have been presented for solving multiphase equilibria problems. Both are sensitive to the initialization values of the unknowns but behave differently. The Newton-Raphson converges quadratically to the solution when it approaches it, while the successive substitution method is at best superlinear. For our particular problem of phase equilibria, the Newton-Raphson is the preferred method because the initial estimates, detailed above, are fairly good and because the successive substitution method tends to converge to the trivial solution when the system exhibits a rather narrow phase envelope. If the Newton-Raphson fails to converge it is always worth trying the successive substitution method. If this fails as well the only remedy is feeding the algorithm with different initial estimates, possibly from the results of similar calculations at easier conditions.

1.6. Validation of the Model and Discussion

It is understood that binary data may be fitted with any flexible enough mathematical equation. In this context, the justification and validation of a VLE model should be based on multicomponent data not used in any sense for obtaining parameters of the model. In this paragraph, the DD and NDD mixing rules are compared by application of the VLE model in multicomponent asymmetric systems. Figure 8a and b depict three-phase VLL experimental data of McKetta and Katz(1948) for the ternary system methane-n-butane-water at 100 °F together with predictions from three-phase flash calculations by both the DD and the NDD mixing rules. It is seen that predictions from both mixing rules are identical and they are very accurate for the concentration of methane in all phases, the total solubility in the water-rich phase and the concentration of

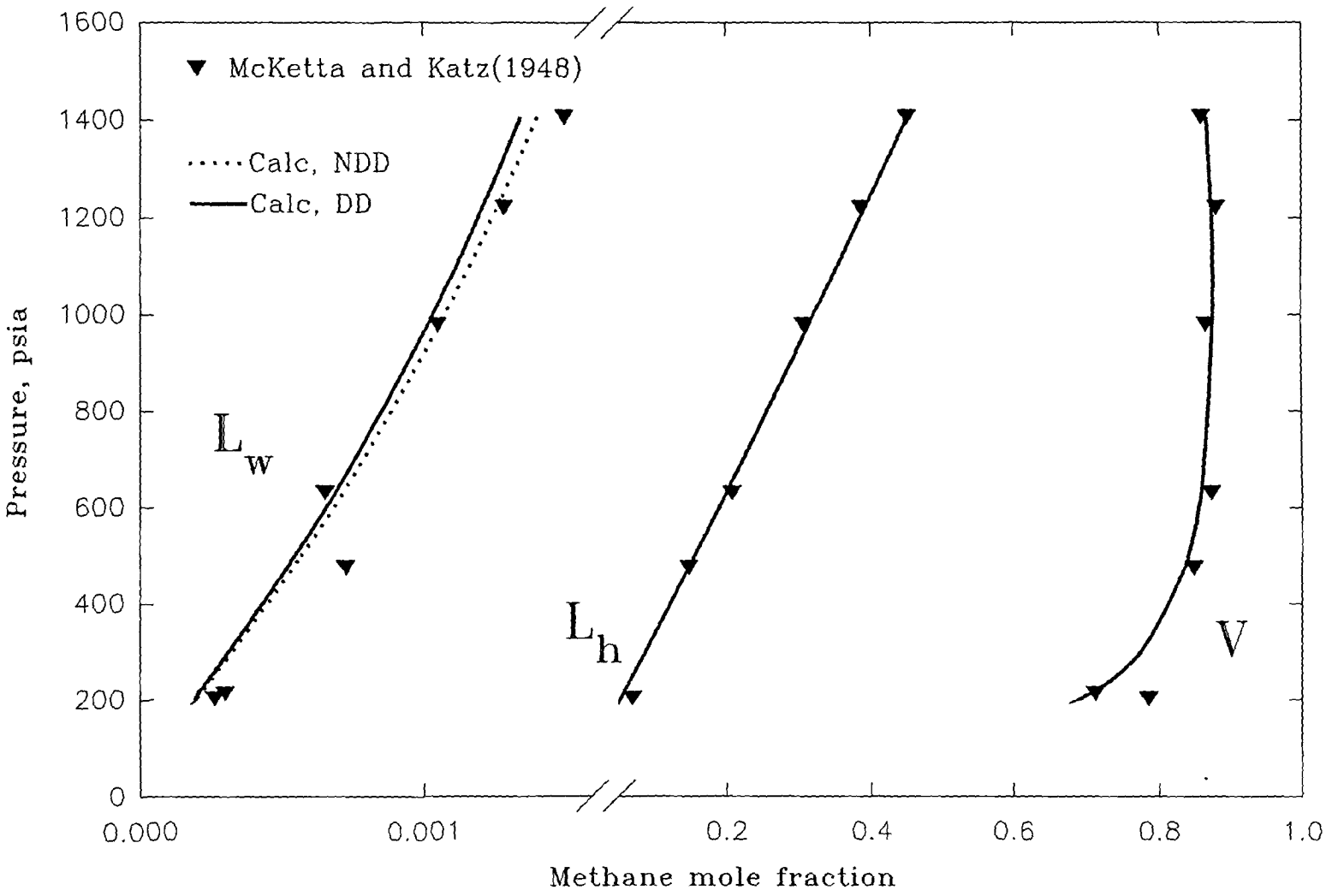

Figure 1.8a. Distribution of methane among the equilibrium V–Lw–Lh phases of the system CH_4–nC_4H_{10}–H_2O at 100^0 F.

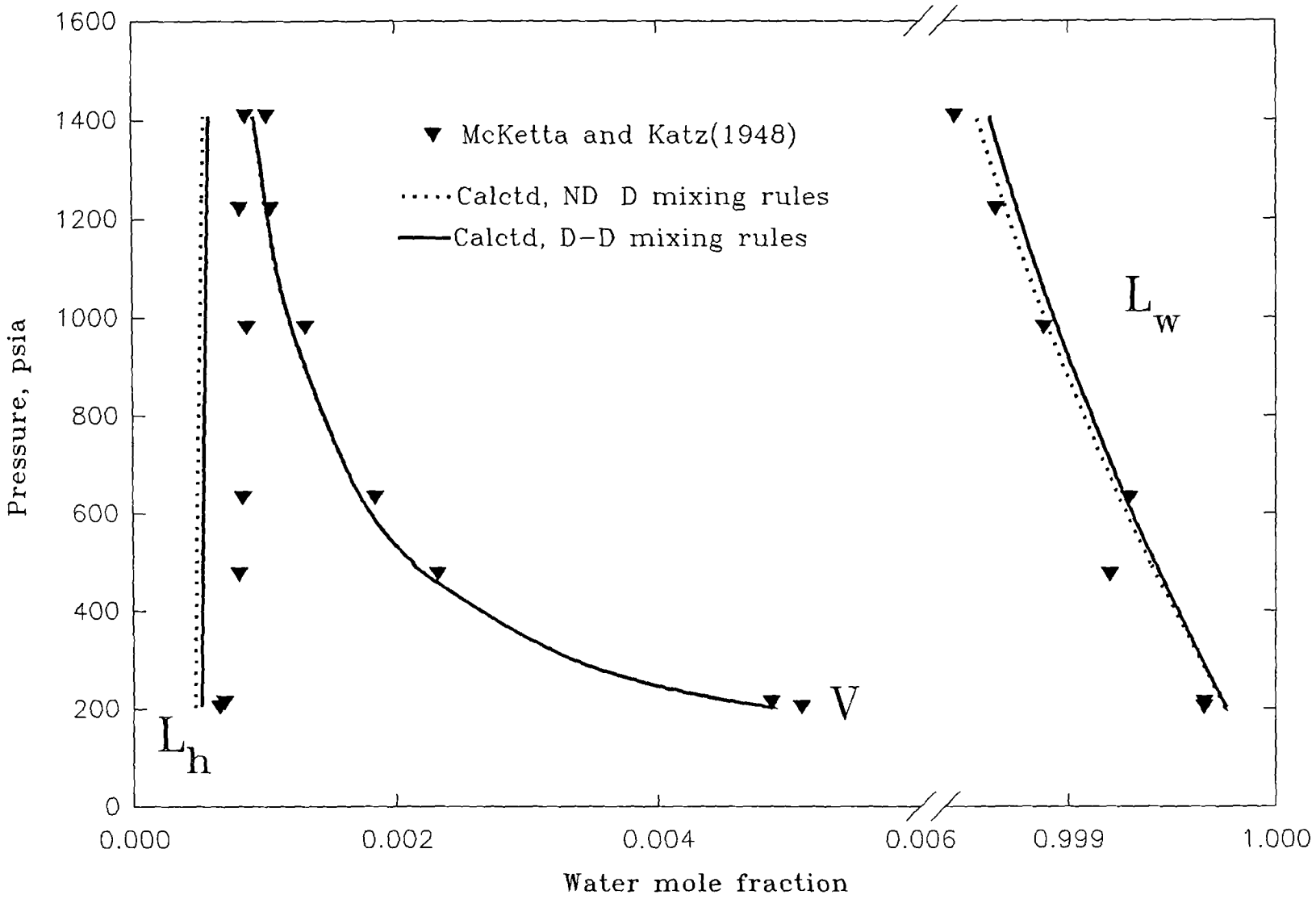

Figure 1.8b. Distribution of water among the equilibrium V-Lw-Lh phases of the methane-n-butane-water system at 100 °F.

water in the vapour phase. Deviations from experiment, however, appear for the concentration of water in the hydrocarbon-rich liquid phase.

Table 7 compares predictions from three-phase flash calculations with experimental data of Huang et al(1985) for the system methane-hydrogen sulfide-carbon dioxide-water in the three phase region. This rich in hydrogen sulfide asymmetric system is particularly difficult to model with conventional mixing rules because a hydrogen sulfide-rich liquid phase is present instead of the normally present hydrocarbon-rich liquid. Successful modelling of the above system has not been attempted by the previous workers and it serves as a severe test for a model based on binary data only. It is seen that both mixing rules predict the composition of any phase with satisfactory accuracy, even for the minor components in each phase. It is significant to note that the direction of deviations of predictions is the same for both models and of similar size.

Tables 8a and 8b compare at two different temperatures predictions from bubble point VL calculations with experimental data of Galivel-Solastiouk et al(1986) for a series of mixtures of propane-carbon dioxide-methanol. Again, this is a highly asymmetric system which has not been modelled by the previous workers. Schwartzentruber et al(1987) have reported a successful representation of these data by means of a cubic EoS with mixing rules involving three temperature dependent binary parameters, which were not correlated. However, such a mixing rule with so many parameters is practically useless for real systems. As is seen all data are predicted successfully with both mixing rules proposed by us. A comparison with the predictions of Schwartzentruber et al(1987) is not easy, because of the particular method employed by them to represent the data.

So far, both the DD and NDD mixing rules are shown to represent successfully experimental data for multicomponent systems with only one polar component. Table 9 compares predictions from flash VL and LL calculations with the experimental data of Ng and Robinson(1985) for a quaternary system containing both water and methanol. For this system the quality of predictions deteriorates. In particular the concentration of hydrocarbons in the water-rich phase is underpredicted and so is the concentration of water in the hydrocarbon-rich phases. Predictions from both mixing rules deviate in the same direction but NDD mixing rules perform consistently better with this system for the prediction of solubilities of hydrocarbons in the water-rich liquid phase.

Table 1.7. Comparison of experimental and calculated equilibrium phase compositions(mole fractions) for a 4-component asymmetric system in the three phase Lw-Lh-V region. Experimental data of Huang et al(1985).

	Methane	Hydr. sulfide	Carbon dioxide	Water
T=37.8. °C, P=6.26 MPa				
Feed	0.0504	0.3986	0.0503	0.5008
Water-rich liquid				
Exptl	0.000490	0.0284	0.00350	0.9677
Caltd, NDD	0.000402	0.0296	0.00326	0.9696
Caltd, DD	0.000314	0.0254	0.00315	0.9714
Hydrogen sulfide-rich liquid				
Exptl	0.0653	0.8197	0.1049	0.0101
Caltd, NDD	0.0602	0.8391	0.0894	0.0113
Caltd, DD	0.0602	0.8391	0.0894	0.0113
Vapour				
Exptl	0.3213	0.5028	0.1739	0.00214
Caltd, NDD	0.3216	0.5248	0.1517	0.00194
Caltd, DD	0.3217	0.5247	0.1516	0.00194
T=65.6 °C, P=8.43 MPa				
Feed	0.0501	0.4016	0.0499	0.4984
Water-rich liquid				
Exptl	0.000385	0.0321	0.00272	0.9684
Caltd, NDD	0.000305	0.0317	0.00242	0.9655
Caltd, DD	0.000245	0.0285	0.00233	0.9691
Hydrogen sulfide-rich liquid				
Exptl	0.0580	0.8287	0.0904	0.0212
Caltd, NDD	0.0612	0.8354	0.0844	0.0191
Caltd, DD	0.0638	0.8312	0.0863	0.0186
Vapour				
Exptl	0.1872	0.6557	0.1484	0.00866
Caltd, NDD	0.1848	0.6791	0.1291	0.00700
Caltd, DD	0.1877	0.6749	0.1303	0.00700

Table 1.8a. VLE predictions and experimental data (Galivel-Solastiouk et al, 1986) for the system C_3H_8(1)-CO_2(2)-MeOH(3) . T=313.1 K.

BP/MPa, exptl	x	y, exptl	BP/MPa, NDD	y, caltd NDD	BP/MPa, DD	y,caltd Dd
0.510	0.0478	0.885	0.542	0.904	0.520	0.901
	0.00078	0.0223		0.0246		0.0258
	0.951	0.093		0.071		0.074
	0.0250	0.529	Q.510	0.553	0.493	0.540
	0.0106	0.366		0.371		0.385
	0.964	0.105		0.076		0.078
	0.0156	0.352	0.485	0.376	0.474	0.360
	0.0146	0.546		0.545		0.560
	0.970	0.102		0.079		0.081
	0.0086	0.191	0.474	0.217	0.467	0.205
	0.0182	0.717		0.702		0.714
	0.9731	0.092		0.081		0.081
1.206	0.194	0.913	1.231	0.917	1.240	0.917
	0.0045	0.051		0.049		0.049
	0.802	0.036		0.034		0.034
	0.128	0.777	1.239	0.784	1.234	0.783
	0.015	0.192		0.182		0.183
	0.857	0.031		0.034		0.035
	0.0508	0.417	1.201	0.440	1.182	0.428
	0.037	0.547		0.525		0.536
	0.912	0.035		0.035		0.036
	0.0353	0.299	1.181	0.330	1.165	0.317
	0.043	0.663		0.635		0.647
	0.922	0.038		0.036		0.036
1.710	0.772	0.802	1.487	0.783	1.481	0.781
	0.0362	0.173		0.190		0.192
	0.192	0.025		0.027		0.027
	0.393	0.775	1.521	0.759	1.518	0.760
	0.031	0.195		0.212		0.211
	0.576	0.029		0.029		0.030
	0.0477	0.283	1.688	0.300	1.675	0.290
	0.067	0.671		0.673		0.683
	0.885	0.036		0.027		0.027
	0 0045	0.0300	1.677	0.0333	1.680	0.0311
	0.088	0.936		0.940		0.943
	0.908	0.034		0.027		0.026
2.203	0.551	0.626	1.781	0.622	1.769	0.620
	0.071	0.356		0.351		0.353
	0.378	0.018		0.027		0.027
	0.434	0.616	1.894	0.598	1.885	0.598
	0.073	0.361		0.376		0.376
	0.494	0.022		0.026		0.026

Table 1.8b. VLE predictions and experimental data (Galivel-Solastiouk et al, 1986) for the system C_3H_8(1)-CO_2(2)-MeOH(3) . T=343.1 K.

BP/MPa, exptl	x	y, exptl	BP/MPa, NDD	y, caltd NDD	BP/MPa, DD	y,caltd Dd
0.510	0.0175	0.540	0.534	0.603	0.510	0.594
	0.00288	0.127		0.145		0.146
	0.9796	0.332		0.252		0.261
	0.0065	0.228	0.478	0.259	0.461	0.251
	0.0081	0.436		0.464		0.463
	0.9853	0.335		0.277		0.286
	0.0030	0.104	0.465	0.124	0.451	0.120
	0.010	0.559		0.592		0.588
	0.9868	0.337		0.284		0.292
	0.00062	0.023	0.448	0.027	0.435	0.026
	0.011	0.656		0.679		0.673
	0.9884	0.321		0.294		0.302
1.206	0.0536	0.673	1.260	0.697	1.227	0.696
	0.0095	0.184		0.187		0.186
	0.937	0.143		0.116		0.118
	0.0435	0.599	1.167	0.633	1.131	0.630
	0.0112	0.248		0.243		0.243
	0.945	0.153		0.124		0.127
	0.0313	0.466	1.120	0.496	1.081	0.491
	0.0162	0.376		0.376		0.377
	0.952	0.157		0.128		0.132
	0.0173	0.252	1.173	0.275	1.132	0.270
	0.0265	0.603		0.603		0.604
	0.956	0.145		0.123		0.126
1.710	0.0864	0.692	1.764	0.722	1.743	0.724
	0.0145	0.193		0.189		0.186
	0.899	0.115		0.089		0.089
	0.045	0.421	1.708	0.452	1.658	0.450
	0.031	0.466		0.457		0.458
	0.924	0.113		0.091		0.092
	0.0284	0.278	1.630	0.316	1.577	0.312
	0.037	0.623		0.591		0.592
	0.934	0.100		0.094		0.100
	0.00750	0.0774	1.656	0.087	1.604	0.085
	0.0506	0.817		0.822		0.822
	0.942	0.105		0.091		0.093
2.203	0.145	0.745	2.300	0.759	2.320	0.765
	0.019	0.171		0.167		0.162
	0.835	0.084		0.074		0.073
	0.0223	0.175	2.116	0.196	2.052	0.193
	0.059	0.739		0.728		0.730
	0.918	0.086		0.076		0.077

Table 1.9. Comparison of experimental and calculated equilibrium phase compositions(mole fractions) for a 4-component asymmetric mixture of methanol and water. Experimental data of Ng and Robinson(1985).

	Ethane	Carbon dioxide	Methanol	Water
		T=270.93 K, P=1.14 MPa		
Feed	0.0059	0.0020	0.1223	0.8698
		Water-rich liquid		
Exptl	0.00098	0.00177	0.12994	0.86731
Caltd, NDD	0.00037	0.00129	0.12307	0.87528
Caltd, DD	0.00010	0.00113	0.12312	0.87565
		Vapour		
Exptl	0.87476	0.12393	0.00062	0.00072
Caltd, NDD	0.88367	0.11532	0.00061	0.00041
Caltd, DD	0.86764	0.13109	0.00085	0.00043
		T=275.76 K, P=2.70 MPa		
Feed	0.0168	0.0056	0.1205	0.8571
		Water-rich liquid		
Exptl	0.00163	0.00381	0.12260	0.87196
Caltd, NDD	0.00063	0.00304	0.12280	0.87353
Caltd, DD	0.00018	0.00258	0.12291	0.87433
		Vapour		
Exptl	0.82653	0.17286	0.00057	0.00041
Caltd, NDD	0.86013	0.13899	0.00062	0.00026
Caltd, DD	0.84323	0.15562	0.00087	0.00028
		T=280.85 K, P=3.60 MPa		
Feed	0.0720	0.0240	0.1114	0.7926
		Water-rich liquid		
Exptl	0.00185	0.01021	0.12178	0.86616
Caltd, NDD	0.00058	0.00716	0.12151	0.87075
Caltd, DD	0.00018	0.00553	0.12140	0.87290
		Ethane-rich liquid		
Exptl	0.77078	0.22668	0.00156	0.00078
Caltd, NDD	0.79612	0.19477	0.00891	0.00020
Caltd, DD	0.78070	0.20627	0.01275	0.00029

Table 1.10 compares predictions from VL flash calculations with experimental data of Ng and Robinson(1983) for natural gas+water+methanol mixtures. Compositions as well as experimental conditions for these systems are more close to the industrial reality than the previous data. It is seen that NDD mixing

rules again produce consistently more accurate predictions than DD mixing rules and that all data are predicted reasonably well.

Table 1.10. Comparison of experimental and calculated equilibrium phase compositions(mole fractions) for a natural gas-water-methanol equilibrium. Experimental data of Ng and Robinson(1983).

	C_1	C_2	C_3	nC_4	nC_5	CO_2	N_2	MeOH	H_2O
T=273.75, P=1.48 MPa(10%W/W MeOH in Lw)									
Feed	0.01722	0.00113	0.00047	0.00019	0.00019	0.00359	0.00143	0.05720	0.91860
Water-rich liquid									
Exptl	0.00059	0.00005	0.00002	-	-	0.00152	0.00005	0.05771	0.94006
NDD	0.00023	0.00003	0.00001	1.3E-6	2.0E-7	0.00141	0.00001	0.05852	0.93980
DD	0.00016	0.00001	2.4E-6	0.3E-6	<1.E-7	0.00139	0.00001	0.05852	0.93991
Vapour									
Exptl	0.74640	0.05241	0.02191	0.00886	0.00925	0.09636	0.06378	0.00058	0.00045
NDD	0.75240	0.04869	0.02047	0.00836	0.00840	0.09814	0.06291	0.00021	0.00044
DD	0.75163	0.04916	0.02060	0.00836	0.00837	0.09836	0.06274	0.00035	0.00044
T=288.85, P=16.71 MPa(10%W/W MeOH in Lw)									
Feed	0.06875	0.00453	0.00187	0.00075	0.00075	0.01435	0.00570	0.5310	0.85020
Water-rich liquid									
Exptl	0.00280	0.00010	0.00002	-	-	0.00521	0.00020	0.05830	0.93337
NDD	0.00139	0.00007	0.00001	7.E-7	1.E-7	0.00479	0.00009	0.05838	0.93528
DD	0.00092	0.00003	0.3E-5	2.E-7	<1.E-7	0.00447	0.00006	0.05840	0.93612
Vapour									
Exptl	0.74194	0.05196	0.02174	0.00872	0.00950	0.10290	0.06219	0.00077	0.00028
NDD	0.74170	0.04913	0.02047	0.00824	0.00824	0.10982	0.06177	0.00039	0.00024
DD	0.73971	0.04903	0.02034	0.00817	0.00817	0.11211	0.06152	0.00071	0.00025
T=269.25 K, P=2.11 MPa(20%W/W MeOH in Lw)									
Feed	0.03503	0.00231	0.00095	0.00039	0.00039	0.00732	0.00291	0.11700	0.83370
Water-rich liquid									
Exptl	0.00107	0.00010	0.00003	-	-	0.00264	0.00009	0.12080	0.87527
NDD	0.00022	0.00004	0.00001	7.E-7	1.E-7	0.00219	0.00001	0.12275	0.87479
DD	0.00011	0.00001	0.1E-5	1.E-7	<1.E-7	0.00180	0.4E-5	0.12281	0.87526
Vapour									
Exptl	0.74828	0.04908	0.02022	0.00982	0.00823	0.09989	0.06357	0.00059	0.00032
NDD	0.74114	0.04846	0.02008	0.00829	0.00830	0.11146	0.06176	0.00030	0.00021
DD	0.73536	0.04844	0.01999	0.00821	0.00821	0.11796	0.06119	0.00042	0.00022
T=282.55 K, P=16.78 MPa(20%W/W MeOH in Lw)									
Feed	0.11803	0.00779	0.00321	0.00130	0.00130	0.02466	0.00981	0.10250	0.73140
Water-rich liquid									
Exptl	0.00355	0.00014	0.00002	-	-	0.00713	0.00028	0.11989	0.86899
NDD	0.00105	0.00006	0.00001	3.E-7	<1.E-7	0.00554	0.00007	0.12196	0.87132
DD	0.00055	0.00002	0.1E-5	<1.E-7	<1.E-7	0.00440	0.00003	0.12211	0.87289
Vapour									
Exptl	0.73245	0.05251	0.02197	0.00804	0.00588	0.11529	0.06242	0.00115	0.00029
NDD	0.72938	0.04820	0.01996	0.00809	0.00809	0.12460	0.06073	0.00078	0.00016
DD	0.72518	0.04795	0.01980	0.00802	0.00802	0.12937	0.06033	0.00117	0.00017

Cubic equations of state with classical mixing rules cannot correlate any of the data presented in this paragraph. The proposed mixing rules are applicable to any cubic equation of state, but no substantial differences should be expected. This is because most popular EoS have been shown by several authors to behave similarly for most VLE calculations of hydrocarbon systems. On the other hand, for asymmetric systems the governing part of the equation is the mixing rules. If it is desired, additional flexibility may be gained by allowing l_{ij} and l_{ji} to take freely any nonzero value in fitting binary data. In that case no physical significance can be attributed to the interaction parameter and such a scheme will not necessarily perform better in multicomponent asymmetric systems.

Though the proposed model fundamentally is only an empirical correlation practically useful for quantitative calculations in a limited region of the phase equilibria area, nonetheless, it is a significant improvement over the traditional approaches to modelling of phase equilibria of asymmetric systems and offers a number of advantages.

(1) The use of a single equation of state for all phases allows critical points to be defined. In principle, it is possible to carry out accurate predictions of critical points of asymmetric systems by taking appropriate care in the choice of the parameters of the EoS.

(2) The computation time is short. In fact for either mixing rule computational time is comparable to that with classical mixing rules. This is because additional summations of mole fraction products are governed by the number of polar components, equations (23), (26) and (28), which in our case are only one or two.

(3) Other useful thermodynamic properties of solutions, such as partial molar volumes, enthalpies etc, can be easily calculated as with any cubic equation of state, and the resulting expressions of the derived quantities are relatively simple.

(4) The number of binary parameters is limited to three only(to include the temperature dependence slope coefficient) and do not impose particular computational memory and space requirements.

(5) It is noted that if l_{ij} is set equal to zero the original form of the cubic EoS proposed by Valderrama(1990) is recovered. This is a useful feature, since this EoS has been shown to represent adequately the phase behaviour of complex

reservoir fluids even without the use of binary interaction parameters(Danesh et al,1991).

The proposed NDD and DD mixing rules were shown to behave similarly for systems with only one polar component. However, when two polars were present(and most probably so with even more polars) the performance of the DD mixing rules deteriorates and it is consistently inferior. Considering that both mixing rules are very similar in form (purposely), while only the DD mixing rules meet the theoretical boundary requirements at low pressures, this observation may be initialy unexpected. In fact, although many publications have adressed density-dependent mixing rules in the last decade(only a few were reviewed in this Chapter) no researcher has presented a successful correlation of multicomponent strongly asymmetric systems. These observations alone suggest that density-dependent mixing rules are fundamentally as far from the correct theoretical basis as any other empirical modification of the attractive term of the vdW EoS.

A possible explanation of the failure of DD mixing rules when two polars are present, can be given from a close examination of the mathematical formulation of the defining equation(27): when the interaction parameter l_{ij} was fitted to binary data, the liquid molar volume of the mixture v was the sum of the partial molar volumes of i and j. When water is the only polar component, due to the very low solubility of hydrocarbons in water, the mixture molar volume v can be considered equal to the molar volume of water. In ternary and multicomponent systems, however, containing methanol the molar volume is not related to the mole fraction of i and j. Therefore, for such a mixture the regressed binary parameter l_{ij} will be not correct; the true value of the binary parameter l^*_{ij} is: $l^*_{ij}=l_{ij}v/(x_i\bar{v}_i+x_j\bar{v}_j)$, where $\bar{v}_i$ and $\bar{v}_j$ denote the partial molar volumes of the respective components in the mixture.

As a result of the above discussion, in the following Chapters DD mixing rules are not employed for mixtures containing both water and methanol, ie for methanol inhibition problems. In other cases where DD mixing rules are used, it is believed that NDD mixing rules would lead to the same results. In conclusion our preference would the NDD mixing rules.

References

Dahl,S. and Michelsen,M.L., "High pressure vapor-liquid equilibria with a UNIFAC-based equation of state", AIChE J., **36**, 1829(1990).

Danesh,A., Xu,D.-H. and Todd,A.C., "Comparative study of cubic equations of state for predicting phase behaviour and volumetric properties of injection gas reservoir oil systems", Fluid Phase Equilibria, **63**, 259(1991).

Dimitrelis,D. and Prausnitz,J.M., "Molecular thermodynamics of fluid mixtures at low and high densities",Chem.Eng.Sci., **45**, 1503(1990).

Elliot,R.J., Suresh,S.J. and Donohue,M.D., "A simple equation of state for nonspherical and associating molecules",IEC Res., **29**, 1476(1990).

Huron,M.J. and Vidal,J., "New mixing rules in the cubic equations of state for representing vapour-liquid equilibria of strongly non-ideal mixtures", Fluid Phase Equilibria, **3**, 255(1979).

IUPAC, Solubility Data Series, Vol. **2**, **9**, **10**, **24**, **27/28**, Pergamon Press, Oxford(1987).

Kabadi,V.N. and Danner,R.P., "A modified Soave-Redlich-Kwong equation of state for water-hydrocarbon phase equilibria", IEC Proc.Des.Dev., **24**, 537(1985).

Luedecke,D. and Prausnitz,J.M., "Phase equilibria for strongly nonideal mixtures from an equation of state with density-dependent mixing rules", Fluid Phase Equilibria, **22**, 1(1985).

Mathias,P.M. and Copeman,T.W., "Extension of the Peng-Robinson equation of state to complex mixtures: Evaluation of the various forms of the local composition concept", Fluid Phase Equilibria, **13**, 91(1983).

Michelsen,M.L., "A modified Huron-Vidal mixing rule for cubic equations of state", Fluid Phase Equilibria, **60**, 213(1990a).

Michelsen,M.L., "A method for incorporating excess Gibbs energy models in equations of state" Fluid Phase Equilibria, **60**, 42(1990b).

Mollerup,J., "A note on excess Gibbs energy models, equations of state and the local composition concept", Fluid Phase Equilibria, **7**, 121(1981).

Mollerup,J., "Correlation of gas solubilities in water and methanol at high pressures", Fluid Phase Equilibria, **22**, 139(1985).

Mollerup,J., "Correlations of thermodynamic properties of mixtures using a random-nonrandom mixture reference state", Fluid Phase Equilibria, **15**, 189(1983).

Mollerup,J., "A note on the derivation of mixing rules from excess Gibbs energy models", Fluid Phase Equilibria, **25**, 323(1986).

Panagiotopoulos,A.Z. and Reid,R.C., "New mixing rules for cubic equations of state for highly polar, asymmetric systems", Amer.Chem.Soc. Symposium Ser., **300**, 571(1986).

Panagiotopoulos,A.Z. and Reid,R.C., "Multiphase high pressure equilibria in ternary aqueous systems", Fluid Phase Equilibria, **29**, 525(1986).

Patel,N.C. and Teja,A.S., "A new cubic equation of state for fluids and fluid mixtures", Chem.Eng.Sci., 37, 463(1982).

Peneloux,A., Rauzy,E. and Freze,R., "A consistent correction for the Redlich-Kwong-Soave volumes", Fluid Phase Equilibria, **8**, 7(1982).

Peng,D.-Y. and Robinson,D.B., "A new two-constant equation of state", Ind.Eng.Chem., Fundam., **15**, 59(1976).

Peschel,W. and Wenzel,H., "Equation-of-state predictions of phase equilibria at elevated pressures in mixtures containing methanol", Ber.Bunsenges.Phys.Chem., **88**, 807(1984).

Soave,G., "Equilibrium constants from a modified Redlich-Kwong equation of state", Chem.Eng.Sci., **27**, 1197(1972).

Sryjek,R. and Vera,J.H., "Vapor-liquid equilibrium of hydrochloric acid solutions with the PRSV equation of state",Fluid Phase Equilibria, **25**, 279(1986).

Schwartzentruber,J. Galivel-Solastiouk,F. and Renon,H., "Representation of the vapor-liquid equilibrium of the ternary system carbon dioxide-propane-methanol and its binaries with a cubic equation of state", Fluid Phase Equilibria, **38**, 217(1987).

Topliss,R., Dimitrelis,D. and Prausnitz,J.M., "Computational aspects of a non-cubic equation of state for phase equilibrium calculations. Effect of density-dependent mixing rules", Comput.Chem.Engng, **12**, 483(1988).

Valderrama,J.O., "A generalized Patel-Teja equation of state for polar and non polar fluids and their mixtures", J.Chem.Eng.Japan, **23**,87(1991).

Valderrama,J.O. and Cisternas,L.A., "On the choice of a third (and fourth) generalizing parameter for equations of state", Chem.Eng.Sci., **42**, 2957(1987).

Wenzel,H. and Kropp,E, "Phase equilibrium by equation of state: A short-cut method allowing for association", Fluid Phase Equilibria, **59**, 147(1990).

Whiting,W.B. and Prausnitz,J.M., "Equations of state for strongly nonideal fluid mixtures: Application of local compositions toward density-dependent mixing rules", Fluid Phase Equilibria, **9**, 119(1982).

Wilson,G.M., "A modified Redlich-Kwong equation of state. Application on general physical data calculations", Paper 15C, AIChE 65th Natnl Meeting, Ohio(1969).

Sources of experimental VLE water-hydrocarbon data

1. Amirijafari,B. and Campbell,J.M., "Solubility of gaseous hydrocarbon mixtures in water", Soc.Pet.Eng.J., p21-, Feb. 1972.

2. Azarnoosh,A. and McKetta,J.J., "The solubility of propane in water", Pet.Ref., **37**, 275(1958).

3. Bartlett,E.P., "The concentration of water vapor in compressed hydrogen, nitrogen and a mixture of these gases in the presence of condensed water",J.Am.Chem.Soc., **49**,65(1927).

4. Burd,S.D. and Braun,W.G., "Vapor-liquid equilibria of some C6 hydrocarbons with water", Proc.Am.Pet.Inst.Ref.Dept., **48**, 464(1968).

5. Culberson, O.L., "Phase equilibria in hydrocarbon-water systrems. III-The solubility of methane in water at pressures to 10000 psia", Petr.Trans.AIME, **192**, 223(1951).

6. Culberson,O.L. and McKetta,J.J., "The solubility of ethane in water at pressures to 10000 psi", Pet.Trans.AIME, **189**, 319(1950).

7. Daneil,A., Toenheide,K. and Frank,E.U., "Verdampfungsgleichgewichte und kritische kurven in den systemen aethan/wasser und n-butan/wasser bei hohen drucken", Ch.-Ing.-Techn., **39**, 816(1967).

8. DeLoos,T.W., Wijen,A.J.M. and Diepen,G.A.M., "Phase equilibria and critical phenomena in fluid(propane+water) at high pressures and temperatures", J.Chem.Thermodynamics, **12**, 193(1980).

9. Duffy,J.R. Smith,N.O. and Nagy,B., "Liquidus surfaces in the system CH4-H2O-NaCl-CaCl2 at room temperatures and pressures below 1000 psia", Geo.Cosmochimica Acta, **24**, 23(1961).

10. Kobayashi, R.K. and Katz,D.L., "Vapor-liquid equilibria for binary hydrocarbon-water systems", Ind.Eng.Chem., **45**, 440(1953).

11. Kudchacker,A.P. and McKetta,J.J., "Solubility of hexane in water", Hydr.Pross.Petr.Ref., **40**, 231(1961).

12. LeBreton,J.G. and McKetta,J.J., "Low pressure solubility of n-butane in water", Hydr.Proc.Pet.Ref., **43**, 136(1964).

13. Leinonen,P.J. and McKay,D., "The multicomponent solubility of hydrocarbons in water", Can.J.Chem.Eng., **51**, 230(1973).

14. Maharajh,D.M. and Walkey,J., "Thermodynamic solubility. Part 1.-Two component gas mixtures in water at 25 C", - ,- ,842(1972).

15. McAuliffe,C., "Solubility in water of paraffin, cyclopaffin, olefin, acetylene, cycloolefin, and aromatic hydrocarbons", J.Phys.Chem., 70, 1267(1966).

16. McAuliffe, C., "Solubility in water of C1-C9 hydrocarbons", Nature, **200**, 1092(1963).

17. McKetta,J.J. and Katz,D.L., "Methane-n-butane-water system in two- and three-phase regions", Ind.Eng.Chem., **40**, 853(1948).

18. Namiot, A.V. and Beider, S.V., " ", Khim.Tekhnol. Topl. Masel, **5**, 52(1960).

19. Nelson,H.D. and deLigny,C.L., "The determinationof the solubilities of some n-alkanes in water at different temperatures, by means of gas chromatography", Recueil, **87**, 528(1968).

20. Nighswander,J.A., Kalogerakis,N. and Mehrotra,A.K., "Solubilities of carbon dioxide in water and 1% NaCl at pressures up to 10MPa and temperatures from 80 to 200 C", J.Chem.Eng.Data, **34**, 355(1989).

21. O'Sullivan, T.D. and Smith,N.O., "The solubility and partial molar volume of nitrogen and methane in water and aqueous sodium chloride from 50 to 125 C and 100 to 600 atm", J.Phys.Chem., **74**, 1460(1970).

22. Olds, R.H., Sage,B.H. and Lacey,W.N., "Composition of the dew-point gas of the methane-water system", Ind.Eng.Chem., **34**, 1223 (1942).

23. Poettmann,F.H. and Dean,M.R., "Water content of propane", Pet.Ref., **25**, 125(1946).

24. Polak,J. and Lu,B., "Mutual solubilities of hydrocarbons in water at 0 and 25 C", Can.J.Chem., **51**, 4020(1973).

25. Reamer,H.H., Olds,R.H., Sage,B.H. and Lacey,W.N., "Composition of dew-point gas in ethane-water system", Ind.Eng.Chem., **35**, 790(1943).

26. Reamer, H.H., Olds,R.H., Sage,B.H. and Lacey,W.N., "Compositions of the coexisting phase of n-butane-water system in the three phase region", Ind.Eng.Chem., **36**,381(1944).

27. Reamer, H.H., Sage,B.H. and Lacey,W.N., "n-Butane-Water in the two-phase region", Ind.Eng.Chem., **44**, 609(1952).

28. Rebert,C.J. and Hayworth,K.E., "The gas and liquid solubility relations in hydrocarbon-water systems", AIChE J., **13**, 118(1967).

29. Rigby,M. and Prausnitz,J.M., "Solubility of water in compressed nitrogen, argon and methane", J.Phys.Chem., **72**, 330(1968).

30. Sanchez, M. and Coll,R., "Sistema propaneo-aqua para altas pressiones y temperaturas. I. Region de dos fases", Anales de Quimica, **74**, 1329(1978).

31. Schatzberg,P., "Solubilities of water in several normal alkanes from C7 to C16", J.Phys.Chem., **67**,776(1963).

32. Selleck,F.T., Carmichael,L.T. and Sage,B.H., "Phase behavior in the hydrogen sulfide-water system", Ind.Eng.Chem., **44**, 2219(1952).

33. Song,K.Y. and Kobayashi,R., "The water content of CO2-rich gas mixture containg 5.31 mol% methane along the three-phase and supercritical conditions", J.Chem.Eng.Data, **35**, 3209(1990).

34. Stoessell, R.K. and Byrne,P.A., "Methane solubilities in clay slurries", Clays and Caly Minerals, **30**, 67(1982).

35. Sultanov,R.G., Skripka,V.G. and Namiot,V.G., " ", Gasovaia Promvshlennost, **17**, 6(1972).

36. Sultanov,R.G., Skripka,V.G. and Namiot,V.G., " ", Gasovaia Promvshlennost, **16**, 6(1972).

37. Takenouchi,S. and Kennedy,G.C., "The binary system H2O-CO2 at high temperatures and pressures", Am.J.Sci., **262**, 1055(1964).

38. Toedheide,K. Frank,E.U., " ", Z.Phys.Chem.Frankf., **37**, 387(1963).

39. Tsonopoulos,C. and Wilson,G.M., "High-temperature mutual solubilities of hydrocarbons and water. Part I:Benzene, cyclohexane and n-hexane", AIChE J., **29**, 990(1983).

40. Villareal,J.F., Bissey,L.T. and Nielsen,R.F., "Dew-point watercontents of methane-ethane mixtures at a series of pressures and temperatures", Producer Monthly, p15, May 1954.

41. Wang, Qi and Chao,K.-C., "Vapor-liquid and liquid-liquid equilibria and critical states of water+n-decane mixtures", Fluid Phase Equilibria, **59**, 207(1990).

42. Wehe, A.H. and McKetta,J.J., "Method for determining total hydrocarbons dissolved in water", Anal.Chem., **33**, 291(1961).

43. Wiebe,R,, Gaddy, V.L. and Heins,C., "The solubility of nitrogen in water at 50, 75 and 100 C from, 25 to 1000 atm",J.Am.Chem.Soc., **55**, 947(1933).

44. Wiebe,R. and Gaddy,V.L., "Vapor-phase composition of carbon dioxide-water mixtures at various temperatures and at pressures up to 700 atm", J.Am.Chem.Soc.,**63**, 475(1941).

45. Wiebe,R. and Gaddy,V.L., "The solubility of carbon dioxide in water at various temperatures from 12 to 40 and at pressures to 500 atm", J.Am.Chem.Soc., **62**,815(1940).

46. Zawisza,A. and Boguslawa,M., "Solubility of carbon dioxide in liquid water and of water in gaseous carbon dioxide in the range 0.2-5MPa and at temperatures up to 473K", J.Chem.Eng.Data, **26**, 388(1981).

47. Coan,C.R. and King,A.D., "Solubility of compressed carbon dioxide, nitrous oxide, and ethane. Evidence of hydration of carbon dioxide and nitrous oxide in the gas phase", J.Am.Chem.Soc., 93, 1857(1971).

48. Brady,C.J. and Wilson,G.M., "Water-hydrocarbon liquid-liquid-vapor equilibrium measurements to 530 F", GPA RR-62, Tulsa, 1982.

49. Gilespie,P.C. and Wilson,G.M., "Vapor-liquid and liquid-liquid equilibria: water-methane, water-carbondioxide, water-hydrogen sulfide, water-n-pentane", GPA RR-48, Tulsa, 1982.

50. Song,K.Y. and Kobayashi,R., "The water content of CO2-rich fluids in equilibrium with liquid water and/or hydrates", GPA RR-99, Tulsa, 1986.

51. Scheffer,F.E., "On the system hexane-water", Proc. Kon. Akad. Wet. Amsterdam, **16**, 404(1913).

52. Dodson,C.R. and Standing,M.B.,"Pressure-volume-temperature and solubility relations for natural-gas-water mixtures", Proc.Am.Pet.Inst., Drilling and Product Practice, 173(1944).

53. Rettich,T.R., Handa,Y.P., Battino,R. and Wilchem,E., "High precision determination of Henry's constants for methane and ethane in liquid water at 275 and 328 K", J.Phys.Chem., **85**, 3230(1981).

54. Crovetto,R., Fernandez-Prini,R. and Japas,M.-L., "Solubilities of inert gases and methane in H_2O and D_2O in the temperature range of 300 to 600 K", J.Chem.Phys., **76**, 1077(1982).

55. Huang,S., Leu,A.-D., Ng,H.-J. and Robinson,D.B., "The two-phase behavior of two mixtures of methane, carbon dioxide, hydrogen sulfide and water", Fluid Phase Equilibria, **19**, 21(1985).

56. Heidman,J.L., Tsonopoulos,C., Brady,C.J. and Wilson,G.M., "High-temperature mutual solubilities of hydrocarbons and water. Part II:Ethylbenzene, ethylcyclohexane and n-octane", AIChE J., **31**, 376(1985).

Sources of experimental VLE methanol-hydrocarbon data

1. Benedict,M., Johnson,C.A., Solomon,E. and Rubin,L.C., "Separation of toluene from paraffins by azeotropic distillation with methanol", Trans.AIChE, **41**, 371(1945).

2. Berthod,A. and Armstrong,D.W., "Centrifugal partition chromatography. VI. Temperature effects", J.Liq.Chromatography, **11**, 1457(1988).

3. Bezdel,L.S. and Teodorovich,V.P., "Solubility of carbon dioxide ...", Gaz. Promst., **8**, 38(1958).

4. Brunner,E., "Fluid mixtures at high pressures. I. Phase separation and critical phenomena of ten binary mixtures of (a gas+methanol)", J.Chem.Thermodynamics, **17**, 671(1985).

5. Brunner,E., Hueltenschmidt,W. and Schlichtaerle,G., "Fluid mixturres at high pressures. IV. Isothermal phase equilibria in binary mixtures consisting of (methanol+hydrogen or nitrogen or methane or carbon monoxide or carbon dioxide)", J.Chem.Thermodynamics, **19**, 273(1987).

6. Budantseva,L.S., Lesteva,T.M. and Nemtsov,M.S., "Liquid-vapor equilibria in systems comprising methanol and C_5 Hydrocarbons of different classes", Russ.J.Phys.Chem., **49**, 1088(1975).

7. Budantseva,L.S., Lesteva,T.M. and Nemtsov,M.S., "Liquid-vapour equilibria in systems comprising methanol and C_6 hydrocarbons of different classes", Russ.J.Phys.Chem., **49**, 155(1975).

8. Budantseva,L.S., Lesteva,T.M. and Nemtsov,M.S., "Liquid-vapor equilibria in systems comprising methanol and C_7 and C_8 Hydrocarbons of different classes", Russ.J.Phys.Chem., **49**, 1087(1975).

9. Chang,T. and Rousseau, R.W., "Solubilities of carbon dioxide in methanol and methanol-water at high pressures: Experimental data and modelling", Fluid Phase Equilibriam **23**, 243(1985).

10. Churkin,V.N. et al, "Liquid-vapour equilibria in C4 hydrocarbon-methanol systems", Russ. J.Phys.Chem., **52**, 278(1978).

11. Clark,W.M. and Rowley,R.L., "The Mutual diffusion coefficient of methanol-n-hexane near the consolute point", AIChE J., **32**, 1125(1986).

12. Ferguson,J.B., "The system methylalcohol-n-hexane at 45 degrees", J.Phys.Chem., **36**, 1123(1932).

13. Francesconi,A.Z., Lentz,H. and Franck,E.U., "Phase equilibria and PVT data for the methane-methanol system to 300 MPa and 240 C", J.Phys.Chem., **85**, 3303(1981).

14. Galivel-Solastiouk,F., Laugier,S. and Richon,D., "Vapor-liquid equilibrium data for the propane-methanol and propane-methanol-carbon dioxide system", Fluid Phase Equilibria, **28**, 73(1986).

15. Gjaldbaek,J.C. and Niemann,H., "The solubility of nitrogen, argon and ethane in alcohols and water", Acta Chemica Scand., **12**, 15(1958).

16. Hemmaplardh,B. and King,A.D., "Solubility of methanol in compressed nitrogen, argon, methane, ethylene, ethane, carbon dioxide and nitrous oxide. Evidence for association of carbon dioxide with methanol in the gas phase", J.Phys.Chem., **78**, 2170(1972).

17. Hoelscher,I.F., Schneider,G.M. and Ott,J.B., "Liquid-liquid phase equilibria of binary mixtures of methanol with hexane, nonane and decane at prressures up to 150 MPa", Fluid Phase Equilibria, **27**, 153(1986).

18. Hong,J.H. and Kobayashi, R., "Vapor-liquid equilibrium studies for the carbon dioxide-methanol system", Fluid Phase Equilibria, **41**, 269(1988).

19. Hong,J.H., Malone,P.V., Jett,M.D. and Kobayashi,R., "The measurement and interpretation of the fluid-phase equilibria of a normal fluid in a hydrogen bonding solvent: The methane-methanol system", Fluid Phase Equilibria, **38**, 83(1987).

20. Hwang,C. and Robinson,R.L.Jr., "Vapor-liquid equilibria at 25 C for nine alcohol-hydrocarbon binary systems", J.Chem.Eng.Data, **22**, 319(1977).

21. Katayama,T. and Nitta,T., "Solubilities of hydrogen and nitrogen in alcohols and n-hexane", J.Chem.Eng.Data, **21**, 194(1976).

22. Kiser,R.W., Johnson,G.D. and Shetlar,M.D., "Solubilities of various hydrocarbons in methanol", J.Chem.Eng.Data, 6, 338(1961).

23. Kretschmer,C.B. and Wiebe,R., "Solubility of gaseous paraffins in methanol and isopropyl alcohol", J.Am.Chem.Soc., **74**, 1276(1952).

24. Kretschmer,C.B., Nowakowska,J. and Wiebe,R., "Solubility of oxygen and nitrogen in organic solvents from -25 to 50 C", Ind.Eng.Chem., **38**, 506(1946).

25. Krichevsky,I.R. and Lebedeva,E.S. "-", Zh.Fiz.Khim., **21**, 715(1947).

26. Luehring,P. and Schumpe,A., "Gas solubilities(H2, He, N2, CO, O2, Ar, CO2) in organic liquids at 293.2 K", J.Chem.Eng.Data, **34**, 250(1989).

27. Ma,Y.H. and Kohn,J.P., "Multiphase and volumetric equilibria of the ethane-methanol system at temperatures between -40 and 100 C", J.Chem.Eng.Data, **9**, 3(1964).

28. Miyano,Y. and Hayduk,W., "Solubility of butane in several polar and nonpolar solvents and in - acetone-butanol solvent solution", J.Chem.Eng.Data, **31**, 77(1986).

29. Nagahama,K., Suda,S. Hakuta,T. and Hirata,M., "Determination of vapor-liquid equilibrium drom total pressure measurement. C3 Hydrocarbon/solvent", Sekiyu Gakkai Shi(Tokyo, Japan), **14**, 252(1971).

30. Noda,K., Sato,K. and Nagatsuka,K., "Ternary liquid-liquid equilibria for the systems of aqueous methanol solutions and propane or n-butane", J.Chem.Eng.Japan, **8**, 492(1975).

31. Ohgaki,K. and Katayama,T., "Isothermal vapor-liquid equlibrium data for binary systems containing carbon dioxide at high pressures: methanol-carbon

dioxide, n-hexane-carbon dioxide, and benzene-carbon dioxide systems", J.Chem.Eng.Data, **21**, 53(1976).

32. Ohgaki,K., Sano,F. and Katayama,T., "Isothermal vapor-liquid equilibrium data for binary systems containing ethane at high pressures", J.Chem.Eng. Data, **21**, 55(1976).

33. Ott,J.B., Hoelscher,I.F. and Schneider,G.M., "(Liquid-liquid) phase equilibria in (methanol+heptane) and (methanol+octane) at pressures form 0.1 to 150 MPa", J.Chem.Thermodynamics, **18**, 815(1986).

34. Raal,J.D., Russel,K.C. and Best,D.A., "Examination of ethanol-n-heptane, methanol-n-hexane systems using new vapor-liquid equilibrium still", J.Chem.Eng.Data, 17, 211(1972).

35. Rousseau,R.W., Matange,J.N. and Ferrell,J.K., "Solubilities of carbon dioxide, hydrogen sulfide and nitrogen mixtures in methanol", AIChE J., **27**, 605(1981).

36. Semenova,A.I. et al, "Phase equilibria in the methanol-carbon dioxide system", Russ.J.Phys.Chem., **53**, 1428(1979).

37. Shenderei,E.R., Zelvenskii,Y.D. and Ivanovskii,F.P., "Solubility of carbon dioxide in methanol at low temperatures and high pressures", Khim. Prom., **4**, 328(1959).

38. Short,I., Sahgal,A. and Hayduk,W., "-",J.Chem.Eng.Data, **28**, 63(1983).

39. Suzuki, K. et al, "Isothermal vapor-liquid equilibrium data for binary systems at high pressures: Carbon-dioxide methanol, ...", J.Chem.Eng.Data, **35**, 63(1990).

40. Takeuchi,K., Matsumura,K. and Yaginuma,K., "Vapor-liquid equilibria for multicomponent systems containing methanol-acid gases", Fluid Phase Equilibria, **14**, 255(1983).

41. Tenn,F.G. and Missen,R.W., "A study of the condensation of binary vapors of miscible liquids", Can.J.Chem.Eng., Feb. 1963.

42. Varym-Agaev,N.L. et al, "-", Zh.Prikl.Khim., **58**, 165(1985).

43. Vorizane,M.S., Adadmoto,S., Masuoka,H. and Eto,Y., "Gas solubilities in methanol at high pressures", Kogyo Kogaku Zashi, **72**, 2174(1969).

44. Weber,W., Zeck,S. and Knapp,H., "Gas solubilities in liquid solvents at high pressures: apparatus and results for binary and ternary systems of N_2, CO_2 and CH_3OH", Fluid Phase Equilibria, **18**, 253(1984).

45. Zeck,S. and Knapp,H., "Solubilities of ethylene, ethane, and carbon dioxide in mixed solvents consisting of methanol, acetone and water", Int.J.Thermophysics, **6**, 643(1985).

46. Zeck,S. and Knapp,H., "Vapor-liquid and vapor-liquid-liquid-liquid phase equilibria for binary and ternary systems of nitrogen, ethane and methanol: experimental data and and data reduction", Fluid Phase Equilibria, **25**, 303(1985).

47. Schneider,R., "Experimentelle bestimmung der dynamischen viscositaet von fluessigkeitsgemishen aus methanol mit CO_2, CH_4, C_2H_6 und C_3H_8", Doctoral Dissertation, Technishe Universitaet Berlin, Berlin(1978).

Sources of experimental VLE data for methanol-water mixtures

1. Dalager,P., "Vapor-liquid equilibria of binary systems of water with methanol and ethanol at extreme dilution of the alcohols", J.Chem.Eng.Data, 14, 299(1969).

2. Griswold,J. and S.Y.Wong, "Phase equilibria of the acetone-methanol-water system from 100°C into the critical region", AIChE Symp. Ser., 48, 18(1952).

3. Kato,M., Konishi,H. and Hirata,M., "New apparatus for isobaric dew and bubble point method",J.Chem.Eng.Data, 15, 435(1970).

4. Kato,M., Konishi,H. and Hirata,M., "Apparatus for measurement of isobaric dew and bubble points and vapor-liquid equilibria",J.Chem.Eng.Data, 15, 501(1970).

5. Kooner,Z.S., Phutela,R.C. and Fenby,D.V., "Determination of the equilibrium constants of water-methanol deuterium exchange reactions from vapor pressure measurements", Aust.J.Chem., 33, 9(1980).

6. Maripuri,V.O. and Ratcliff,G.A., "Measurement of isothermal vapor-liquid equilibria for acetone-n-heptane mixtures using modified Gillespie still", J.Chem.Eng.Data, 17, 366(1972).

7. McGlashan,M.L. and Williamson,A.G., "Isothermal liquid-vapor equilibria for system methanol-water", J.Chem.Eng.Data, 21,196(1976).

Sources of experimental data for the freezing point of methanol-water mixtures

1. Miller,G.A. and Carpenter,D.K., "Solid-liquid phase diagram of the system methanol-water", J.Chem.Eng.Data, **9**,371(1964).

2. Ross,H.K., "Cryoscopic studies: Concentrated solutions of hydroxycompounds", Ind.Eng.Chem., **46**, 601(1954).

Sources of experimental VLE data for mixtures containing methanol, water and hydrocarbons

1. Chen,C.J., Ng,H.-J. and Robinson,D.B., "The solubility of methanol or glycol in water-hydrocarbon systems", GPA RR-117, Tulsa(1988).

2. Ng,H.J. and Robinson,D.B., "Equilibrium phase composition and hydrating conditions in systems containing methanol, light hydrocarbons, carbon dioxide and hydrogen sulfide", GPA RR-66, Tulsa(1983).

3. Ng,H.-J., Chen,C.J. and Robinson,D.B., "Hydrate formation and equilibrium phase composition in the presence of methanol: Selected systems containing hydrogen sulfide, carbon dioxide, ethane of methane", GPA RR-87, Tulsa(1987).

CHAPTER II

DETERMINATION OF KIHARA POTENTIAL PARAMETERS FROM GAS HYDRATE DATA

2.1. Introduction

Gas hydrates of water are crystalline compounds stabilized by inclusion of small gas molecules inside cavities formed by water molecules. They resemble ice in appearance, but unlike ice they may form at temperatures well above the ice point. The most common gas hydrates exist in either of two distinct structures, each of which contains two different types of cavities. The thermodynamic properties of gas hydrates may be predicted from the ideal solid solution theory presented by van der Waals and Platteeuw(1959). These authors have conceived each cavity as a spherical cage which may contain only one gas molecule. Only gas-water interactions were allowed which were described by the Lennard-Jones 12-6 potential. Subsequently, McKoy and Sinanoglu(1963) have demonstrated that application of the Kihara potential with a spherical core yields improved predictions of hydrate dissociation pressures. Both of the above works use gas-water potential parameters obtained from second virial coefficient data for gas parameters, constant values for water parameters along with the hard sphere mixing rule for the size parameter and the geometric mean approximation for the energy parameter.

Saito et al(1964) were the first to adjust the potential parameters to fit experimental hydrate dissociation pressures of pure gases. This approach was shown to result in a substantial improvement in predictions and it has been adopted in most subsequent works. Hŏwever, there is hardly any agreement in the published values of the parameters (Parrish and Prausnitz, 1972; Anderson and Prausnitz,1986, Sloan,1990) although, presumably, they have all been obtained from the same data, which are available in the open literature.

The present work attempts to elucidate the nature of the problem and to present a consistent methodology for obtaining the potential parameters from experimental hydrate equilibrium data. Following a recommendation by Holder and Hand(1982), we restrict this study to the distance and energy parameters only.

We obtain values of the core diameter from second virial coefficient data. The proposed scheme is supported by favourable comparisons of predictions with experimental hydrate equilibrium data of multicomponent and real systems. For nearly perfect gases, predicted second virial coefficients also agree well with experimental data.

2.2. Thermodynamic Description of the Hydrate Phases

The basic equations of the theory presented by van der Waals and Platteeuw(1959) relate the chemical potential of water in a hydrate phase μ_w^H to that in the hypothetical empty hydrate lattice μ_w^β :

$$\mu_w^H = \mu_w^\beta - RT\sum_m \nu_m \ln(1+\sum_j C_{jm} f_j) \qquad (2.1)$$

where R is the gas constant, T is the absolute temperature, ν_m is the number of cavities of type m per water molecule in the unit cell, f_j is the fugacity of the gas component j in the hydrate phase. At equilibrium it is equal to that of the same component in any other coexisting phase. C_{jm} is a Langmuir type constant which depends on temperature according to the relation:

$$C_{jm}(T) = \frac{4\pi}{kT}\int_0^\infty \exp(-\frac{w(r)}{kT}) r^2 dr \qquad (2.2)$$

where k is Boltzmann's constant and w(r) is the spherically symmetric cell potential function of the cell radius r. Following the suggestion of McKoy and Sinanoglu(1963), we use the Kihara potential with a spherical core:

$$U(r)=\infty \,,\ r \le 2\alpha$$

$$U(r)=4\varepsilon\left[\left(\frac{\sigma^*}{r-2\alpha}\right)^{12}-\left(\frac{\sigma^*}{r-2\alpha}\right)^{6}\right] \,,\ r>2\alpha \qquad (2.3)$$

where α is the core radius, $\sigma=\sigma^*+2\alpha$ is the collision diameter and ε is the depth of the energy well. The chemical potential of the empty hydrate lattice is a function of temperature and pressure only and it is given by the following equation(Holder et al, 1980):

$$\frac{\mu_w^{\beta}(T,P)}{RT} = \frac{\mu_w^{\alpha/L}(T,P)}{RT} + \frac{\Delta\mu_w^0}{RT_0} - \int_{T_0}^{T} \frac{\Delta h_w^{\beta-\alpha/L}}{RT^2} dT + \int_0^P \frac{\Delta v_w^{\beta-\alpha/L}}{RT} dP \qquad (2.4)$$

where $\mu_w^{\alpha/L}$ is the chemical potential of pure water in the ice or the liquid state depending on the temperature, P is the equilibrium pressure and T_0 is the absolute temperature at the ice point. $\Delta v_w^{\beta-\alpha/L}$ are molar volume differences between an empty hydrate lattice and ice or liquid water. We have obtained the molar volumes of hydrate I and II by fitting the X-ray diffraction data of Davidson et al(1986,1987) to the equation $v=v_0[1+k_1(T-T_0)+k_2(T-T_0)^2+k_3(T-T_0)^3]$. The numerical values of the parameters of this equation are given in Table 1 along with the corresponding values for ice and liquid water.

Table 2.1. Values of the parameters of the molar volume of water function of temperature

Water Form	T Range,K	v_0, cc/mol	$k_1 x 10^4$, K^{-1}	$k_2 x 10^7$, K^{-2}	$k_3 x 10^{10}$, K^{-3}
Ice I[1]	100-273	19.6522[4]	1.6070	3.4619	-0.2637
Hydrate I[2]	100-273	22.35[5]	3.1075	5.9537	1.3707
Hydrate II[2]	100-273	22.57[6]	1.9335	2.1768	-1.4786
Liquid[3]	273.2-300	18.0182	-0.6427	85.053	-679.0

[1]Calculated from data of Leadbetter(1965). [2]Calculated from data of Davidson et al(1987). [3]Smithsonian Tables, Table 269. [4]Ginnings and Gorruccini(1947).[5]Calculated assuming a(0°C)=11.95A for the empty lattice(Davidson et al,1987). [6]Calculated assuming a(0°C)=17.21A for the empty lattice(Davidson et al,1986).

The molar enthalpy differences between an empty hydrate lattice and ice are functions of temperature:

$$\Delta h_w^{\beta-\alpha/L} = \Delta h_w^0 + \Delta h_w^f + \int_{T_0}^{T} \Delta c_{p_w}^{\beta-\alpha/L} dT \qquad (2.5)$$

where Δh_w^f is the molar difference in enthalpy between ice and liquid water. At temperatures below the ice point it is set equal to zero. $\Delta c_{p_w}^{\beta-\alpha/L}$ is the heat capacity difference between the empty hydrate and ice(α) or water(L), as appropriate. For the heat capacity difference between ice and liquid water we use the equation recommended by Holder et al(1980) in cal/mol/K:

$$\Delta c_{p_w}^{\alpha-L} = -9.05+0.0423(T-T_0)\ ,\ T>T_0 \qquad (2.6a)$$

For the heat capacity difference between hydrate structure I and II and ice, we have regressed the following equations in cal/mol/K, by a procedure detailed in Chapter IV:

$$\Delta c_{p_w}^{\beta^I-\alpha} = 0.2606-0.00043(T-T_0) \qquad (2.6b)$$

$$\Delta c_{p_w}^{\beta^{II}-\alpha} = 0.3542+0.0040(T-T_0) \qquad (2.6c)$$

Equations (6b, c) have been derived from ethane and propane data respectively and they are meant to be applicable for systems containing these components. For pure gases of relatively small molecules, like methane, nitrogen etc, the heat capacity difference between the empty hydrate lattice and ice is set equal to zero. $\Delta\mu_w^0$ and Δh_w^0 are respectively chemical potential and enthalpy differences between the empty hydrate lattice and ice at the ice point and zero pressure. We use the values obtained experimentally by Dharmawardhana et al(1980). Equations (1) through to (4) give the value of the chemical potential of water in the hydrate phase relative to that of a pure water phase as a function of temperature, pressure and hydrate composition(implicitly). The corresponding fugacity of water in the hydrate phase may be obtained from:

$$f_w^H = f_w^{\alpha/L} \exp\left[\frac{\Delta\mu_w^{H-\alpha/L}}{-RT}\right] \qquad (2.7)$$

where $f_w^{\alpha/L}$ is the fugacity of pure water in its stable state at T and P and $\Delta\mu_w^{H-\alpha/L}$ is the chemical potential difference between hydrate and pure water in the ice or liquid state, depending on temperature.

The mole fractions of gases in a hydrate phase are calculated from the equations:

$$x_i^H = \frac{\sum_m \nu_m \Theta_{im}}{1+\sum_m \sum_j \nu_m \Theta_{jm}} \tag{2.8a}$$

where

$$\Theta_{im} = \frac{C_{im} f_i}{1+\sum_j C_{jm} f_j} \tag{2.8b}$$

The fugacities of any component in the vapour and liquid phases are calculated from a cubic equation of state with the density-dependent mixing rules developed in the present study as presented in Chapter I. The fugacity of ice is calculated by correcting the saturation fugacity at the same temperature by the Poynting factor.

2.3. Determination of Kihara Potential Parameters

Kihara potential parameters of pure gases from second virial coefficient and viscosity data have been reported by Tee et al(1966). However, more recent experimental second virial coefficient data indicate the necessity for a new determination of Kihara parameters. We determined parameters α, σ and ε/k from the compilation of second virial coefficient data of Dymond et al(1985) and Dymond and Smith(1980,1968). The relative equations, originally derived by Kihara(1951), are listed in Appendix B. We used the most recent compilation of data, unless it is otherwise specified. The results appear in Table 2 together with the quality of the fit in AAD%. It is noted that in certain cases our values are significantly different from those reported by Tee et al(1966).

We have obtained values of the Kihara potential parameters for gas-water interactions by matching experimental hydrate dissociation point data in the V-Lw-H region in the following manner: At the experimental conditions of temperature and pressure, we perform a two phase V-Lw flash calculation of a mixture of a single gas and water. The Kihara collision diameter σ^* is fixed to an arbitrary value and the energy parameter ε is adjusted so that the fugacity of water in the hydrate phase matches the fugacity of water in either of the two other equilibrium phases obtained from the flash calculation. The convergence criterion is: $e=\ln(f_w^H/f_w^V)<10^{-8}$. A series of such calculations are carried out for several values of σ^* and the obtained values of ε are plotted against σ^*. The same procedure is repeated for other experimental hydrate dissociation points.

Table 2.2. Kihara Potential Parameters from Second Virial Coefficient Data

Component	α,Å	σ*, Å	ε/k, K	AAD %
Xenon[1]	0.327(0.286)[2]	3.156(3.308)	315.4(298.15)	0.49
Methane	0.295(0.393)	3.067(2.779)	199.3(227.13)	2.7
Ethane	0.488(0.463)	3.331(2.578)	338.4(496.69)	0.51
Propane	0.730(0.737)	2.908(3.137)	547.2(501.89)	0.42
iso-Butane	0.798(-)	2.570(-)	789.8(-)	6.4
nButane	1.029(0.939)	2.724(2.839)	721.6(701.15)	0.58
Nitrogen	0.335(0.000)	2.845(3.694)	136.7(96.26)	1.4
Carbon Dioxide[3]	0.753(0.716)	2.349(2.328)	420.3(424.16)	1.1
Hydrogen Sulfide[4]	0.7178(-)	1.710(-)	737.5(-)	0.44

[1]From the data for xenon of Dymond and Smith(1969). [2]Values in parentheses have been reported by Tee et al(1966). [3]From the data of Lichtenhaler et al(1969) and Waxman et al(1973). [4]Insufficient and probably inadequate data(Dymond, 1980).

Xenon and Water

At a fixed temperature the equilibrium pressure of binary systems is constant in the three phase equilibria region and it is fairly easy to obtain highly accurate experimental hydrate dissociation points for single gases. Dissociation points of the xenon hydrate in the three phase V-Lw-H region have been reported by Ewing and Ionescu(1974). Determinations of potential parameters for two dissociation points are presented in Figure 1a. It is seen that there is an infinite set of pairs of potential parameters, such that the experimental hydrate dissociation points are exactly matched. The pairs of optimum parameters appear to be independent of temperature. This behaviour is common to all simple hydrates and it relates to the particular mathematical form of the potential function. Though it may be possible to prove this phenomenon by analytical techniques, the graphical approach presented here is much easier to implement. It is concluded therefore that *in no case can the correct values of the potential parameters be obtained from dissociation points of simple gas hydrates alone.*

Figure 1b shows at 273.15 and 279.15 K the calculated hydrate numbers and cavity occupancy ratios (θ_1/θ_2) of xenon hydrate in the three phase region as functions of the set of pairs (σ^*,ε) obtained from dissociation pressure data. The values of the composition and the occupancy ratio of xenon hydrate obtained

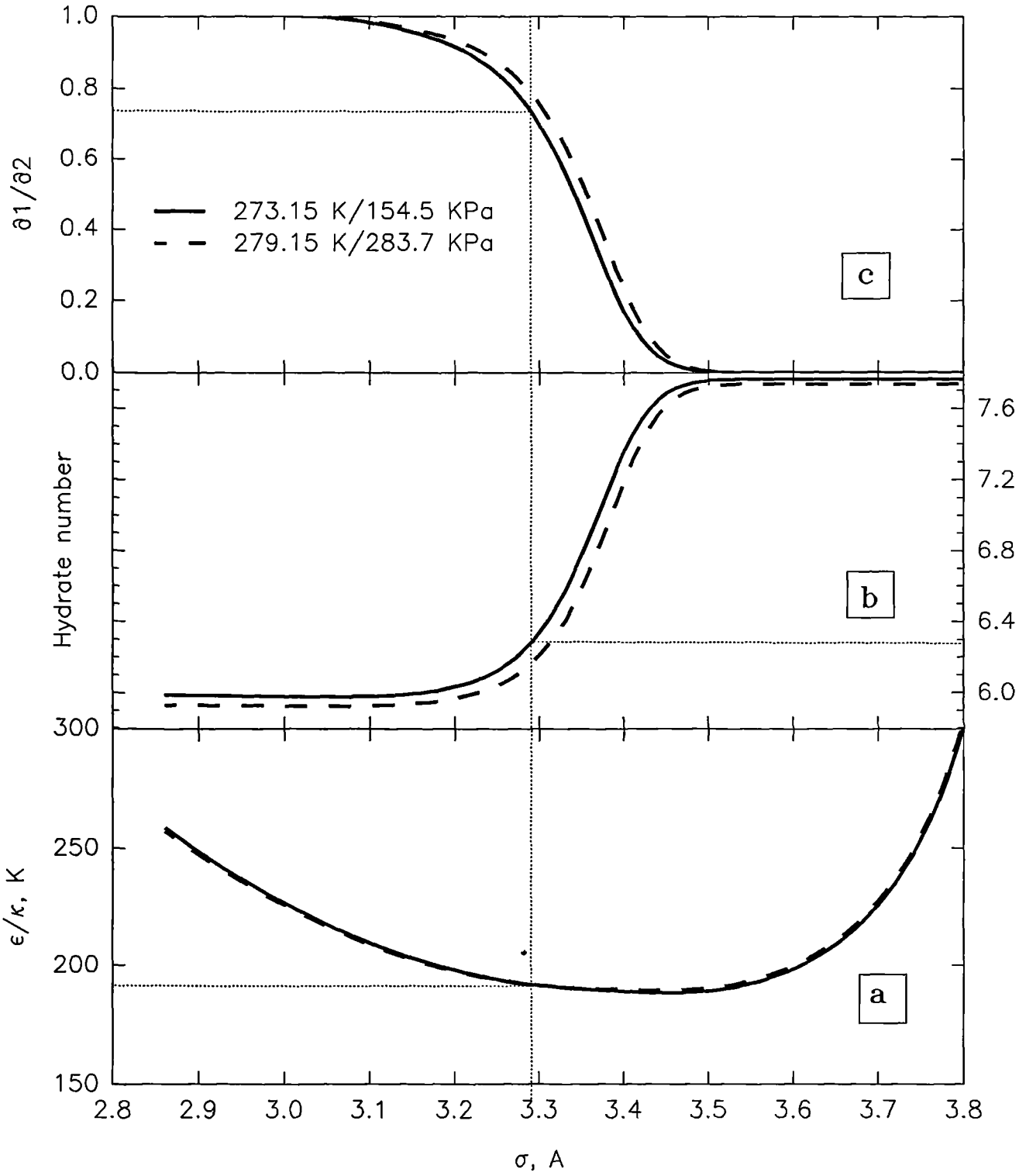

Figure 2.1. Calculated hydrate numbers(b) and cavity relative occupancies(c) of xenon hydrate from pairs of Kihara potential parameters optimized from dissociation point data(a).

experimentally by Davidson et al(1986) are also indicated. It is seen that *one single pair of potential parameters matches the experimental dissociation pressure, the composition and the cavity occupancy ratio* without any bias and within the uncertainties reported by the experimentalists. This observation is concrete proof of the validity of the ideal solid solution theory of gas hydrates(van der Waals and Platteeuw,1959) at least for small spherical molecules. The optimum values of the Kihara potential parameters for xenon-water interactions and the associated uncertainties are σ^*=3.291±0.006 Å and ε/k=191.6±0.3 K. It is noted that uncertainties in the experimental composition result in uncertainties in the values of the potential parameters of the same level with those caused by uncertainties in the experimental cavity occupancy ratio.

The parameters for xenon-water interactions may be used to calculate the Kihara potential parameters of water from the values of the corresponding parameters of pure xenon gas, obtained from second virial coefficient data. Assuming that the hard-sphere and the geometric mean approximations are effective, i.e. $\sigma_{AB}^*=(\sigma_A^*+\sigma_B^*)/2$ and $\varepsilon_{AB}=(\varepsilon_A\varepsilon_B)^{1/2}$, we obtain for water: σ_W=3.426 Å and ε_W/k=116.4 K.

Ethane and propane

The set of Kihara potential parameters obtained from two hydrate dissociation points of ethane are depicted in Figure 2a. As was the case with xenon, the correct unique values of the potential parameters can not be determined from hydrate dissociation points alone. Figure 2b shows calculated Langmuir constants of ethane hydrate in the large cavity of structure I at two different T,P conditions as function of the corresponding optimum potential parameters. Since any pair of these potential parameters produces the same value of the Langmuir constant, it is concluded that, unlike xenon, the correct values of the potential parameters of ethane *can not be obtained from any hydrate dissociation pressure and composition data.* Any choice of Kihara parameters of ethane from the set obtained from dissociation points is expected to reproduce the dissociation points and predict the hydrate composition as well.

Figure 3 shows the spherically symmetrical potential in the large cavity of the structure I hydrate of ethane, for two different optimum pairs of Kihara potential parameters, from those depicted in Figure 2a. For the first pair (solid line), we use the value of the Kihara distance parameter σ^* obtained from the values in Table 1 and the corresponding parameter of water, by using the hard sphere approximation. Conversely, for the second pair (dashed line), the energy

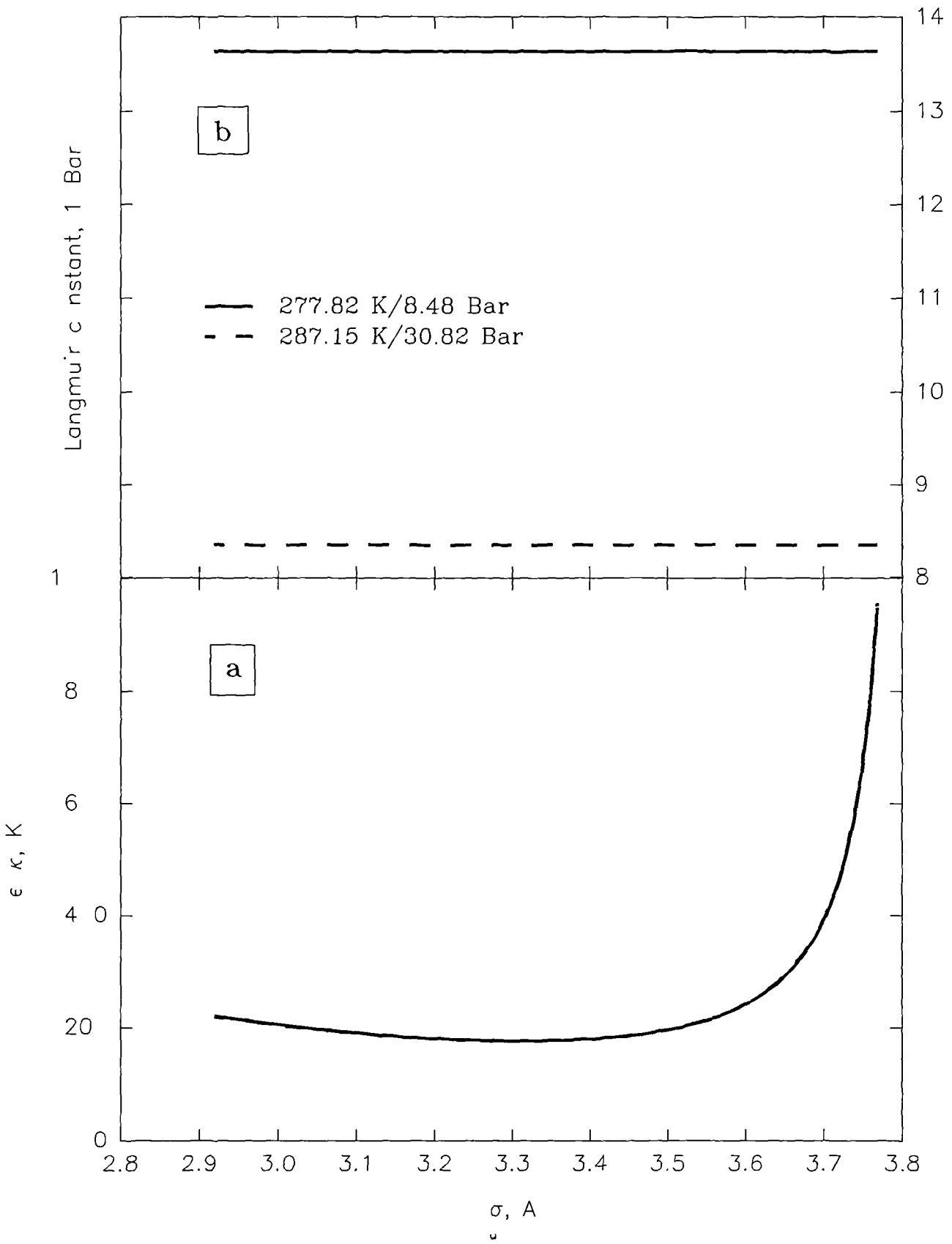

Figure 2.2. Calculated Langmuir constants(b) in the large cavity of ethane hydrate from optimum Kihara potential parameters(a).

parameter was fixed from the value in Table 1 and the parameter of water, by using the geometric mean approximation. According to van der Waals(1961), differences in the shape of the field within the cage will be reflected in differences in heat capacities. The same author argues that "the heat capacity provides a very sensitive experimental criterion for the distance parameter while it hardly depends on the energy parameter". We have, therefore, optimized the Kihara potential parameters of ethane from mixed dissociation and heat capacity data. In doing so it has been necessary to optimize simultaneously with the potential parameters the heat capacity of the (hypothetical) empty hydrate lattice. This procedure is detailed in Chapter IV. The regressed value for the distance parameter was very close to that obtained by the arithmetic mean approximation and it was fixed to the last value. The optimum value obtained for the energy parameter, however, is significantly different from the one listed in Table 1. Consequently, the calculated virial coefficients of ethane from Kihara parameters obtained from hydrate data differ from experimental values about 50%. We attribute this discrepancy to a failure of the classical mixing rules. A successful alternative, however, does not exist. For heavier molecules, therefore, the effort to match the Kihara parameters from virial coefficient data has been abandoned.

The parameters for propane-water interactions could not be found as accurately as those of ethane, although propane is expected to behave in a similar manner. This is because of the very large hydrate number of the structure II simple hydrate of propane (17 moles of water per mole of guest), makes the regression routine almost insensitive to the heat capacity contribution of the guests.

Methane, Nitrogen ,Carbon Dioxide and Hydrogen Sulfide

Small molecules capable of entering all cavities exhibit the same behaviour as xenon. Since highly accurate hydrate compositions and distribution ratios in the cavities data are not currently available for these gases, Kihara potential parameters can not be obtained in a manner similar to that of xenon. Here we adopt a different approach. In Figure 4a we plot the function $\varepsilon/k=f(\sigma^*)$ of the pairs of energy and distance parameters of methane which match dissociation points of pure methane, methane/ethane (structure I) and methane/propane (structure II) mixtures. The potential parameters of ethane and propane were fixed as detailed above. It is noted that within a very small range of potential parameters, all three dissociation points are matched. It is believed that the region defined by the three curves would have collapsed to a single point if the data were of sufficient accuracy.

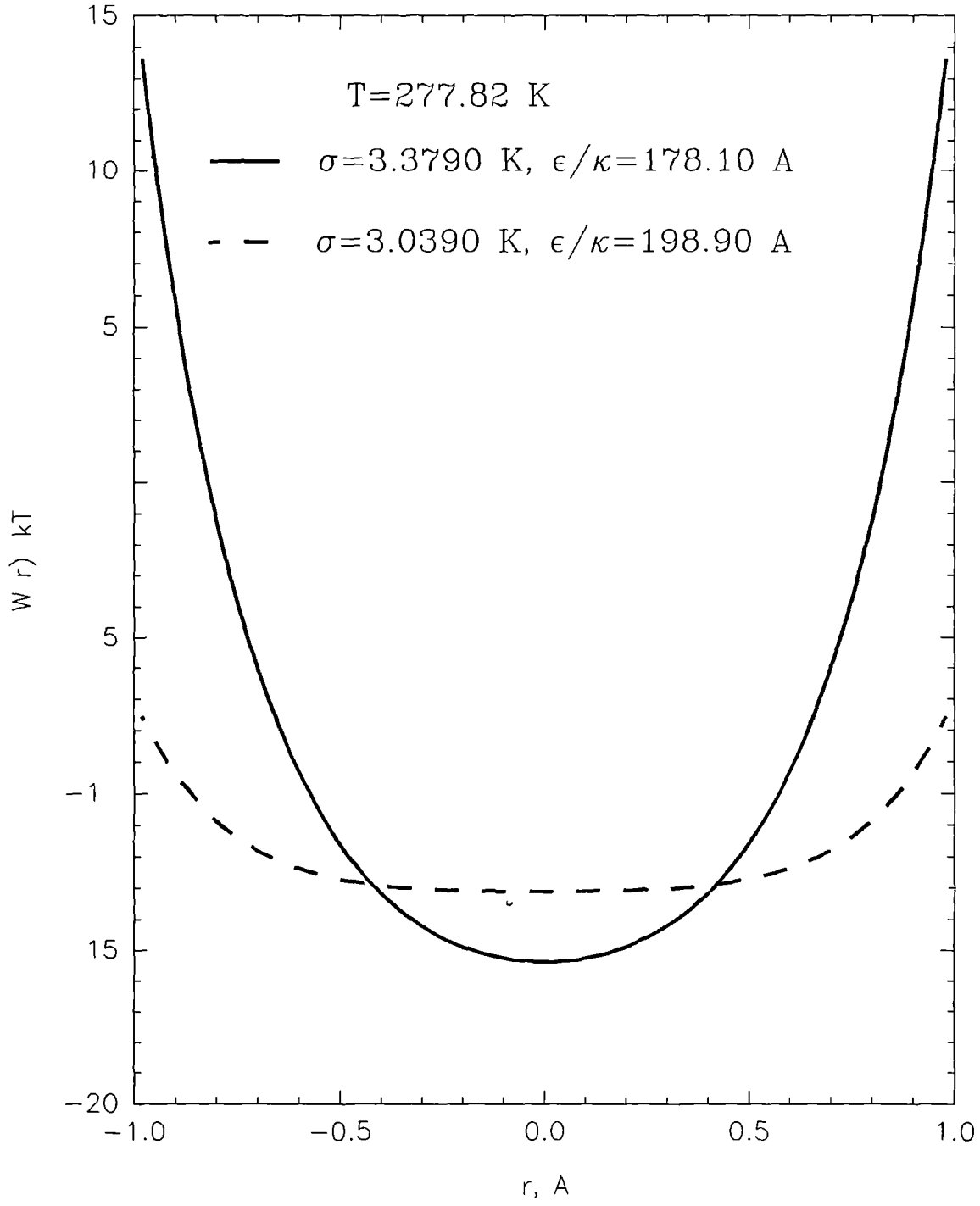

Figure 2.3. Cell potential in the large cavity of structure I hydrate of ethane calculated from two pairs of optimum Kihara potential parameters, for the dissociation pressure.

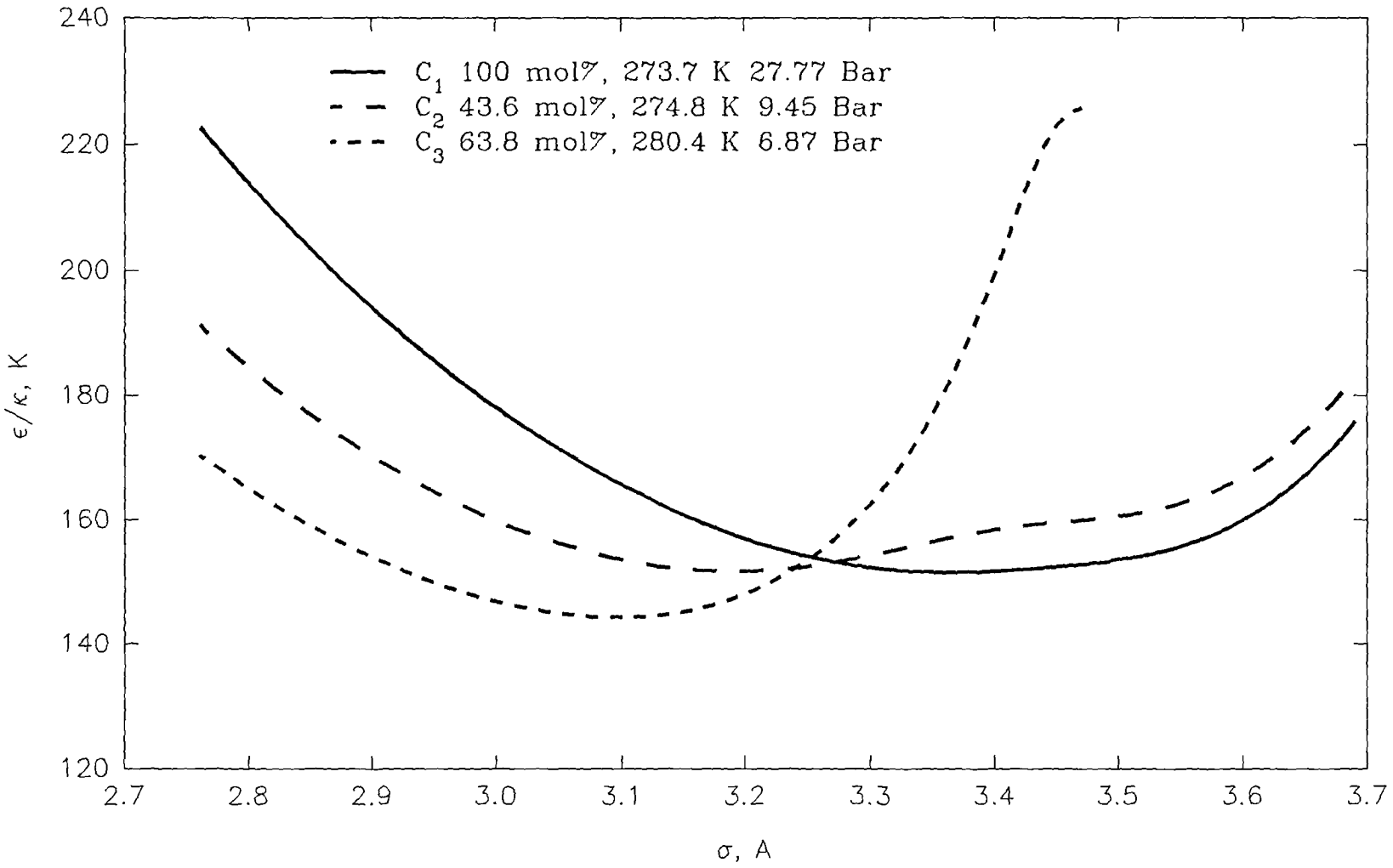

Figure 2.4a. Determination of the Kihara potential parameters of methane from hydrate dissociation point data.

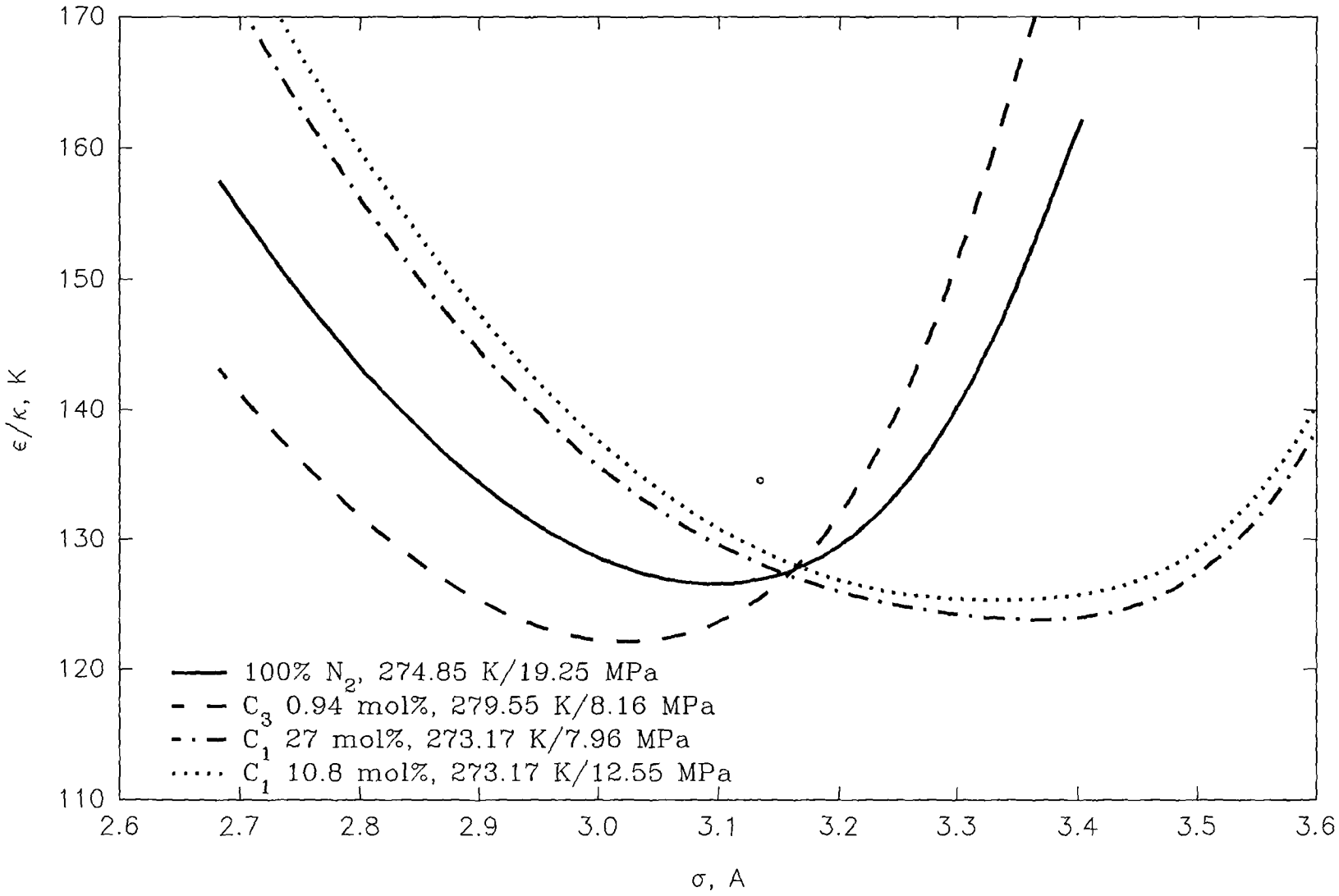

Figure 2.4b. Determination of the Kihara potential parameters of nitrogen from hydrate dissociation point data.

The parameters of methane were obtained by forcing agreement of predictions with all hydrate dissociation point data, retrieved from Sloan(1990), of pure methane and its binary mixtures with ethane (structure I) and propane (structure II). Data have been appropriately weighed so that each of the three sets of data gets equal importance. Similar approach was followed for nitrogen (Figure 4b), carbon dioxide and hydrogen sulfide. It is noted that no binary data of these gases with ethane are available in the open literature. All the potential parameters for gas-water interactions obtained in the course of this study are listed in Table 3, along with the quality of the fit in AAD%.

Table 2.3. Kihara potential parameters for gas-water interactions, obtained from gas-hydrate data.

Component	σ*, Å	ε/k, K	AAD %
Xenon	3.291	191.6	0.04
Methane	3.250	153.8	3.5
Ethane	3.379	178.1	3.4
Propane	3.608	195.3	4.2
Nitrogen	3.190	127.8	4.5
Carbon Dioxide	2.903	172.5	5.7
Hydrogen Sulfide	2.822	216.4	7.3

In Figures 5a, b and c we compare experimental second virial coefficient data for methane, xenon and nitrogen with predictions, calculated from the Kihara parameters in Table 2 along with the hard sphere and the geometric mean mixing rules for gas-water interactions. Good agreement is obtained, which justifies the use of the mixing rules for these gases and proves the validity of the proposed methodology. Further evidence is gained by comparing the calculated composition of methane hydrate with the experimental value 0.1429±0.0002 mole fraction of methane reported by Handa(1986) at 253.0±0.5 K and 3.40±0.1 MPa. Our prediction is 0.1432±0.0001 at the hydrate point of the three phase V-I-H equilibria (253.0 K, 1.45 MPa) and it is within the error bounds of the experiment.

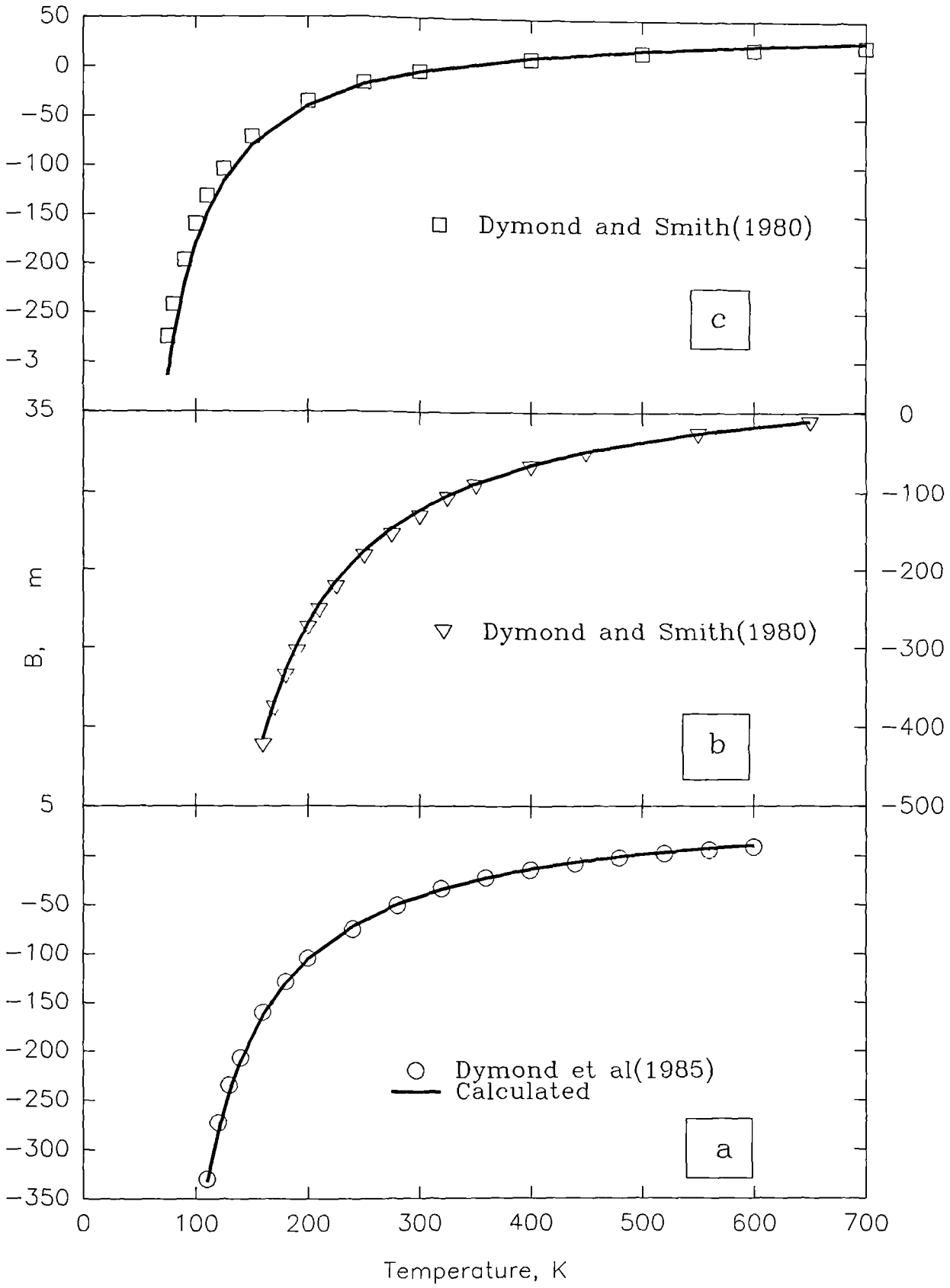

Figure 2.5. Comparison of virial coefficeints calculated from hydrate data with experimental measuremnts: (a) methane, (b) xenon and (c) nitrogen.

The Kihara potential parameters obtained for carbon dioxide-water interactions are not useful for prediction of second virial coefficient data. Conversely, the corresponding parameters obtained from fitting second virial coefficient data along with the hard sphere and geometric mean approximations are σ^*=2.666 Å and ε/k= 245.9 K and it is noted that they are significantly different from those listed in Table 2. Similar results were obtained for hydrogen sulfide, but in this case the experimental values of the second virial coefficients cannot be considered adequate.

2.4. Discussion

John (1982) questions the use of Kihara potential parameters of water in structure I to describe the structure II lattice. Because for krypton hydrate(the "perfect" structure II hydrate) there are not available accurate data corresponding to those of xenon, the significance of the suggestion of John (1982) cannot be accurately verified. However, since nitrogen also forms structure II hydrates and since a fair agreement (14.0 AAD%) has been obtained between the predicted virial coefficients obtained from hydrate data and the Kihara parameters of water in structure I hydrate, it is evident that Kihara parameters of water can be considered the same for both structures.

It is believed that the cause of the apparent failure of the corresponding states approach to obtain a consistent set of Kihara potential parameters from hydrate data for carbon dioxide, ethane and propane is the inadequacy of the traditional mixing rules for such molecules. It is known (see Hirschfelder et al, 1964) that these mixing rules fail to give reasonable results for mixtures of molecules very different in size and/or polarity. In these cases empirical modification of the mixing rules to incorporate higher order interactions might improve the representation of certain experimental data (Reddy et al, 1988) but with little theoretical or practical significance.

John et al(1985) have observed that there are several sets of Kihara parameters which can produce a single Langmuir constant so that correct values may not be achieved. To overcome the problem, they used a constrained optimization technique to fit experimental hydrate dissociation pressures with potential parameters close to those recommended by Tee et al(1966) from second virial coefficient data. Several binary mixtures of heavier hydrocarbons were regressed, by using the classical mixing rules and a generalized formula to adjust the Langmuir constant to fit experimental binary data. In doing so they have assumed that the values of potential parameters of individual gases

obtained from second virial coefficient and viscosity data are correct, the mixing rules are effective and that the cause of the discrepancies is the size and shape of the cage and the enclathrated molecule. However, they have reported very limited success in the prediction of dissociation pressures of multicomponent systems. The failure of their model is not surprising. As it is demonstrated in Chapter IV, the asymmetry of the cavities can be safely neglected, and the restriction of the motion of the enclathrated molecule as well as the subsequent distortion of the hydrate lattice have a comparatively small energetic effect. We conclude, therefore, that the difficulty to apply a corresponding states approach arises mainly from the inadequacy of the classical mixing rules.

The proposed procedure for obtaining correct values of the potential parameters of ethane could not be applied for propane. Also, for iso-butane and n-butane relevant heat capacity data are not available in the open literature. There is no other known technique to obtain the potential parameters for the interactions of these molecules with water, from the currently available physicochemical data.

2.5. Conclusions

It was demonstrated that the correct values of the potential parameters for gas-water interactions might not be obtained from dissociation pressure data alone. It was further shown that compositional data are not useful for obtaining these parameters for gases entering only the large cavity of either structure. Subsequently, correct values of the Kihara potential parameters of ethane for gas-water interactions, have been obtained and reported for the first time, by using the hydrate heat capacity data of this gas, reported by Handa(1986).

The corresponding states approach, used by several authors to obtain the correct values of the Kihara potential parameters for gas-water interactions was shown to be valid only for relatively small molecules. It was demonstrated that the Kihara potential parameters of water are the same for both structure I and II. However, lack of data for isobutane and n-butane did not permit the use of this finding to develop more appropriate mixing rules for the interaction of larger molecules with water in hydrate cavities. It is to be noted, however, that the normally incorrect values of the pairs of potential parameters for the heavier hydrocarbons, obtained simultaneously by fitting dissociation pressures and compositions, lead to the identical values of the Langmuir constant. Therefore they still reproduce dissociation pressures and compositions of simple gas hydrates and predict correctly these properties of mixed gas hydrates.

References

Anderson, F.E. and Prausnitz, J.M., "Inhibition of Gas Hydrates by Methanol", AIChE J., **32**(8),1321(1986).

Davidson,D.W., Handa,Y.P. and Ripmeester,J.A., "Xenon-129 and the thermodynamic parameters of xenon hydrate", J.Phys.Chem., **90**, 6549(1986).

Davidson,D.W., Handa,Y.P., Ratcliffe,C.I., Ripmeester,J.A., Tse,J.S. Dahn,J.R. Lee,F. and Calvert,L.D., "Crystallographic studies of clathrate hydrates", Mol.Cryst.Liq.Cryst., **141**, 141(1986).

Davidson,D.W., Desando,M.A., Gough,S.R., Handa,Y.P., Ratcliffe,C.I., Ripmeester,J.A. and Tse,J.S., "Some physical and thermophysical properties of clathrate hydrates", J.Inclusion Phenom., **5**, 219(1987).

Dharmawardhana, P.B., Parrish, W.R., Sloan, E.D., "Experimental Thermodynamic Parameters for the Prediction of Natural gas Hydrate Dissociation Pressures", IEC Fund., **19**, 410(1980).

Dymond,J.H., Cholinski,J.A., Szafranski,A. and D.Wyrzykowska-Stankiewicz, "Second virial coefficients for n-alkanes; Recommendations and predictions", in "Measurement, evaluation and prediction of phase equilibria", edited by Kehiaian and Renon, Elsevier, (1986).

Dymond,J.H. and Smith,E.B., "The virial coefficients of gases: a critical compilation", Clarendon Press, Oxford, (1969).

Dymond,J.H. and Smith,E.B., "The virial coefficients of pure gases and gas mixtures", Clarendon Press, Oxford, (1980).

Ewing,G.J. and Ionescu,L.G.,"Dissociation pressure and other thermodynamic properties of xenon-water clathrate", J.Chem.Eng.Data, **19**, 367(1974).

Handa,Y.P., "Compositions, enthalpies of dissociation and heat capacities in the range 85 to 270K for clathrate hydrates of methane, ethane, and propane, and enthalpy of dissociation of isobutane hydrate, as determined by a heat-flow calorimeter", J.Chem.Thermodynamics, **18**, 915(1986b).

Hirschfelder,J.O., Curtiss,C.F. and Bird,R.B., "Molecular theory of gases and liquids", John Willey, NY(1964).

Holder,G.D., Corbin,G. and Papadopoulos,K.D., "Thermodynamic and molecular properties of gas hydrates from mixtures containing methane, argon, and krypton", I&EC Fundam., **19**, 282(1980).

Holder, G.D. and Hand, J.H., "Multiple-Phase Equilibria in Hydrates from Methane, Ethane, Propane and Water Mixtures", AIChE J., **28**(3), 440(1982).

John,V.T., Papadopoulos,K.D. and Holder,G.D., "A generalized model for predicting equilibrium conditions for gas-hydrates", AIChE J., **31**, 252(1985).

John,V.T., "Improved predictions of gas hydrate phase equilibria", Ph.D. Dissertation, Columbia University(1982).

Kihara, T, "The second virial coefficient of non-spherical molecules", J. Phys. Soc. Japan, **6**, 289(1951).

McKoy,V. and Sinanoglou,O., "Theory of dissociation pressures of some gas hydrates", J.Chem.Physics, **38**, 2946(1963).

Parrish, W.R. and Prausnitz, J.M., "Dissociation Pressures of Gas Hydrates Formed by Gas Mixtures", IEC Proc. Des. Dev., **11**(1), 26(1972).

Reddy,M., O'Shea,S.F. and Cardini, "Analytical approximations to virial coefficients for pure and mixed systems", Mol.Phys., 57, 841(1986).

Saito, S., Marshall, D.R., Kobayashi, R., "Hydrates at High Pressures", AIChE J., 10(5) 734(1964).

Sloan, E.D., "Clathrate Hydrates of Natural Gases", Marcel Dekker Inc, New York(1990).

Tee,S.L., Gotoh,S. and Stewart,W.E., "Molecular parameters for normal fluids", I&EC Fundam., **5**, 363(1966).

van der Waals, J.H. and Platteeuw, J.C., "Clathrate Solutions", Adv. Chem. Phys., **2**, 1(1959).

van der Waals,J.H., "Some observations on clathrates", J.Phys.Chem.Solids, **18**, 82(1961).

CHAPTER III

VALIDATION OF THE MODEL

3.1. Objective

Hydrate equilibria can be predicted by coupling the ideal solid solution theory, presented in Chapter II, together with the cubic equation of state presented and tested in Chapter I. The method is thermodynamically rigorous and the model has built-in capability of performing any type of hydrate equilibria calculations, as it is detailed in Chapter V. Prediction of the thermal properties of gas hydrates can also be carried out with an efficient algorithm presented and tested in Chapter IV.

The extent of validity and reliability of the PVT predictions of the hydrate model, is investigated in this Chapter. We focus our attention on the three phase Vapour[V]-Water-rich liquid[Lw]-Hydrate[H] boundary predictions, for several reasons. First, a plethora of data is available in this region, which allows for identification of deviations in the experimental data. Second, the water-rich liquid phase is the most difficult to model and the ability of the program to predict the properties of this phase is crucial. Third, this is the most commonly encountered case in gas pipelines and therefore adequate predictions are of industrial importance.

Almost all experimental V-Lw-H hydrate point data of synthetic and natural gases collected by Sloan(1990) - where we refer for complete data references - have been used for the validation of our model. Of these the multicomponent data have not been used in any sense to obtain or to readjust the parameters of the model, and therefore they provide a stringent test of its reliability. The model is further tested in other equilibrium regions in Chapter V.

3.2. Simple Gas Hydrate Equilibria

Most of the data referred to in this paragraph have been used in someway to obtain the potential parameters of the model, as required by the ideal solid solution theory. Nonetheless, a comparison of predictions with experimental data has been considered worthy mainly for two reasons. First, for gas

components capable of entering both cavities (methane, nitrogen, carbon dioxide, etc), pure component data were not the only used data(see Chapter 2 for details). On the other hand, for gas components entering only the large cavity of either structure, ie ethane and propane, in addition to hydrate dissociation pressure data, heat capacity data have also been simultaneously used (see Chapter 4 for details). In either case, it is interesting to see how the extension of the feed data affects simple gas hydrate dissociation pressure predictions. Second, since the accuracy of the data is not usually specified by the experimentalists, it is interesting to visualize potentially deviating data and relevant inconsistencies.

Figure 1 shows calculated and experimental data for the methane hydrate above the ice point. There is a limited scatter of the experimental data and the agreement of the model is very good.

Figure 2 shows calculated and experimental data for ethane hydrate above the ice point but below the upper quadruple point(UQP). It is noted that there is a significant scatter in the experimental data and the exact location of the UQP is rather diffuse, reflecting experimental difficulties in this region. The model represents well most of the data with the exception of some of the older data which are overpredicted.

Figure 3 shows calculated and experimental data for the propane hydrate above the ice point and up in the neighbourhood of the upper quadruple point. There are systematic deviations in the experimental data. The model follows the data of Verma(1974) which are the mainstream data.

Calculations and experimental dissociation pressures for carbon dioxide hydrate are compared in figure 4. There is fair agreement between several sets of data. The model seems unable to follow consistently the mainstream line and overpredicts the low temperature data while it underpredicts the data at higher temperatures.

Only two sets of data have been reported for hydrogen sulphide and there is fair agreement between them as depicted in figure 5. The model represents satisfactorily these data.

The experimental data for the dissociation pressures of pure nitrogen hydrate are plotted and compared with predictions in figure 6. The overall agreement is good.

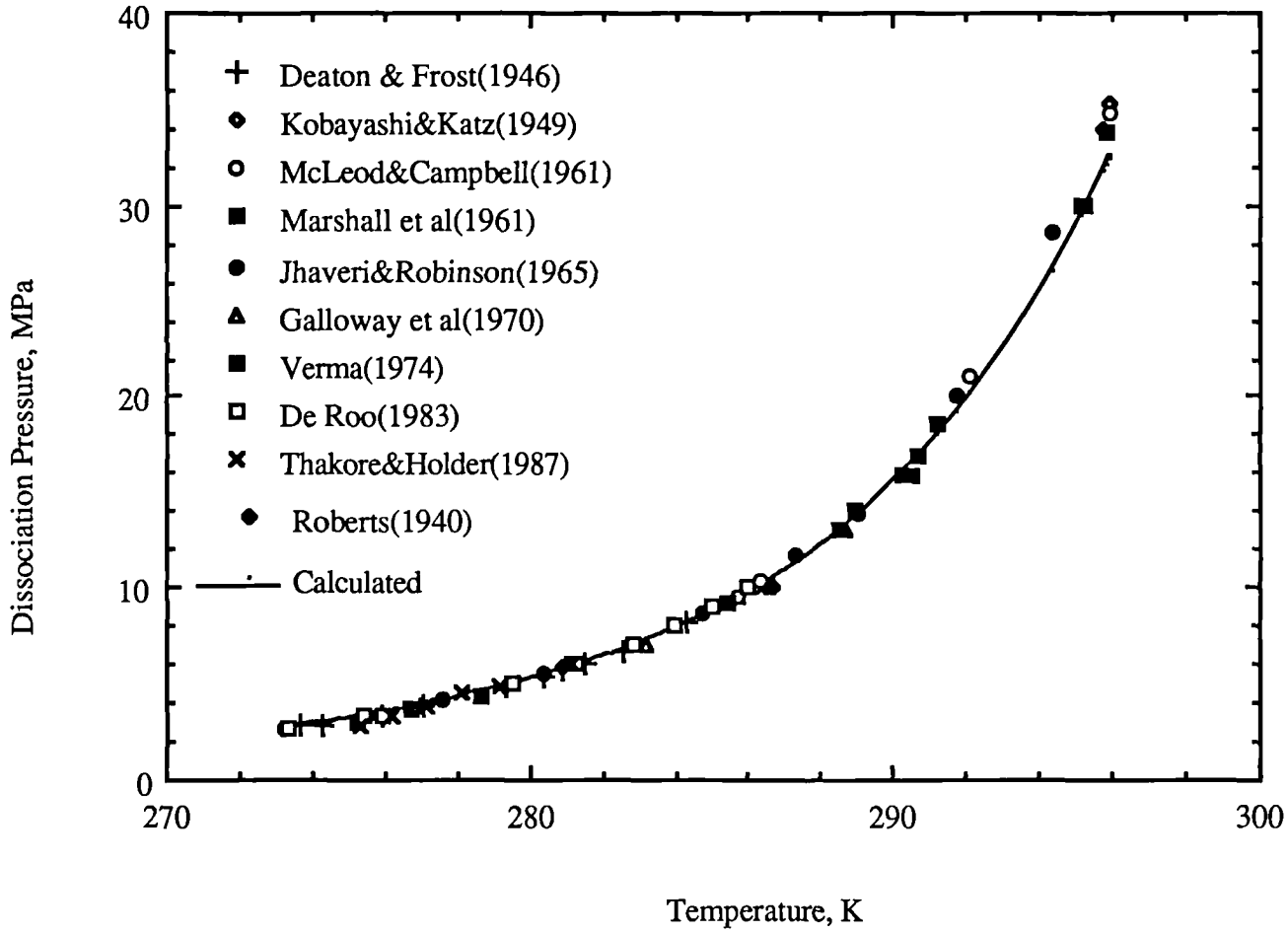

Figure 3.1. Experimental and calculated dissociation conditions of methane hydrate in the Lw-H-V region.

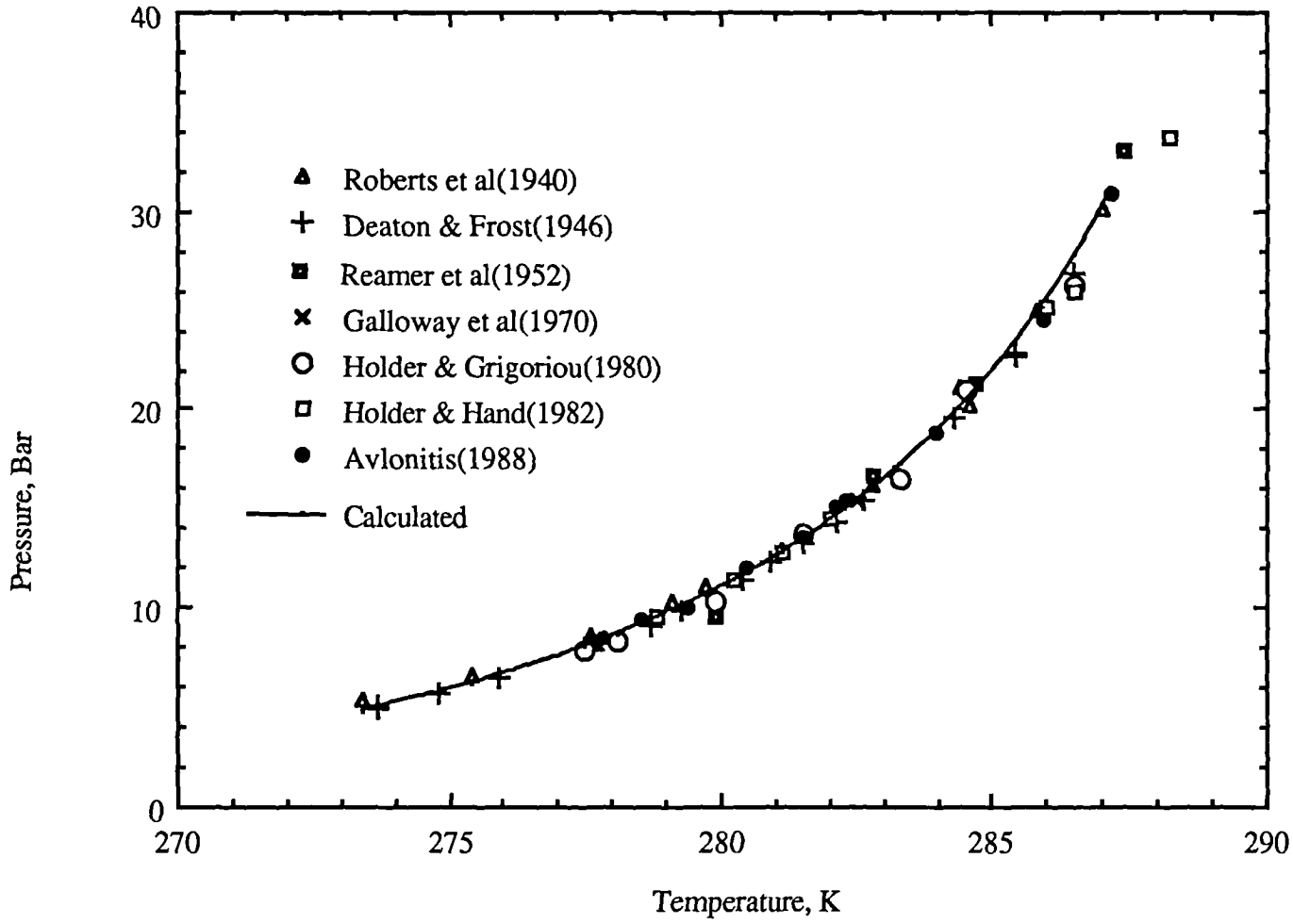

Figure 3.2. Experimental and calculated dissociation pressures of ethane hydrate in the Lw-H-V region

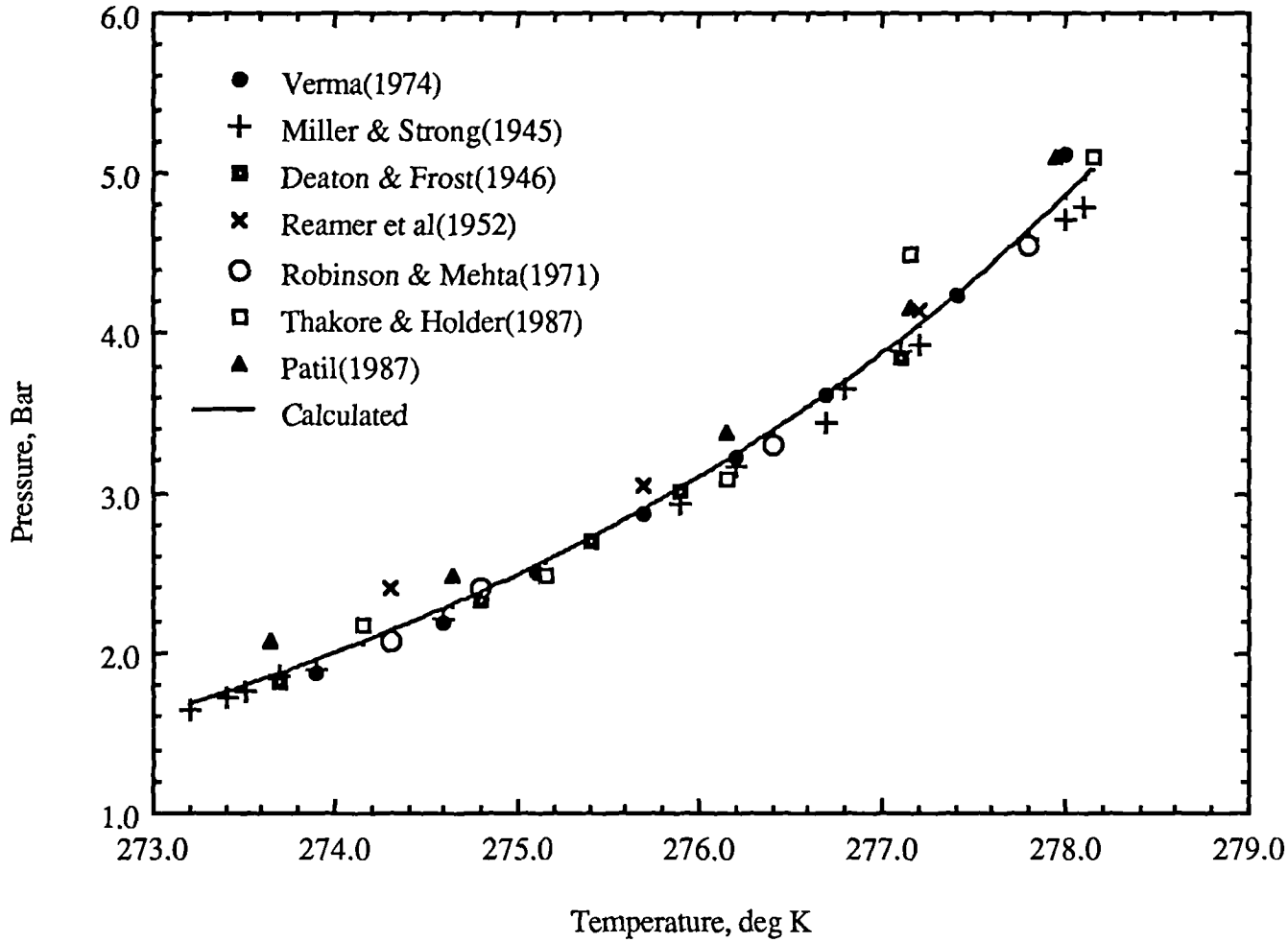

Figure 3.3. Experimental and calculated dissociation conditions of propane hydrate in the Lw-V-H region

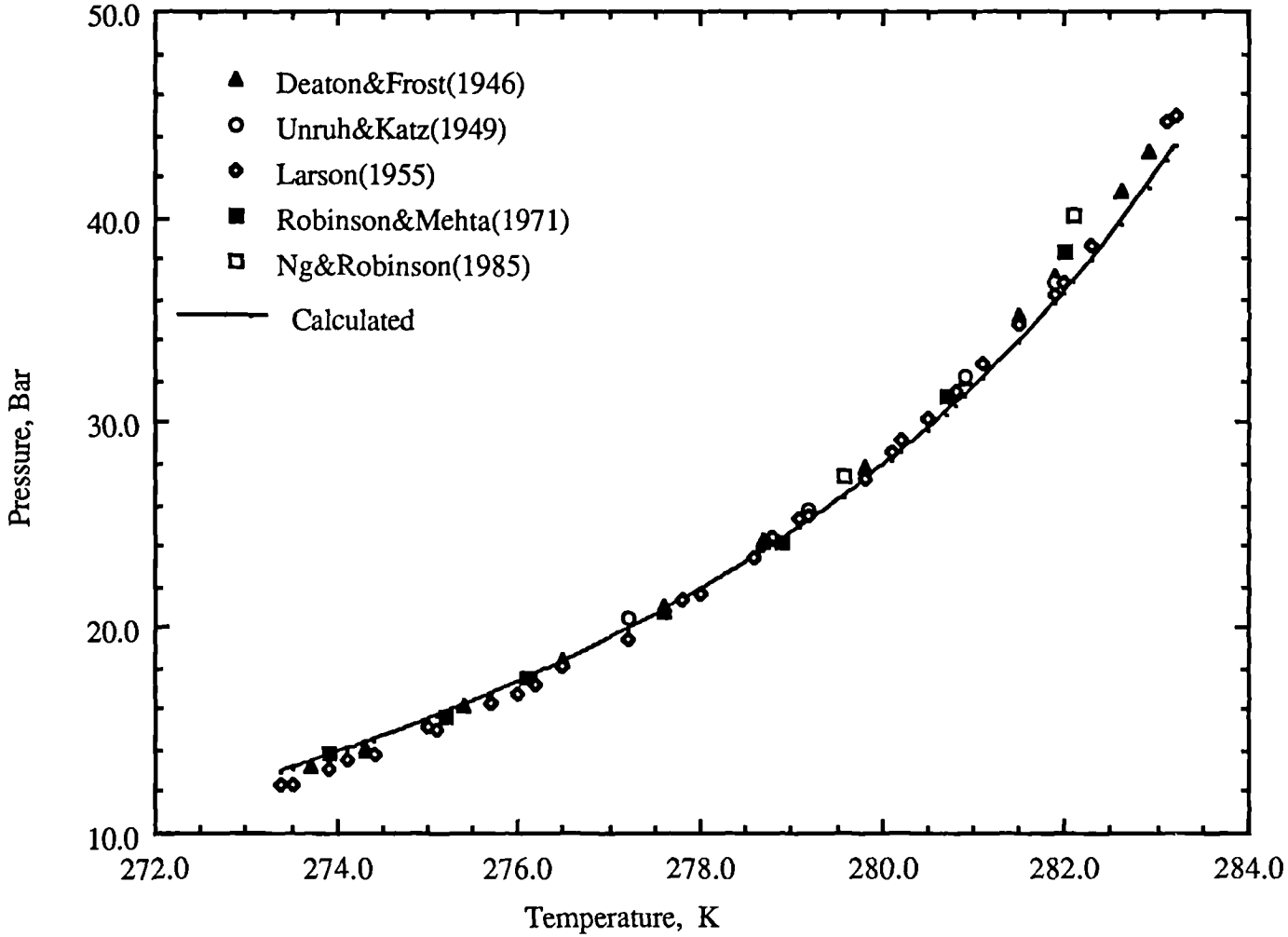

Figure 3.4. Experimental and calculated dissociation pressures of carbon dioxide hydrate in the Lw-H-V region

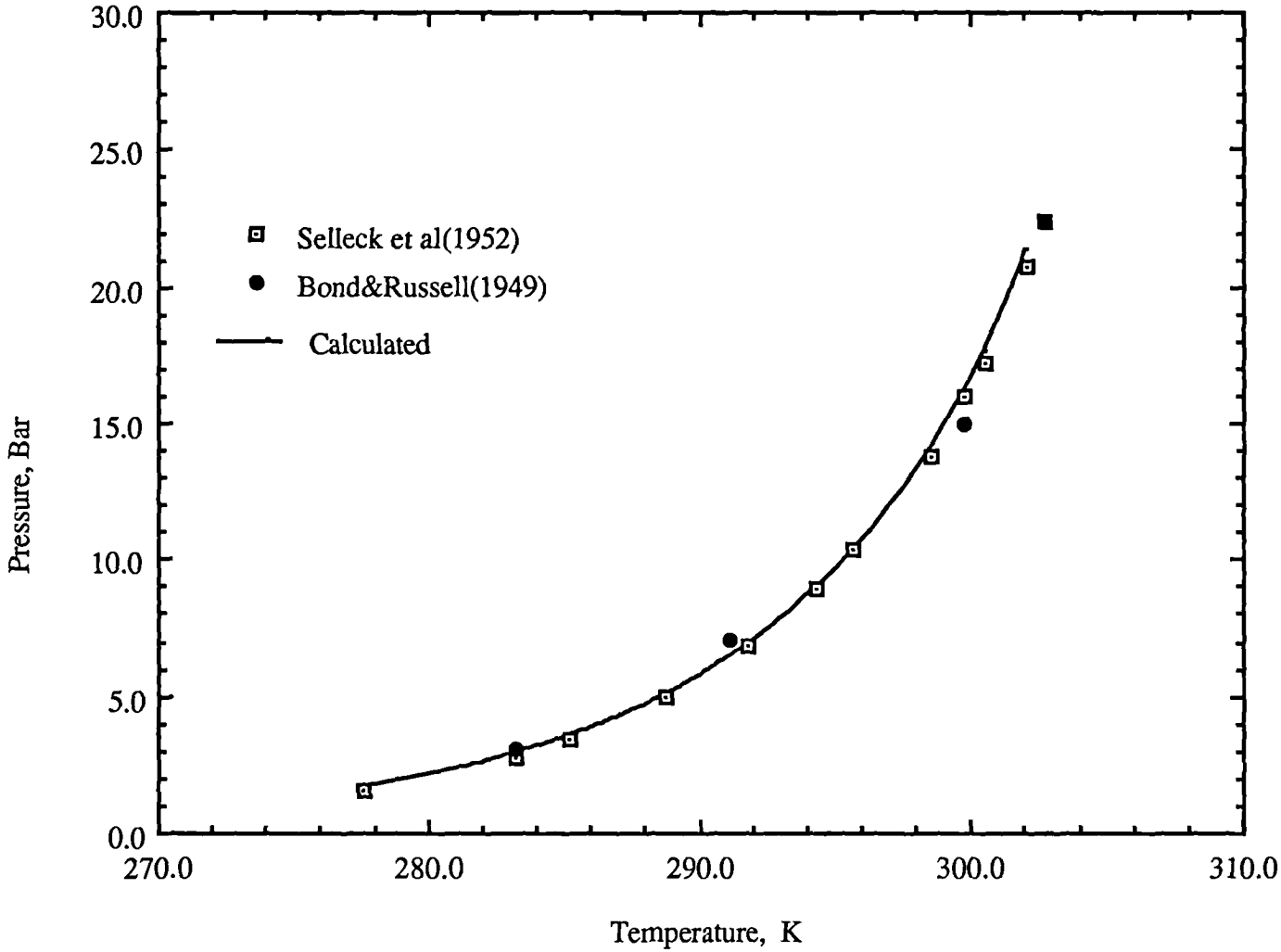

Figure 3.5. Experimental and calculated dissociation pressures of hydrogen sulfide hydrate in the Lw-H-V region

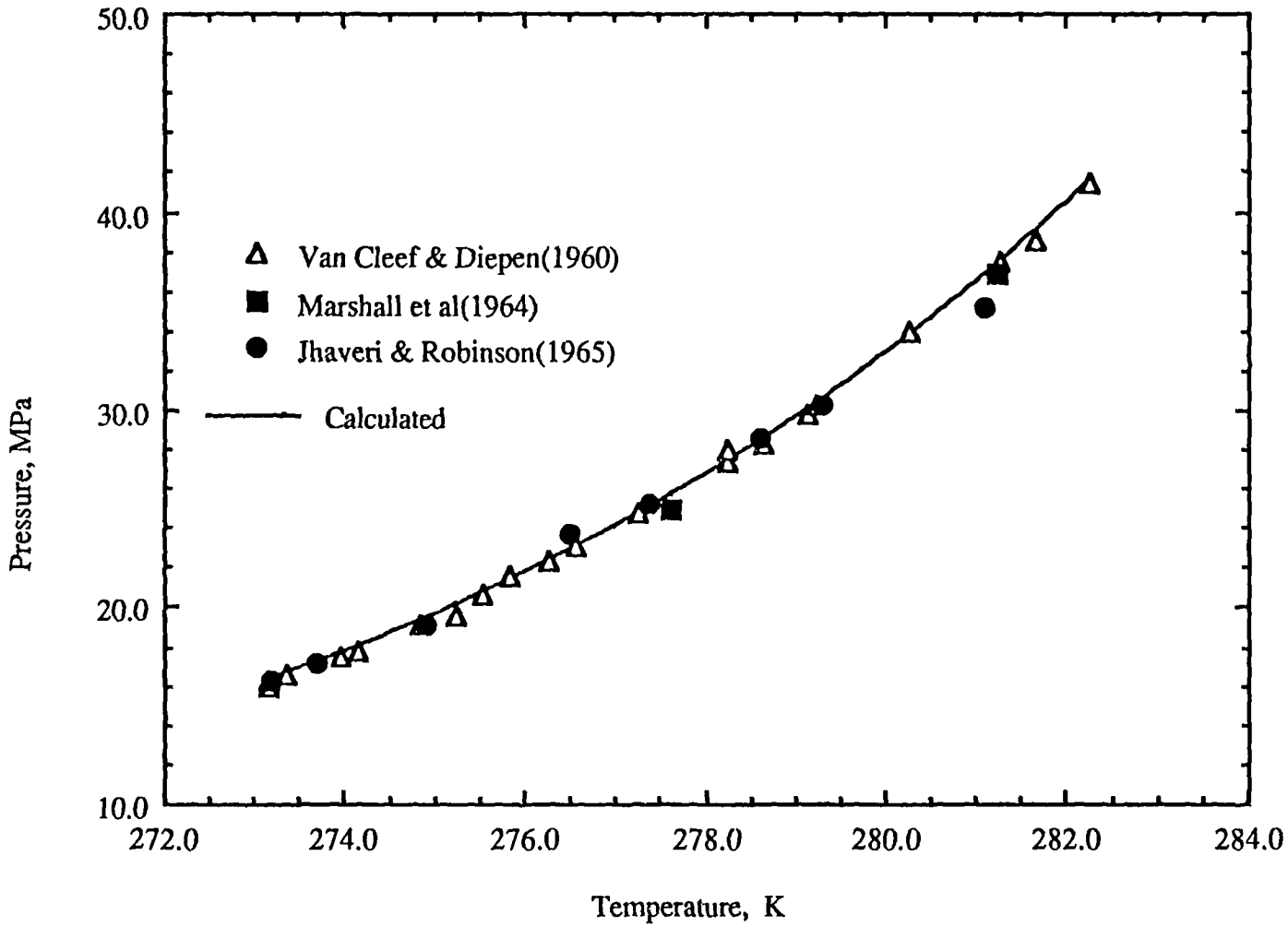

Figure 3.6. Experimental and calculated dissociation pressures of nitrogen hydrate in the Lw-H2-V region.

3.3. Hydrates of Natural Gases and Synthetic Mixtures

There are rather limited data in the open literature for the hydrate dissociation pressures of multicomponent synthetic and natural gas mixtures in the three phase V-Lw-H region. All data reported by Sloan(1990) are used below for evaluation of our model. The compositions of all mixtures are given on the respective figures.

Figure 7 depicts the behaviour of a six component natural gas hydrocarbon mixture. The heavy end of the gas has been arbitrarily characterized as normal pentane but this is not expected to affect predictions. The agreement of predictions to the data, which is good at low temperatures, deteriorates as the temperature increases and the model underpredicts the data.

Figure 8 represents the hydrate dissociation pressures of a five component synthetic gas mixture studied at relatively high pressures. The agreement is not very good and this could be attributed to the fact that the parameters of the model - and in particular, the parameters of the VLE model - have been regressed at much lower pressures.

Figure 9 compares predictions with experimental hydrate dissociation pressures of a natural gas containing some nitrogen. The agreement is very good even at higher temperatures.

Figure 10 depicts data and predictions for a natural gas containing both nitrogen and carbon dioxide. The agreement is excellent throughout.

Figure 11 represents the behaviour of a very lean natural gas hydrate, which forms in structure II, despite the fact that the equilibrium gas contains 96.5% methane. The observed deviations are significant at higher temperatures and, as it always has been the case so far, the model underpredicts the experimental dissociation pressures.

In figure 12 experimental data and predictions are plotted for a natural gas mixture rich in nitrogen. It seems that not all the experimental data belong to the same line. Predictions in this case are fair, but it is noted that the model consistently overpredicts the dissociation pressures.

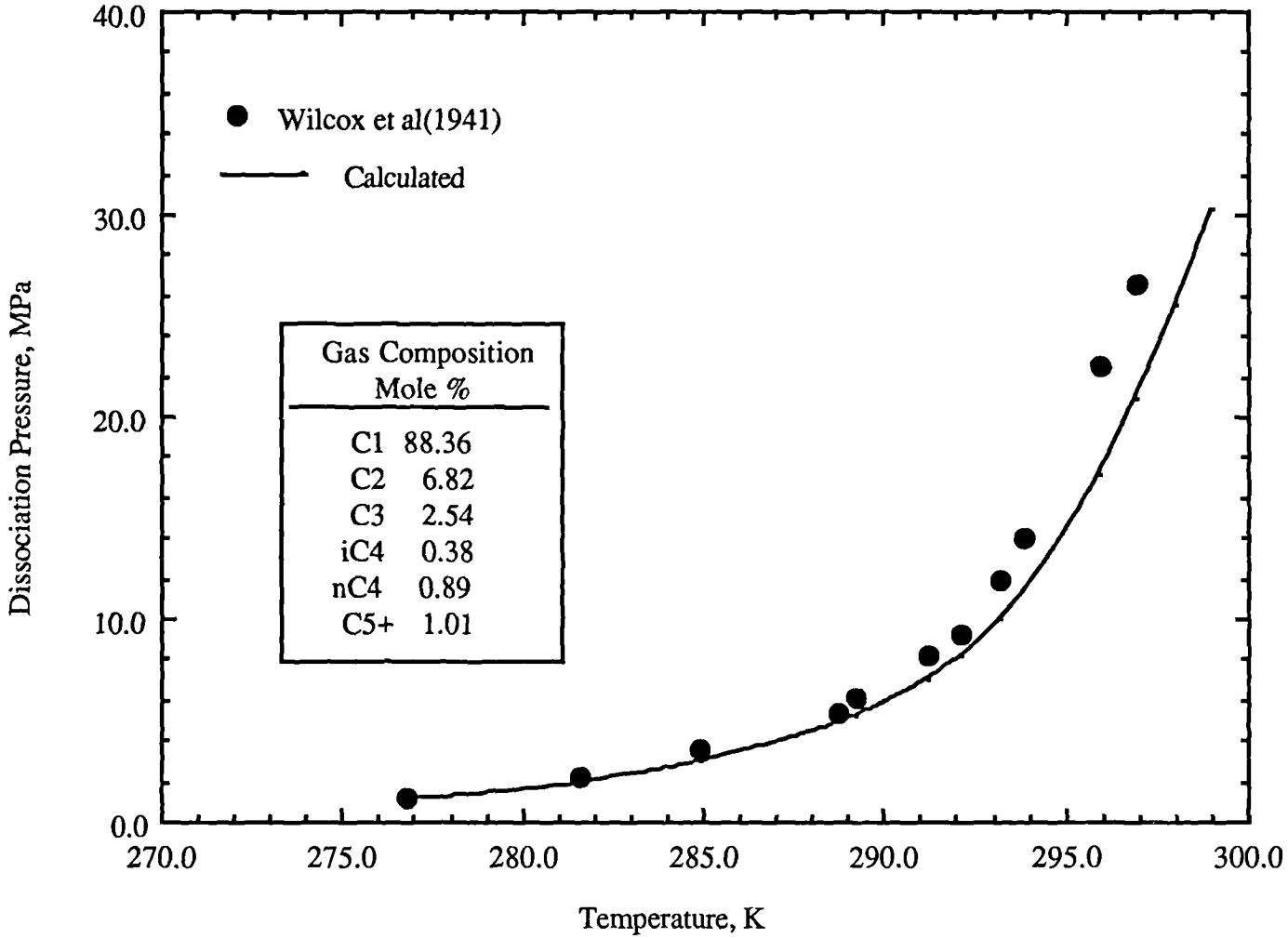

Figure 3.7. Dissociation conditions of the hydrate of a hydrocarbon natural gas.

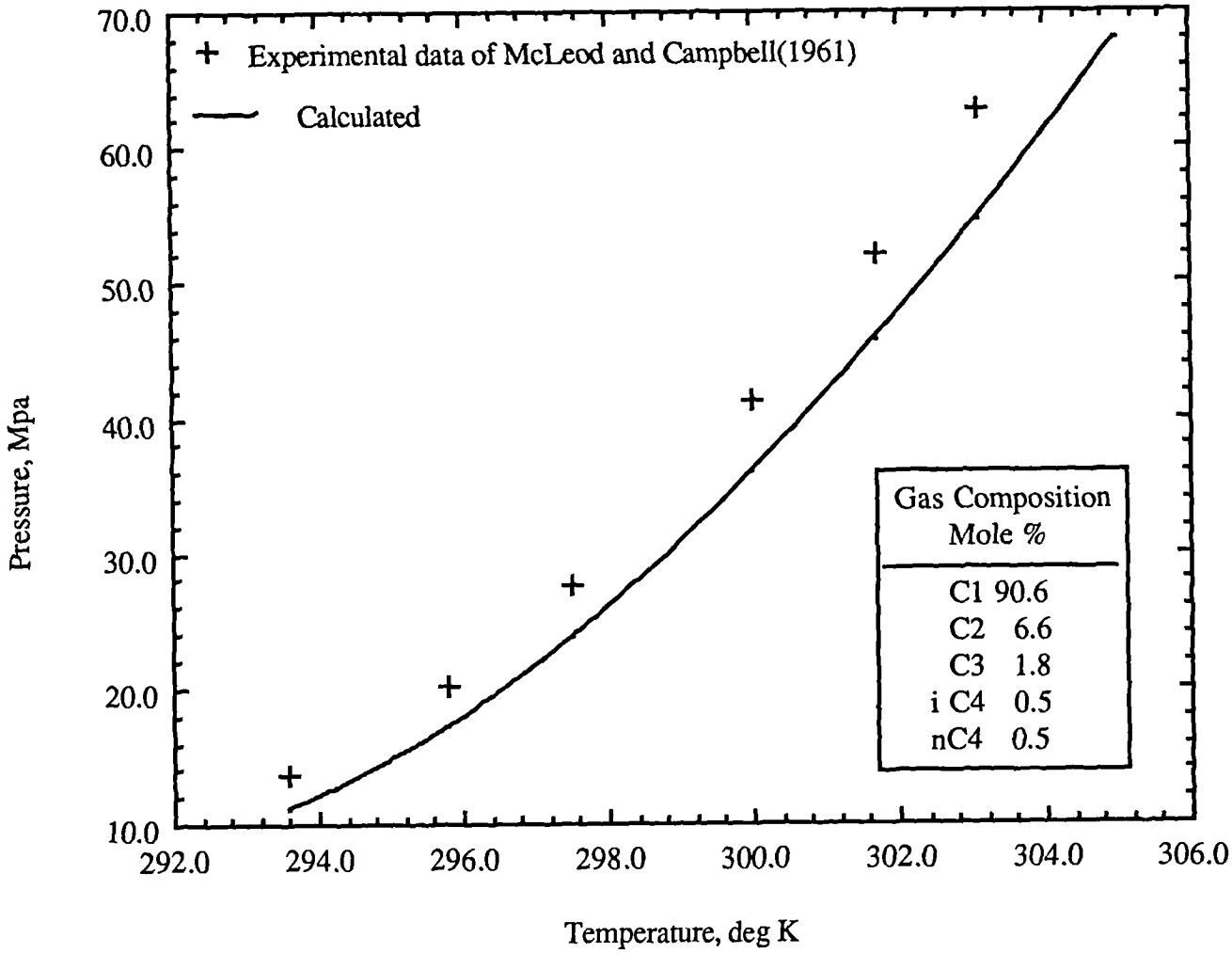

Figure 3.8. Hydrate dissociation conditions for a synthetic gas mixture.

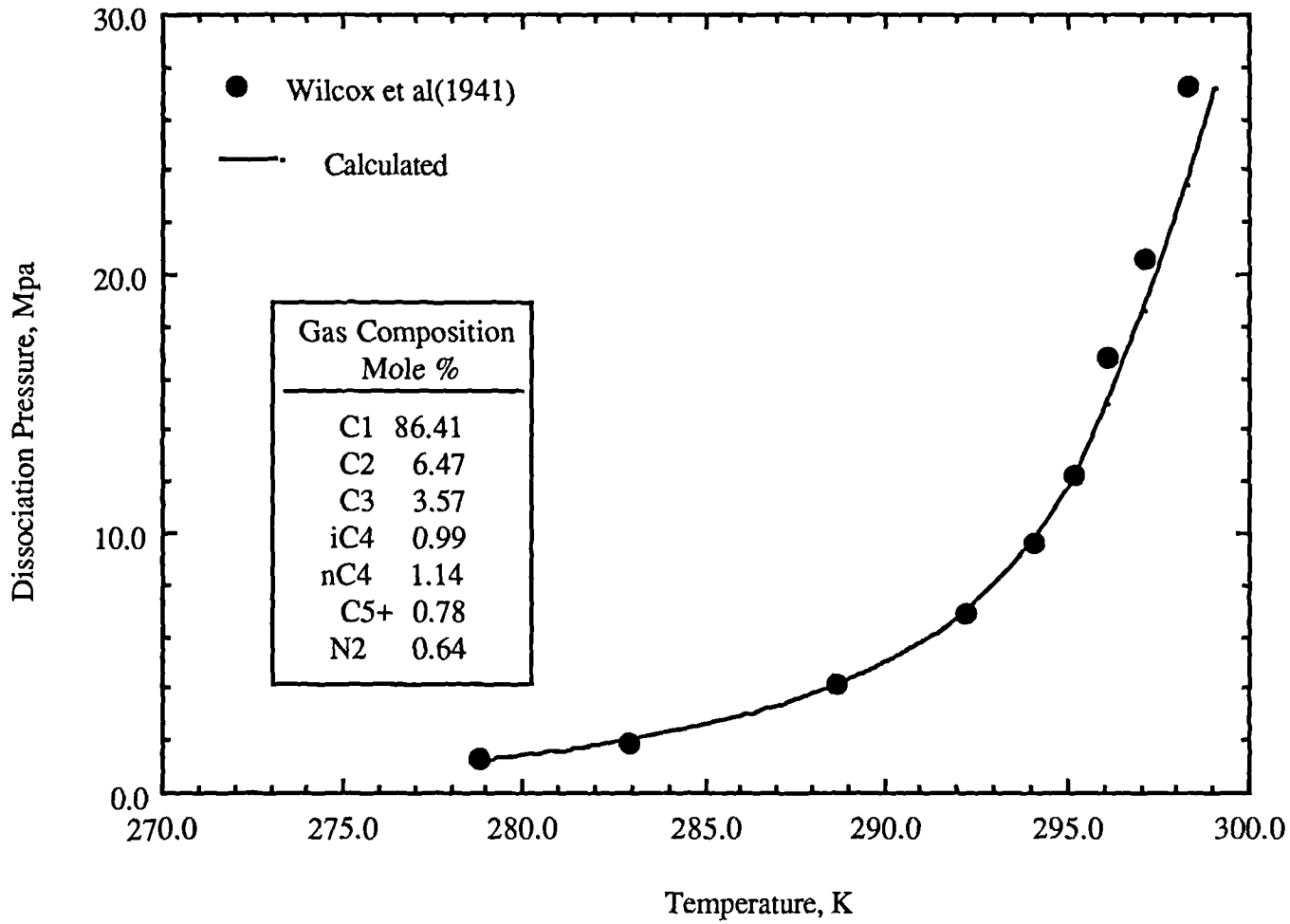

Figure 3.9. Dissociation conditions of the hydrate of a natural gas containing some nitrogen.

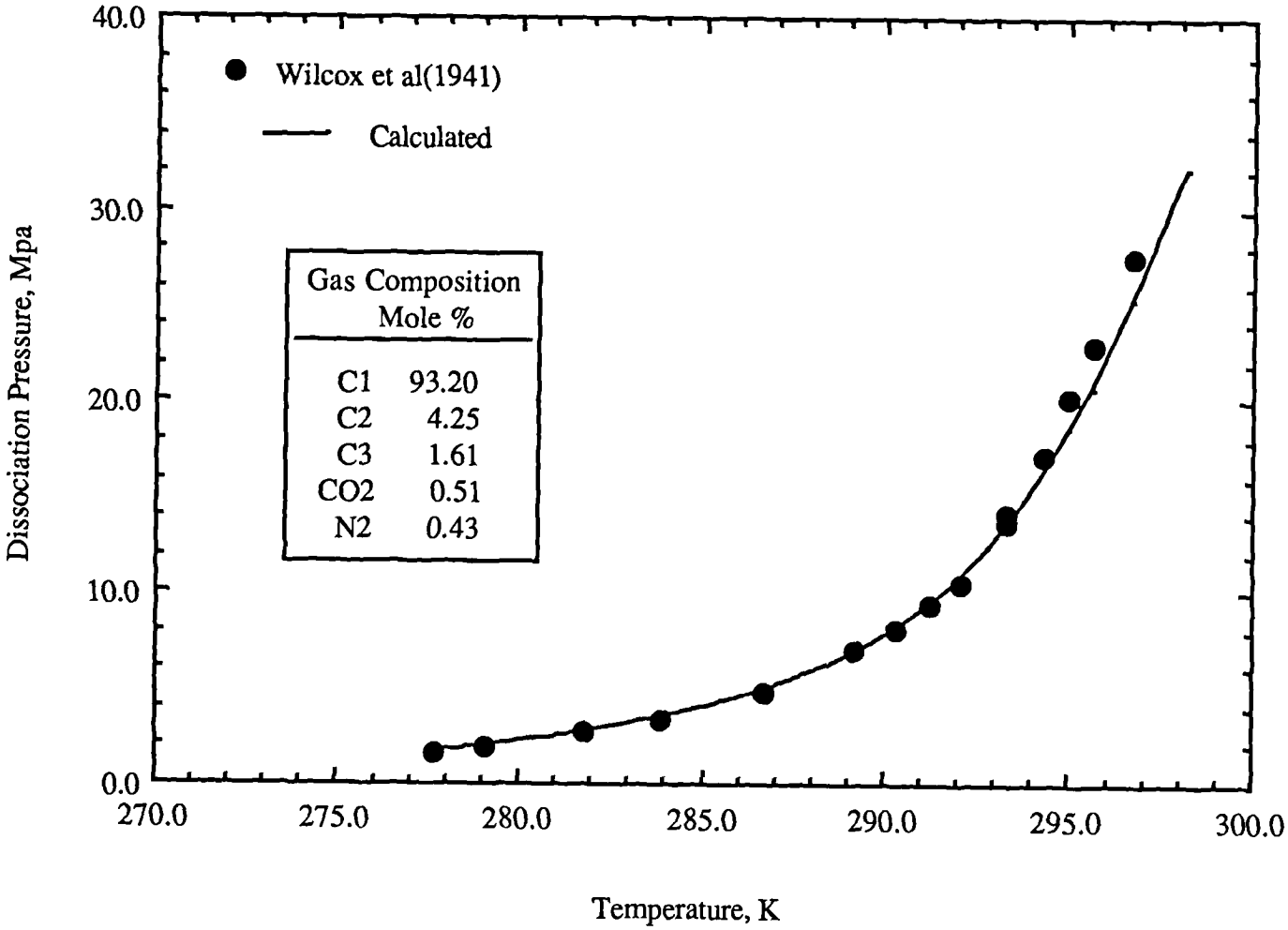

Figure 3.10. Dissociation conditions of the hydrate of a natural gas containing both nitrogen and carbon dioxide.

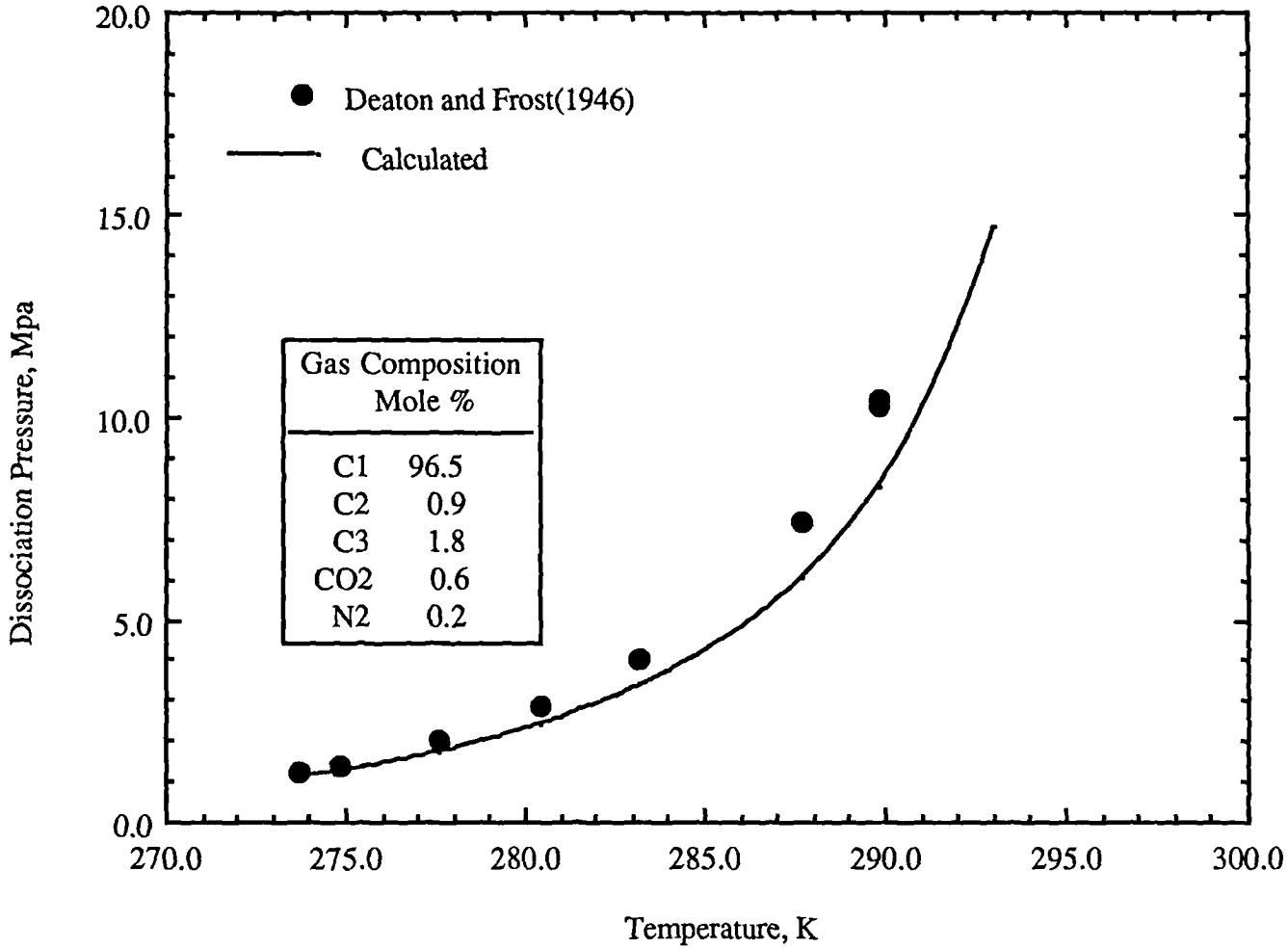

Figure 3.11. Dissociation conditions of the hydrate of a lean natural gas containing both nitrogen and carbon dioxide.

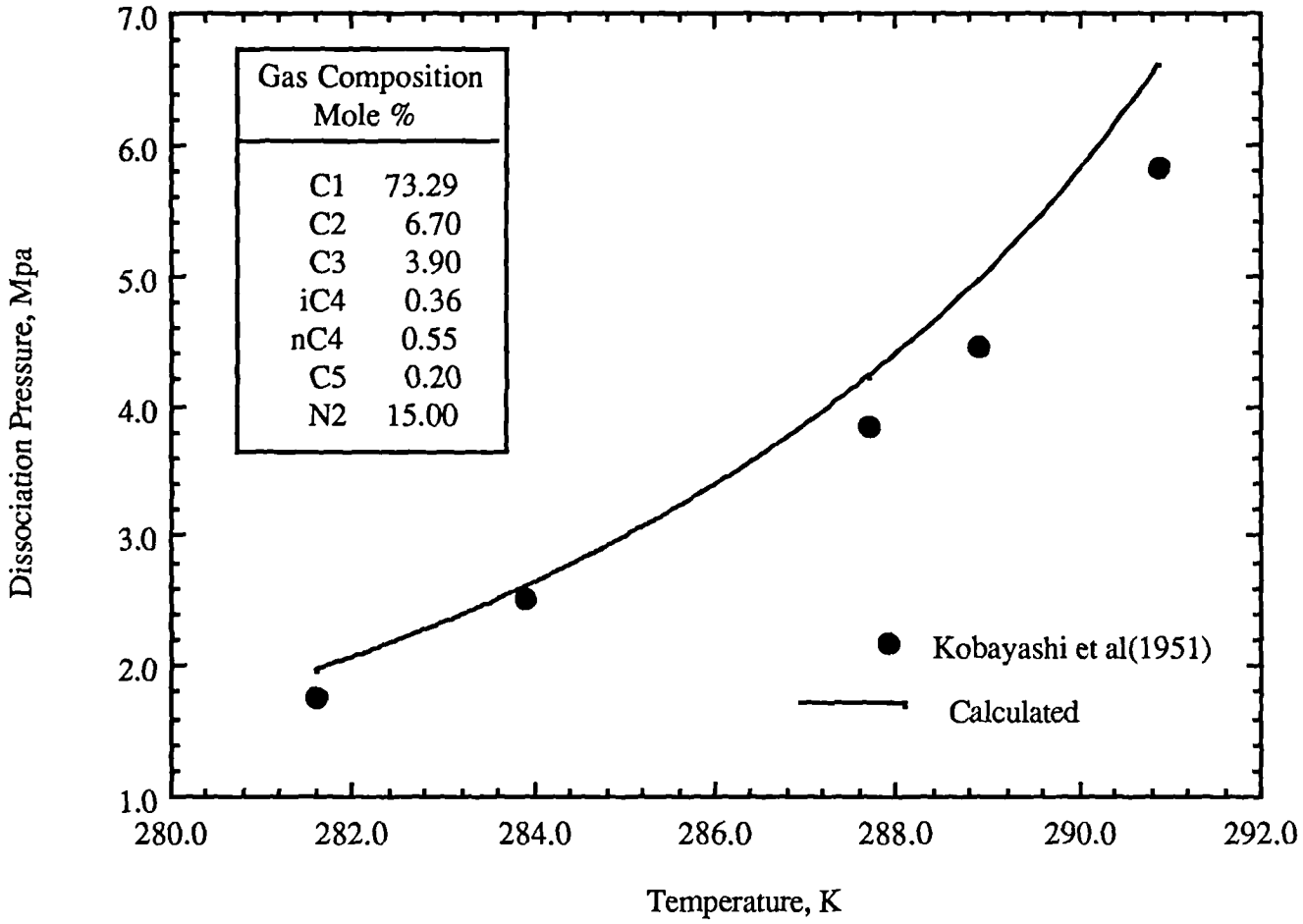

Figure 3.12. Dissociation conditions of the hydrate of a natural gas rich in ntrogen.

3.4. Hydrate Inhibition by Methanol

The effect of methanol on the conditions of hydrate formation of the most common single gases is depicted in figures 13 to 17. All experimental data reported in the literature for the three phase V-Lw-H region have been used for this comparison. For hydrogen sulphide with 35 % w/w methanol, where the largest deviations appear, we note that the quality of the fit of the binary vapour-liquid equilibria data is about 4% AAD but since these data do not include vapour compositions, the determined parameters may be in error. For the same system, it appears that the experimental data of Ng and Robinson (1985) with 20% methanol overlap with those of Bond and Russell (1949) with 16.5% methanol. This disagreement indicates the necessity of reproduction of data generated by one laboratory only. For all gases, the observed deviations do not exceed 2 K and the average absolute deviation is much less than 1 K. In general the agreement with the experimental measurements are good even at the highest reported concentration of methanol.

Figures 18 to 20 compare predictions with experimental hydrate inhibition data of several synthetic 4-component mixtures. The agreement is consistently good in all cases, indicating that hydrocarbon-hydrocarbon interactions as well as asymmetric interactions are efficiently described by our model.

Figures 21 and 22 show calculated and experimental hydrate formation conditions for two multicomponent synthetic gas mixtures. The model appears to be systematically conservative for the predicted dissociation pressures. For the first gas the predictions are quite good and deviations do not exceed 1 K. Lack of experimental data on the hydrate formation of the uninhibited gas does not permit attribution of the deviations. However, since the deviations appear unaffected by the quantity of methanol, it is reasonable to assume that they would be the same for the uninhibited gas. For the second carbon dioxide rich gas significant deterioration appears at the higher methanol concentrations rendering the model even more conservative. Surprisingly, the prediction of the effect of methanol on the hydrate formation of the pure carbon dioxide gas, show the opposite effect and a reasonable explanation cannot be given.

3.5. Discussion

The present model predicts the hydrate dissociation pressures of natural and synthetic gas mixtures(figures 7 to 12) with an average absolute deviation(AAD) 10.5 %, for all points tested. Deviations are mostly observed at the higher pressures. Overall, the performance of the model may be considered

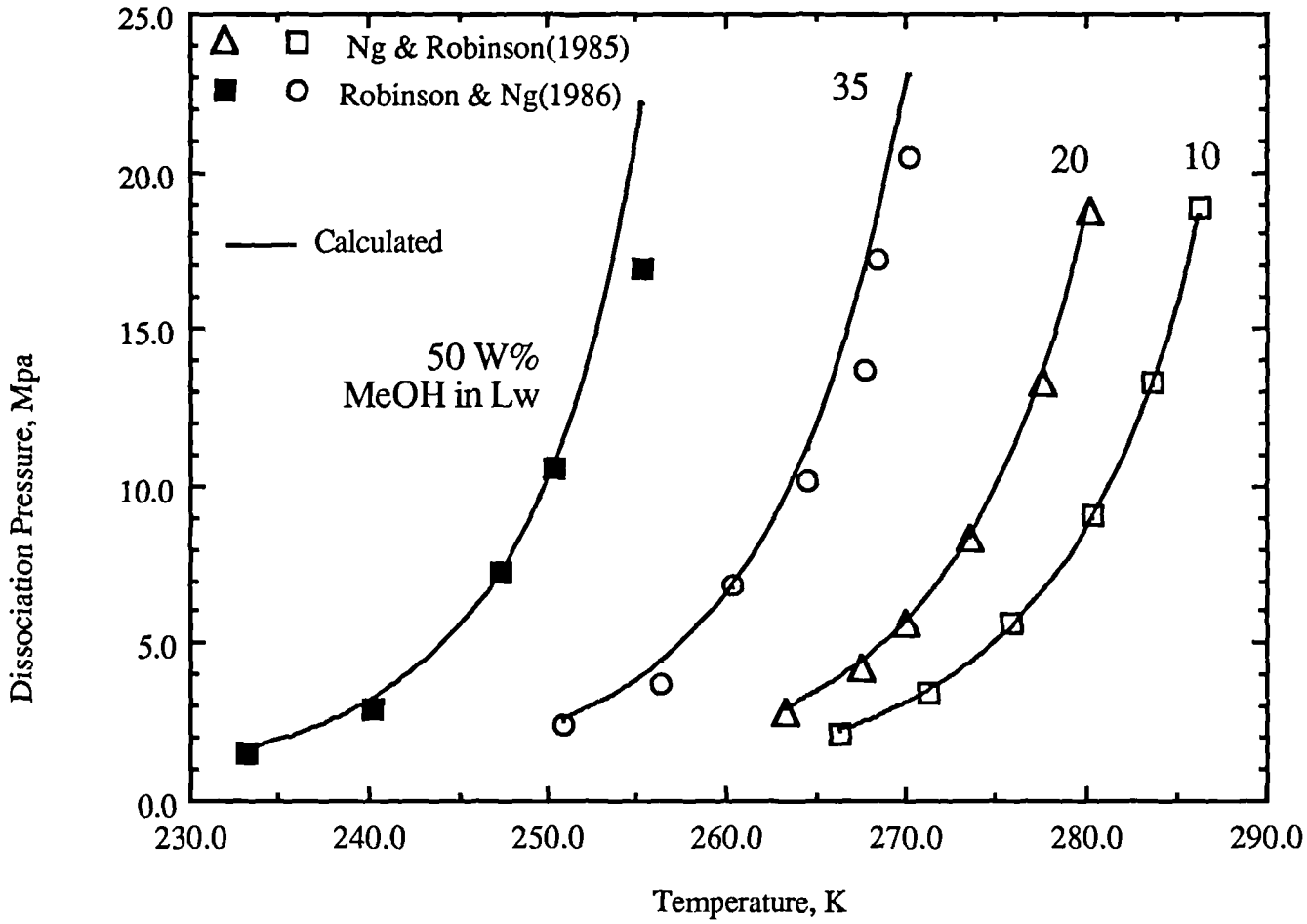

Figure 3.13. Inhibition of methane hydrate by methanol in the Lw-H(I)-V region.

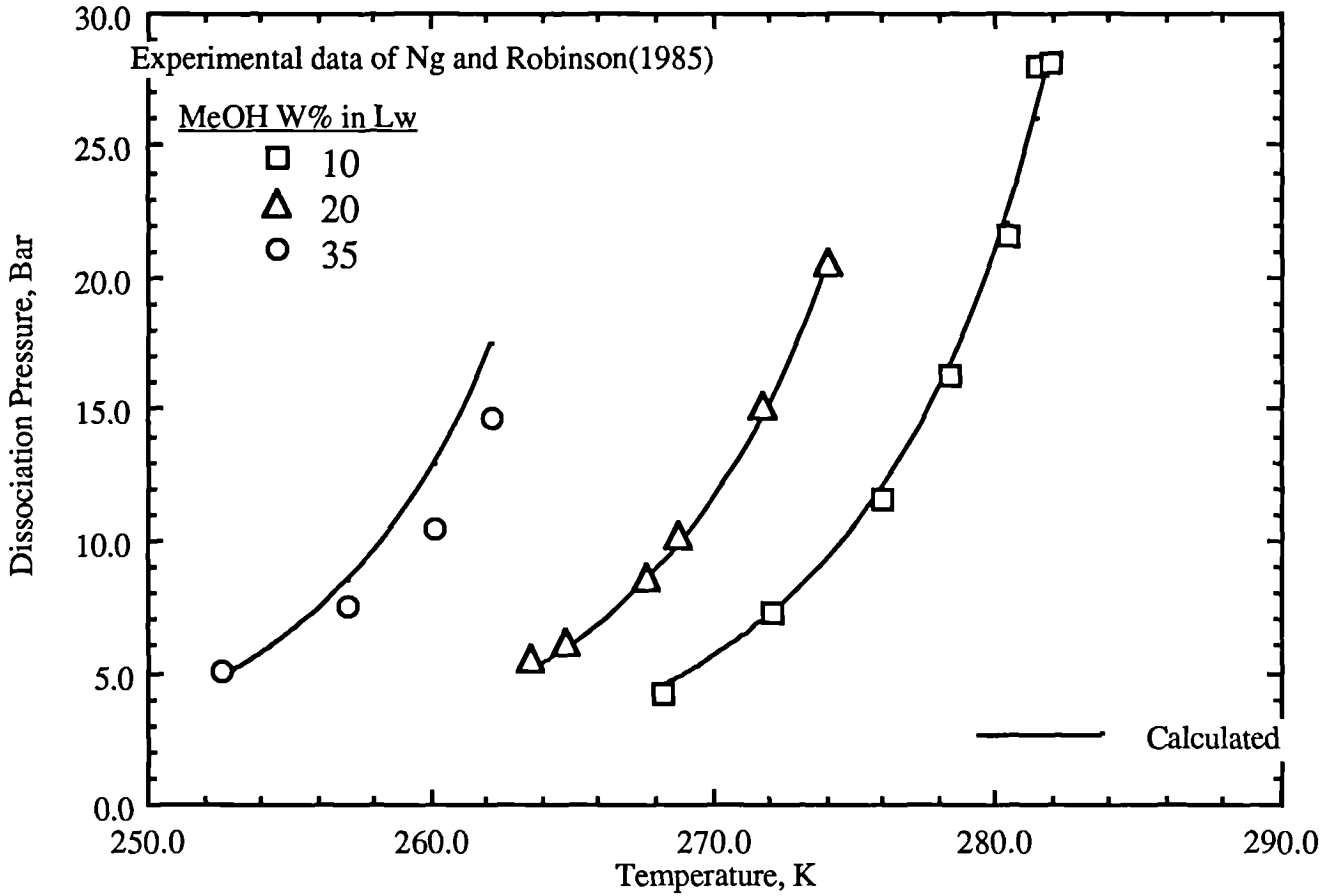

Figure 3.14. Inhibition of ethane hydrate by methanol in the Lw-H(I)-V region.

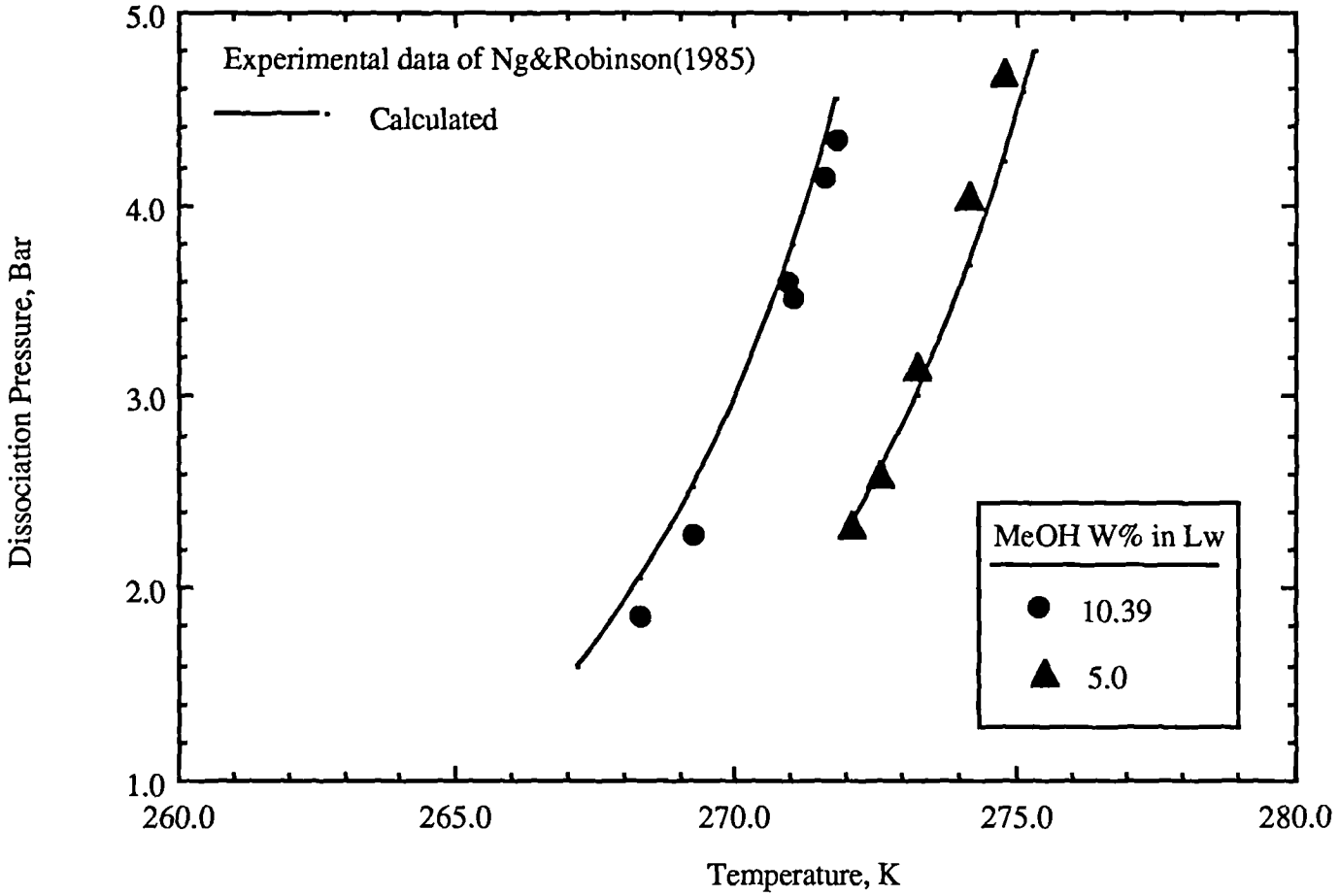

Figure 3.15. Inhibition of propane hydrate by methanol in the Lw-H(II)-V region.

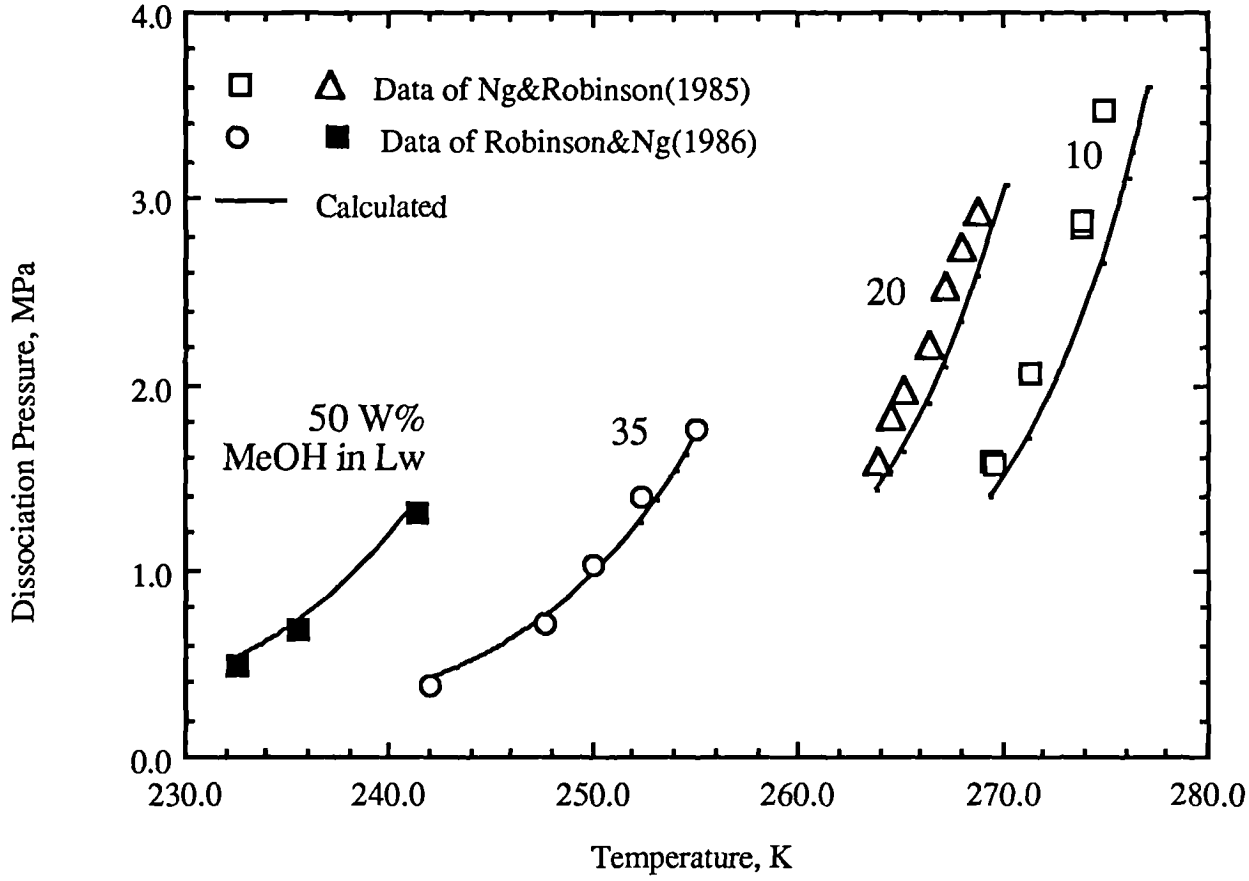

Figure 3.16. Inhibition of carbon dioxide hydrate in the Lw-H(I)-V region.

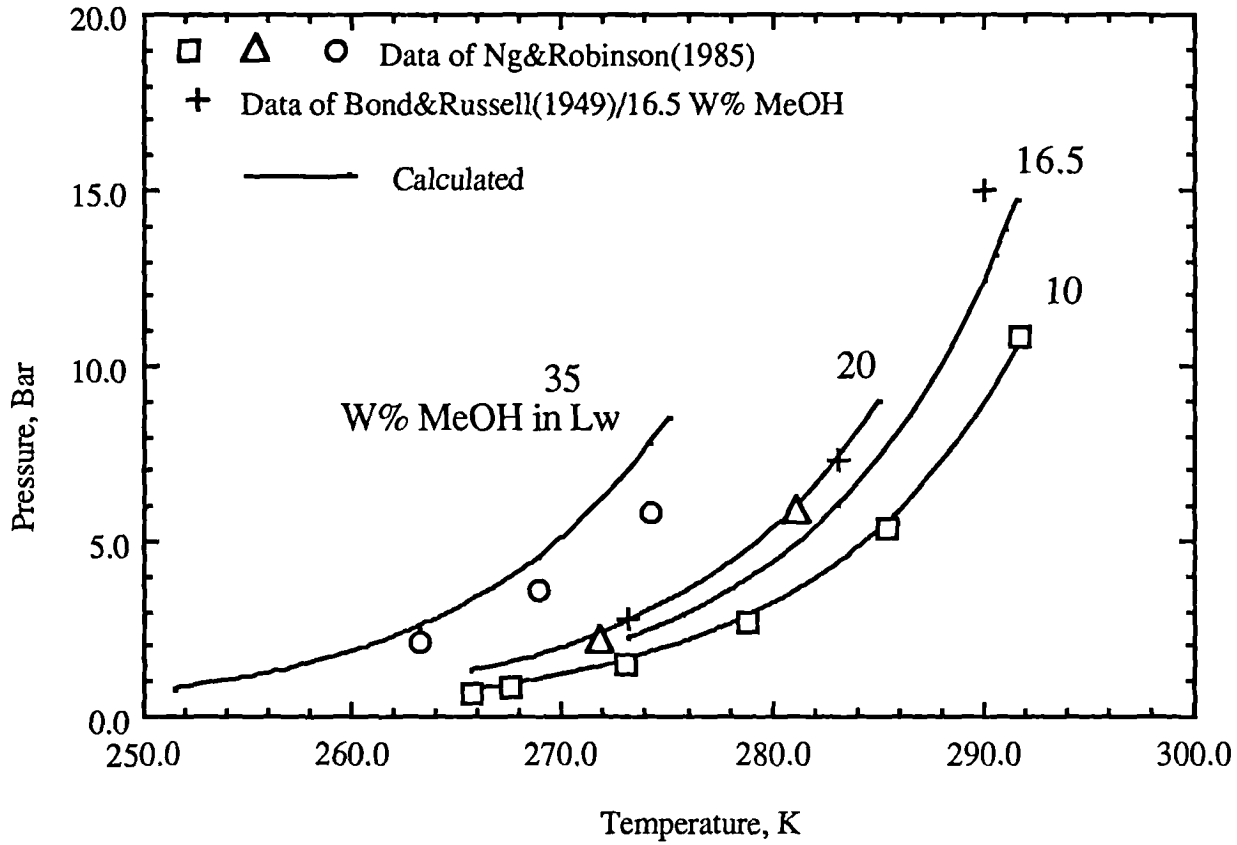

Figure 3.17. Inhibition of hydrogen sulfide hydrate by methanol in the Lw-H(I)-V region.

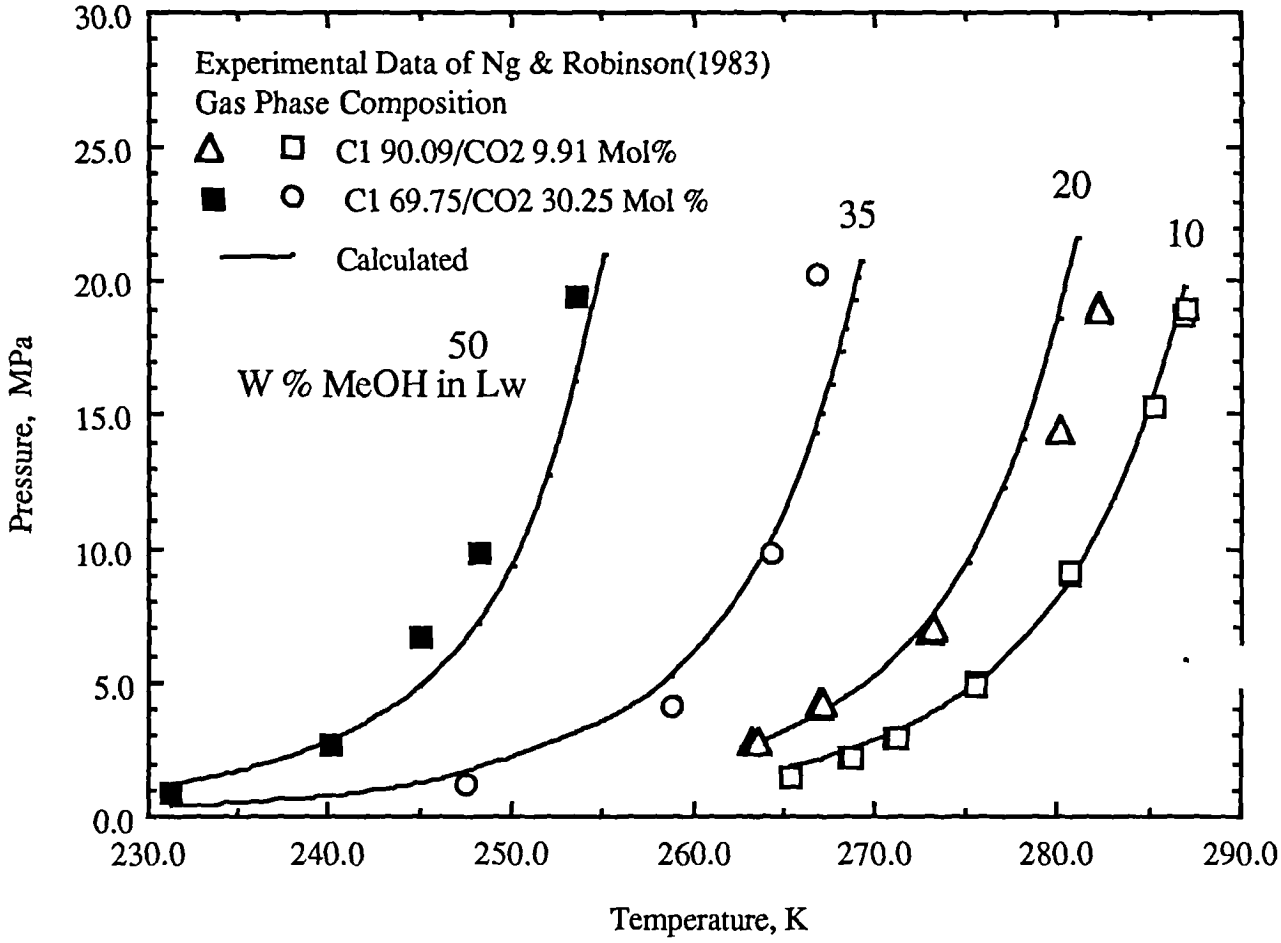

Figure 3.18. Inhibition of methane-carbon dioxide mixtures by methanol in Lw-H(I)-V region.

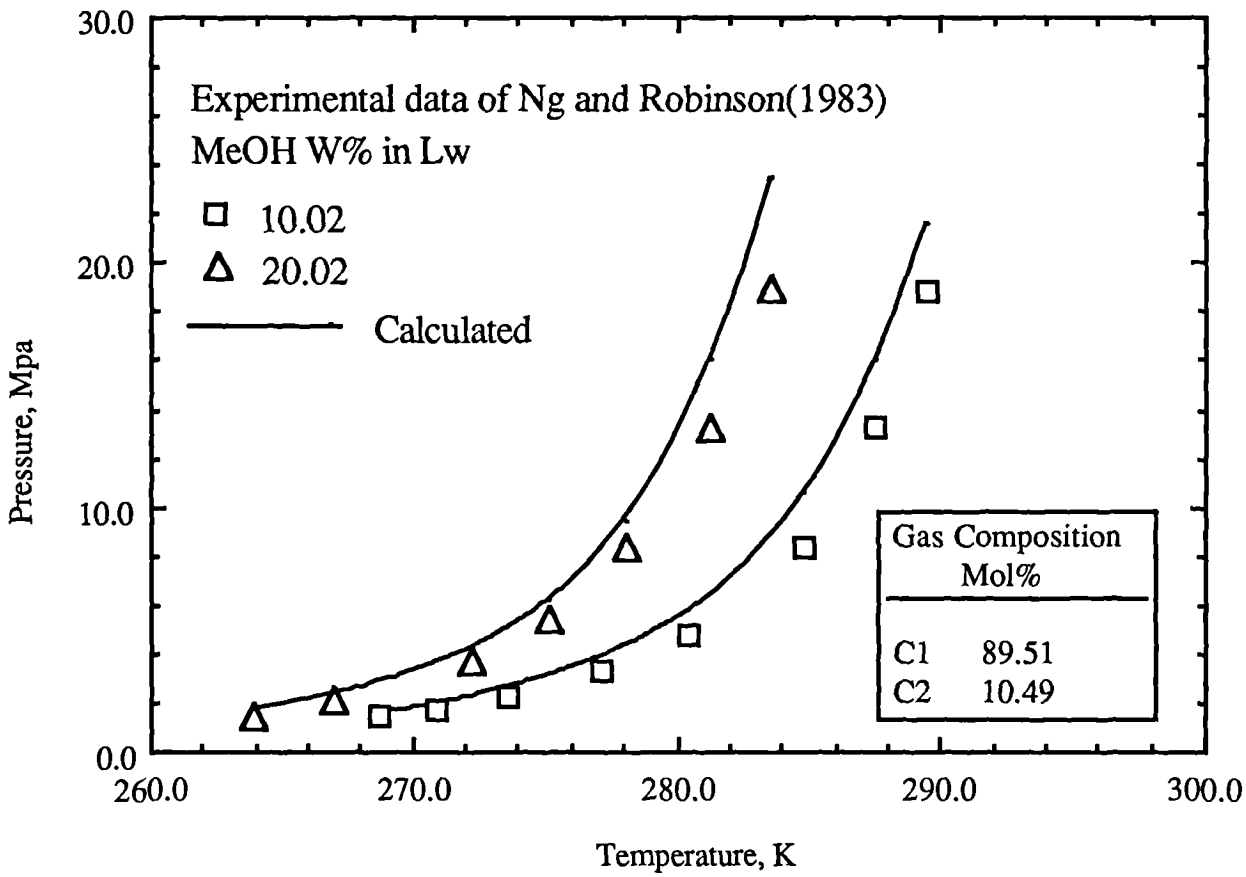

Figure 3.19. Inhibition of a methane-ethane gas mixture by methanol in the Lw-H(I)-V region.

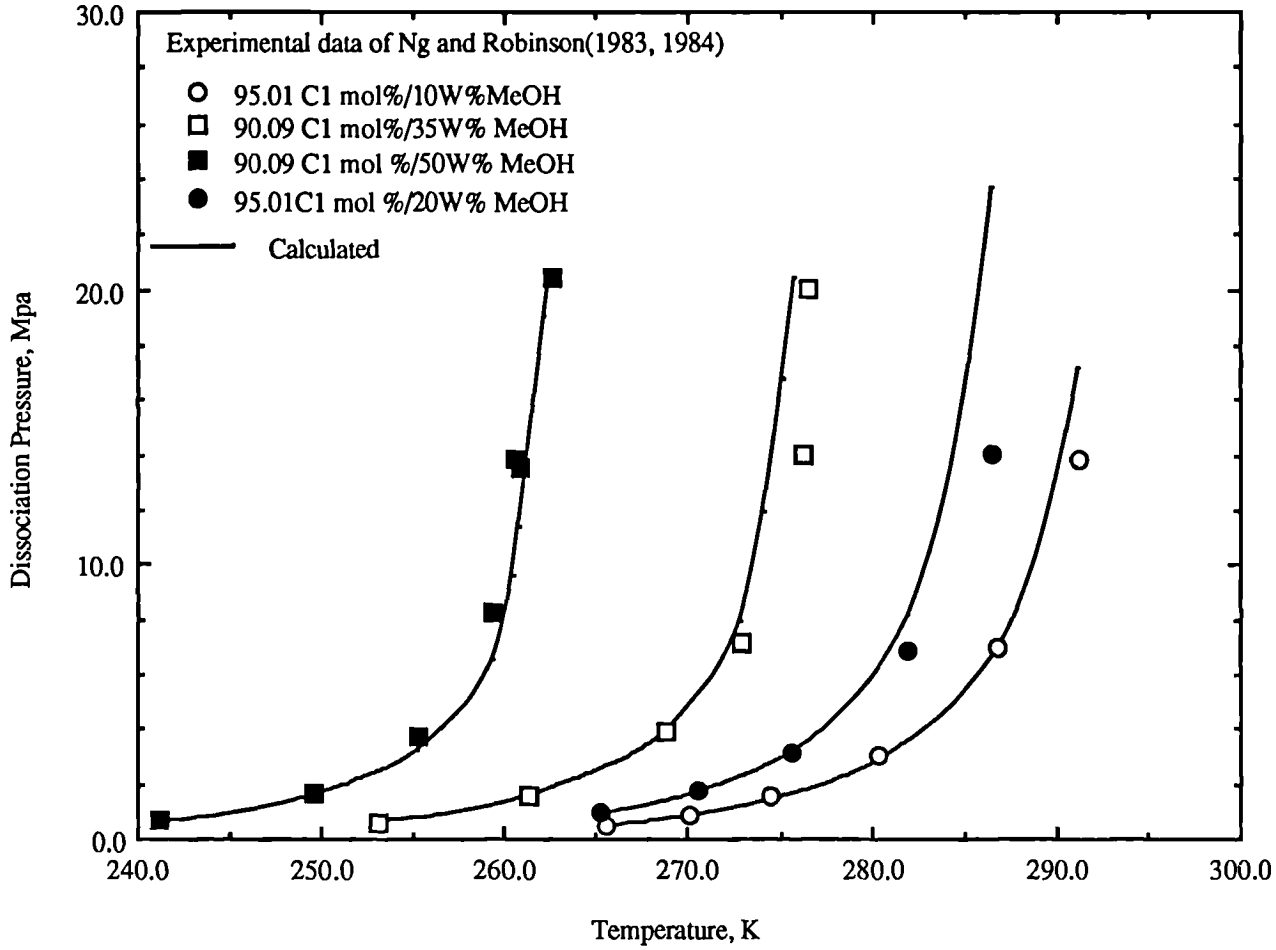

Figure 3.20. Inhibition of methane-propane mixtures by methanol.

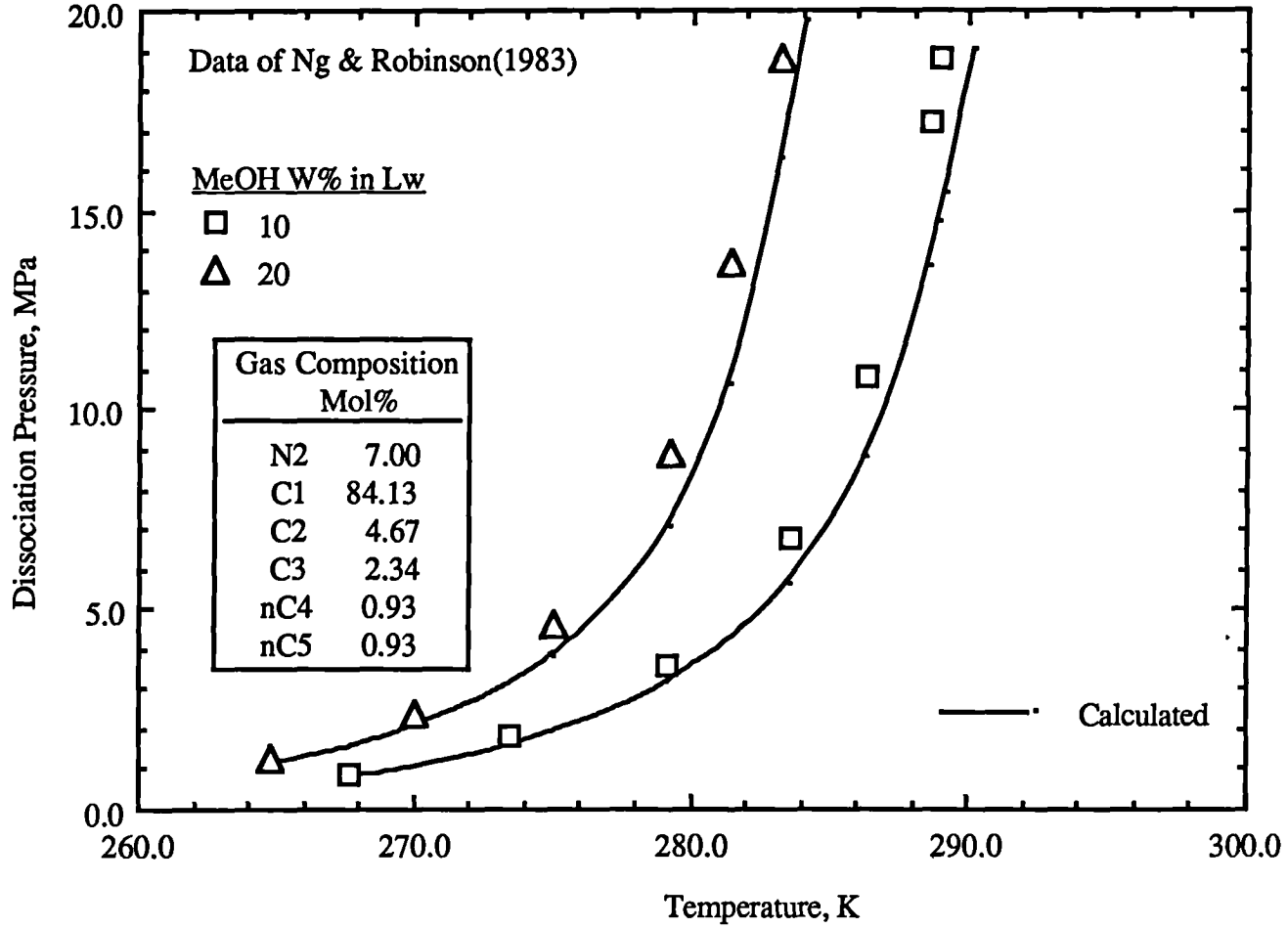

Figure 3.21. Inhibition of a synthetic gas mixture by methanol in the Lw-H(II)-V region.

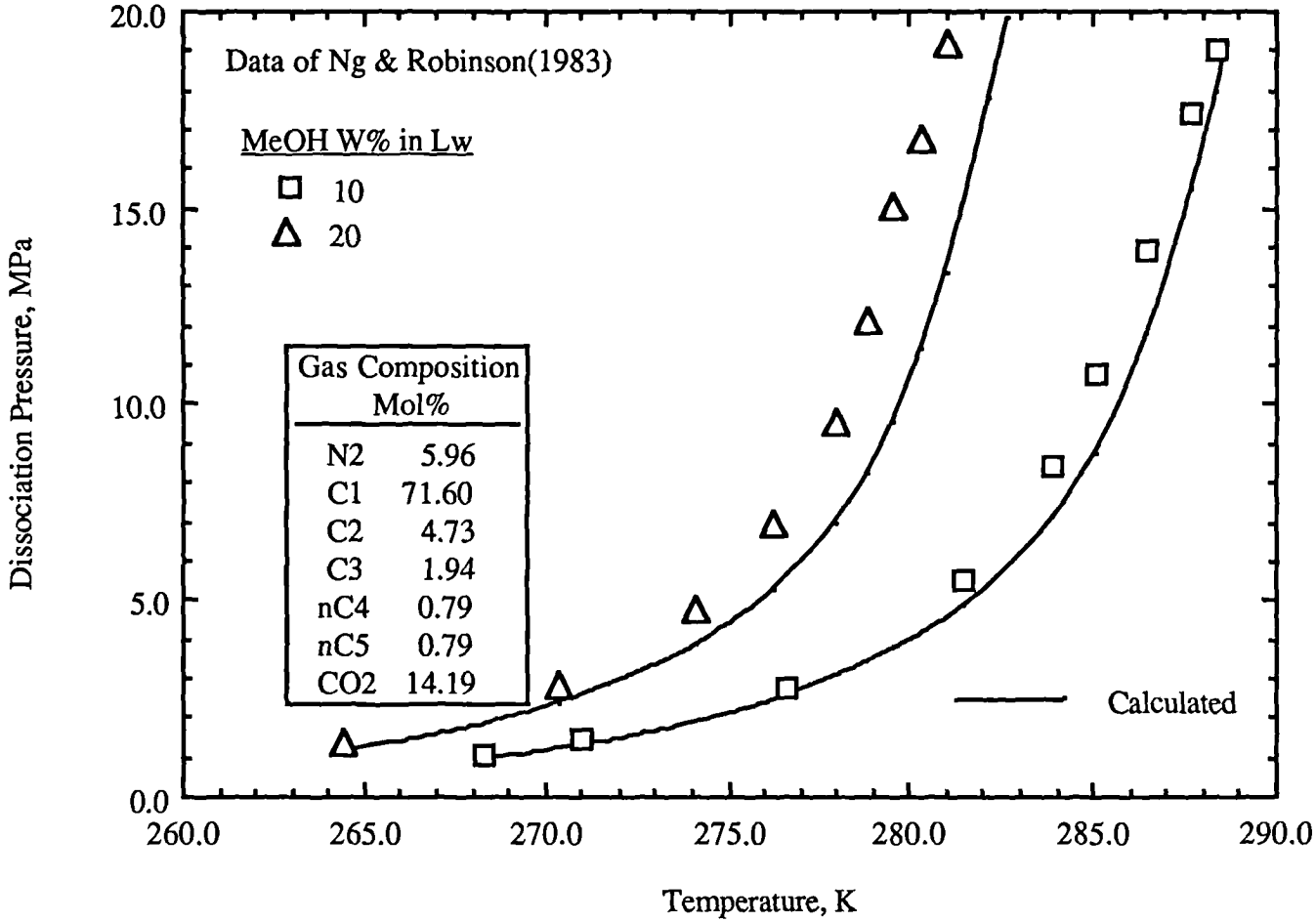

Figure 3.22. Inhibition of a synthetic carbon dioxide-rich gas mixture in the Lw-H(II)-V region.

satisfactory, considering that the quality of the fitted simple gas hydrate dissociation pressures is about 5%. It is noted that in all but one case the model tends to be conservative in the prediction of the dissociation pressures.

The effect of methanol on hydrate formation conditions in most tested cases was predicted within ±1 K with a maximum deviation ±2 K. This is a significant improvement over previously published predictive methods. Anderson and Prausnitz (1986), who employ an activity model for the water-rich liquid phase, report deviations ±5 K for multicomponent systems. Du and Guo (1990) calculate all fugacities with the Peng-Robinson equation of state with local composition mixing rules, except for water in the water-rich liquid, where they employ the activity model of Anderson and Prausnitz (1986). Despite the complexity of their model, for the carbon-dioxide rich synthetic gas with 20 w% methanol (Figure 22) their deviations are over 4 K on the optimistic side. The same authors using the program of Skjold-Jorgensen (1986) report a similar order of deviation, but on the conservative side. This is also based on an activity model for the description of the water-rich liquid.

It is noted that none of the above authors report any predictive ability for the distribution of methanol among the equilibrium phases. However, methanol losses to the hydrocarbon-rich vapour and liquid phases are quite significant and cannot be neglected. As a closing note we would like to report that this work had finished when it came to our attention that Englezos et al(1991) were also able to predict successfully hydrate inhibition by methanol using one equation of state together with the classical cell model.

3.6. Conclusions

A model, based on consistent thermodynamic descriptions of phases, has been tested for the prediction of hydrate dissociation pressures with and without methanol as inhibitor. The method is based on one cubic equation of state for all fluid phases with simple non-density dependent mixing rules and the ideal solid solution theory for the hydrate phases. An extensive comparison with experimental data demonstrates the reliability of the proposed model and its superiority over previously available methods, particularly for hydrate inhibition by methanol. Although the present work is confined to the study of methanol, clearly, it can be rigorously extended to include any polar inhibitor, subject to availability of binary VLE data.

References

Anderson, F.E. and Prausnitz, J.M., "Inhibition of Gas Hydrates by Methanol", AIChE J., **32**(8), 1321(1986).

Englezos, P., Huang, Z. and Bishnoi, P.R., "Prediction of natural gas hydrate formation conditions in the presence of methanol using the Trebble-Bishnoi equation of state", J. Can. Petrol. Techn., **30**(2), 148(1991).

Du, Y. and Guo, T.-M.,"Prediction of Hydrate Formation for Systems Containing Methanol", Chem.Eng.Sci., **45**(4), 893(1990).

Sloan,E.D., "Clathrate Hydrates of Natural Gases", Marcel Dekker Inc., NY(1990).

CHAPTER IV

PREDICTION OF HEAT CAPACITIES OF NATURAL GAS HYDRATES

4.1. Introduction

Accurate knowledge of the thermal properties of natural gas hydrates is required for the development of novel technology for the recovery of natural gas from hydrates in the earth and for storing of natural gas in hydrate form (Sloan,1990; Berecz and Balla-Achs,1983). Though the enthalpies of dissociation can be obtained reliably by the use of the Clapeyron equation (Fleyel and Sloan,1991; Rueff et al,1988) no general scheme has been documented for the prediction of heat capacities of natural gas hydrates. Handa(1986a,b) has measured the heat capacities of single gas hydrates of xenon, krypton, methane, ethane and propane with a calorimetric technique from 85 to 270 K with accuracy better than 1%. Handa and Tse(1986) have analyzed the data for the first three gases and they have concluded that over the temperature range of 100-270 K the heat capacity of the empty hydrate lattice of both structures is essentially equal to that of ice, within the experimental uncertainties. These authors did not consider the data for ethane and propane.

In this work classical thermodynamics together with the ideal solid solution theory of van der Waals and Platteeuw(1959) is used for the prediction of heat capacities of natural gas hydrates. No additional assumptions are needed. The formulae are particularly simple for ethane and propane hydrates, where the gas occupies the large cavity only. For multicomponent mixtures the system of equations is solved numerically.

4.2. Previous implementations of the classical statistical model

The statistical mechanics theory of van der Waals(1956) provides a formula for the calculation of the isothermal energy of formation $\Delta U_m^{\beta+g->H}$ of a clathrate per mole of gas. Parsonage and Staveley(1958) were the first to apply the statistical mechanics theory of van der Waals(1956) to calculate the heat capacity of the argon quinol clathrates. Briefly, by differentiation of ΔU_m they arrive at an

expression for the constant volume heat capacity difference $\Delta C_v^{\beta+g->H}$ between the heat capacities of the occupied cage and that of the empty cage plus that of the guest molecule per mole of gas. The heat capacity contribution of the enclathrated guest, was calculated as the difference between the heat capacity of the hydrate minus the heat capacity of the empty lattice:

$$C_{v_g}^H = C_v^H - C_v^\beta \tag{4.1}$$

Equation (1) is independent of composition and this is an implicit crucial assumption in the above model, suggesting that guest-guest interactions are negligible, the lattice is not distorted by the guest and there is no coupling between the guest and lattice modes (Handa and Tse,1986).

Finally, assuming ideal gas heat capacity for the gas phase, the constant volume heat capacity contribution of the guest molecule in the clathrate lattice is given by:

$$C_{v_g}^H = \Delta C_v^{\beta+g->H} + \frac{3}{2}R \tag{4.2}$$

Parsonage and Staveley(1958) have reduced their experimental data by observing that the heat capacity of the clathrate is a linear function of composition at constant temperature. Then a plot of the heat capacity of the clathrate versus composition would give the heat capacity of the empty lattice at the intercept y=0 and the heat capacity of the encaged molecule from the slope of the curve. The agreement between theory and experiment was considered satisfactory. This model has been used to predict successfully the heat capacities of the β-quinol clathrates of Ar, Kr, N_2, O_2 ,CO and CH_4 all of which were linear functions of composition (Parsonage and Staveley,1984), indicating validity of equation (1). The same model has also been used by Handa and Tse(1986) as part of their analysis of the heat capacity data of Handa(1986) for xenon, krypton and methane gas hydrates.

4.3. Proposed thermodynamic model

The heat capacity C_p of any system at constant pressure P is defined by:

$$C_p = \left[\frac{\partial H}{\partial T}\right]_P = T\left[\frac{\partial S}{\partial T}\right]_P = -T\left[\frac{\partial^2 G}{\partial T^2}\right]_P \tag{4.3}$$

where H, S and G are the enthalpy, entropy and free energy of the system and T the absolute temperature. By partial differentiation of the last relation we obtain:

$$\bar{c}_{p_i} = -T\left[\frac{\vartheta^2\mu_i}{\vartheta T^2}\right]_{P,x} \tag{4.4}$$

where **x** is the array of mole fractions of all components and μ_i and $\bar{c}_{p_i}$ are the chemical potential and the partial molar heat capacity of component i respectively. The heat capacity of the mixture is given by the weighed sum: $C_p=\Sigma_i x_i \bar{c}_{p_i}$. From eqn (4) and the defining equation of fugacity f_i of a component in a mixture, we obtain:

$$\bar{c}_{p_i}=c^{+}_{p_i} - 2RT\left[\frac{\vartheta \ln f_i}{\vartheta T}\right]_{p,x} - RT^2\left[\frac{\vartheta^2 \ln f_i}{\vartheta T^2}\right]_{p,x} \tag{4.5}$$

where R is the gas constant and $c^{+}_{p_i}$ is a unique function of temperature only, characteristic of the pure substance i. It is the same for all states of the substance and it may be determined by forcing agreement of the model eqn (5) to pure component experimental heat capacity data.

Table 4.1. Parameters for fitting the quantity $c^{+}_{p_i}$

Gas	a	bx10^2	cx10^4	dx10^8	AAD %
	cal·mole^{-1}·K^{-1}	cal·mole^{-1}·K^{-2}	cal·mole^{-1}·K^{-3}	cal·mole^{-1}·K^{-4}	
Xe	4.712430	0.000738	-	-	0.07
Kr	4.837330	0.000380	-	-	0.03
CH_4	7.706430	-0.265672	0.196906	-0.241807	0.54
C_2H_6	6.519231	0.925880	0.471700	-3.578000	0.10
C_3H_8	3.697170	4.756530	-0.033294	-0.036224	0.37
C_4H_{10}	2.640850	7.733960	-0.239008	-0.063755	0.40
CO_2	4.486210	1.916040	-0.174884	0.743337	0.17
N_2	6.973140	-0.066320	0.017739	-0.003831	0.03

We have fitted ideal gas heat capacity experimental data (API, Technical Data Book, 1977) to the equation $c^{+}_{p_i} = a+bT+cT^2+dT^3$, where $c^{+}_{p_i}$ is in cal·mole^{-1}·K^{-1}.

The parameters of this equation, for the temperature range 120 to 600 K, are listed in Table 1 together with the attained quality of the fit.

Calculation of $\bar{c}^{H}_{p_i}$ of a gas component in a hydrate phase

The composition in mole fraction of a hydrate phase may be calculated from the following relations:

$$x_i^H = \frac{\sum_m \nu_m \Theta_{mi}}{1+\sum_m \sum_k \nu_m \Theta_{mk}} \tag{4.6a}$$

and

$$\frac{x_i^H}{x_w^H} = \sum_m \nu_m \Theta_{mi},\ i \neq w \text{ and } m=1,2 \tag{4.6b}$$

where ν_m is the number of cavities of type m per water molecule in the unit cell and Θ_{mi} is calculated from the corresponding Langmuir type constant C_{mi}:

$$\Theta_{mi} = \frac{C_{mi} f_i}{1+\sum_j C_{mj} f_j} \tag{4.7}$$

From eqns (6b) and (7) by taking logarithms and differentiating while keeping all x_i and x_w constants we obtain:

$$\frac{\vartheta}{\vartheta T}\left(\sum_m \nu_m \Theta_{mi}\right)_{P,x_{i,w}} = 0 \text{ or equivalently } \sum_m \nu_m \Theta_{mi} \frac{\vartheta \ln \Theta_{mi}}{\vartheta T} = 0 \tag{4.8}$$

$$\frac{\vartheta \ln \Theta_{mi}}{\vartheta T} = \frac{\vartheta \ln C_{mi}}{\vartheta T} + \frac{\vartheta \ln f_i}{\vartheta T} - \sum_j \Theta_{mj} \left[\frac{\vartheta \ln C_{mj}}{\vartheta T} + \frac{\vartheta \ln f_j}{\vartheta T}\right] \tag{4.9}$$

$$\sum_m \nu_m \Theta_{mi} \left[\frac{\vartheta \ln C_{mi}}{\vartheta T} + \frac{\vartheta \ln f_i}{\vartheta T} - \sum_j \Theta_{mj} \left[\frac{\vartheta \ln C_{mj}}{\vartheta T} + \frac{\vartheta \ln f_j}{\vartheta T}\right]\right] = 0 \tag{4.10}$$

The last system of eqns (10) may be solved for the derivatives of the logarithms of the fugacities of gas components as functions of T and the composition of

the hydrate phase. It is noted that these equations are independent of pressure and the constant pressure requirement for differentiation is dropped. For single gas hydrates the system of equations is reduced to a single analytical expression:

$$\frac{\vartheta \ln f_1}{\vartheta T} = - \frac{\sum_m \nu_m \Theta_{m1}(1 - \Theta_{m1}) \frac{\vartheta \ln C_{m1}}{\vartheta T}}{\sum_m \nu_m \Theta_{m1}(1 - \Theta_{m1})} \qquad (4.10a)$$

If the gas component enters the large cavities only, the equation is particularly simple:

$$\frac{\vartheta \ln f_1}{\vartheta T} = - \frac{\vartheta \ln C_{21}}{\vartheta T} \qquad (4.10b)$$

Equations (10) can be further differentiated to obtain the second derivative of the logarithm of the fugacities of gas components. The corresponding final expressions are:

$$\frac{\vartheta^2 \ln f_i}{\vartheta T^2} \sum_m \nu_m \Theta_{mi}$$

$$+\sum_m \nu_m \Theta_{mi} \left[\frac{\vartheta \ln^2 C_{mi}}{\vartheta T^2} - \sum_j \Theta_{mj} \frac{\vartheta \ln \Theta_{mj}}{\vartheta T} \left[\frac{\vartheta \ln C_{mj}}{\vartheta T} + \frac{\vartheta \ln f_j}{\vartheta T} \right] - \sum_j \Theta_{mj} \left[\frac{\vartheta^2 \ln C_{mj}}{\vartheta T^2} + \frac{\vartheta^2 \ln f_j}{\vartheta T^2} \right] \right]$$

$$+\sum_m \nu_m \Theta_{mi} \frac{\vartheta \ln \Theta_{mi}}{\vartheta T} \left[\frac{\vartheta \ln C_{mi}}{\vartheta T} - \sum_j \Theta_{mj} \left[\frac{\vartheta \ln C_{mj}}{\vartheta T} + \frac{\vartheta \ln f_j}{\vartheta T} \right] \right] = 0 \qquad (4.11)$$

$$\frac{\vartheta^2 \ln f_1}{\vartheta T^2} =$$

$$- \frac{\sum_m \nu_m \Theta_{m1}(1-\Theta_{m1}) \left[\left[\frac{\vartheta \ln C_{m1}}{\vartheta T} \right]^2 - \left[\frac{\vartheta \ln f_1}{\vartheta T} \right]^2 + \frac{\vartheta \ln^2 C_{m1}}{\vartheta T^2} - 2\Theta_{m1} \left[\frac{\vartheta \ln C_{m1}}{\vartheta T} + \frac{\vartheta \ln f_1}{\vartheta T} \right]^2 \right]}{\sum_m \nu_m \Theta_{m1}(1-\Theta_{m1})}$$

(4.11a)

$$\frac{\vartheta^2 \ln f_1}{\vartheta T^2} = - \frac{\vartheta \ln^2 C_{21}}{\vartheta T^2} \qquad (4.11b)$$

The Langmuir type constants and the derivatives of their logarithms are functions of temperature only. The necessary expressions for the calculation of the derivatives of the Langmuir type constants are listed in Appendix C.

For multicomponent systems, equations (10) and (11) can be solved easily for the unknown values of the first and second derivatives of fugacity by application of the method of successive substitutions. The procedure can be initialized by assigning zero values to all unknowns. At some extra computational time cost, alternative good initial estimates may be obtained by assuming each hydrate former to be the only hydrate forming gas and applying equations (10a) and (11a) respectively. In the present implementation, solution is considered to be achieved when the Euclidian Norm of the unknowns is less than a tolerance set equal to 10^{-8}.

Calculation of $\bar{c}^{H}_{p_w}$ of water in a hydrate phase

The partial molar heat capacity of water in the hydrate phase is calculated from the expression:

$$\bar{c}^{H}_{p_w} = c^{\beta}_{p_w} + \Delta c^{H-\beta}_{p_w} \tag{4.12}$$

where $c^{\beta}_{p_w}$ is the heat capacity of water in the empty hydrate lattice and $\Delta c^{H-\beta}_{p_w}$ the difference between heat capacities of water in the hydrate phase and water in the empty lattice at the same temperature. $\Delta c^{H-\beta}_{p_w}$ can be calculated by application of the thermodynamic equation (4):

$$\Delta c^{H-\beta}_{p_w} = -T\frac{\vartheta^2(\Delta\mu^{H-\beta}_w)}{\vartheta T^2} \tag{4.13}$$

The ideal solid solution theory gives:

$$\Delta\mu^{H-\beta}_w = -RT\sum_m \nu_m \ln(1+\sum_j C_{mj} f_j) \tag{4.14}$$

It is noted that if the composition of the hydrate is fixed, equation (14) is independent of pressure. The final general expression for the calculation of $c^{H}_{p_w}$ is :

$$\bar{c}^{H}_{p_w} = c^{\beta}_{p_w} - 2RT\sum_m \nu_m \sum_j \Theta_{mj}\left[\frac{\vartheta \ln C_{mj}}{\vartheta T} + \frac{\vartheta \ln f_j}{\vartheta T}\right]$$

$$-RT^2\sum_m \nu_m \sum_j \Theta_{mj}\left[\frac{\vartheta^2 \ln C_{mj}}{\vartheta T^2} + \frac{\vartheta^2 \ln f_j}{\vartheta T^2} + \left[\frac{\vartheta \ln C_{mj}}{\vartheta T} + \frac{\vartheta \ln f_j}{\vartheta T}\right]^2\right]$$

$$+RT^2\sum_m \nu_m\left[\sum_j \Theta_{mj}\left[\frac{\vartheta \ln C_{mj}}{\vartheta T} + \frac{\vartheta \ln f_j}{\vartheta T}\right]\right]^2 \qquad (4.15)$$

For single gas hydrates eqn(15) is simplified:

$$\bar{c}^{H}_{p_w} = c^{\beta}_{p_w} - 2RT\sum_m \nu_m \Theta_{m1}\left[\frac{\vartheta \ln C_{m1}}{\vartheta T} + \frac{\vartheta \ln f_1}{\vartheta T}\right]$$

$$-RT^2\sum_m \nu_m \Theta_{m1}\left[\frac{\vartheta^2 \ln C_{m1}}{\vartheta T^2} + \frac{\vartheta^2 \ln f_1}{\vartheta T^2} + (1 - \Theta_{m1})\left[\frac{\vartheta \ln C_{m1}}{\vartheta T} + \frac{\vartheta \ln f_1}{\vartheta T}\right]^2\right] \qquad (4.15a)$$

Considering eqns (10b) and (11b) the heat capacity of water for single gas hydrates where the gas enters the large cavity only is equal to that of the empty lattice:

$$\bar{c}^{H}_{p_w} = c^{\beta}_{p_w} \qquad (4.15b)$$

4.4. The heat capacity of the empty hydrate lattice

Handa(1986a) argues that the composition of the hydrate sample during his experiments should be considered constant for the whole range of the scan temperatures, although hydrate, ice and gas coexisted at pressures higher than the hydrate dissociation pressure. Theoretical calculations, however, show that for xenon, krypton and methane the composition of the hydrate as well as the distribution of the guest between the two types of cavities change appreciably with temperature. To apply classical thermodynamics we consider the hydrate as a closed homogeneous phase having the reported experimental composition at any fixed temperature. Then, the heat capacity of the hydrate is calculated as the weighted sum of the partial molar heat capacities of gas and water. The value of $c^{\beta}_{p_w}$ is adjusted until agreement is obtained between experimental and predicted heat capacities of single gas hydrates. The results of this procedure are presented in figures 1 and 2 together with the experimental heat capacity data for ice reported by Handa et al(1984).

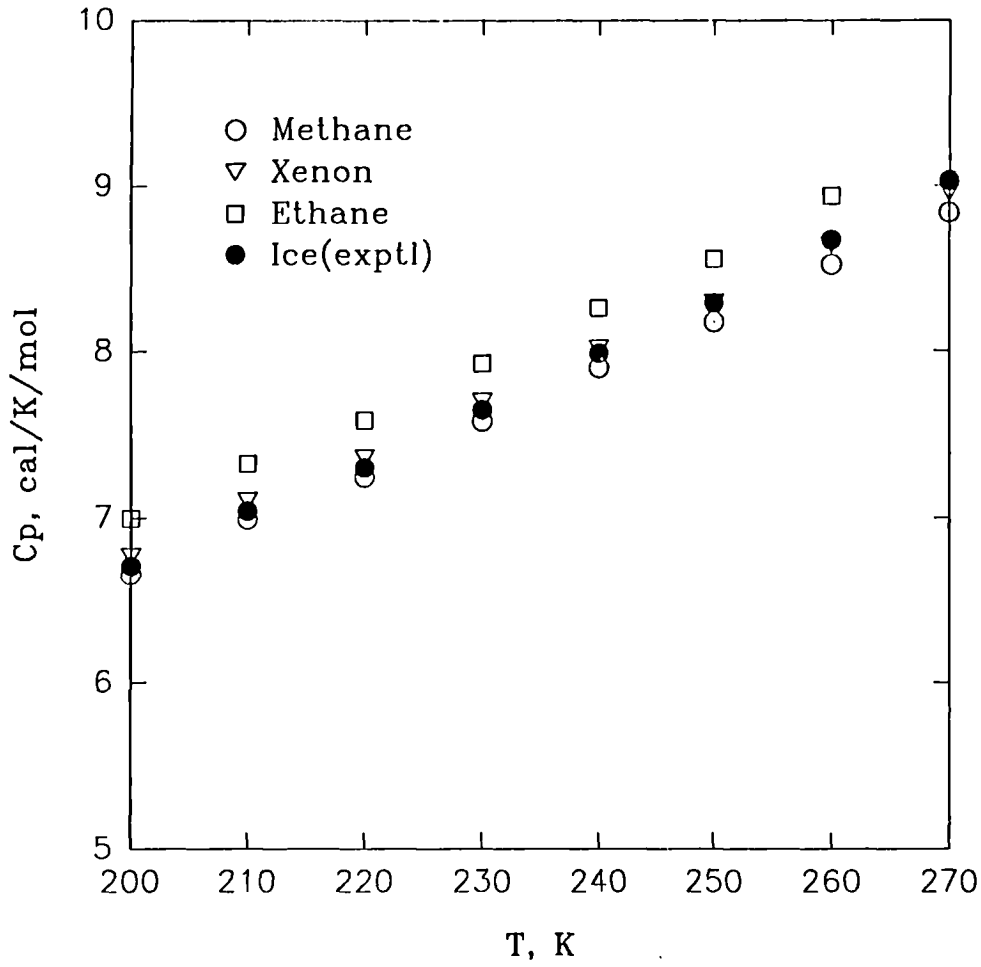

Figure 4.1. Comparison of calculated heat capacities of the empty hydrate structure I from heat capacity data of ethane, methane and xenon hydrates.

For single gas hydrates where the guest can only enter the large cavity, the composition of the hydrate is less sensitive to temperature and can be considered constant within the present experimental capabilities. Therefore, for the case of ethane and propane hydrates no assumption regarding the state of equilibrium is necessary and heat capacities calculations are straightforward by application of eqns (5), (10b), (11b) and (15b). It is seen that only the derivatives of the Langmuir type constants are required from the ideal solid solution model.

Figure 1 indicates that $c_{p_w}^{\beta}$ for structure I calculated from ethane hydrate heat capacity data is always higher than that from methane data, which in turn is very close to the one calculated from xenon. The heat capacity of the empty structure II hydrate has been obtained from the propane heat capacity data. Krypton hydrate is excluded from the present study, mainly because there are inadequate data for dissociation pressures and compositions to allow undisputed determination of the Kihara potential parameters. In particular, the six HLV data points of Holder et al(1980), assumed as structure II, do not fit very well on the same model with the six low temperature HIV data points of Barrer and Edge(1967). On top of this discrepancy, it was found that the solid solution model cannot match with the required accuracy both the above 12 dissociation points and the composition $Kr{\cdot}6.10H_2O$ at 253.0 K and 2.72 MPa reported by Handa(1986). However, Handa and Tse(1986) claim successful prediction of the composition $Kr{\cdot}6.10H_2O$ at the three phase HIV hydrate point at 273.15 K. Of course, the prediction of their model is just irrelevant to the experimental datum of Handa(1986) and thus our conclusion for inadequacy of the available experimental data for krypton is verified.

The heat capacity of the empty hydrate structure II lattice, as determined from the heat capacity data of propane, is also higher than that of ice and on average it is higher than the one of structure I hydrate derived from the ethane hydrate heat capacity data.

We have fitted, the heat capacity differences between the empty hydrate lattice and ice, in the temperature region 200-270 K to the equation:

$$\Delta C_{p_w}^{\beta-\alpha} = C_1 + C_2(T-T_0) \qquad (4.16)$$

where T_0 is the ice point. The regressed parameters from each hydrate are given in Table 4.2. Heat capacities are never linear functions of temperature, and it is

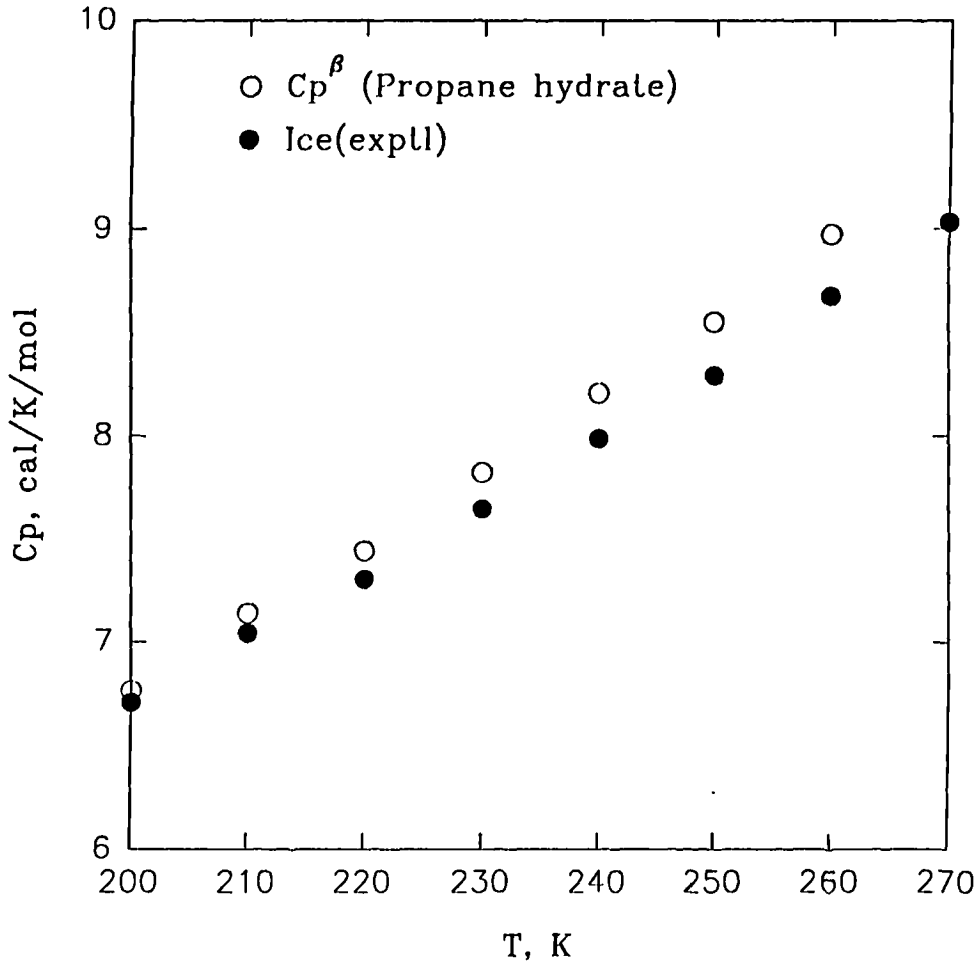

Figure 4.2. Heat capacity of the empty hydrate structure II lattice calculated from heat capacity data of propane single gas hydrate.

understood that these linear equations are approximations only, and they may not be valid outside the specified temperature region.

Table 4.2. Regressed parameters for the heat capacity of the empty hydrate lattice relative to ice from the single gas hydrate heat capacity data of Handa(1986a,b).

Parameter	Gas Hydrate			
	$Xe{\cdot}5.90H_2O$	$CH_4{\cdot}6.00H_2O$	$C_2H_6{\cdot}7.67H_2O$	$C_3H_8{\cdot}17.01H_2O$
C_1/cal·mol^{-1}·K^{-1}	-0.0483	-0.1709	0.2606	0.3542
C_2/cal·mol^{-1}·K^{-2}	-0.0019	-0.0020	-0.00043	0.00403

4.5. Partial molar heat capacity of guest molecules in the hydrate phase

The heat capacity contributions of guest molecules to their hydrate heat capacity can be calculated by direct application of equation (5) with derivatives obtained from equations (10) and (11). It is noted that equation (5) is a generally valid thermodynamic relation and as such does not depend on adjustable parameters other than those used to calculate fugacities. The results of application of equation (5) for the hydrates $Xe{\cdot}5.90H_2O$, $CH_4{\cdot}6.00H_2O$, $C_2H_6{\cdot}7.67H_2O$ and $C_3H_8{\cdot}17.01H_2O$ are presented in figures 3 to 6. For comparison, the experimental ideal gas heat capacities (API Techical Data Book, 1982) of the respective gases are also plotted in the same figures.

Figures 3 and 4 show that in the temperature range 200 to 270 K, enclathrated xenon and methane have the same heat capacity, within the experimental error, as the corresponding ideal gases. Figure 5 shows that enclathrated ethane gas has a heat capacity about 2.7 % higher than the corresponding gas, while in figure 6 the propane guest appears having heat capacity not more than 3% less than the propane ideal gas. These differences, however, are indeed very small, and although they may represent real situations, one should take into account that the combined experimental errors of the heat capacity determinations of the gas hydrate(±1%) and the ideal gas(±1.5%) might be mainly responsible for these differences.

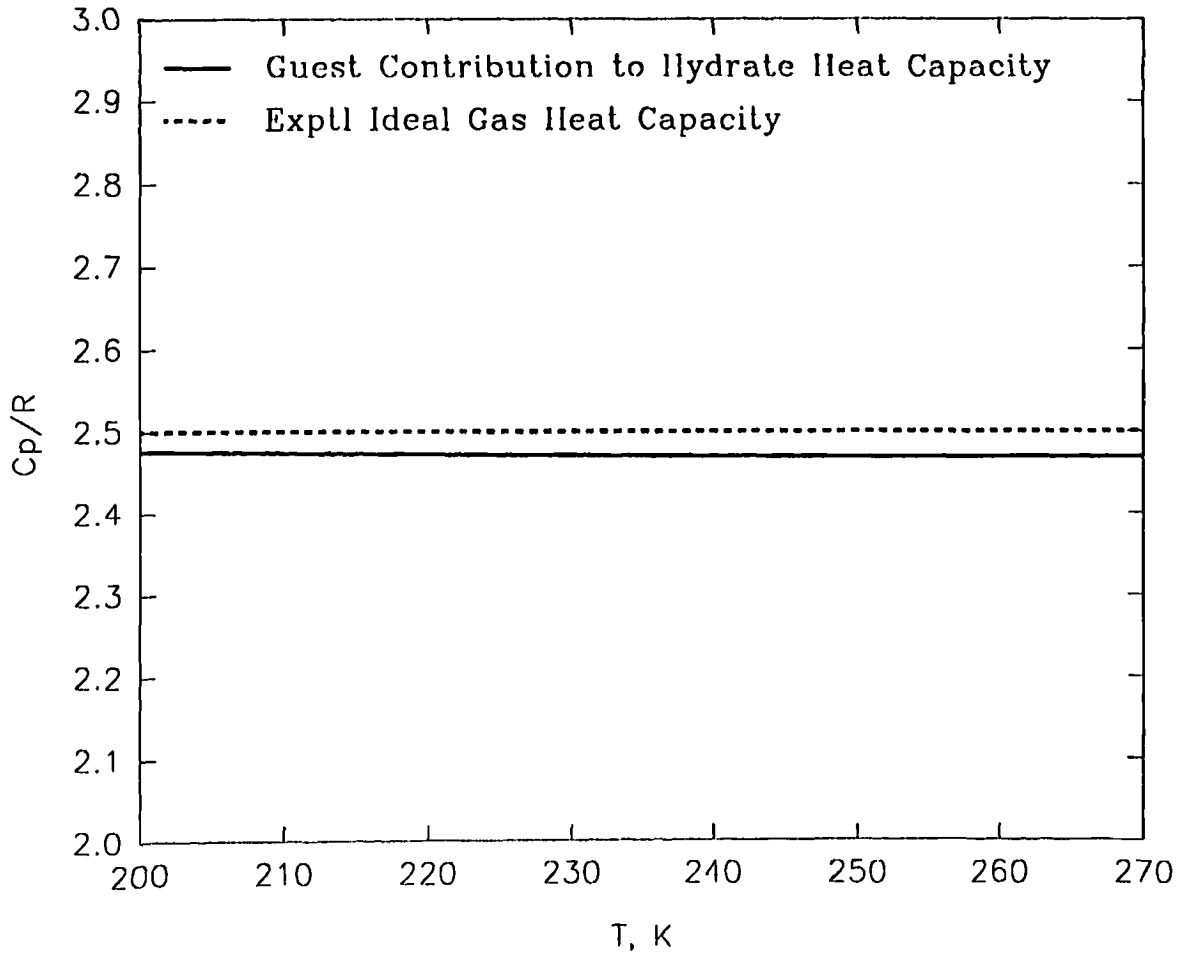

Figure 1.3. Predicted contribution of xenon guest to its hydrate structure I heat capacity.

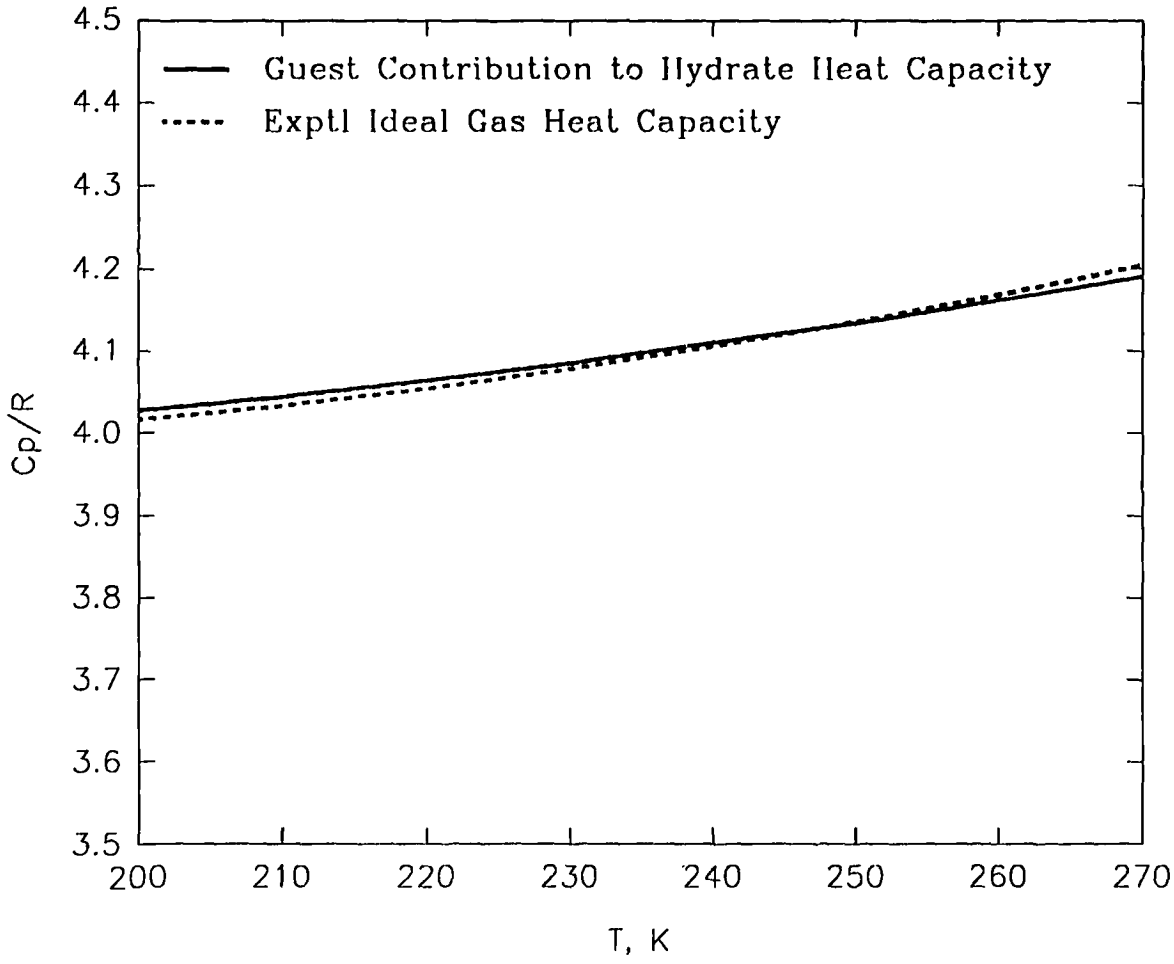

Figure 4.4. Predicted contribution of methane guest to its hydrate structure I heat capacity.

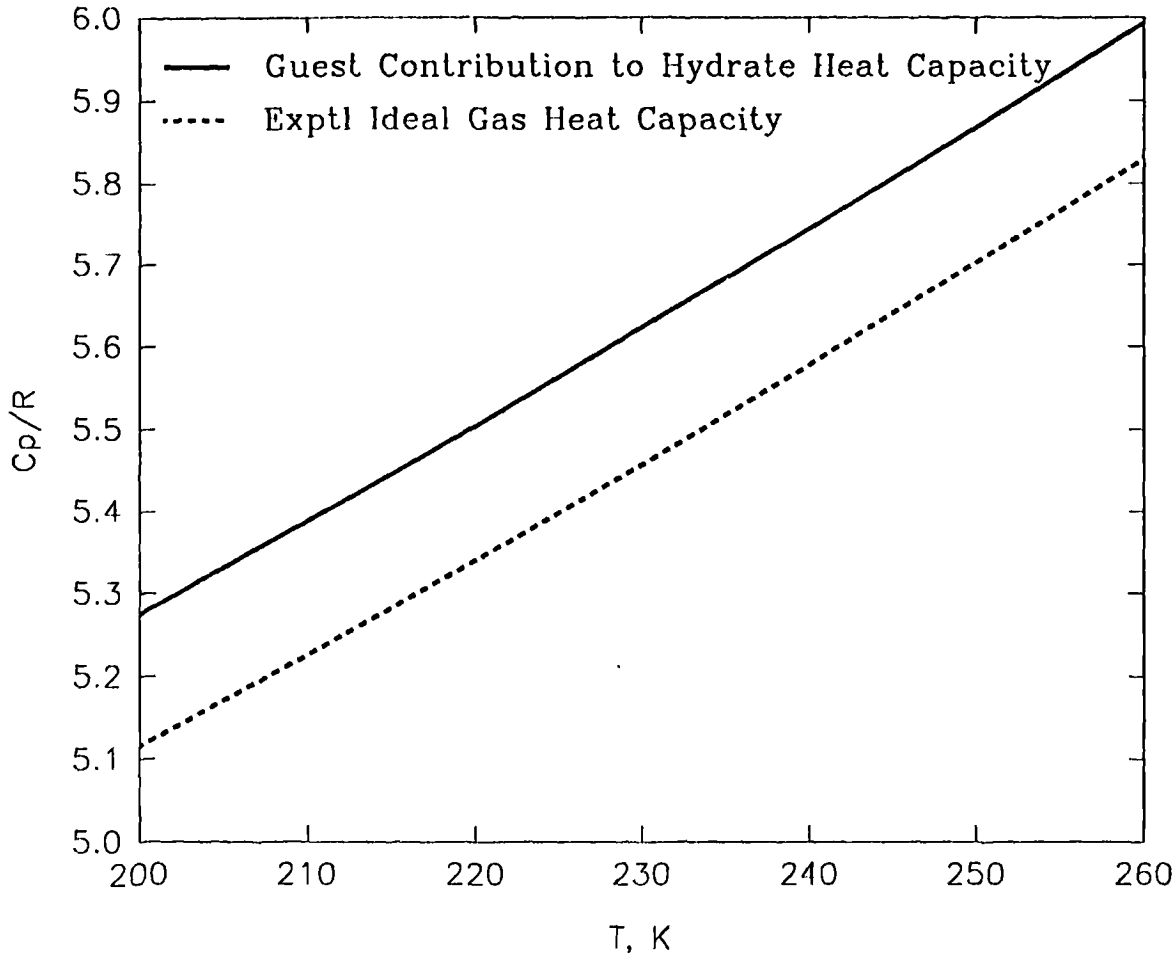

Figure 4.5. Predicted contribution of ethane guest to its hydrate structure I heat capacity.

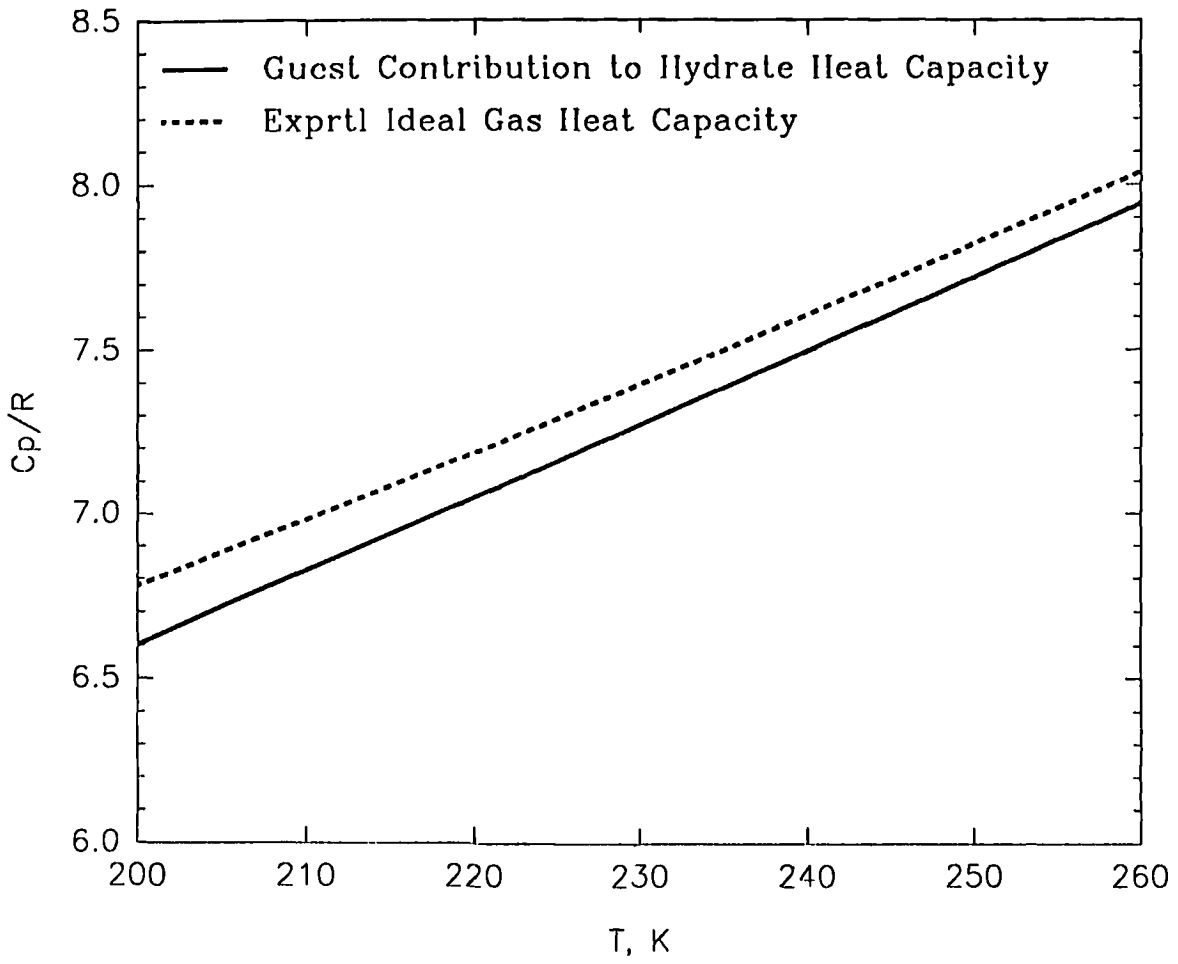

Figure 1.6. Predicted contribution of propane guest to its hydrate structure II heat capacity.

4.6. Results and discussion

The thermodynamic model is applied to predict the heat capacities of the natural gas hydrate studied by Cherskii et al(1983). The composition of the gas used by the experimentalists to produce the hydrate is given in Table 3 in volume % at some unspecified temperature and pressure conditions. We assume therefore the same percentage in mole fraction. The composition of the synthetic gas hydrate has not been reported and the details of its preparation are rather diffuse. We assume that the hydrate has been produced at 258 K and 5 MPa(conditions for the preparation of the silica sand/hydrate mixture) in equilibrium with excess of the natural gas. We further assume that the composition of the hydrate did not change during the heat capacity measurements. The experimental data were reported in the form of a fitted equation with unspecified range of validity. We assume reasonably that this equation is valid in the temperature range 235-270 K. Figure 7 presents the experimental data for the hydrate heat capacities and the associated error bars as reported by the experimentalists. For comparisons the heat capacities of ice (Handa et al, 1984) and the predictions of our model are also plotted in figure 7. Since the gas mixture corresponds to a structure II hydrate, we have used for the heat capacity difference between the empty hydrate lattice and ice, the value obtained from the propane hydrate(Table 2). The predictions of the model are about 10% lower than the experimental line and they are very close to the experimental heat capacity data of ice. Such deviation can be considered satisfactory considering the uncertainties associated with the experimental data. It is noted that Rueff et al(1988) have also found the data of Cherskii et al(1983) to be too high and questioned their reliability.

Table 4.3. Composition of the natural gas of Cherskii et al(1983) in V%[1].

CH_4	C_2H_6	C_3H_8	C_4H_{10}	C_5H_{12}	N_2	O_2
91.51	3.94	1.22	0.59	0.20	2.00	0.40

[1]Temperature and pressure were not specified. The composition is not normalized.

An experimental study of the heat capacities of naturally occurring hydrates has been carried out by Handa(1988). The gas in the first sample was almost pure methane but the composition of the hydrate was slightly different from the synthetic sample studied before(1986) by the same author, reflecting different preparation conditions. The second sample was a structure II hydrate with high propane content. Unfortunately, precise heat capacity measurements could not be

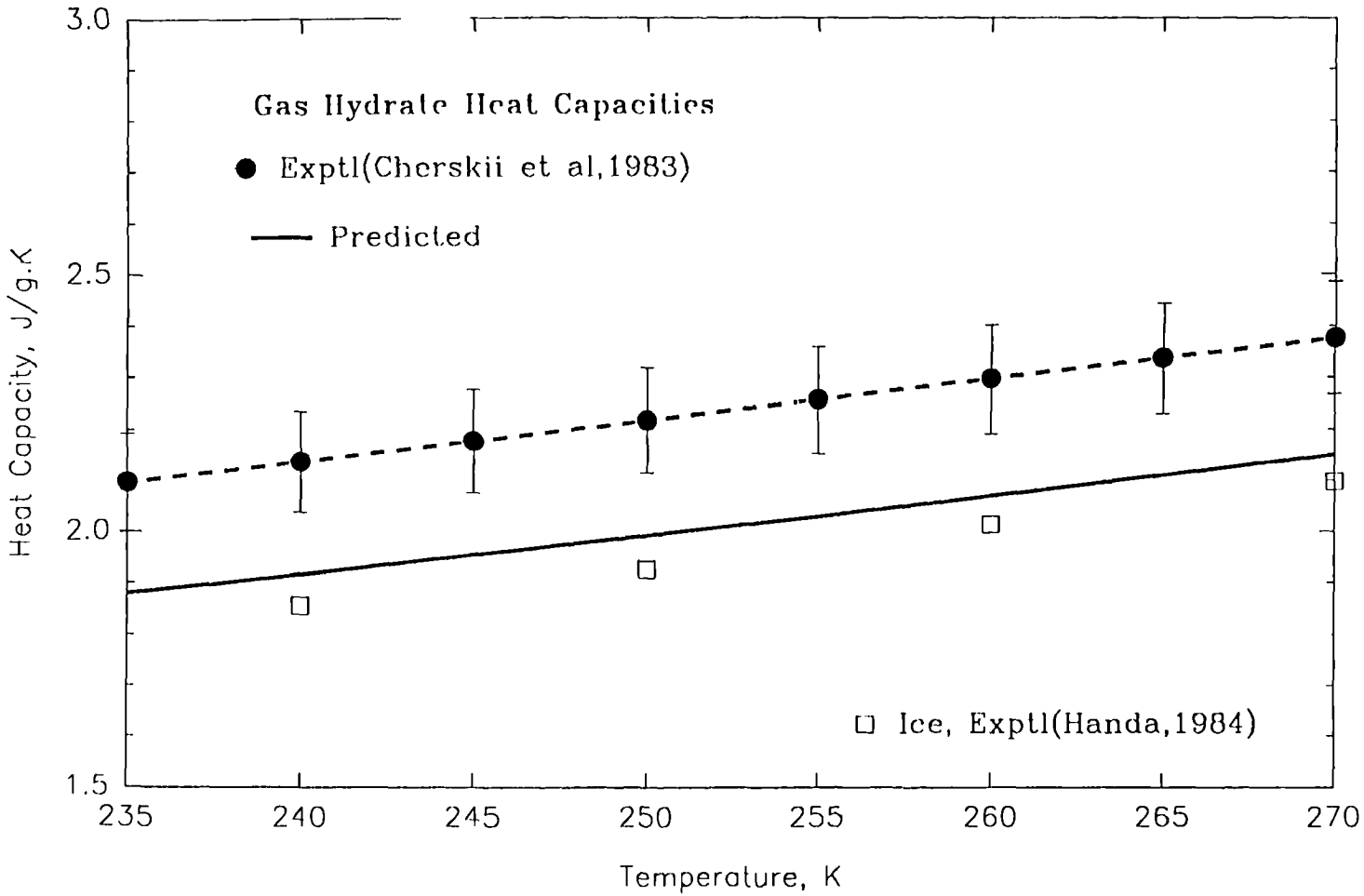

Figure 1.7. Experimental and calculated heat capacities of a natural gas hydrate.

reported for either sample, due the amount of impurities in the samples. No other experimental heat capacity data of multicomponent hydrate systems have been reported in the open literature.

Our analysis of the heat capacity data of Handa(1986a,b) for methane and xenon leads essentially to the same conclusion as that reached by Handa and Tse(1986): For hydrates of small molecules, the heat capacities of the guest and water are - within the experimental error - equal to those in the gas and ice phase respectively. It was not possible to analyse the data of krypton. It may be that the hydrate number of the krypton hydrate reported by Handa(1986b) is too high, leading to wrong values for the respective heat capacity data. In any case, more dissociation point data for krypton are needed. Alternatively, the discrepancy might be resolved when heat capacity data for nitrogen, which is also a structure II hydrate former, become available. Note, however, that a potential barrier has been reported (van der Waals, 1961) for the nitrogen β-quinol clathrate, the cavity radius of which is similar in size to the small hydrate cavities.

The scheme used by Handa and Tse(1986) to reduce the heat capacity data for xenon, krypton and methane is not applicable to ethane and propane. No analysis of the data for these components has come to our attention. The application of the methodology proposed by us leads to the conclusion that the ethane guest causes a small but definite increase of the heat capacity of water in the hydrate lattice as well as an increase of the heat capacity of the guest itself. It is noted that, according to our proposal, the heat capacity of the guest molecules is independent of the pressure while the heat capacity of water depends on pressure to the same extent as ice. Our results for propane, however, are not conclusive, although the regression algorithm always converges to the reported values . This is because the hydrate number of propane is too large (17 moles of water per mole of propane guest). Accordingly, the contribution of the guest to the heat capacity of its hydrate is very small and our multivariable regression algorithm may not sense the correct values.

Davidson et al(1977) have recorded nuclear magnetic resonance spectra of the clathrate hydrates and/or deuteriorates of methane, ethane, propane, isobutane and conducted dielectric relaxation measurements in hydrogen sulfide, propane, isobutane and n-butane-hydrogen sulfide hydrates. They have estimated that there are no reorientation barriers for the hydrogen sulfide and methane encaged molecules and they report average barriers to reorientation ("activation energies") 1.2 Kcal/mol for ethane(str.I) and 0.6, 1.2 and 1.4 Kcal/mol for

propane, iso-butane and n-butane in structure II hydrates. Our calculations for methane and ethane are in agreement with these findings.

It has not been possible to reach a unique function for the heat capacity of the (hypothetical) empty hydrate lattice, but different approximations were obtained from hydrates of different guest molecules. Although this finding is contrary to the conventional approach of assigning unique values to the thermodynamic properties of the empty hydrate lattice, it does support the suggestion of Holder et al(1988) for different values of the reference chemical potential for different guests. Moreover, Davidson et al(1977) were able to detect wide distributions of reorientation rates in all hydrates studied by them. They attribute this phenomenon to variations of distortion from cage to cage. Then, if variable composition heat capacity data were available for the mixed with methane hydrates of ethane and propane, application of our model would be expected to lead to varying calculated values of the heat capacity of the respective empty hydrate lattices.

4.7. Conclusions

Classical thermodynamics and the ideal solid solution theory were applied to reduce the heat capacity experimental data for single gas hydrates obtained by Handa(1986a,b) and a general methodology was detailed for the prediction of the heat capacity of single and multicomponent gas hydrates. The heat capacities of the empty hydrate lattices of structure I and II hydrates were regressed as functions of temperature and it was shown that the heat capacities of the empty lattice of propane and ethane hydrates are always larger than those of xenon and methane, which in turn are very close to that of ice. The calculated partial molar heat capacities of the enclathrated gases of methane and xenon were always ideal gas like, while ethane demonstrated a definite increase. No conclusive results could be obtained for propane hydrate. It has been indicated that the experimental heat capacity data of gas hydrates are insufficient. To establish generalized correlations for the thermodynamic properties of the empty hydrate lattice more heat capacity data are needed. In particular, heat capacity data are needed for multicomponent systems of both structures, for binary mixtures of the gas hydrates studied by Handa(1986a, b) in a range of compositions and for the simple gas hydrates of carbon dioxide, nitrogen and n-butane, which have not been studied so far. In addition, dissociation pressure and compositional data are needed for the krypton hydrate.

References

API, Technical Data Book, Petroleum Refining, Volume II, Procedure 7A1.1, Fourth Edition(1977).

Barrer,R.M. and Edge,A.V.J., "Gas hydrates containing argon, krypton and xenon: kinetics and energetics of formation and equilibria", (1967).

Berecz and Balla-Achs,"Gas hydrates", Elsevier,NY(1983).

Cherskii,N.V., Groisman,V.P., Tsarev,V.P. and Nikitina,L.M., "Thermophysical properties of natural gases", Doklady Akademii Nauk SSSR, **207**(4), 949(1983).

Davidson,D.W., Garg,S.K., Gough,S.R., Hawkins,R.E. and Ripmeester,J.A., "Characterization of natural gas hydrates by nuclear resonance and dielectric relaxation", Can.J.Chem., **55**, 3641(1977).

Handa,Y.P., "Calorimetric determinations of the compositions, enthalpies of dissociation, and heat capacities in the range 85 to 270K for clathrate hydrates of xenon and krypton", J.Chem.Thermodynamics, **18**, 891(1986a).

Handa,Y.P., "Compositions, enthalpies of dissociation and heat capacities in the range 85 to 270K for clathrate hydrates of methane, ethane, and propane, and ethalpy of dissociation of isobutane hydrate, as determined by a heat-flow calorimeter", J.Chem.Thermodynamics, **18**, 915(1986b).

Handa,Y.P., "A calorimetric study of naturally occurring gas hydrates", Ind.Eng.Chem.Res., **27**, 872(1988).

Handa,Y.P., Hawkins,R.E. and Murray,J.J. "Calibration and testing of a Tian-Calvet heat-flow calorimeter. Enthalpies of fusion and heat capacities for ice and tetrahydrofuran hydrate in the range 85 to 270K", J.Chem.Eng.Thermodynamics, **16**, 623(1984).

Handa,Y.P. and Tse,J.S., "Thermodynamic properties of the empty lattices of structure I and II clathrate hydrates", J.Phys.Chem., **90**, 5917(1986).

Holder, G.D., Zetts,S.P. and Pradhan,N, "Phase Behaviour in systems containing clathrate hydrates. A review", Reviews in Chem. Eng.,2(1988).

Holder, G.D., Corbin,G. and Papadopoulos, "Thermodynamic and molecular properties of gas hydrates from mixtures containing methane, argon and krypton", Ind.Eng.Chem.Fund., **19**, 282(1980).

Parsonage,N.G. and Staveley,L.A.K.,"Thermodynamic properties of clathrates: The heat capacity and entropy of argon in the argon quinol clathrate", Mol.Phys., **2**,212(1958).

Parsonage,N.G. and Staveley,L.A.K., "Thermodynamic studies of clathrates and inclusion compounds", in Inclusion Compounds, Vol 3, Chapter 1, Academic Press, London(1984).

Rueff,R.M., Sloan,E.D. and Yesavage,V.F., "Heat capacity and heat of dissociation of methane hydrates", AIChE J., **9**(34), 1469(1988).

Sloan,E.D., "Clathrate hydrates of natural gases", Marcel Dekker,Inc., NY(1990).

Fleyel,F. and Sloan,E.D., "Prediction of natural gas hydrate dissociation enthalpies", ISOPE-91, Edinburgh, 11-16 Aug.1991.

van der Waals,J.H., "The statistical mechanics of clathrate compounds", Trans.Faraday Soc., **52**, 184(1956).

van der Waals,J.H., "Some observations on clathrates", J.Phys.Chem.Solids, **18**, 82(1961).

van der Waals,J.H and Platteeuw,J.C.,"Clathrate compounds", in Advances in chemical physics, Edited by I.Prigogine, Interscience,NY(1959).

CHAPTER V

THERMODYNAMIC STABILITY

5.1. Objective

A major problem in multiphase equilibria calculations is that the number and the identity of the equilibrium phases is not known in advance. In the previous chapters this problem was not faced because the identity of the equilibrium phases was experimentally known. The right approach to this problem is the minimisation of the Gibbs free energy, since if a system is at true equilibrium the Gibbs free energy is at a global minimum. Accordingly, the conventional method to solve this problem had been to assume a combination of phases and formulate a Gibbs free energy minimisation problem(Heidemann,1974). Obviously, this is a tedious approach which not necessarily converges to the correct solution(Gautam and Seider, 1979). Currently, the established methodology makes use of the Gibbs tangent plane criterion, as implemented by Michelsen(1982), to search for the Gibbs free energy surface global minimum.

In this chapter the thermodynamic principles governing multiphase equilibria and stability are clearly stated in an effort to elucidate the thermodynamic nature of the problem. Methods based on the tangent plane criterion are presented and reviewed. Next, the development of a new approach particularly suitable for multiphase equilibria calculations involving solid hydrate phases is presented and the computational implementation is detailed. The efficiency of the proposed methodology is demonstrated by application in several situations and by comparison of predictions with experimental data.

The present treatment ignores metastable states as an immediate result of the particular methods employed to minimise the Gibbs free energy of the system. Also, equilibrium states at the limit of stability(critical states), which represent a special case of the general stability analysis, are not considered here. These limitations do not interfere with the solution of the specified(Chapter 1) heterogeneous equilibrium problem.

5.2. Thermodynamic equilibrium and stability criteria

A direct consequence of the Second Law of thermodynamics is the principle of maximum entropy: The state of equilibrium of an isolated system composed of a number of open phases is defined by the values of the independent variables which maximize the entropy function $S(U,V,n_1,...,n_c)$ of the system. In mathematical notation, that is:

$$dS = 0 \qquad (5.1a)$$

and

$$d^2S < 0 \qquad (5.1b)$$

If U is the internal energy of the system, V the total volume and n_i the total number of moles of component i in the system and π the number of the open phases composing the system, then the independent variables should meet the imposed conditions of isolation, that is:

$$dU = \sum_j^{\pi} dU_j = 0,\ dV = \sum_j^{\pi} dV_j = 0 \text{ and } dn_i = \sum_j^{\pi} dn_{ij} = 0,\ i=1,...,c \qquad (5.1c)$$

where U_j, V_j and n_{ij} are the corresponding values of internal energy, volume and mole numbers of component i in the (open)phase j and c the number of components.

The maximum entropy principle for isolated systems can be used to derive the equilibrium conditions at different imposed restraints, practically more interesting. In particular, the condition of thermodynamic equilibrium in a composite closed system of open phases at constant temperature and pressure, is characterized by those values of the independent variables which minimize the Gibbs free energy of the system $G(T,P,n_1,...,n_c)$. In mathematical notation this is:

$$dG = 0 \qquad (5.2a)$$

and

$$d^2G > 0 \qquad (5.2b)$$

under the constraints:

$$T, P = \text{constant and } dn_i = \sum_j^{\pi} dn_{ij} = 0,\ i=1,...,c \qquad (5.2c)$$

Equation (2a) and the inequality (2b) form respectively the criteria of thermodynamic equilibrium and stability in Gibbs free energy representation of the fundamental equation.

If the virtual boundaries separating the phases are diathermal and movable, then equation (2a) under the restraints (2c) can be shown to be equivalent to the following set of equations, which relate the thermodynamic properties of the open phases at the state of thermodynamic equilibrium:

$$T_1 = T_2 = ... = T_\pi \tag{5.3a}$$

$$P_1 = P_2 = ... = P_\pi \tag{5.3b}$$

$$\mu_{11} = \mu_{12} = ... = \mu_{1j} = ... = \mu_{1\pi}$$

. . .

$$\mu_{i1} = \mu_{i2} = ... = \mu_{ij} = ... = \mu_{i\pi}$$

. . .

$$\mu_{c1} = \mu_{c2} = ... = \mu_{cj} = ... = \mu_{c\pi} \tag{5.3c}$$

where $\mu_{ij} = (\vartheta G/\vartheta n_{ij})_{T,P,n_{kj}}$ is the chemical potential of component i in phase j.

For an homogeneous closed phase under constant temperature and pressure, the inequality (2b) results in the following criterion for the intrinsic stability of a phase:

$$\left[\frac{\vartheta^2 G}{\vartheta n_i^2}\right]_{T,P,n_k} = \left[\frac{\vartheta \mu_i}{\vartheta n_i}\right]_{T,P,n_k} > 0,\ i=1,...,c \tag{5.4}$$

This is a necessary and sufficient criterion and states that addition to a stable phase of an amount of some component will always result in an increase of the chemical potential of that component. To fix ideas, consider that a phase meeting this criterion, can develop a heterogeneous region within it. Initially both phases will have the same composition and will differentiate by transfer of mass of components 1,...,i,...,c from the first to the second phase. According to eqn (4), this results in a decrease of the chemical potential of each component in the first phase and a corresponding increase in the second phase and, therefore equilibrium is not possible due to violation of equation (3c).

Mole fractions x_i are commonly the preferred variables in chemical engineering calculations and it is desired to express the stability criteria in terms of mole fractions as well. Since the fundamental equation is a homogeneous polynomial of the first degree it follows that the mean Gibbs energy g = G/n is:

$$g = (1/n)G(T,P,n_1,...,n_c) = G(T,P,x_1,...,x_c) \tag{5.5a}$$

and

$$g = \sum_i^c x_i \frac{\vartheta G}{\vartheta n_i} = \sum_i^c x_i \mu_i \tag{5.5b}$$

where n is the (constant) total number of moles:

$$n = \sum_i^c n_i \tag{5.6}$$

It is noted that because of the normalization equation, one(anyone) of the mole fractions is a dependent variable. Therefore equation (5a) may be rewritten as:

$$g = g(T,P,x_1,...,x_{c-1}) \tag{5.5c}$$

Direct comparison of the total differentials dg of equations (5a) and (5b) yields the following important relation:

$$\frac{\vartheta g}{\vartheta x_i} = \mu_i - \mu_c \tag{5.7}$$

where c is the indice of the dependent mole fraction. For a binary system, with x_1 the independent mole fraction, differentiation of (7) by taking into consideration the Gibbs-Duhem equation leads to another useful relation:

$$\frac{\vartheta^2 g}{\vartheta x_1^2} = \frac{1}{x_2} \frac{\vartheta \mu_1}{\vartheta x_1} \tag{5.8}$$

The stability criterion inequality (4) may also be expressed in terms of mole fractions:

$$\left[\frac{\vartheta \mu_i}{\vartheta n_i}\right]_{T,P,n_k} = \left[\frac{\vartheta \mu_i}{\vartheta x_i}\right]\left[\frac{\vartheta x_i}{\vartheta n_i}\right] = \frac{1-x_i}{N}\left[\frac{\vartheta \mu_i}{\vartheta x_i}\right] > 0 \Rightarrow \left[\frac{\vartheta \mu_i}{\vartheta x_i}\right] > 0 \tag{5.9}$$

Comparison of (8) and (9) results in another equivalent stability criterion:

$$\frac{\vartheta^2 g}{\vartheta x_i^2} > 0 \qquad (5.10)$$

The last inequality and the equilibrium relations (3c) allow for a simple geometrical representation of the equilibrium and stability criteria, as it is discussed in section 4.

5.3. Equilibrium relations in multicomponent heterogeneous systems

According to the first postulate(Modell and Reid,1984), an open phase consisting of c nonreacting species can be fully characterized from the values of c+2 independent variables of which c variables correspond to the values of the mole numbers of each component and the remaining two can be any independently variable properties. However, the physico-chemical state of a phase can be defined by intensive variables only and if the actual mass of the phase is not to our concern, we can replace mole numbers by the corresponding mole fractions. Thus, all variables can be intensive properties of which only c+1 are independent because of the existing (normalization) relation between mole fractions. Therefore, the physico-chemical state of a heterogeneous system of π phases can be described by $\pi(c+1)$ intensive variables. At equilibrium there exist $(c+2)(\pi-1)$ independent equations (5.3a, b, c) and the number of independent variables is:

$$F = \pi(c+1) - (c+2)(\pi-1) = c+2-\pi \qquad (5.11)$$

Equation (11) is known as the Gibbs Phase Rule. It is very useful for immediate recognition of the maximum number of permissible phases for a given mixture at specified conditions. For example, at fixed temperature and pressure (F=2), the maximum number of phases is as many as the number of components (π=c), the composition of each of which is fixed and independent of the overall composition of the multiphase system.

The first postulate can be extended to heterogeneous systems. A closed heterogeneous system of π phases is described by 2π intensive variables such T and P, πc mole fractions and π phase fractions(the number of moles of each phase). At equilibrium there exist the $(c+2)(\pi-1)$ independent equations (5.3a, b, c), π normalization equations for the mole fractions in each phase and the c conditions for the material balance of each component in the system. The total number of unknowns is $\pi(c+3)$, the total number of equations is $\pi(c+3)-2$ and, therefore, the number of independent variables is 2. Thus, if the overall composition of any closed system is given, its equilibrium state is completely determined by two independent variables(Duhem's theorem). However, *indifferent states* do not obey this rule (for details, see Prigogine and Defay, 1954).

5.4. Geometrical representation of the conditions of thermodynamic equilibrium and stability

Consider, first, a simple system of two components at constant temperature and pressure, which is assumed stable everywhere in the interior of the permissible region($1 > x_{ij} > 0$, $\Sigma_i x_{ij} = 1$). If the mean Gibbs free energy g of the system is plotted against the composition as in figure 1, the stability condition inequality (10), requires that the curve is everywhere concave upward. The chemical potentials of each component of the system have also a simple geometrical representation. From equations (5b) and (7) we obtain:

$$\mu_c = g - \sum_i^{c-1} x_i \frac{\vartheta g}{\vartheta x_i} \qquad (5.12a)$$

For a binary system, having the composition $z_1(z_2=1-z_1)$, this reduces to:

$$\mu_2 = g^A - z_1 \frac{\vartheta g}{\vartheta z_1} \qquad (5.12b)$$

which shows that the chemical potentials of a binary system define a line tangent to the surface g at the point $\{g(z_1),z_1\}$ which intersects the ordinate at μ_2 ($z_1=0$) and, by virtue of eqn(7), at μ_1 ($z_1=1$). The discussion has been restricted to the two-dimensional space only for ease of representation, but the arguments are general and apply to multidimensional space equally well. In general, therefore, for a simple stable system the mean Gibbs energy surface g should be concave upward everywhere in the interior of the permissible region and the chemical potentials of the single phase define a plane tangent to the g surface at the point of the overall composition of the mixture. The intersections of this plane with the ordinates are the values of respective chemical potentials.

Suppose now that there is a region where the g surface do not fulfil (10) and, therefore it is not concave upward, as shown in figure 2. Then, it is always possible to define a plane tangent to the g surface to replace the convex part of it. At the points of tangency A and B the inequality (10) is satisfied, indicating the existence of stable single phases. Application of equation (12) at the points A and B results in the following equations:

$$\overset{A}{\mu_2} = g^A - \overset{A}{x_1} \frac{\vartheta g^A}{\vartheta \overset{A}{x_1}} \qquad (5.13a)$$

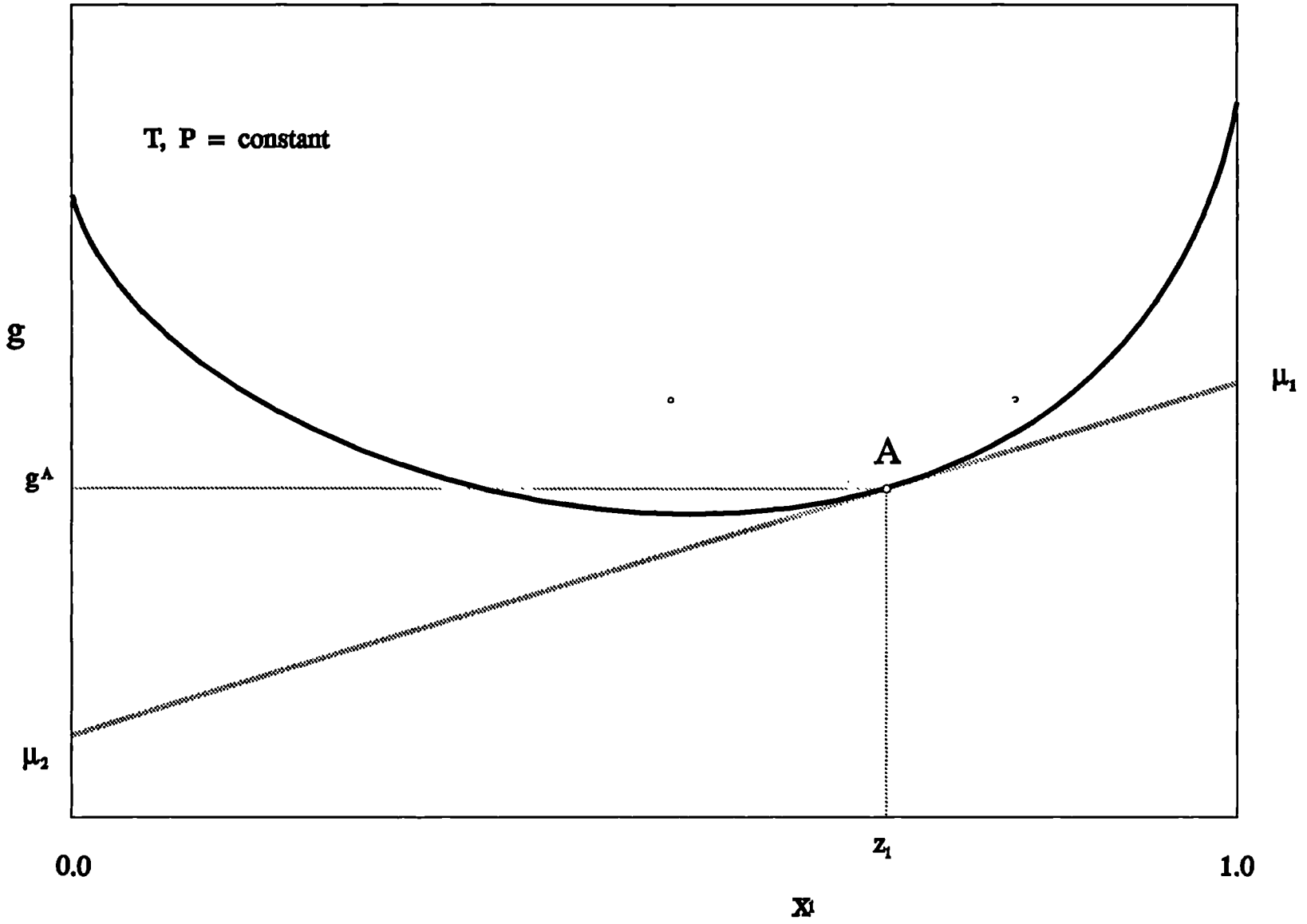

Figure 5.1. Mean Gibbs free energy of a homogeneous binary system.

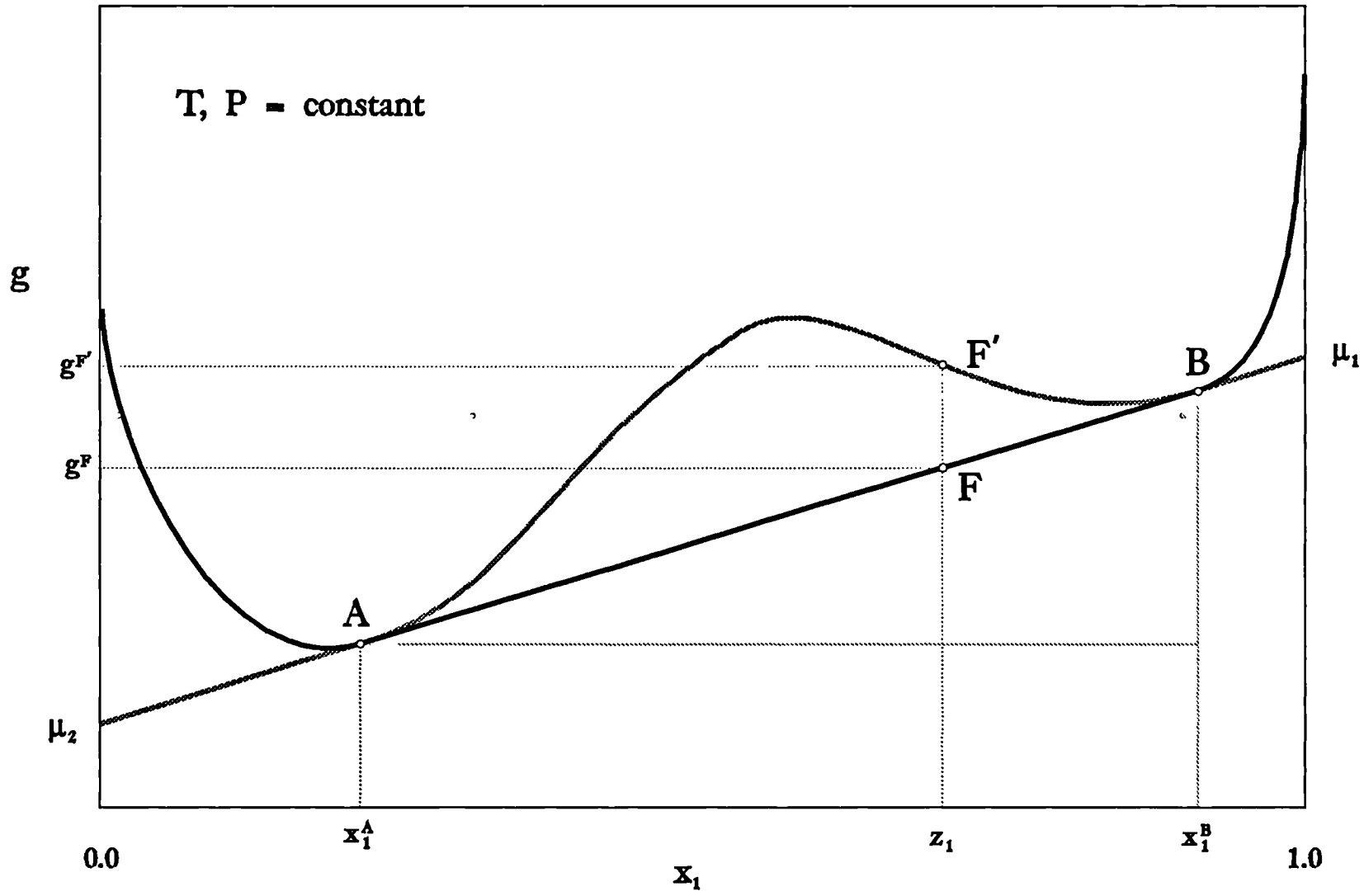

Figure 5.2. A binary system showing a region of intrinsic instability.

$$\mu_2^B = g^B - x_1^B \frac{\vartheta g^B}{\vartheta x_1^B} \tag{5.13b}$$

Subtraction of (13b) from (13a) gives:

$$\mu_2^A - \mu_2^B = g^A - g^B - (x_1^A - x_1^B) \frac{\vartheta g^A}{\vartheta x_1^A} = 0 \tag{5.13c}$$

as it is evident from figure 2. Similarly,

$$\mu_1^A = g^A - x_2^A \frac{\vartheta g^A}{\vartheta x_2^A} \tag{5.14a}$$

$$\mu_1^B = g^B - x_2^B \frac{\vartheta g^B}{\vartheta x_2^B} \tag{5.14b}$$

$$\mu_1^A - \mu_1^B = g^A - g^B - (x_2^A - x_2^B) \frac{\vartheta g^A}{\vartheta x_2^A} \tag{5.14c}$$

Notice, that

$$\frac{\vartheta g^A}{\vartheta x_1^A} = - \frac{\vartheta g^A}{\vartheta x_2^A} \tag{5.15}$$

and subtract (14c) from (13c):

$$\left[\mu_2^A - \mu_2^B\right] - \left[\mu_1^A - \mu_1^B\right] = \frac{\vartheta g^A}{\vartheta x_1^A} [(x_1^A - x_1^B) + (x_2^A - x_2^B)] = 0 \tag{5.16}$$

Thus, we obtain:

$$\mu_2^A = \mu_2^B \quad \text{and} \quad \mu_1^A = \mu_1^B \tag{5.16b}$$

which is simply the equilibrium condition, equation (3c). We conclude, therefore, that the points of the mean Gibbs energy surface having a common tangent plane may represent phases at equilibrium. In this case, the mean Gibbs energy defined by the tangent plane is always lower than that of the corresponding unstable homogeneous phase. Therefore, any mixture with

composition between x_1^A and x_1^B, where g is convex, is unstable and splits in two equilibrium phases A and B with compositions x_1^A and x_1^B respectively.

If g is convex in more than one regions, then more than one plane tangent to g may be drawn, so that *all* regions where g is convex are substituted by tangent planes connecting stable phases. Thus, the remaining original g surface is the locus of *all* possible stable phases within the permissible region. Planes tangent to the g surface at points where the inequality (10) is violated are not acceptable, because they leave convex areas. Besides, since the g surface should be concave upward everywhere, no tangent plane should intersect it.

We may state therefore that:

a. *Of the tangent planes which do not intersect the g surface, it is only the one which meets the material balance constraints that defines the equilibrium state.*

An alternative but equivalent expression, is:

b. *Of the tangent planes which satisfy the material balance constraints, the one which represents the equilibrium state should not intersect the g surface.*

The last statement forms the Gibbs tangent plane criterion. To fix ideas, consider the hypothetical binary system, the Gibbs mean free energy of which is depicted in figure 3, at some fixed temperature and pressure. Depending on the feed composition z, this system can be in any of two heterogeneous regions, where phases A and B or phases B and C, correspondingly, are at equilibrium, or in any of three homogeneous phases, namely A, B or C. The shaded tangent plane is rejected because it violates criterion (b) put forward above. It is to be noted, that in any case the correct tangent plane is the one which minimizes the mean Gibbs free energy of the system. This is expected since inequality (10) was derived from the Gibbs free energy minimisation concept and it is equivalent to it.

Tangent planes can also give quantitative information about the relative proportions of the equilibrium phases. For a binary system in the two phase region, this is demonstrated in figure 4. Let n be the total number of moles of the mixture, n_1^A the number of moles of component 1 in phase A and n_1^B in phase B respectively and n^A, n^B the total number of moles of phases A and B respectively. Then it is:

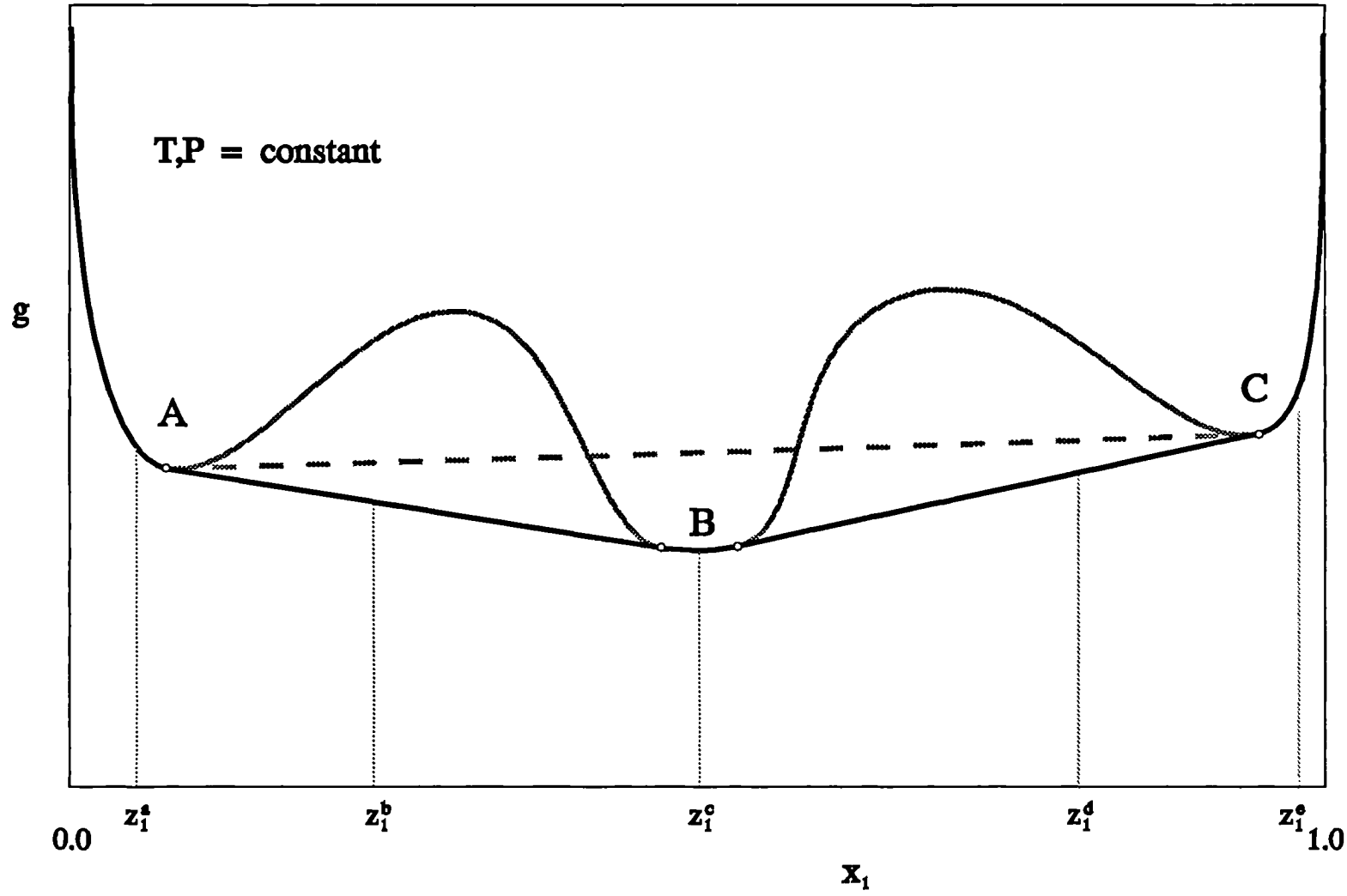

Figure 5.3. Mean Gibbs free energy of a binary system showing three homogeneous and two heterogeneous regions.

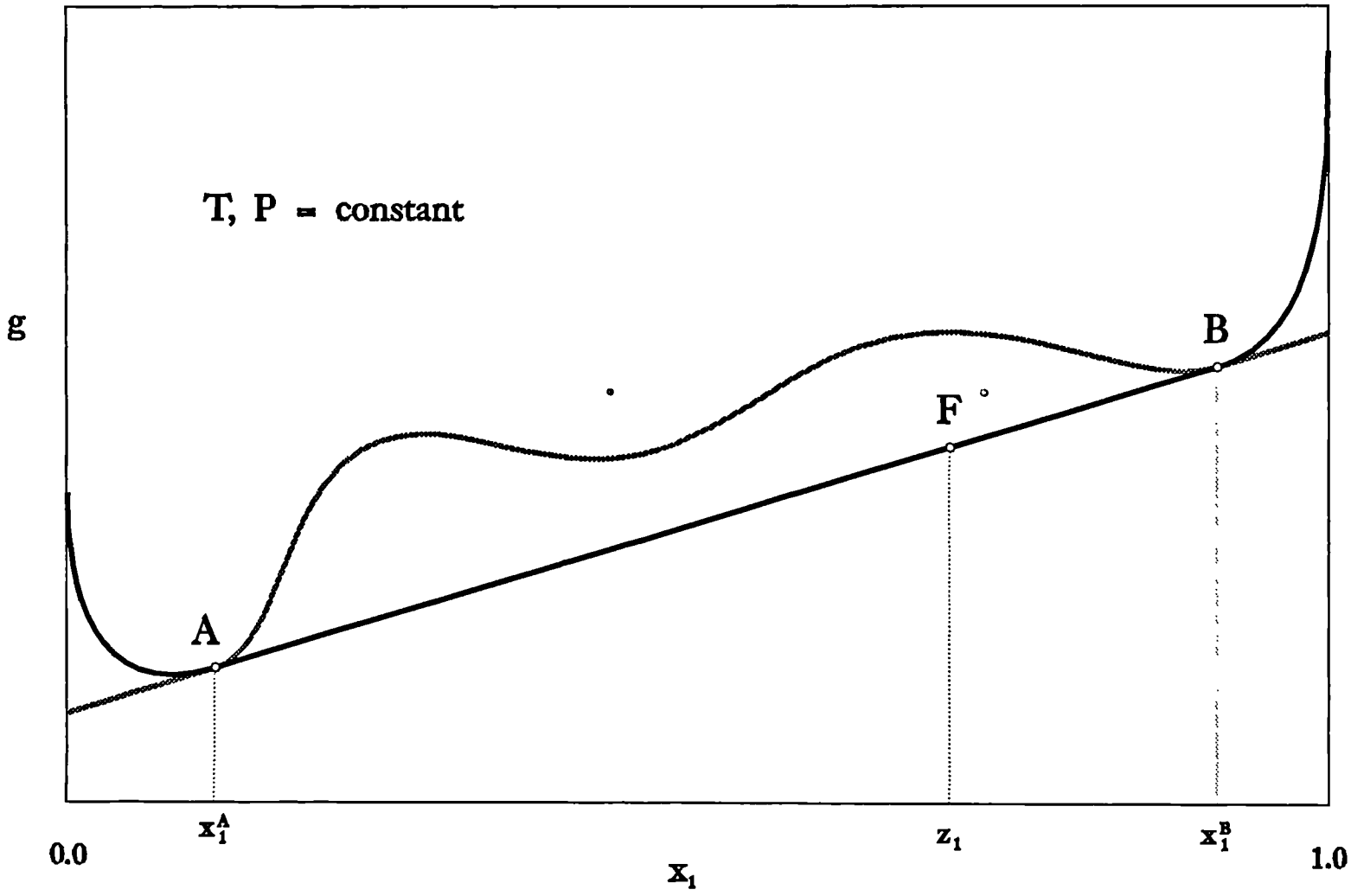

Figure 5.4. The lever rule for a binary system in the two phase region.

$$\frac{\overline{FA}}{\overline{FB}} = \frac{f_1 - x_1^A}{x_1^B - f_1} = \frac{n_1/n - n_1^A/n^A}{n_1^B/n^B - n_1/n} = \frac{n^B}{n^A} \qquad (5.17)$$

which is known as the *lever rule* since it applies around a "fulcrum"(in the present example this is point F). If this system is at the three phase pressure, as shown in figure 5, the lever rule can not be strictly applied, unless we assume phase boundary conditions and assign to one of the phases zero mass. In that case the lever rule applies for the remaining two phases.

The arguments presented so far are not specific to the two dimensional space and apply to any multicomponent heterogeneous system. The presentation was restricted only for the sake of convenience and clarity. For example, assume a ternary system with three equilibrium phases. Relations equivalent to the lever rule can be applied on the triangle formed by the projection of the points of tangency on the (x_1,x_2) plane (x_3 is not independent). Of course, the lever rule could be directly applied to this ternary system or to any multicomponent system in the two-phase region. A complete presentation of the properties of ternary diagrams is given by Durell(1961).

5.5. Predictive methods

Locating the Gibbs free energy surface global minimum permits - at least in principle - correct identification of the equilibrium phases and simultaneous determination of their composition. Several reports in the literature concentrate on Gibbs free energy minimisation. Of all methods, only the Gibbs tangent plane criterion deserves practical interest for the general heterogeneous equilibrium problem and will be referred here.

The properties of the tangent plane criterion have been extensively studied by Baker et al.(1981) but they did not give numerical implementations. Michelsen(1982) presented a technique, based on the tangent plane criterion, to locate regions indicating intrinsic instability in an initially assumed homogeneous phase. Schematically, the method of Michelsen(1982) involves the following steps:

(1) A plane is drawn tangent to the g surface at the feed composition.

(2) A second phase is assumed present. The composition of the new phase is adjusted so that a plane parallel to the first one can be drawn tangent to the g surface at the composition of the new phase.

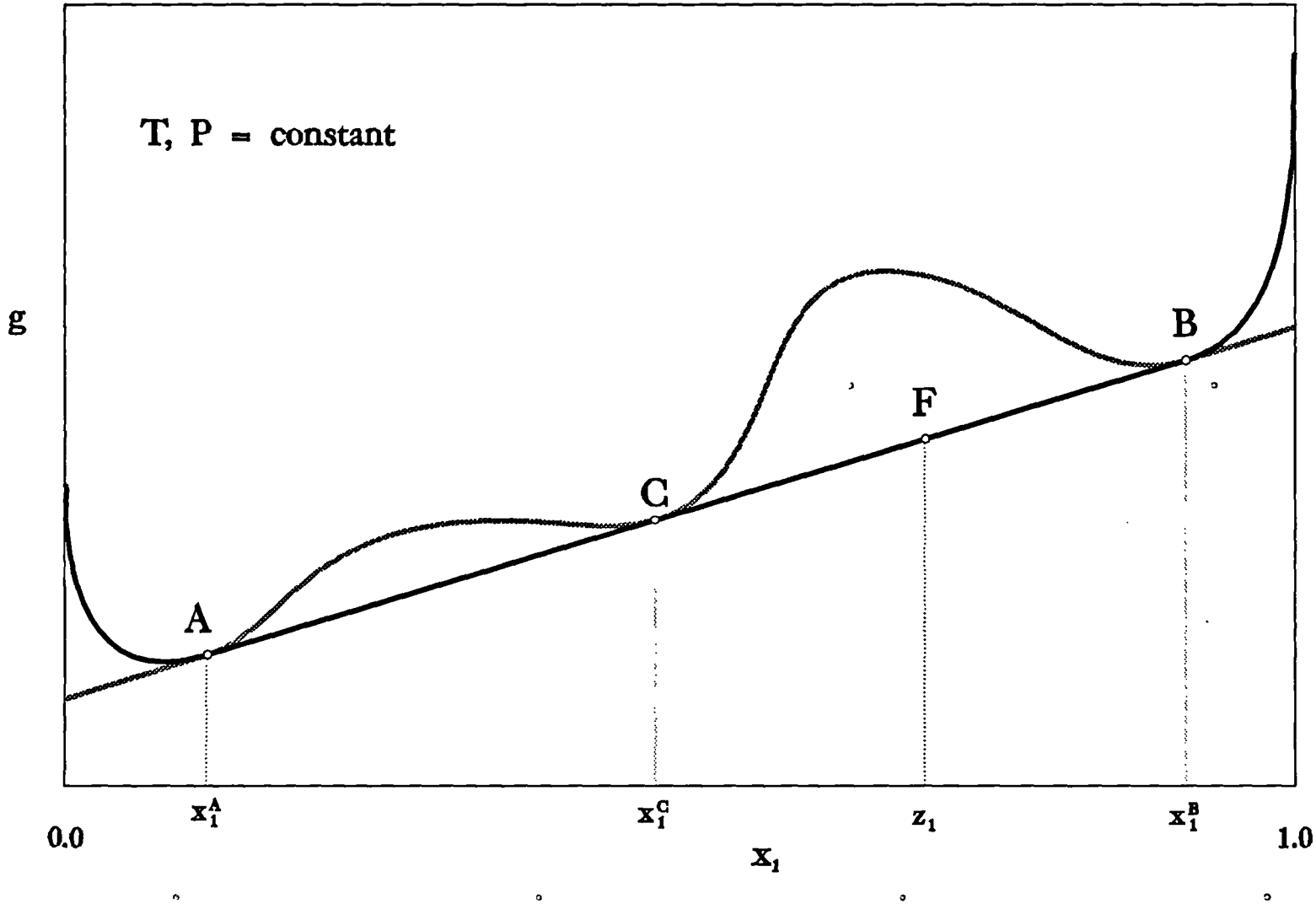

Figure 5.5. Gibbs mean free energy of a binary system at the three phase point.

(3) If the tangent plane of the second plane is above the first one, the analysis has indicated the stability of the original mixture with respect to that phase. The analysis ends here, if all admissible compositions were tested. If, however, the second plane is below the first one, then the tangent plane criterion is violated and the feed composition does not represent a stable single phase and further steps are taken.

(4) The original mixture is flashed at the specified temperature and pressure. The initial guess for the composition of the second phase is taken from the previous step.

(5) For each one of the present phases the above procedure (1) to (4) is repeated until all present phases are found to be stable.

The crucial move in this procedure is step (2). In thermodynamic terms, it is required that the difference in chemical potential of all components in the second phase from the corresponding ones in the first phase assume a constant difference independent of the component index. To prove it, consider the function $g=g(x_1,...,x_{c-1})$ in the c-dimensional space. From equation (12a), the equation $g'=g'(x_1,...,x_{c-1})$ of the plane tangent to g at the point $A=\{g^A, x_i^A, i=1,...,c-1\}$, is :

$$g' = \mu_c^A - \sum_i^{c-1} x_i \frac{\vartheta g^A}{\vartheta x_i^A} \qquad (5.18a)$$

Similarly, for a plane tangent to g at point B, we have:

$$g'' = \mu_c^B - \sum_i^{c-1} x_i \frac{\vartheta g^B}{\vartheta x_i^B} \qquad (5.18b)$$

At any point $\{x_i^*,1=1,...,c-1\}$, by subtracting (18b) from (18a) and taking into consideration that the slopes are equal(because the planes were assumed parallel), we get:

$$g' - g'' = \mu_c^A - \mu_c^B \qquad (5.18c)$$

However, equations (18a, b) are independent of the choice of the dependent mole fraction c and equation (18c) should be valid for any such choice. We conclude, therefore, that the vertical distance of two parallel planes tangent to the mean Gibbs free energy surface is simply the difference in chemical potential of

any two corresponding components in the phases defined by the points of tangency. Thus we may rewrite (5.18c) in a more general form:

$$D = g' - g'' = \mu_i^A - \mu_i^B, \; i=1,...,c \qquad (5.18d)$$

where D is independent of the component index.

The method of Michelsen(1982) has been used for phase splitting in diverse situations such as the three phase flash of polar fluids(Cairns et al,1990), two and three phase flash of water-hydrocarbon mixtures at high temperatures(Nutakki et al, 1988) and multiphase hydrate flash(Cole and Goodwin,1990). Nonetheless, it requires increased computational effort, it cannot guarantee convergence to a nontrivial solution when phases have close composition, it does not provide good estimates for a second liquid phase(Trebble,1989) and it becomes awkward as the number of equilibrium phases increases.

In figure 6 we plot the mean Gibbs energy g of a hypothetical binary system versus the composition in mole fraction. Application of the tangent plane criterion demonstrates that the system with overall composition F is a stable single phase. The same conclusion may be reached, however, by application of the lever rule which indicates immediately that phase B, assumed as equilibrium phase, must have a negative phase fraction.

Whitson and Michelsen(1989) have studied this phenomenon as it appears in the case of two phase flash by the method of successive substitutions and have indicated some further applications. In general the two criteria are thermodynamically equivalent in the sense that the stability of a simple or heterogeneous system against any additional phase may be tested by either of the them.

We propose an alternative algorithm for multiphase flash calculations which starts closer to the final solution in realistic hydrate problems. If hydrate formers and water are present in the feed, generally up to six phases may be present at equilibrium. All phases which can be potentially present under the specified conditions are automatically assumed either actively present or *marginally* present due to restrictions imposed initially by the phase rule. The compositions of marginal phases are stored outside the algorithm. The program generates initial guesses for all phases on the basis of the feed information, as detailed in section 1.5. The case is considered as a typical multiphase flash problem and a Newton-Raphson algorithm is called to solve the material balance and the diffusional stability equations. As the algorithm proceeds by forcing equality of

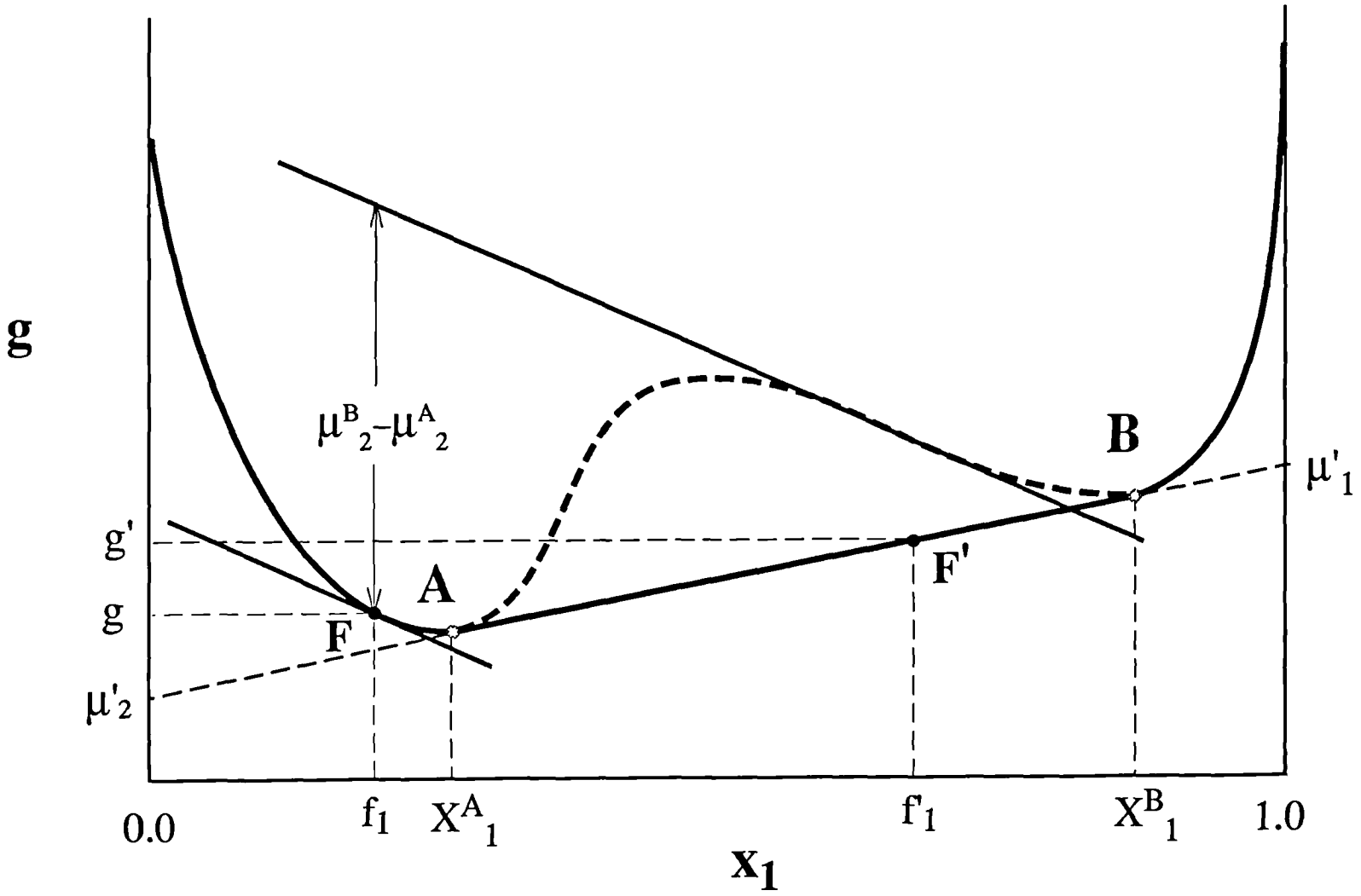

Figure 5.6. Thermodynamic stability criteria.

the fugacities of each species in all phases, it may be observed that one or more phases start having components with negative mole fractions. It has been noticed that a phase which persists having negative mole fractions is very unlikely to change behaviour later. It is therefore removed and stored at the margins of the algorithm with its mass distributed appropriately among the remaining active phases. Since the points of tangency of a hyperplane to a surface in a multidimensional space may be as many as the dimensions of the space, the Newton-Raphson will anyway find one apparent solution to the problem and will define the associated tangent plane. A plane parallel to that is drawn tangent to each one of the marginal phases, that is the composition of all marginal phases is adjusted until their chemical potentials obtain a constant difference (independent from the component index) from those of the solution. Any phase with tangent plane lower than that of the solution is reintroduced and the Newton-Raphson is called again. An apparent solution is accepted as final only if the tangent planes of all marginal phases lie above the one of the solution. Single phase conditions are indicated when one phase alone appears with positive mole fractions but confirmation by application of the tangent plane criterion is generally recommended due to the sensitivity of the Newton-Raphson to the initial estimates.

It is rather impossible to give a geometrical visualization of this technique in the multidimensional space to which it is specific. To fix ideas, we have chosen the system propane-water, the behaviour of which has been recently reviewed(Harmens and Sloan,1990). Figure 7 presents the calculated mean Gibbs free energy of mixing of the propane(1)-water(2) system as a function of composition at 273.60 K and 485.774 Kpa. The Gibbs free energy of the system is denoted by the lower line with lines above corresponding to unstable homogeneous phases. For the sake of clarity, this diagram is only qualitatively correct but all the essential features are retained. It is noted that on the left the curves of $\Delta g/RT$ of all phases are tangent to the vertical line $X_1=0$, on the right the curves of the vapour and the liquid phases are tangent to the line $X_1=1$. The hydrate curve is tangent on the right to the line $X_1=X_c$, where X_c is a constant corresponding to the maximum filling of the hydrate lattice which depends on the type of the hydrate structure and on the type of the hydrate formers (for propane $X_c=8/(136+8)=0.055556$). All curves are concave upward at the points of tangency and their relative position determines which phases will be present at equilibrium and what will be their composition. It is seen that at the chosen conditions of temperature and pressure our system may be in anyone of four homogeneous(L_w, H_2, V, L_p) and three heterogeneous two-phase(L_w-H_2, H_2-V, V-L_p) regions depending on the overall composition.

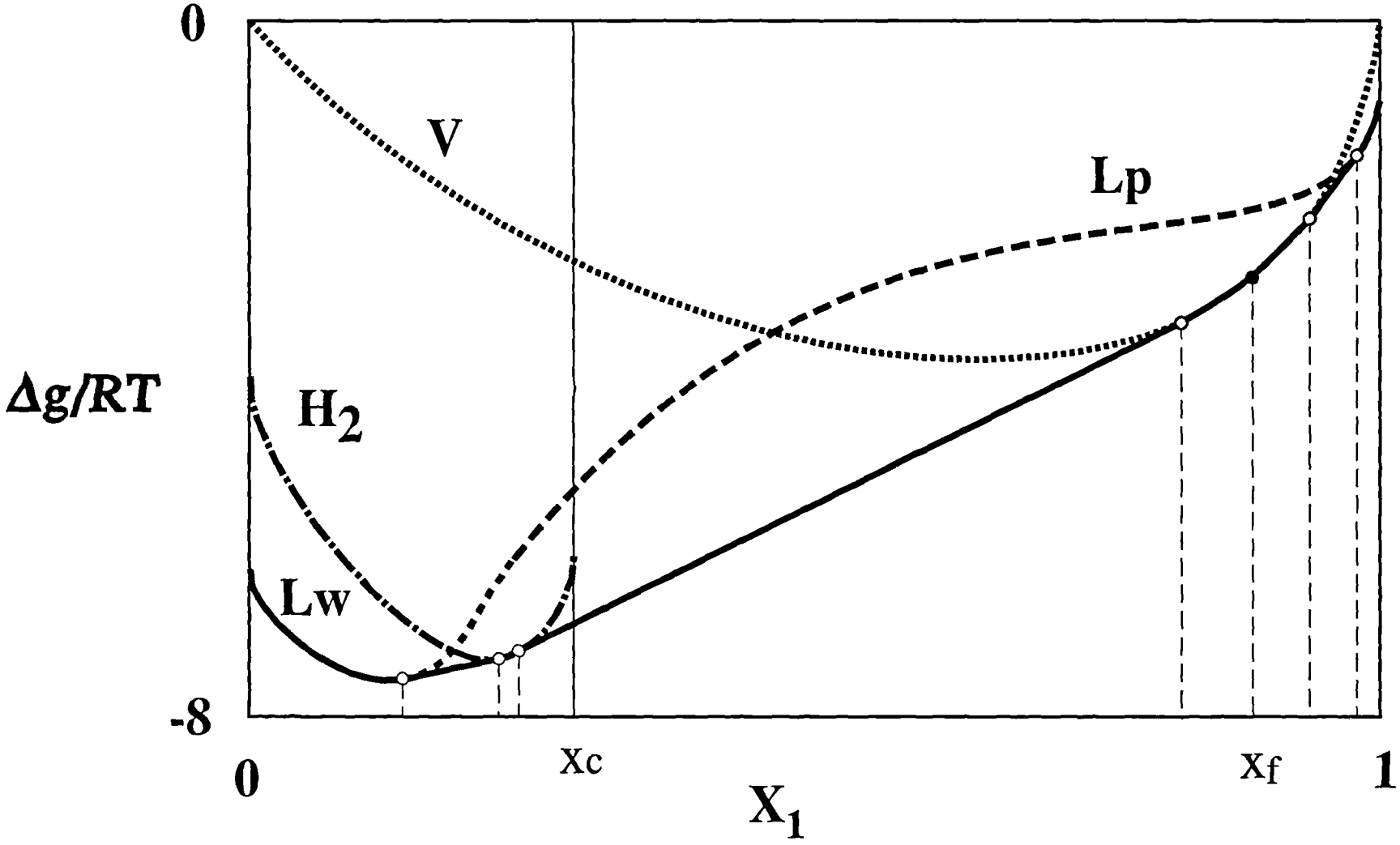

Figure 5.7. Gibbs free energy of mixing of propane(1)-water(2) at 273.60K and 485.774KPa.

As an example application of the proposed algorithm, consider the indicated feed X_f which corresponds to a single vapour phase. The algorithm identifies four probable phases(L_w, H_2, V, L_p), makes an initial guess of their composition, chooses two of them(L_w,H_2) - in accordance with the phase rule - and tries to equal their fugacities while preserving the material balance. The mass of the water-rich liquid phase should become negative and it is eliminated. The hydrate phase is examined for stability and the vapour phase is introduced resulting in the hydrate phase being negative this time. Examination of the stability of the remaining vapour phase reveals that the system is an homogeneous vapour phase, the properties of which are calculated and reported. The calculated phase diagram of the propane-water system is shown in Figure 8 by successive area diagrams. For multicomponent systems the algorithm may assume up to six phases or as many as the number of components and tries to converge to any solution of the problem with positive mole fractions. Thereafter additional phases from those initially assumed as probable may be reintroduced as indicated by application of the tangent plane criterion.

5.6. Numerical implementation

The numerical calculations of multiphase equilibria are carried out essentially by the scheme defined by the system of equations (1.32) appropriately modified to include any solid hydrate phases. If s is the number of solid hydrate phases, it is:

$$G(\Psi) = 0 \tag{5.19}$$

where **G** is the vector of the $\pi(c+1)+s$ equations defined below:

$$G_i = z_i - \sum_{j}^{\pi} F_j x_{ij} - \sum_{j=\pi+1}^{\pi+s} F_j x_{ij}\,,\ i = 1,\ldots,c \tag{5.19a}$$

$$G_{c+1} = 1 - \sum_{i}^{c} x_{i1} \tag{5.19b}$$

$$G_{(m-1)(c+1)+i} = \ln\frac{f_{i1}}{f_{im}}\,,\ m = 2,..,\pi \tag{5.19c}$$

$$G_{m(c+1)} = P - \sum_{i}^{c} \frac{f_{i1}}{\phi_{im}}\,,\ m = 2,..,\pi \tag{5.19d}$$

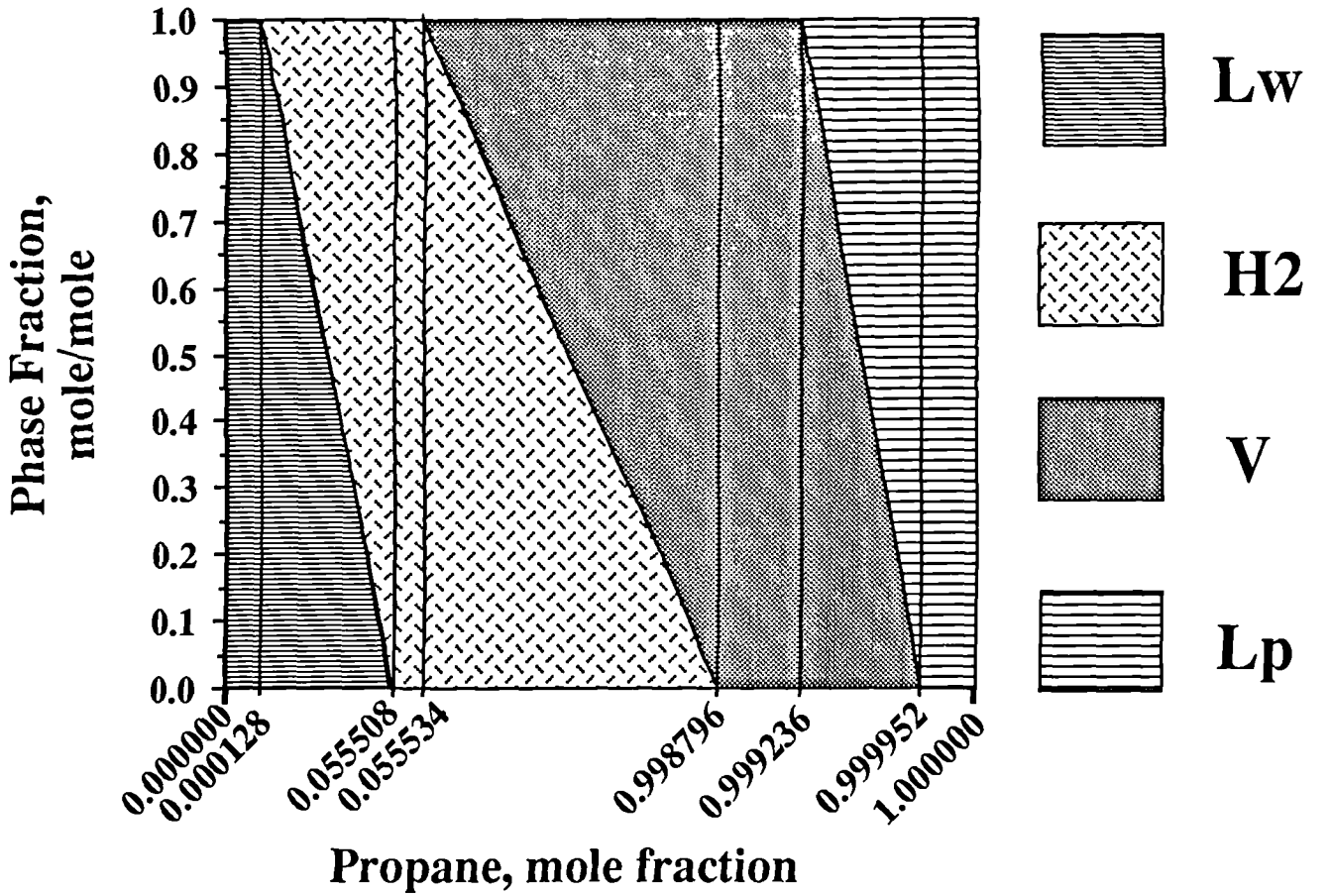

Figure 5.8. Calculated phase diagram of the propane-water system at 273.60K and 485.774 KPa.

$$G_{m(c+1)+k} = \ln\frac{f_{w1}}{f_{wk}}\ , k = 1,s \qquad (5.19e)$$

where symbols have the same significance as in paragraph 1.4. The vector of the unknowns Ψ is defined by:

$$\Psi = \Psi(x_1, F_1, x_2, F_2, ..., x_\pi, F_\pi, F_k)^T\ , k = 1,s \qquad (5.19f)$$

where x_j is the vector of the mole fractions composing the fluid phase j. The mole fractions of the hydrate phases are considered as dependent variables and they are calculated from the following relations together with the normalization equation:

$$x_i = \frac{\Sigma_l^2 \nu_l \theta_{il}}{1 + \Sigma_l^2 \Sigma_j^{c'} \nu_l \theta_{jl}},\quad i \neq w \qquad (5.20a)$$

$$\theta_{il} = \frac{C_{il} f_i}{1 + \Sigma_j^{c'} C_{jl} f_j} \qquad (5.20b)$$

where ν_l is the number of cavities of type l per water molecule in the hydrate lattice, f_i is the fugacity of the hydrate former i, c' is the number of hydrate formers and C_{il} is the Langmuir-type constant of component i in cavity l, a function of temperature. In equation (20) the hydrate phase index has been dropped for simplicity.

The formulation above permits easy physical removal or introduction of a phase by appropriately contracting or expanding the Jacobian and the related matrices by as many columns and rows as the number of unknowns associated with that phase. Switching of the reference phase can also be readily carried out. Some modification is needed when only solid phases are participating in equilibrium; the mole fractions of one of the hydrate phases, which now is assigned as the reference phase, become independent variables and equations (20a) and (20b) are solved for the fugacities, as suggested by Cole and Goodwin(1990). It is noted, however, that in such cases the physical constraints in the hydrate composition may not allow the Newton-Raphson to take a full step and may curb convergence.

The plane tangent to the g surface of a vapour or liquid phase j which is parallel to that of the reference phase (indice 1) can be located by solving the system of equations (18d) or the equivalent

$$\ln(f_{ij}/ f_{i1})=D_j/ RT \tag{5.21a}$$

together with the normalisation equation, for the composition x_{ij} of phase j and the vertical distance D_j. Michelsen(1982), by introducing the new independent variables $Y_{ij}= x_{ij}\exp(-D_j/ RT)$, brings it in the form:

$$\ln Y_{ij}+ \ln\phi_{ij} - \ln(x_{i1}\phi_{i1}) = 0 \tag{5.21b}$$

with the dependent variables given by the normalization equation:

$$x_{ij}=\frac{x_{ij}}{\Sigma_i x_{ij}} =\frac{Y_{ij}}{\Sigma_i Y_{ij}} \tag{5.21c}$$

In the present implementation, following Michelsen(1982), the system of equations (21b) is solved by applying both the Successive Substitution and the Newton-Raphson techniques as indicated below.

The method of Successive Substitutions(SS)

$$\ln Y_{ij}^{t+1}= \ln(x_{i1}\phi_{i1}) - \ln\phi_{ij}^{t} \tag{5.22}$$

The Newton-Raphson method(NR)

The vector **G** of the c equations is defined by the equations:

$$G_k =\ln Y_k +\ln\phi_k - h_k = 0 \tag{5.23}$$

where the phase indices where dropped for simplicity. The significance of the symbols in equation (23) becomes apparent by comparison to equation (21b). The elements of the Jacobian matrix are calculated from the equations:

$$\frac{\vartheta F_k}{\vartheta Y_i}=\frac{1}{Y_k}\delta_{ki}+\frac{1}{\phi_k}\Sigma_j\frac{\vartheta\phi_k}{\vartheta x_j}\frac{\vartheta x_j}{\vartheta Y_i} \tag{5.24a}$$

where δ_{ki} is the Kronecker delta, and

$$\frac{\vartheta x_j}{\vartheta Y_i}=\frac{1}{\Sigma_i Y_i}\delta_{ji}-\frac{Y_j}{\Sigma_i Y_i} \tag{5.24b}$$

In certain cases, either of these methods may fail either to converge or to find a solution other than the trivial. In this implementation, we start with the NR and in case of failure we switch to SS. If convergence is indicated by a small objective function($\cong 10^{-2}$), the NR is called again. However, if the SS is fluctuating most probably it will not converge to the solution and it is abandoned. Then, the algorithm is restarted with a new initial guess for the composition of the phase under test, as suggested by Michelsen(1982).

For a hydrate phase we write for the tangent plane:

$$f_{ih}^{t+1} = \left[\frac{f_{i1}}{f_{w1}}\right] f_{wh}^{t} \tag{5.25}$$

where f_{ih} and f_{wh} are the fugacities of the hydrate former i and water in the hydrate phase and f_{i1} and f_{w1} are the corresponding fugacities in the reference phase at the solution under test. Convergence of the above scheme is usually achieved in 4 to 5 iterations when the tolerance is set equal to 10^{-4}. The tangent plane to the hydrate phase is lower than that of the solution if the ratio of the fugacity of water in the hydrate phase to the same in the reference state is lower than 1.

As a final note, the initial guesses of the composition of the hydrate phases are estimated from the fugacities of the vapour phase assumed in equilibrium and the Langmuir constants taken from the ideal solid solution theory.

5.7. Results and discussion

The characteristic ability of the proposed algorithm to identify correctly the equilibrium phases in heterogeneous systems is demonstrated on a quaternary mixture of methane, ethane, propane and water at 285 K. The results, appearing in Figure 9 as an area diagram and in Table 1, indicate that in the pressure region from 100 to 10000 KPa this system assumes seven phase combinations. In Figure 9, hydrate structure 1 appears at slightly higher pressure than hydrate structure 2 (this contrasts a prediction by Holder and Hand, 1982), passes through a maximum at the expense of hydrate 2 and disappears almost together with the vapour phase, leaving hydrate 2 as the sole stable solid phase in equilibrium with a hydrocarbon-rich liquid. It is confirmed that water-liquid/water-solid phase changes thermodynamically must take place abruptly, as reported by Bishnoi et al(1989). The presence, however, of non-hydrate formers effects lower rate of phase transformation. The boundaries of phase transitions, shown in Table 1, have been approached here within the third decimal digit of the mass (in mole fraction) of the appearing or disappearing phase, but evidently the approximation is only limited by machine accuracy. Phase transitions in the following examples have been located by linear extrapolation to zero of two predictions of the fraction of the phase of interest.

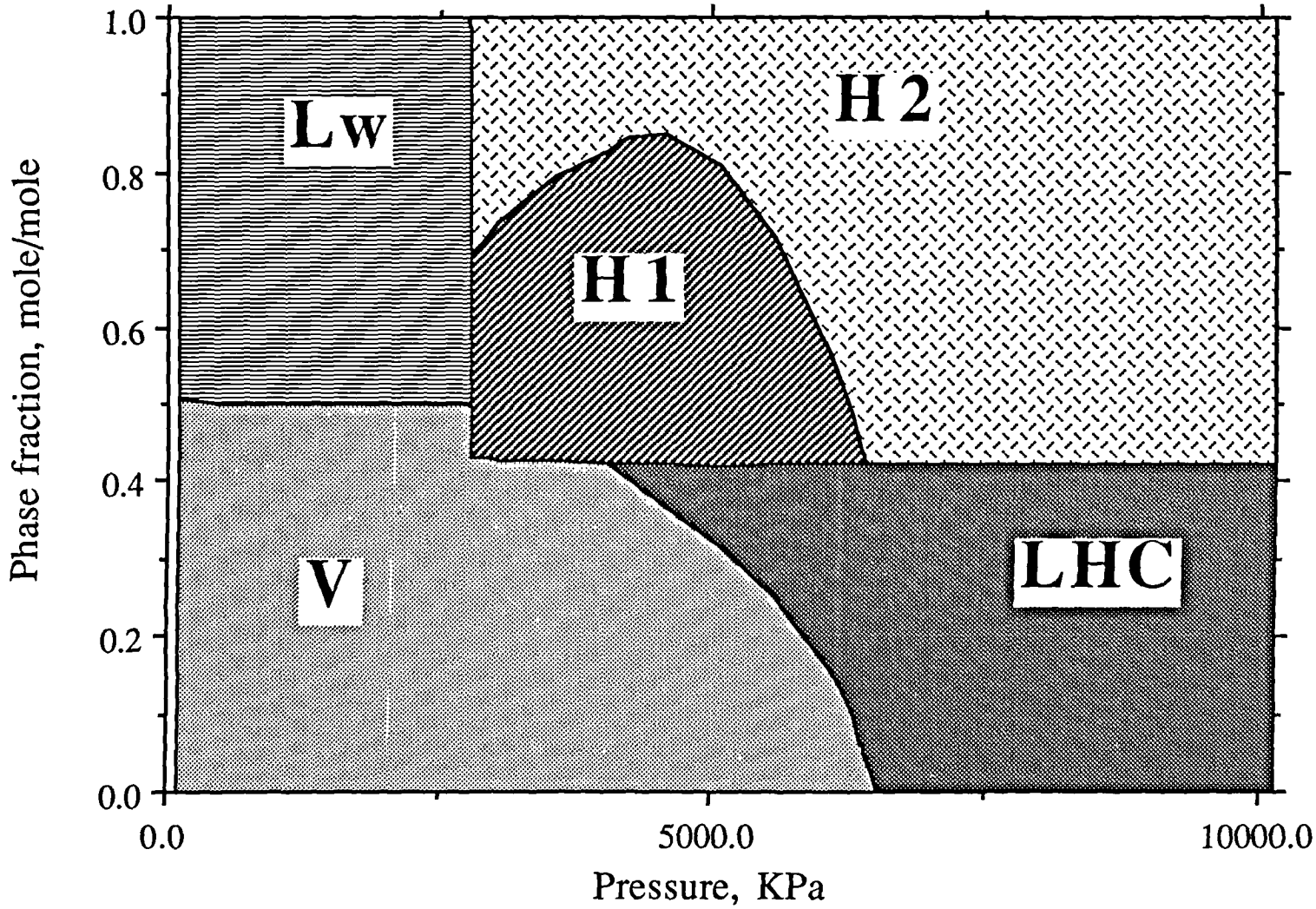

Figure 5.9. Calculated phase diagram of the system C1=0.1820, C2=0.2705, C3=0.0475, H2O=0.50 at 285.0K.

Table 5.1. Predicted phase behaviour at 285.0 K of the system C_1=0.1820, C_2=0.2705, C_3=0.0475, H_2O=0.5000 moles.

Pressure, KPa	Equilibrium Phases
101.3 - 2771.7	V - L_w
2771.7 - 2791.0	V - L_w - H^2
2791.0 - 2791.2	V - L_w - H^2 - H^1
2791.2 - 4053.0	V - H^2 - H^1
4053.0 - 6408.8	V - L_{HC} - H^2 - H^1
6408.8 - 6535.5	V - L_{HC} - H^2
6535.5 - 10132.5	L_{HC} - H^2

Experimental data on the water content of the gas phase in equilibrium with hydrate in the two phase region have been published by Song and Kobayshi(1982) for a ternary system and by Aoyagi and Kobayashi(1978) for two multicomponent systems and they are presented in Figure 10 and Table 2 respectively, together with the predictions of our algorithm. For the system C1 10.1%, C2 4.4%, C3 26.1%, nC5 59.4% at 3.447 MPa, studied by Sloan et al(1986), at 264.1 and 270.7 K L_{HC}-H2 equilibrium is predicted with concentration of water in the hydrocarbon-rich phase 33 and 55 ppm respectively. The corresponding experimental values are 56 and 124 ppm. The significant error in this case may be partly attributed to the high content of n-pentane, the Equation of State binary interaction parameters of which have been calculated from limited data at significantly higher temperatures (310-470 K).

Figure 11 shows some typical predictions of hydrate dissociation points in the three phase H-L_w-L_{HC} region in comparison with experimental data of Ng and Robinson(1976). A part of the calculated four phase H-L_w-L_{HC}-V equilibria is also shown. The calculated upper quadruple point has been located as the intersection of these two lines. The feed compositions in moles are listed in Table 3. Latin numbers refer to the original publication. Deviations in the calculated hydrate point temperature do not exceed 1 K.

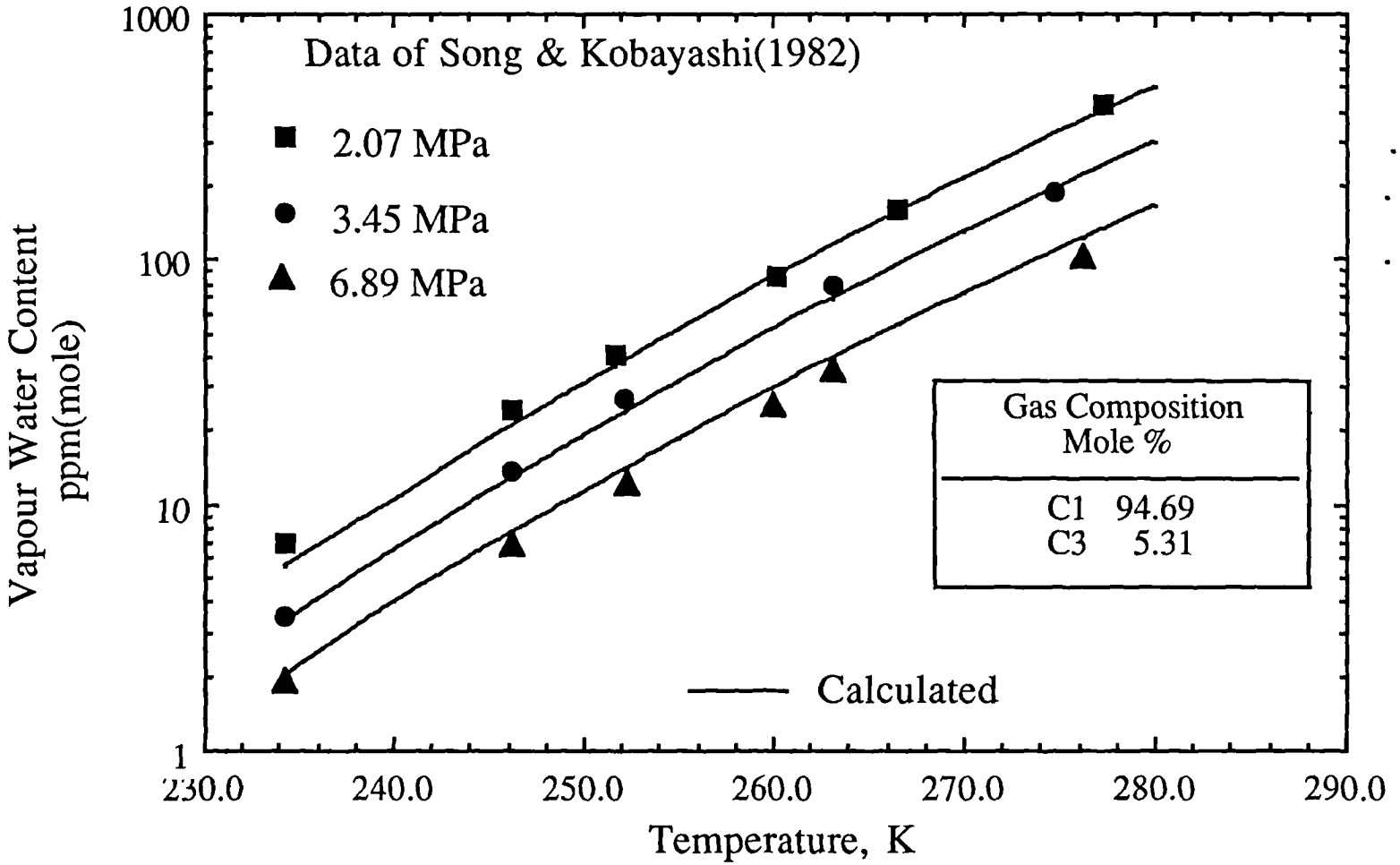

Figure 5.10. Prediction of the water content of a vapour phase in equilibrium with hydrates.

Table 5.2. Experimental and predicted vapour phase water concentration over a hydrate phase for two natural gas mixtures.

T/K	P/MPa	Vapour phase water mole fraction $x10^{-5}$	
		Exptl	Pred
Gas I: C_1 0.7502, C_2 0.0795, C_3 0.0399, CO_2 0.1304			
267.1	4.499	9.89	8.53
	5.857	8.71	7.06
	12.068	6.30	5.41
260.9	4.458	5.88	4.88
261.2	5.836	5.67	4.18
260.9	12.048	4.16	3.30
251.8	5.857	2.52	1.72
249.0	4.499	2.06	1.52
249.8	12.078	1.84	1.32
243.2	4.479	1.05	0.84
243.7	5.847	1.03	0.77
243.2	12.048	1.05	0.74
237.2	12.088	0.452	0.43
233.9	12.068	0.250	0.32
Gas II: C_1 0.8706, C_2 0.0796, C_3 0.0388, CO_2 0.0110			
277.6	10.345	11.8	10.9
	3.445	25.2	25.3
260.9	10.345	2.84	2.70
	3.445	6.30	5.72
249.8	10.345	1.00	0.99
	3.445	1.97	1.91

Table 5.3. Composition of natural gas liquids, moles.

	Liquid		
Component	II	III	VI
Methane	2.2	21.9	-
Ethane	30.6	24.7	17.0
Propane	50.8	40.8	38.6
iso-Butane	16.2	12.4	18.9
Carbon dioxide	-	-	25.5
Nitrogen	0.2	0.2	-
Water	50.0	50.0	1.0

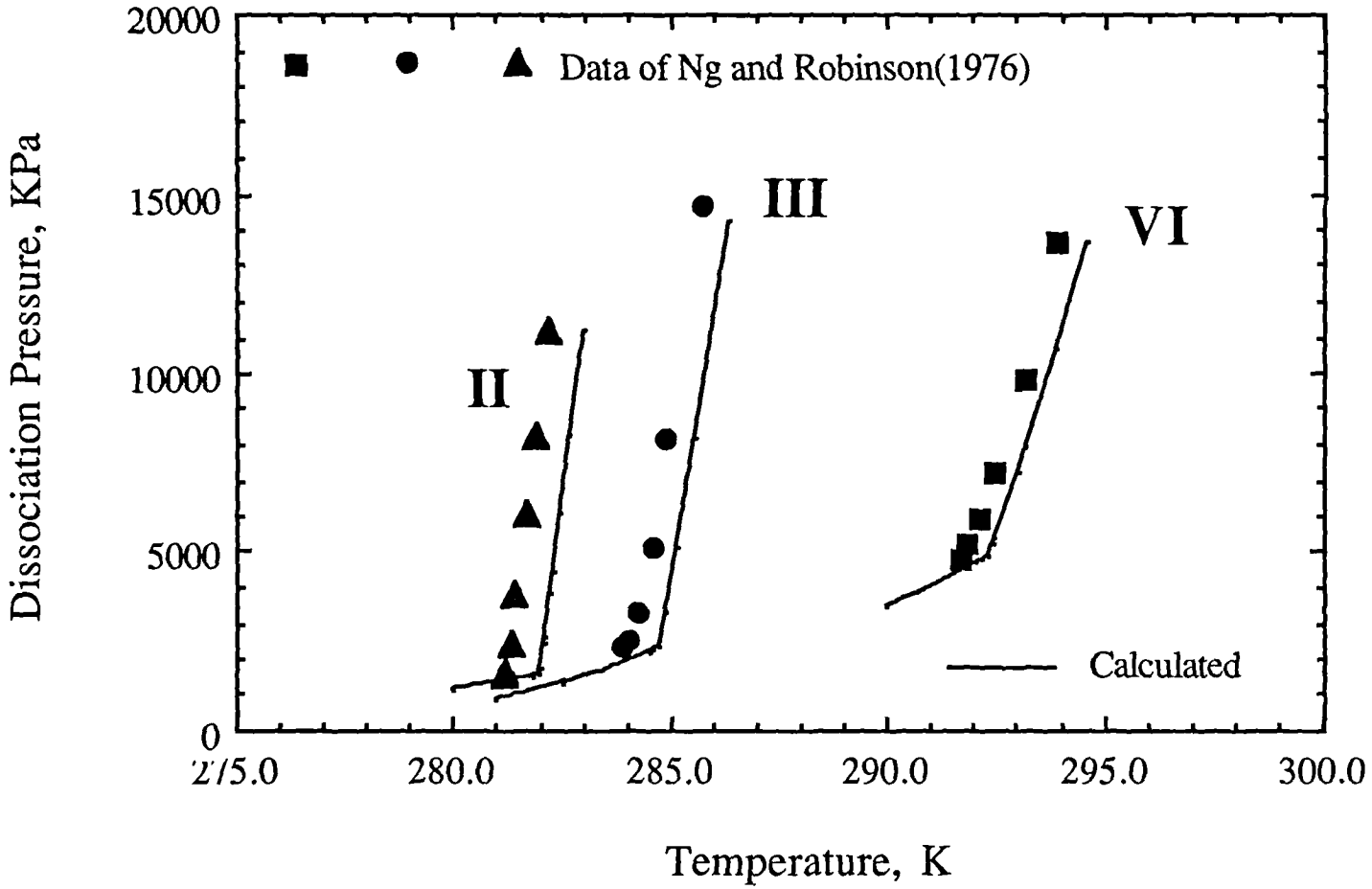

Figure 5.11. Prediction of hydrate dissociation conditions of some natural gas liquid systems.

Table 5.4a. Prediction of dissociation conditions of a gas condensate wellstream.

Pressure, MPa	Dissociation Temperature/K	
	Exptl	Pred
6.01	290.75	290.51
11.07	293.75	294.06
15.01	294.95	295.56
19.99	296.25	296.94

Table 5.4b. Dry base composition of the gas condensate wellstream.

Component	Mole %
Methane	73.03
Ethane	8.04
Propane	4.28
iso-Butane	0.73
n-Butane	1.50
iso-Pentane	0.54
n-Pentane	0.60
Pentadecane	7.53
Carbon dioxide	3.11
Nitrogen	0.64

Table 4 compares predictions with experimental hydrate dissociation point data of a gas condensate wellstream studied by Ng et al(1987) in the four phase H-L_w-L_{HC}-V region. The heavy end has been characterized as pentadecane to match the reported retrograde saturation pressure. The characterization does not affect materially the predictions. The water content of the feed was 33.3 mole %. The average absolute deviation of predicted hydrate point temperature is 0.46 K. The composition of the condensate is given in Table 4b.

The method of Gupta, first presented by Bishnoi et al(1989) and documented later by Gupta et al(1991), deserves particular attention. The fundamental stability equations of this method are:

$$x_{ik}=K_{ik}x_{ir}e^{\theta_k} \qquad (5.26a)$$

where $\theta_k = D_k/RT$, $K_{ik} = \phi_{ir}/\phi_{ik}$ and

$$F_k\theta_k=0 \qquad (5.26b)$$

subject to

$$F_k \geq 0 \text{ and } \theta_k \geq 0. \qquad (5.26c)$$

Equations (26a) can be derived by rearranging equations (22a) which define a plane tangent to phase k and parallel to the plane tangent to the reference phase r. Equations (26b) under the restrictions (26c) are mathematical expressions of the fact that either an equilibrium phase ($\theta_k=0$) must have positive phase fraction ($F_k \geq 0$) or any non-equilibrium phase ($F_k=0$) must have a tangent plane parallel to the equilibrium one but above that ($\theta_k \geq 0$).

The solution of these equations is not an easy task as discussed by Gupta et al(1991). However, as it was demonstrated in paragraph 5.4, the same conclusions may be reached simply by allowing F_k to be positive or negative. It seems, therefore, that the method of Gupta - in comparison to our proposal - suffers from unnecessary complexity.

The combined employment of two thermodynamically equivalent stability criteria, as implemented in the proposed algorithm for multiphase flash calculations, was shown to work efficiently and reliably in an extreme variety of situations, although the user is not requested to provide any information other than the specifications of the problem. This in itself demonstrates the power of the method but it must be noted that the algorithm has been presented and applied here in the most general form and therefore it is computationaly expensive for two-phase systems in comparison to the phase splitting approach. If the user would indicate the starting active phases, some computational time might be saved without loss of generality or limitation of the reliability of the predictions since at the end the tangent plane criterion would still be applied to all phases potentially present.

A non-technical note on the terminology "negative flash" introduced by Whitson and Michelsen(1989) appears to be necessary. In our view this term is at best unfortunate for several reasons. Strictly speaking a flash calculation cannot be either "negative" or "positive". Further, if a phase has indeed negative phase fraction, this can not be known in advance. In this context, one should first perform the calculation and later should name it. Moreover, if a phase has negative phase fraction then one or more coexisting phases should have phase fractions greater than 1. To avoid misunderstandings, we would prefer the term "free flash", meaning a flash calculation free from constraints.

References

Aoyagi, K. and Kobayashi, R.,"Report of the Water Content Measurement of High Carbon Dioxide Content Simulated Prudhoe Bay Gas in Equilibrium with Hydrates", Proc. 57th Annual Convention, Gas Processors Association, New Orleans, La, 1978.

Baker, L.E., Pierce, A.C., Luks, K.D., "Gibbs Energy Analysis of Phase Equilibria", SPE J., 731(1982).

Bishnoi, P.R., Gupta, A.K., Englezos, P., Kalogerakis, N., "Multiphase Equilibrium Flash Calculations for Systems Containing Gas Hydrates", Fluid Phase Equilibria, **53**, 97(1989).

Durell, C.V., "Homogeneous Coordinates", G. Bell and Sons(1961).

Cairns, B.P. and Furzer, I.A., "Multicomponent Three-Phase Azeotropic Distillation. 2.Phase-Stability and Phase-Splitting Algorithms", IEC Res., **29**, 1364(1990).

Cole, W.A., Goodwin, S.P., "Flash Calculations for Gas Hydrates: A Rigorous Approach", Chem. Eng. Sci., **45**(3), 569(1990).

Gautam, R. and Seider, W.D., "Computation of Phase and Chemical Equilibrium: Part II. Phase Splitting", AIChE J., **25**(6), 999(1979).

Gupta, A.K, Bishnoi, P.R. and Kalogerakis, N., "A method for the simultaneous phase equilibria and stability calculations for multiphase reacting and non-reacting systems", Fluid Phase equilibria, **63**, 65(1991).

Harmens, A. and Sloan, E.D., " The Phase Behaviour of the Propane-Water System: A Review", Can.J.Chem.Eng., **68**, 151(1990).

Heidemann, R.A., "Three-Phase Equilibria Using equations of State", AIChE J., **20**(5), 847(1974).

Michelsen, M.L., "The Isothermal Flash Problem, Part I. Stability", Fluid Phase Equilibria, **9**, 1(1982).

Ng, H.J., Chen, C.J. and Saeterstad, T, "Hydrate Formation and Inhibition in Gas Condensate and Hydrocarbon Liquid Systems", Fluid Phase Equilibria, **36**, 99(1987).

Ng, H.J. and Robinson,D.B., "The Measurement and Prediction of Hydrate Formation in Liquid Hydrocarbon-Water Systems", IEC Fund., **15**(4), 293(1976).

Nutakki, R., Firoozabadi, A, Wong, T.W., Aziz, K., "Calculation of Multiphase Equilibrium for Water-Hydrocarbon Systems at High Temperature", SPE/DOE 17390, 733(1988).

Prigogine, I. and Defay, R., "Chemical Thermodynamics", Translated by D.H. Everett, Longmans, London(1954).

Sloan, E.D., Khoury, F.M., Kobayashi, R., "Water Content of Methane Gas in Equilibrium with Hydrates", IEC Fund., **15**(4) 318(1976).

Sloan, E.D., "Clathrate Hydrates of Natural Gases", Marcel Dekker Inc, New York(1990).

Song, K.Y. and Kobayashi, R., "Measurement and Interpretation of the Water Content of a Methane-Propane Mixture in the Gaseous State in Equilibrium with Hydrate", IEC Fundam, **21**, 391(1982).

Trangenstein, J.A., "Customized Minimization Techniques for Phase Equilibrium Computations in Reservoir Simulation", Chem. Eng. Sci., **42**(12), 2847(1987).

Trebble, M.A., "A Preliminary Evaluation of Two and Three Phase Flash Initiation Procedures", Fluid Phase Equilibria, **53**, 113(1989).

Whitson, C.H. and Michelsen, M.L., "The Negative Flash", Fluid Phase Equilibria, **53**, 51(1989).

CHAPTER VI

CONCLUSIONS AND RECOMMENDATIONS FOR FURTHER WORK

6.1. Conclusions

Modelling of asymmetric systems

In Chapter I all experimental data of water and methanol binaries with common reservoir fluid constituents, reported in the open literature (including unpublished data in Theses, Dissertations and Research Reports), were systematically collected. Based on these data, the phase behaviour of some typical binary mixtures has been presented as qualitative diagrams and non-idealities in these systems have been highlighted. Subsequently, the literature on modelling asymmetric systems was reviewed and the ideas considered most successful or promising were briefly presented. Consequently, we developed a new mixing rule for asymmetric systems with two interaction parameters per binary system, one of which was temperature dependent. The theoretical requirement for quadratic dependence of the mixing rules on mole fractions for gaseous states, was fulfilled by a density-dependent modification of the proposed mixing rules. We have regressed interaction parameters for binary mixtures of water and methanol with hydrocarbons up to n-octane, nitrogen, hydrogen sulfide and carbon dioxide, both for the density-dependent and for the nondensity-dependent mixing rules. In doing so, we have developed efficient general algorithms for multiphase phase flash and phase boundary calculations. To enhance the stability of the implementation, two numerical methods were used for solving the systems of nonlinear equations, namely the Newton-Raphson and the Successive Substitutions method. Finally, the model has been extensively tested against diverse experimental data of highly asymmetric systems preferably in multiphase regions.

A number of conclusions can be drawn, as a result of the above work.

(1) The phase behaviour of the system water-methanol-reservoir fluids can be modelled with accuracy adequate for engineering applications with a cubic equation of state with unconventional mixing rules. The methodology is general

and it is applicable to any asymmetric system, subject to availability of adequate binary data for regression of interaction parameters.

(2) The proposed mixing rules can be applied to any equation of state. However, since most equations of state behave similarly in most cases, significant differences should not be expected for asymmetric systems.

(3) The concept of density-dependent mixing rules does not offer any significant advantage as far as quality of predictions is concerned. On the contrary, it was shown to perform consistently worse than the nondensity-dependent equivalent when both methanol and water were present. More over, it was found that it is computationally inferior to the nondensity-dependent alternative. This is because the cubic form of the equation of state is lost and a numerical method must be used for solving the equation for the compressibility factor.

(4) No convergence problems were encountered during the extensive testing of the algorithm although the Newton-Raphson method has been the main tool for solving the system of nonlinear equations. This must be attributed to two main reasons: First, the implemented methodology for obtaining initial estimates, works successfully in the tested cases. Second, our implementation of the Newton-Raphson method makes use of the most extensive set of independent variables. This results in an improved stability of the algorithm, at the cost of increased computational time.

The Classical Cell Model

In Chapter II it is attempted to determine a unique set of parameters for the ideal solid solution model for gas hydrates. The classical cell model was implemented as it is appropriate to work with an equation of state for calculation of the fugacities of all components in equilibrium phases. We have used experimental data on the expansion coefficients of ice, liquid water and hydrates of both structures to regress a cubic equation of the molar volume of water in the above states as a function of temperature. Using heat capacity data for pure components, we have also regressed equations for the heat capacity differences between ice and the empty hydrate lattice at the ice point. The rest of the reference thermodynamic properties were used as reported by Dharmawardhana et (1980). Subsequently, a number of methods were applied to determine a consistent and unique set of potential parameters for the most common hydrate

forming gases. In doing so, it has been necessary to develop a rigorous method for the determination of the heat capacities of gas hydrates.

The following conclusions can be drawn from the application of the above methodology.

(1) The potential parameters of small molecules capable of entering both cavities of either structure cannot be determined from the simple gas hydrate dissociation pressure data alone. Though a regression algorithm may converge to a solution of the optimization problem, this solution can be shown not to be unique. More importantly, since the so obtained "optimum" solution is normally wrong, when the method is applied to multicomponent systems incorrect predictions will be obtained.

(2) If compositional data of simple hydrates are available for the guest entering the small cavity, the correct potential parameters can be isolated. Then dissociation point data together with the compositional data can be used to determine a unique set of potential parameters. The weak point of this method is that highly accurate determinations of the composition of simple gas hydrates is required. The method is extremely tedious and sophisticated equipment and extreme care are necessary. Only very few data have been reported, which are widely different.

(3) We have developed an alternative method for the determination of the potential parameters of gas hydrate formers entering both cavities when accurate compositional data are not available. As we demonstrate it is possible to locate accurately the unique set of potential parameters by using simple and mixed gas hydrate data.

(4) None of the above techniques is applicable for the determination of the potential parameters of components entering only the large cavity. Although a unique set of these parameters cannot be determined from any dissociation point and compositional data, any optimum set can be used to predict these properties for simple and mixed gas hydrates.

(5) It has been possible to determine a consistent unique set of potential parameters of ethane, which can enter large cavities only, by using heat capacity data. As shown in Chapter IV our result is consistent with the experimentally determined rotation barriers.

(6) Propane potential parameters could not be determined with confidence from heat capacity data, as explained in Chapter IV. Corresponding heat capacity data are not available for other larger hydrate formers. If infrared and Raman spectroscopic data for the enclathrated molecules of the above gases were available, they could be used to calculate corresponding heat capacities, which in turn is the only method which can lead to the determination of the potential parameters of these components.

(7) It has been shown that the potential parameters of water can be considered the same for both structures I and II. This finding ends an ambiguity raised in the literature.

(8) For small components, dissociation pressure data can be used to calculate reliable second virial coefficients.

Application of the model

Extensive comparison of the model with experimental data in Chapters I, III and V leads to the following conclusions:

(1) The model can predict reliably hydrate dissociation points of any natural or synthetic gas mixture. In most cases the model has demonstrated conservative predictions.

(2) Hydrate dissociation pressures in the presence of methanol inhibitor were also calculated reliably for any mixture.

(3) The water content of a vapour phase in equilibrium with hydrates can also be calculated reliably.

(4) The model predicts reliably the concentrations of major components in any phase. Predictions of the water and methanol content of the vapour phase are also reliable. However, corresponding predictions of the water and methanol content of a hydrocarbon-rich liquid phase often give only the order of the experimental values.

Stability Analysis

In Chapter V we have presented an algorithm for multiphase-multicomponent flash calculations, alternative to the well established phase-splitting approach, effectively equipped with stability analysis capabilities. The algorithm has been

applied in a variety of hydrate equilibria problems and results were compared with experimental data and the following conclusions may be drawn:

(1) The proposed algorithm can be used to solve any phase equilibria PVT problem, including location of phase boundaries (by trial and error), for binary or multicomponent systems.

(2) The proposed methodology is superior to the phase-splitting approach for hydrate problems because normally more than two phases coexist at equilibrium.

(3) The algorithm of Gupta is also an alternative to the phase splitting approach. However, in comparison to the method proposed here, it suffers from unnecessary complexity.

6.2. Recommendations for further work

Modelling of asymmetric systems

The experimental vapour-liquid equilibrium data reported in the open literature on the system water-methanol-reservoir gases and its binaries seem to be sufficient in most cases for supporting our modelling work. Note, however, that experimental data have not been reported at all in the open literature, for the vapour phase of the systems water-isobutane and methanol-isobutane. The modelling of this system plays an important role for hydrate predictions.

The computational scheme for modelling asymmetric systems, presented in Chapter I, has been based on one cubic equation of state for all fluid phases. Although this scheme offers a number of significant advantages over the activity coefficient models used previously, it is not free of shortcomings. In particular, the accuracy of the predictions of the minor components in each phase needs to be enhanced. Further, the accuracy of predictions in the near critical region needs to be greatly improved. It is doubtful whether these tasks can be accomplished by a modified form of the mixing rules for polar-nonpolar interactions. We base this statement on the immense international effort which has been directed towards modelling of asymmetric systems with cubic and noncubic equations of state, as it is evidenced by the number of publications on the subject every month in the past decade. Albeit almost every possible combination has been tried, even with relaxation of the corresponding states principle, the reported results seem to be limited. It appears, therefore, that there are certain limitations inherent in the current approach to this problem. It is believed that the solution of this problem can not be set on a sound basis, until

fundamental progress is made towards understanding critical phenomena and molecular forces. Even then it is questionable whether equations derived from statistical mechanics will be simple enough for engineering applications.

For a short-term development, it appears that an increased flexibility of the EoS can be achieved empirically, as necessary to achieve a good fit of vapour pressures of *binary* mixtures at low and high temperatures including the near critical region. The systems *methanol-ethane* and *methanol-propane* should be chosen for the modelling studies, because of the high degree of non-idealities they demonstrate and the availability of sufficient and adequate experimental data. The binary interaction parameters, incorporated in the model should meet certain limitations. No more than three interaction parameters per binary should be considered for simultaneous regression. In our experience, any multivariable regression technique would have difficulties in converging to unique values with more parameters. This is a natural result of the inherent extreme complexity of the model. These parameters should be neither temperature nor pressure dependent. Pressure dependence leads to thermodynamic inconsistency, since molecular forces should not depend on pressure. On the other hand, a temperature dependence of the parameters indicates a limited predictive power of the model, inadequate flexibility and might result in thermodynamic inconsistencies for certain properties. The model should meet certain boundary conditions, similar to those appearing in paragraph 1.3., which also may provide guidance in deciding the mathematical formulation of the model.

In Chapter IV we reported a correlation for the prediction of ideal gas heat capacities. As noted in paragraph 1.2., these correlations combined with the equation of state could serve as a fundamental equation from which any thermodynamic or mechanical property of a system could be derived. It has not been possible to develop the necessary routines within the time-schedule of the present study, but this is strongly recommended since it will allow, for example, prediction of enthalpy changes during a range of industrial processes.

The Classical Cell Model

It has been demonstrated that the classical theory of van der Waals and Platteeuw is perfectly valid for rather small nearly spherical molecules entering either of the hydrate structures. For the interactions of such molecules with water, a corresponding states approach could be successfully applied. It is not so for large nonspherical molecules like ethane, propane, isobutane and n-butane. The interactions of the latter guest molecules with the hydrate host lattice need

to be further investigated. More information on guest-host interactions could be gained by heat capacity measurements for mixed gas hydrates of ethane with methane as a help-gas, over a wide range of temperatures. A series of such experiments should be performed with different compositions. Application of the methodology detailed in Chapter IV, will reveal the extent of the guest-host interactions, as evidenced by the change in the heat capacity of the guest and that of the empty hydrate lattice. Infrared and Raman spectra of the guest molecules in the hydrate cages could directly provide information about the guest-host interactions. Such spectra for gas hydrates have not been reported in the open literature as far as we know. A knowledge of the heat capacities of enclathrated ethane, propane, isobutane and n-butane from spectroscopic data together with the methodology detailed in Chapter 4, will lead to an exact calculation of the heat capacity of the empty lattice of each guest. It might be possible then to achieve a generalized description of these interactions.

As an aside, if correct values of the Kihara potential parameters for gas-water interactions are achieved for the hydrates of the above guests, it would be then possible to derive mixing rules honouring the corresponding states principle. In turn, this could be proven to have some practical significance, at least for approximate estimation of hydrate properties, since more than one hundred hydrate forming gases appear to be known .

Although there are adequate experimental dissociation pressure data for almost all simple gas hydrates of reservoir gases, data for the binary mixtures of nitrogen, carbon dioxide and hydrogen sulfide with ethane, isobutane and n-butane have not been reported in the open literature. Such data would be useful in determining the effect of the size of the molecules on guest-host interactions. For example, nitrogen has a very small diameter (4.0 Å) and it is accommodated comfortably in the small cavities of either structure. Therefore the potential parameters of nitrogen-water interactions should be the same in all structures independently of the presence of other guests. Then the experimental data of its binary mixtures with heavier components might be used to match properties which are expected to depend on the size of the guest, namely the differences between the thermodynamic properties of the hypothetical empty hydrate lattice and ice.

Calculations algorithm

The algorithm detailed in Chapter I for the determination of phase boundaries of multiphase systems is limited to cases when the identity of the present phases is known. On the other hand, the method described in Chapter V for the

determination of phase boundaries of multiphase systems is not very convenient for everyday use. It might be possible to write a more specific algorithm where the pressure, which makes zero the phase fraction of one particular phase at a specified temperature, is one of the unknowns and the algorithm would still be able to decide the identity of the actually present phases. Provision however should be taken because a physically meaningful solution to a specified problem might not exist.

A routine needs to be developed for calculation of the minimum required amount of methanol for a required inhibition effect, considering losses in the vapour and liquid phases. Currently, such calculations can be carried out by a trial and error procedure. For computer implementation, the problem may be defined as follows: For a given fluid the incipient hydrate formation temperature T_i at a specified operating pressure P_i is calculated and is considered known. It is required to find what amount of methanol needs to be injected in the original fluid to depress to incipient hydrate formation temperature by ΔT K. Then the operating pressure and temperature are given(P_i, $T_i^*=T_i+\Delta T$) and the following formulation is suggested for a Newton-Raphson implementation of the problem:

$$\mathbf{G}(\Psi) = 0 \tag{6.1}$$

where the vector of the unknowns Ψ is given by the equation:

$$\Psi = \Psi(x_1, F_1, x_2, F_2, \ldots, x_{\pi-1}, F_{\pi-1}, z_m)^T \tag{6.2}$$

where z_m is the mole fraction of methanol in the feed composition of the mixture and x_j, F_j are the composition and phase fraction of phase j. Here, index π indicates the (incipient) hydrate phase, with phase fraction equal to zero and mole fractions dependent variables. There are $(c+1)(\pi-1)+1$ unknowns. The array **G** of the independent equations is defined by the following equations:

$$G_i = z_i - \sum_{j}^{\pi-1} F_j x_{ij}, \quad i = 1,\ldots,c \tag{6.3}$$

$$G_{c+1} = 1 - \sum_{i}^{c} x_{i1} \tag{6.3}$$

$$G_{(m-1)(c+1)+i} = \ln\frac{f_{i1}}{f_{im}}, \quad m = 2,..,\pi-1 \tag{6.4}$$

$$G_{m(c+1)} = P - \sum_{i}^{c} \frac{f_{i1}}{\phi_{im}} \tag{6.5}$$

$$G_{m(c+1)+1} = \ln\frac{f_{w1}}{f_{wH}} \tag{6.6}$$

APPENDICES

APPENDIX A

CALCULATION OF FUGACITIES FROM THE VALDERRAMA EOS WITH UNCONVENTIONAL DENSITY-DEPENDENT MIXING RULES

The starting formula for the calculation of fugacity coefficients is the thermodynamic relation:

$$RT\ln\phi_k = \int_V^{\infty}\left[\left(\frac{\partial P}{\partial n_k}\right)_{T,V,n_j} - \frac{RT}{V}\right]dV - RT\ln Z \qquad (A.1)$$

The derivative of pressure for the Valderrama EoS is given by the following relation:

$$\left(\frac{\partial P}{\partial n_k}\right)_{T,V,n_{j\neq k}} = \frac{RT}{V-n_T b} + \frac{n_T b_k RT}{(V-n_T b)^2} - \frac{\dfrac{\partial n_T{}^2 a}{\partial n_k}}{V(V+n_T b)+n_T c(V-n_T b)}$$

$$+\frac{n_T{}^2 a}{[V(V+n_T b)+n_T c(V-n_T b)]^2}\frac{\partial[V(V+n_T b)+n_T c(V-n_T b)]}{\partial n_k} =$$

$$\frac{RT}{V-n_T b} + \frac{n_T b_k RT}{(V-n_T b)^2} - \frac{\dfrac{\partial n_T{}^2 a^C}{\partial n_k}}{V(V+n_T b)+n_T c(V-n_T b)}$$

$$-\frac{1}{RTV}\frac{\dfrac{\partial n_T{}^3 a^A}{\partial n_k}}{V(V+n_T b)+n_T c(V-n_T b)}$$

$$+\frac{n_T{}^2 a^C}{[V(V+n_T b)+n_T c(V-n_T b)]^2}\frac{\partial[V(V+n_T b)+n_T c(V-n_T b)]}{\partial n_k}$$

$$+\frac{1}{RTV}\frac{n_T{}^3 a^A}{[V(V+n_T b)+n_T c(V-n_T b)]^2}\frac{\partial[V(V+n_T b)+n_T c(V-n_T b)]}{\partial n_k} \qquad (A.2)$$

where $V=n_T v$. The derivatives appearing in eqn (2) are calculated from the equations:

$$\frac{\vartheta n_T^2 a^C}{\vartheta n_k} = 2\sum_j n_j a_{jk} \tag{A.2a}$$

$$\frac{\vartheta n_T^3 a^A}{\vartheta n_k} = 2n_k a_k \sum_j n_j a_{kj} l_{kj} + \sum_p n_p^2 a_p a_{pk} l_{pk} \tag{A.2b}$$

$$\frac{\vartheta[V(V+n_T b)+n_T c(V-n_T b)]}{\vartheta n_k} = V(b_k + c_k) - n_T b c_k - n_T c b_k \tag{A.2c}$$

Equation (1) is combined with equation (2) and the integral is calculated as the sum of individual integrals, which are given by the following equations:

$$\int_V^\infty \left[\frac{RT}{V-n_T b} - \frac{RT}{V}\right] dV = -RT\ln\frac{v-b}{v} \tag{A.3}$$

$$\int_V^\infty \frac{n_T b_k RT}{(V-n_T b)^2} dV = RT\frac{b_k}{v-b} \tag{A.4}$$

The rest of the integrals require formulas for the appearing specific types of integrals, which are listed below:

$$\int_v^\infty \frac{1}{v(v+b)+c(v-b)} dv = -\frac{1}{2d}\ln\frac{q-d}{q+d} \tag{A.5}$$

where $q=v+(b+c)/2$ and $d=[bc+(b+c)^2/4]^{1/2}$.

$$\int_v^\infty \frac{1}{v[v(v+b)+c(v-b)]} dv = -\frac{1}{2bc}\ln\frac{q^2-d^2}{v^2} - \frac{b+c}{4bcd}\ln\frac{q-d}{q+d} \tag{A.6}$$

$$\int_v^\infty \frac{1}{[v(v+b)+c(v-b)]^2} dv = \frac{1}{4d^3}\left[\frac{2qd}{q^2-d^2} + \ln\frac{q-d}{q+d}\right] \tag{A.7}$$

$$\int_{v}^{\infty} \frac{v}{[v(v+b)+c(v-b)]^2} dv = \frac{1}{2(q^2-d^2)} - \frac{b+c}{8d^3}\left[\frac{2qd}{q^2-d^2} + \ln\frac{q-d}{q+d}\right] \qquad (A.8)$$

$$\int_{v}^{\infty} \frac{1}{v[v(v+b)+c(v-b)]^2} dv = \frac{1}{2(bc)^2}\ln\frac{q^2-d^2}{v^2} + \frac{2d^2+q(b+c)}{4bcd^2(q^2-d^2)} + \frac{(b+c)(2d^2+bc)}{8(bc)^2d^3}\ln\frac{q-d}{q+d} \qquad (A.9)$$

$$\int_{V}^{\infty} \frac{2\sum_j n_j a_{jk}}{V(V+n_T b)+n_T c(V-n_T b)} dV = \int_{v}^{\infty} \frac{2\sum_j x_j a_{jk}}{v(v+b)+c(v-b)} dv = \frac{\sum_j x_j a_{jk}}{d} \ln\frac{q-d}{q+d} \qquad (A.10)$$

$$\frac{1}{RT}\int_{V}^{\infty} \frac{2n_k a_k \sum_j n_j a_{kj} l_{kj} + \sum_p n_p^2 a_p a_{pk} l_{pk}}{V[V(V+n_T b)+n_T c(V-n_T b)]} dV = \frac{1}{RT}\int_{v}^{\infty} \frac{2x_k a_k \sum_j x_j a_{kj} l_{kj} + \sum_p x_p^2 a_p a_{pk} l_{pk}}{v[v(v+b)+c(v-b)]} dv$$

$$= -\frac{2x_k a_k \sum_j x_j a_{kj} l_{kj} + \sum_p x_p^2 a_p a_{pk} l_{pk}}{2RT}\left[\frac{1}{bc}\ln\frac{q^2-d^2}{v^2} + \frac{b+c}{2bcd}\ln\frac{q-d}{q+d}\right] \qquad (A.11)$$

$$a^c(b_k + c_k)\int_{v}^{\infty} \frac{v}{[v(v+b)+c(v-b)]^2} dv =$$

$$\frac{a^c(b_k + c_k)}{2(q^2-d^2)} - \frac{a^c(b_k + c_k)(b+c)}{8d^3}\left[\frac{2qd}{q^2-d^2} + \ln\frac{q-d}{q+d}\right] \qquad (A.12)$$

$$a^c(cb_k + bc_k)\int_{v}^{\infty} \frac{1}{[v(v+b)+c(v-b)]^2} dv = \frac{a^c(cb_k + bc_k)}{4d^3}\left[\frac{2qd}{q^2-d^2} + \ln\frac{q-d}{q+d}\right] \qquad (A.13)$$

$$\frac{a^A(b_k + c_k)}{RT}\int_{v}^{\infty} \frac{1}{[v(v+b)+c(v-b)]^2} dv = \frac{a^A(b_k + c_k)}{RT}\frac{1}{4d^3}\left[\frac{2qd}{q^2-d^2} + \ln\frac{q-d}{q+d}\right] \qquad (A.14)$$

$$\frac{a^A(cb_k + bc_k)}{RT}\int_v^\infty \frac{1}{v[v(v+b)+c(v-b)]^2}dv =$$

$$\frac{a^A(cb_k + bc_k)}{2bcRT}\left[\frac{1}{bc}\ln\frac{q^2-d^2}{v^2}+\frac{2d^2 + q(b+c)}{2d^2(q^2-d^2)} +\frac{(b+c)(2d^2+bc)}{4bcd^3}\ln\frac{q-d}{q+d}\right] \qquad (A.15)$$

Finally, combining equations (1), (2) and (3),(4) (10), (11), (12), (13), (14) and (15) we get:

$$RT\ln\phi_k = - RT\ln Z - RT\ln\frac{v-b}{v} + RT\frac{b_k}{v-b} + \frac{\sum_j x_j a_{jk}}{d}\ln\frac{q-d}{q+d}$$

$$+\frac{a^C(b_k + c_k)}{2(q^2-d^2)}$$

$$-\frac{a^C(b_k + c_k)(b+c)}{8d^3}\left[\frac{2qd}{q^2-d^2} + \ln\frac{q-d}{q+d}\right]$$

$$-\frac{a^C(cb_k + bc_k)}{4d^3}\left[\frac{2qd}{q^2-d^2} + \ln\frac{q-d}{q+d}\right]$$

$$+\frac{2x_k a_k\sum_j x_j a_{kj} l_{kj} + \sum_p x_p^2 a_p a_{pk} l_{pk}}{2bcRT}\left[\ln\frac{q^2-d^2}{v^2} + \frac{b+c}{2d}\ln\frac{q-d}{q+d}\right]$$

$$+\frac{a^A(b_k + c_k)}{RT}\frac{1}{4d^3}\left[\frac{2qd}{q^2-d^2} + \ln\frac{q-d}{q+d}\right]$$

$$-\frac{a^A(cb_k + bc_k)}{2bcRT}\left[\frac{1}{bc}\ln\frac{q^2-d^2}{v^2}+\frac{2d^2 + q(b+c)}{2d^2(q^2-d^2)} +\frac{(b+c)(2d^2+bc)}{4bcd^3}\ln\frac{q-d}{q+d}\right] \qquad (A.16)$$

Divide both sides of equation (16) by RT and collect similar terms to obtain:

$$\ln\phi_k = - \ln(Z - B) + \frac{B_k}{Z-B} + \frac{\sum_j x_j A_{jk}}{D}\ln\frac{Q-D}{Q+D}$$

$$+\frac{A^C(B_k + C_k)}{2(Q^2-D^2)}$$

$$-\frac{A^C}{8D^3}\left[\frac{2QD}{Q^2-D^2} + \ln\frac{Q-D}{Q+D}\right][B_k (B+3C)+ C_k(3B+C)]$$

$$+\frac{2x_kA_k\sum_j x_jA_{kj}l_{kj}+\sum_p x_p^2A_pA_{pk}l_{pk}}{2BC}\left[\ln\frac{Q^2-D^2}{Z^2}+\frac{B+C}{2D}\ln\frac{Q-D}{Q+D}\right]$$

$$+\frac{A^A(B_k+C_k)}{4D^3}\left[\frac{2QD}{Q^2-D^2}+\ln\frac{Q-D}{Q+D}\right]$$

$$-\frac{A^A(CB_k+BC_k)}{2BC}\left[\frac{1}{BC}\ln\frac{Q^2-D^2}{Z^2}+\frac{2D^2+Q(B+C)}{2D^2(Q^2-D^2)}+\frac{(B+C)(2D^2+BC)}{4BCD^3}\ln\frac{Q-D}{Q+D}\right]$$

(A.17)

The capital symbols in the final expression were defined by equations (1.25) and (1.26).

APPENDIX B

CALCULATION OF KIHARA POTENTIAL PARAMETERS FROM SECOND VIRIAL COEFFICIENT DATA (KIHARA, 1951).

The formulas of Kihara(1951) have been rearranged by Tee et al(1966) in terms of more familiar variables. These formulas are reproduced below.

$$B(T)=\frac{2}{3}\pi Ns^3[a^{*3}+3(2^{1/6})a^{*2}F_1(T^*)+3(2^{1/3})a^*F_2(T^*)+(2^{1/2})F_3(T^*)]/(1+a^*)^3 \qquad (B.1)$$

where $T^*= kT/\varepsilon$ and $a^*=2a/(\sigma - 2a)$. The dimensionless functions $F_1(T^*)$, $F_2(T^*)$ and $F_3(T^*)$ are given by

$$F_s(T^*) = -\frac{s}{12}\sum_{j=0}^{\infty}\frac{2^j}{j!}\Gamma(\frac{6j-s}{12})T^{*-(6j+s)/12}\text{ , where } s=1, 2, 3 \qquad (B.2)$$

The Gamma function Γ is approximated numerically.

APPENDIX C

CALCULATION OF THE TEMPERATURE DERIVATIVES OF THE LANGMUIR-TYPE CONSTANT FOR GAS-WATER INTERACTIONS IN HYDRATE CAVITIES.

The Langmuir-type constant, which accounts for gas-water interactions in the hydrate cavities, is given by the relation(van der Waals and Platteeuw,1959):

$$C_{mi}(T) = \frac{4\pi}{kT}\int_0^R \exp(-\frac{w(r)}{kT})r^2dr \qquad (C.1)$$

where m and i are the cavity and guest indices, respectively, and R the radius of the cavity. To simplify notation we assign the symbol $\mathbf{I}_{mi}$ to the integral:

$$\mathbf{I}_{mi} = \int_0^R \exp(-\frac{w(r)}{kT})r^2dr \qquad (C.2)$$

By taking the logarithm of (1) and differentiating, we obtain for the derivatives:

$$\frac{\vartheta \ln C_{mi}}{\vartheta T} = \frac{\vartheta \mathbf{I}_{mi}}{\mathbf{I}_{mi}\vartheta T} - \frac{1}{T} \qquad (C.3)$$

and

$$\frac{\vartheta^2 \ln C_{mi}}{\vartheta T^2} = \frac{1}{\mathbf{I}_{mi}}\frac{\vartheta^2 \mathbf{I}_{mi}}{\vartheta T^2} - \frac{1}{\mathbf{I}_{mi}^2}\left[\frac{\vartheta \mathbf{I}_{mi}}{\vartheta T}\right]^2 + \frac{1}{T^2} \qquad (C.4)$$

The derivatives of the integral with respect to temperature are calculated as follows:

$$\frac{\vartheta \mathbf{I}_{mi}}{\vartheta T} = \frac{\vartheta}{\vartheta T}\int_0^R \exp(-\frac{w(r)}{kT})r^2dr = \int_0^R \frac{\vartheta}{\vartheta T}\exp(-\frac{w(r)}{kT})r^2dr$$

$$= \int_0^R \exp(-\frac{w(r)}{kT})\frac{\vartheta}{\vartheta T}(-\frac{w(r)}{kT})r^2dr = \int_0^R \frac{w(r)}{kT^2}\exp(-\frac{w(r)}{kT})r^2dr \Rightarrow$$

$$\frac{\vartheta \mathbf{I}_{mi}}{\vartheta T} = \frac{1}{T}\int_0^R \frac{w(r)}{kT}\exp(-\frac{w(r)}{kT})r^2dr \qquad (C.5)$$

$$\frac{\vartheta^2 \mathbf{I}_{mi}}{\vartheta T^2} = \frac{\vartheta}{\vartheta T}\frac{\vartheta \mathbf{I}_{mi}}{\vartheta T} = -\frac{2}{kT^3}\int_0^R w(r)\exp(-\frac{w(r)}{kT})r2dr + \frac{1}{T}\int_0^R \frac{w(r)}{kT}\exp(-\frac{w(r)}{kT})\frac{\vartheta}{\vartheta T}(-\frac{w(r)}{kT})r^2dr$$

$$\frac{\vartheta^2 \mathbf{I}_{mi}}{\vartheta T^2} = -\frac{2}{T}\frac{\vartheta \mathbf{I}_{mi}}{\vartheta T} + \frac{1}{T^2}\int_0^R \left[\frac{w(r)}{kT}\right]^2 \exp(-\frac{w(r)}{kT})r^2dr \qquad (C.6)$$

The two new integrals appearing in equations (5) and (6) are calculated numerically in the same manner as $\mathbf{I}_{mi}$.